

# DISSERTATION

## Physics of Magnetoelectric Composites

performed in application for the degree of Doctor of Technical Sciences

under the supervision of

a.o. Prof. Dr. Roland Grössinger

E138

Institut für Festkörperphysik

submitted to

Technische Universität Wien

Fakultät für Physik

*by*

**GIAP Van-Duong**

Hardtmuthgasse 88/3/9

A-1100, Vienna, Austria

Matr. Nr. 0327351

born on February 23<sup>th</sup>, 1976, in Vietnam

*Vienna, September 13<sup>th</sup>, 2006*

.....

To my family

*...contraria sunt complementa...*

Niels Bohr

# Content

<b>Abstract</b> .....	6
<b>Abstrakt</b> .....	8
<b>Preface</b> .....	10
<b>Introduction</b> .....	14
Magnetoelectric Materials-New Materials for Applications.....	15
Magnetoelectric Composites: An Overview .....	26
<b>Experiments</b> .....	47
Sample preparation.....	48
Structural characterization.....	54
Magnetic characterization .....	56
Magnetoelectric characterization .....	58
Other experiments .....	62
<b>Results and Discussion</b> .....	64
<i>Structural &amp; Magnetic Studies</i> .....	65
Monodispersed Nanocrystalline $\text{Co}_{1-x}\text{Zn}_x\text{Fe}_2\text{O}_4$ Particles by Forced Hydrolysis: Synthesis and Characterization .....	66
Magnetic properties of nanocrystalline $\text{Co}_{1-x}\text{Zn}_x\text{Fe}_2\text{O}_4$ prepared by forced hydrolysis method..	78
Ultrafine $\text{Co}_{1-x}\text{Zn}_x\text{Fe}_2\text{O}_4$ particles synthesized by forced hydrolysis: Effect of thermal treatment and its relationship with magnetic properties.....	90
Magnetic properties of nanocrystalline $\text{CoFe}_2\text{O}_4$ synthesized by modified citrate-gel method ..	98
Magnetic properties of nanocrystalline cobalt ferrite in $\text{CoFe}_2\text{O}_4$ - $\text{BaTiO}_3$ core-shell structure composite. ....	109

<i>Magnetoelectric Studies</i> .....	119
The Lock-in Technique for Studying Magnetoelectric Effect .....	120
Magnetoelectric Properties of CoFe <sub>2</sub> O <sub>4</sub> -BaTiO <sub>3</sub> Core-Shell Structure Composite. ....	128
Effect of Preparation Conditions on Magnetoelectric Properties of CoFe <sub>2</sub> O <sub>4</sub> -BaTiO <sub>3</sub> Magnetoelectric Composites .....	137
Effect of Structure on Magnetoelectric Properties of CoFe <sub>2</sub> O <sub>4</sub> -BaTiO <sub>3</sub> Multiferroic Composites. ....	145
Driving Mechanism for Magnetoelectric Effect in CoFe <sub>2</sub> O <sub>4</sub> -BaTiO <sub>3</sub> Multiferroic Composite...	151
Evidence of direct magneto-electric dipole interaction in CoFe <sub>2</sub> O <sub>4</sub> – BaTiO <sub>3</sub> core-shell structure composite. ....	156
Magnetoelectric properties of CoFe <sub>2</sub> O <sub>4</sub> – BaTiO <sub>3</sub> core-shell structure composite studied by magnetic pulse method.....	166
Magnetoelectric properties of Co <sub>0.7</sub> Zn <sub>0.3</sub> Fe <sub>2</sub> O <sub>4</sub> – BaTiO <sub>3</sub> core-shell structure composite.....	175
<b>Conclusion</b> .....	186
<b>Appendix</b> .....	193
<b>Acknowledgement</b> .....	197
<b>Curriculum vitae</b> .....	199

## Abstract

Magnetolectric composites between the magnetic  $\text{CoFe}_2\text{O}_4$  and the piezoelectric  $\text{BaTiO}_3$  were produced using a variety of chemical methods.  $\text{CoFe}_2\text{O}_4$ - $\text{BaTiO}_3$  composites were chosen in order to obtain a composite with a reasonable magnetolectric coefficient at room temperature. Within this work the understanding of the magnetolectric (ME) properties of these composites shall be improved. Using different preparation methods, new composite structures could be produced with the aim to achieve a better coupling between the constituents. Various kind of nanocrystalline  $\text{CoFe}_2\text{O}_4$ , Zn substituted Co-ferrites and  $\text{CoFe}_2\text{O}_4$ - $\text{BaTiO}_3$ ,  $\text{Co}_{0.7}\text{Zn}_{0.3}\text{Fe}_2\text{O}_4$ - $\text{BaTiO}_3$  composites have been synthesized, mostly by wet chemical methods. All samples were structural characterised (x-ray diffraction) as well as magnetically (magnetization, magnetostriction) investigated. An important aim of this work is to come to an understanding of the responsible driving mechanism which is in charge for the ME effect of such composites and to investigate the possibility of a direct coupling between magnetic and electric components (domains) by reducing the grain size of the constituents to nanoscale.

In order to investigate the magnetolectric effect of the composites different measuring methods were developed and compared. Especially two measuring systems were used to study the ME effect: i) the so-called Lock-in Technique which is an ac-method and ii) the Pulse Field Method, which allows to measure the total magnetolectric coefficient.

It was shown that the wet chemical method is a powerful tool to synthesize high quality nanocrystalline  $\text{CoFe}_2\text{O}_4$  as well as its Zn-substituted derivatives with average grain size of 3-40 nm and very good magnetic properties, which are close to that of bulk material. Such nanocrystalline ferrites can be used not only as initial materials for preparing ferrite-barium titanate ME composites but also for many other applications such as ferrofluids, magnetic drug carriers, etc. This wet chemical method also allows to synthesize ME  $\text{CoFe}_2\text{O}_4$ - $\text{BaTiO}_3$  and  $\text{Co}_{0.7}\text{Zn}_{0.3}\text{Fe}_2\text{O}_4$ - $\text{BaTiO}_3$  composites in a core-shell structure. This type of microstructure is new and proved to have a better coupling between the magnetostrictive and piezoelectric constituents, resulting in a ME coefficient of almost 18 times higher than that of the conventional mixed composites. The microstructure which is determined by sample preparation procedure is found to affect seriously the ME properties of the composites. The ME coefficient is found to be proportional to an efficiency factor  $k_0$  and a

coupling coefficient  $k$ , defined as  $k=\lambda.\partial\lambda/\partial H$  where  $\lambda$  is the linear magnetostriction. This is different from previous knowledge that the ME coefficient of composites is just proportional to the piezomagnetic coupling  $q=d\lambda/dH$ . It was also found that the charging and discharging processes, which occur simultaneously determines the measured value of the magnetoelectric coefficient depending on the time scale (period of ac-field, pulse duration) of the experiment. The total ME coefficient as measured by the Pulse Field Method is generally larger than that obtained by the Lock-in Technique. Besides the mechanical coupling where the magnetostriction is most important, a direct coupling between magnetic and electric domains is evidenced. However, more experiments need to be carried out to characterize the nature of this new coupling phenomenon.

## Abstrakt

Magnetoelektrische Verbundwerkstoffe zwischen dem magnetischen  $\text{CoFe}_2\text{O}_4$  und dem piezoelektrischen  $\text{BaTiO}_3$  wurden mittels verschiedener chemischer Methoden hergestellt. Der  $\text{CoFe}_2\text{O}_4$ - $\text{BaTiO}_3$  Verbundwerkstoff wurde gewählt um eine Substanz mit einem vernünftigen magnetoelektrischen Koeffizienten (ME) bei Raumtemperatur zu entwickeln. Mit dieser Arbeit soll das Verständnis der magnetoelektrischen Eigenschaften dieser Verbundwerkstoffe verbessert werden. Durch die Verwendung verschiedener Herstellungsmethoden sollen neue Verbundstrukturen hergestellt werden, mit dem Ziel eine bessere Kopplung zwischen den Komponenten zu erhalten. Mittels nasschemischer Methoden wurden verschiedene Arten von nanokristallinem  $\text{CoFe}_2\text{O}_4$ , Zn substituierten Co-Ferrit und  $\text{CoFe}_2\text{O}_4$ - $\text{BaTiO}_3$  Verbundwerkstoff hergestellt. Alle Proben wurden sowohl strukturell charakterisiert (Röntgen Diffraktometrie), als auch in Bezug auf die magnetischen Eigenschaften (Magnetisierung, Magnetostriktion) untersucht. Ein wichtiges Ziel dieser Arbeit war zu einem tieferen Verständnis der für den ME Effekt verantwortlichen Mechanismen in derartigen Verbundwerkstoffen zu kommen. Außerdem soll durch eine Reduktion der Korngröße der Komponenten in den Nanometerbereich untersucht werden, ob es möglicherweise eine direkte Kopplung zwischen den magnetischen und elektrischen Komponenten (Domänen) gibt.

Um den magnetoelektrischen Effekt der Verbundwerkstoffe zu untersuchen, wurden verschiedenen Meßmethoden entwickelt und verglichen. Es wurden speziell zwei Meßsysteme verwendet um den ME Effekt zu untersuchen: i) die sogenannte Lock-in Methode welche ein Wechselstromverfahren darstellt und ii) die Puls-Feld-Methode, welche den gesamten magnetoelektrischen Effekt zu messen gestattet.

Es wird gezeigt, dass das nasschemische Verfahren eine sehr wirkungsvolle Methode zur Herstellung qualitativ hochwertigen nanokristallinen  $\text{CoFe}_2\text{O}_4$  mit einer mittleren Korngröße von 3-40 nm darstellt. Diese Proben haben dann sehr gute magnetische Eigenschaften die nahe bei denen von grobkristallinen Material liegen. Solche nanokristalline Ferrite können in der Herstellung nicht nur als Startmaterial für den ME Verbundwerkstoff  $\text{CoFe}_2\text{O}_4$ - $\text{BaTiO}_3$  verwendet werden, sondern auch für viele andere Anwendungen wie z.B.: als Ferroflüssigkeiten, magnetische Arzneimittelträger, usw. Die nasschemische Methode erlaubt die Herstellung des ME Verbundwerkstoffes  $\text{CoFe}_2\text{O}_4$ -



BaTiO<sub>3</sub> in einer „Kern-Schalen“ Mikrostruktur. Diese Art von Mikrostruktur ist neu und es wird gezeigt, dass man damit eine bessere Kopplung zwischen der magnetostruktiven und der piezoelektrischen Komponente erzielt. Man erhält einen ME Koeffizient der fast 18 mal höher ist als der von gewöhnlich gemischten Verbundwerkstoffen. Die Mikrostruktur wird durch das verwendete Herstellungsverfahren festgelegt und bestimmt in entscheidender Weise die ME Eigenschaften des Verbundwerkstoffes. Es wurde festgestellt, dass der ME Koeffizient proportional zu einem „Effektivitätsfaktor“  $k_0$  bzw. einem Kopplungskoeffizient  $k$  ist, welcher definiert durch  $k = \lambda \cdot \partial \lambda / \partial H$  ist, wobei  $\lambda$  die lineare Magnetostriktion darstellt. Dies ist unterschiedlich zu dem bisherigen Verständnis, dass der ME Koeffizient eines Verbundwerkstoffes gerade proportional zu einem piezomagnetischen Kopplungsfaktor  $q = d\lambda/dH$  ist. Es wurde festgestellt, dass der Lade- und Entladevorgang, welcher gleichzeitig während der Messung abläuft, wesentlich den gemessenen Wert des magnetoelektrischen Koeffizienten bestimmt, abhängig auch von der verwendeten Zeitskala (Periode des Wechselfeldes, Pulsdauer) des Experimentes. Der mit der Pulsfeldmethode gemessene gesamte ME Koeffizient ist im Allgemeinen größer als jener durch die Lock-In Methode bestimmte Wert. Neben der magneto-mechanischen Kopplung wo die Magnetostriktion von entscheidender Bedeutung ist, wurde auch eine „direkte“ Kopplung zwischen den magnetischen und elektrischen Domänen gefunden. Es müssen aber sicher noch mehr Experimente durchgeführt werden um die genaue Natur dieser neuen Form der Kopplung in Verbundwerkstoffen voll zu verstehen.

*...a journey of thousand miles starts with a single step...*

Ancient idiom

## **Preface**

# History of the Magnetoelectric Effect

It is already more than a century ago since P. Currie mentioned for the first time the magnetoelectric (ME) effect, in 1894, when he considered the symmetry of crystals [1]. However, it took almost seven decades, of course after many failures of pioneer works, to the first experimental observation of this effect, in  $\text{Cr}_2\text{O}_3$  system by Astrov in 1960 [2]. Due to the possibility of mutual control between magnetic and electric order, ME materials exhibit novel physics and exotic properties, and become very attractive not only for fundamental understanding of the materials, but also for important potential technological applications such as sensors, transducers, actuators, multiple state memory elements, etc. Already in 1973, Wood and Austin proposed 15 different types of applications based on ME materials [3]. However, due to the requirement of the coexistence of magnetic moments and electric dipoles in an asymmetry structure, which is generally due to the important role of the 3d-levels for these effects chemically incompatible [4], the number of compounds that exhibits ME effect is limited, and the ME effect occurs mostly at low temperature with a quite low ME coefficient. The reason for this may be also due to the fact that mostly oxides were studied up to now which in low symmetry structures generally exhibit a low ordering temperature. This prevents them from practical applications and also lowers down its initial attractiveness.

The story becomes different in 1972 when Van Suchetelene introduced the concept of “product property” and for the first time successfully prepared ME composite of CoO-FeO-BaO-TiO system at eutectic composition by using a unidirectional solidification method [5]. Generally a ME composite consists of a magnetostrictive and a piezoelectric phase, which should be mixed together as good as possible in order to achieve “good” coupling. When exposing such a ME composite to an external magnetic field, a strain in the magnetostrictive constituent is produced. This strain will be passed into the piezoelectric component, causing a stress and as a result of it, producing an electric polarization. With this breakthrough step, the limitations of single phase materials such as the chemical incompatibility, the low temperature requirement and the smallness of the ME coefficient are overcome as the magnetic and electric ordering (magnitude and temperature) are introduced in a controlled way and can be optimised independently. This makes the proposed applications of the ME materials more promising. Nevertheless, the lack of complete understanding of such composites as well as the difficulties in controlling the microstructure of such samples again prevents them up to now from practical applications.

Today, the ME effect in single phase materials as well as in various types of composites is investigated intensively which means that this effect see some kind of renaissance [6-7]. The reason is the discovery of large ME effect in laminar and multilayer composites, which allows a good control of the reproducibility of the samples. However, the lack of knowledge in both experimental aspects and fundamental understanding of the ME effect, such as the nature of coupling between magnetic and electric domains together with still rather low values of the ME coefficient makes none of the practical applications based on ME materials commercially available. Additionally a defined experimental determination of the ME coefficient is still a point of discussion.

## References

- [1] P. Curie, J. Physique 3<sup>e</sup> series, 3, 393 (1894).
- [2] D.N. Astrov, Sov. Phys.—JETP, 11, 708 (1960).
- [3] V. E. Wood, A. E. Austin, Int. J. Magn. 5 (1973) 303.
- [4] N.A. Hill, J. Phys. Chem. B 104 (2000) 6694-6709.
- [5] J. Van Suchetelene, Philips Res. Rep., 27 (1972) 28.
- [6] Manfred Fiebig, J. Phys. D: Appl. Phys. 38 (2005) R123–R152
- [7] N. A. Spaldin, M. Fiebig, Science, 309 (2005) 391.

## Aims of the thesis

Within the scope of this thesis, the following problems shall be investigated and if possible solved:

1. Developing and comparing measuring techniques to study the ME effect in composite.
2. Preparing new composite structures which may have a better coupling between constituents.
3. Understanding of the driving mechanism which is in charge for the ME effect in composite.
4. Finding a possible direct coupling between magnetic and electric domains by reducing the grain size of the constituent to nanoscale.

The main experimental results in this area are reported in this thesis. Basically, it consists of 15 different but related articles that are published, accepted to publish or to be submitted for publication, where the author of this thesis is the main author of 14 articles and co-author of the remaining ones, and some additions such as preface, details of experiment and conclusion. The thesis is divided into four different parts: Introduction, Experiment, Results and Discussion and Conclusion. The introduction part includes 2 articles that give an overview of the recent studies on ME materials. The experimental part describes the experimental methods used to synthesize the samples and the experiments to characterise the structural and magnetic properties. The chapter “Results and discussion” consists of 13 articles, arranged in two different subgroups, called Structural & Magnetic Studies and Magnetoelectric Studies, reporting the main results and discussion of the work. Finally, in the “Conclusion” some concluding remarks about what is achieved within this thesis and open questions which should be solved in future investigating and improving ME composites.

*...what is truth?*

Pontius Pilate

## **Introduction**

*This part will give an overview about the magnetoelectric effect in both single phase and composite materials.*

# Magnetoelectric materials-New materials for applications

R.Grössinger<sup>1</sup>, Giap Van Duong<sup>1</sup>, D. Bueno-Baqués<sup>2</sup>

<sup>1</sup>*Inst. f. Festkörperphysik, T.U. Wien, Wiedner Hauptstr. 8-10; A-1040 Vienna, Austria*

<sup>2</sup>*CIMAV, Miguel de Cervantes, 120; 31109 Chihuahua, Mexico*

Invited talk at Internatinal Symposium on Interdisciplinary Electromagnetic, Mechani & Biomedical Problems (ISEM 2005), September 12-14, 2005, Bad Gastein (Salzburg), Austria.

Proceedings in press, published as a special issue of the International Journal of Applied Electromagnetics and Mechanics (IJAEM).

---

## Abstract

A survey of the development of magnetoelectric materials is given. The limitations of single phase materials are shown. The concept of magnetoelectric composites is discussed. A measuring method based on modulating the dc-field and using a lock-in amplifier for determining the magnetoelectric coefficient is described. Results on a composite of 50%BaTiO<sub>3</sub>-50%CoFe<sub>2</sub>O<sub>4</sub> are demonstrated.

*Keywords:* Magnetoelectricity, ME effect, multiferroic, magnetostriction, piezoelectricity

---

## Introduction

Magnetoelectric (ME) materials become magnetized when placed in an electric field and electrically polarized when placed in a magnetic field. The history of the ME effect dates back to as early as 1894, when Curie stated that it would be possible for an asymmetric molecular body to polarize directionally under the influence of a magnetic field [1]. Later, Landau and Lifshitz [2] showed from symmetry considerations that a linear ME can predicted the existence of the ME effect in antiferromagnetic Cr<sub>2</sub>O<sub>3</sub>. This was confirmed by Astrov [4] by measuring the electric field induced magnetization and later by Rado and Folen [5] by detection of the magnetic field-induced polarization. The primary requirement for the observance of this effect is the coexistence of magnetic and electric dipoles. Materials exhibiting the ME effect can be classified into two classes: single phase and composites.

Single phase materials exhibiting the ME effect have an ordered structure and require the presence of a ferroelectric/ferrielectric/antiferroelectric state. These materials should show two transitions—one from a ferroelectric to a paraelectric state and the other from a ferromagnetic/ferrimagnetic/antiferromagnetic to a paramagnetic state. The ME effect arises due to the local interaction between the ordered magnetic and ferroelectric sublattices. The conditions for the occurrence of ferroelectricity and magnetic order in the same material often accompanied by ferroelasticity implies (a) the presence of adequate structural building blocks permitting ferroelectric-type ionic movements, (b) magnetic-interaction pathways, usually of the superexchange type, and (c) the fulfillment of symmetry conditions [6].

The achievable magnitude of the magnetoelectric voltage coefficient in the single phase materials is of the order of 1–20 mV/cm·Oe, which is not sufficient for practical applications. Another limitation on the usage of these materials is the working range of temperature. Most of the single phase materials can be used only at very low temperatures, involve expensive materials and processing technique and suffer from degradation under cyclic conditions. In the last few decades, the ME effect has been found in numerous compounds [3, 7–23].

The solution to these limitations was offered by shifting to composites. In composite materials, the ME effect is realized by using the concept of product properties introduced by Van Suchetelene [24]. A suitable combination of two phases can yield the desirable property such as a combination of piezomagnetic and piezoelectric phases.

Most ferromagnetic materials show the magnetostrictive effect, however, piezomagnetic effect in these materials has not been observed. This means that the strain caused by a magnetic field in these materials is not linearly proportional to the field strength but is related to the square of the magnetic field strength. This makes the product property, the magnetoelectric effect in the piezoelectric-magnetostrictive composites, a non-linear effect unlike the single phase materials where the magnetoelectric effect is a linear one over a wide range of the values of the magnetic or electric field. Also the magnetoelectric effect in these composites shows a hysteretic behaviour. This makes the applications of such composites difficult in linear devices. The ME effect obtained in composites can be more a hundred times than that of single-phase ME materials such as  $\text{Cr}_2\text{O}_3$ .

In this paper, examples of the magnetoelectric effect found in single phase materials as well as in composites or layer structures will be given. Additionally methods suitable for measuring the magnetoelectric effects will be described.



## Single phase materials

According to a theoretical investigation of Fuentes [25], a quantitative Texture Analysis procedures for characterization of polycrystal pyromagnetic, magnetoelectric and piezomagnetic effects was proposed. The considered phenomena link the thermic, electric and elastic subsystems of a given body with its magnetic subsystem. According to his considerations the magnetoelectric coefficient can be defined as:

$$m_{ij}^{or} = \left( \frac{\partial D_i}{\partial H_j} \right)_{or} = \left( \frac{\partial H_i}{\partial E_j} \right)_{or}, \text{ magnetoelectricity (axial, } r = 2)$$

where  $\mathbf{D}$  is the electric displacement;  $\mathbf{E}$  the field intensity;  $\mathbf{B}$  the magnetic induction and  $\mathbf{H}$  the magnetic field intensity. These coefficients are in fact material's properties and therefore they are generally tensors of ranks  $r$ . This leads to Table 1 which resumes the possible electric and magnetic coupling effects in the 32 crystallographic point groups. In electric as well as in magnetic cases, pyro-susceptible materials are a sub-set of piezo-susceptible ones.

Table 1: Electric and magnetic coupling effect crystallographic point groups [25].

<b>Point group</b>								
Cryst. Syst.	Int	Sch	Type	PRE	PZE	PRM	PZM	ME
Triclinic	1	C <sub>1</sub>	e	+	+	+	+	+
	-1	C <sub>1</sub>	c			+	+	
Monoclinic	2	C <sub>2</sub>	e	+	+	+	+	+
	m	C <sub>2</sub>	nc-ne	+	+	+	+	+
	2/m	C <sub>2h</sub>	c			+	+	
Orthorombic	222	D <sub>1</sub>	e		+		+	+
	2mm	C <sub>2v</sub>	nc-ne	+	+		+	+
	mmm	D <sub>2h</sub>	c				+	
Tetragonal	4	C <sub>4</sub>	e	+	+	+	+	+
	-4	S <sub>1</sub>	nc-ne		+	+	+	+
	4/m	C <sub>4h</sub>	c			+	+	
	422	D <sub>1</sub>	e		+		+	+
	4mm	C <sub>4c</sub>	nc-ne	+	+		+	+

	-42m	D <sub>2d</sub>	nc-ne				+	+	+
	4/mmm	D <sub>4h</sub>	c					+	
Trigonal	3	C <sub>3</sub>	e	+	+	+		+	+
	-3	S <sub>6</sub>	c				+	+	
	32	D <sub>3</sub>	e				+	+	+
	3m	C <sub>3v</sub>	nc-ne	+	+			+	+
	-3m	D <sub>3d</sub>	c					+	
Hexagonal	6	C <sub>6</sub>	e	+	+	+		+	+
	-6	C <sub>3h</sub>	nc-ne				+	+	+
	6/m	C <sub>6h</sub>	c				+	+	
	622	D <sub>6</sub>	e				+	+	+
	6mm	C <sub>6v</sub>	nc-ne	+	+			+	+
	-6m2	D <sub>3h</sub>	nc-ne				+	+	
	6/mmm	D <sub>6h</sub>	c					+	
Cubic	23	T	e				+	+	+
	m3	T <sub>h</sub>	c					+	
	432	O	e						+
	-43m	T <sub>d</sub>	nc-ne				+		
	m3m	O <sub>h</sub>	c						

As an example, measurements of a polycrystalline ceramics of the composition Bi<sub>5</sub>Ti<sub>3</sub>FeO<sub>15</sub> were tested for ME effect. Fig.1 shows as an example the field dependence of the magnetoelectric coefficient of this compound [26]. The ME effect in the studied material is weak, but measurable. Hysteresis phenomenon is present. From the intercepts of the curves, an estimate of the longitudinal polycrystal ME coupling coefficient can be given:  $m \approx 7/0.61 \approx 11 \text{mVcm}^{-1} \cdot \text{Oe}^{-1}$ .

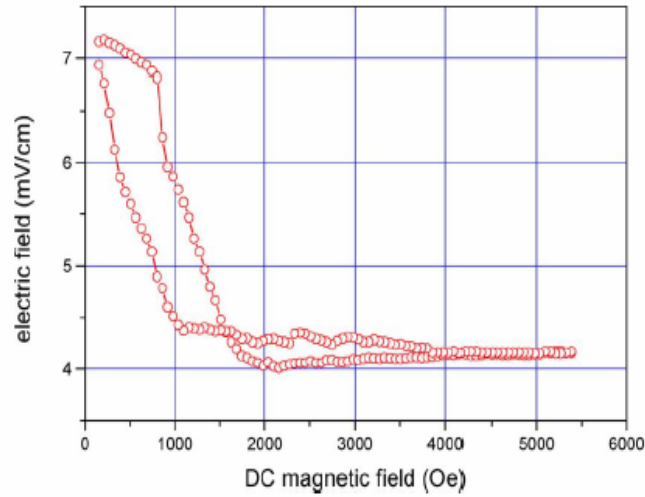


Fig. 1. ME effect in  $\text{Bi}_5\text{Ti}_3\text{FeO}_{15}$  ceramic. Static magnetic field in absciss determines the operating point. Alternating electric field in ordinates is the ME response to a superimposed ac magnetic field.

## Composites

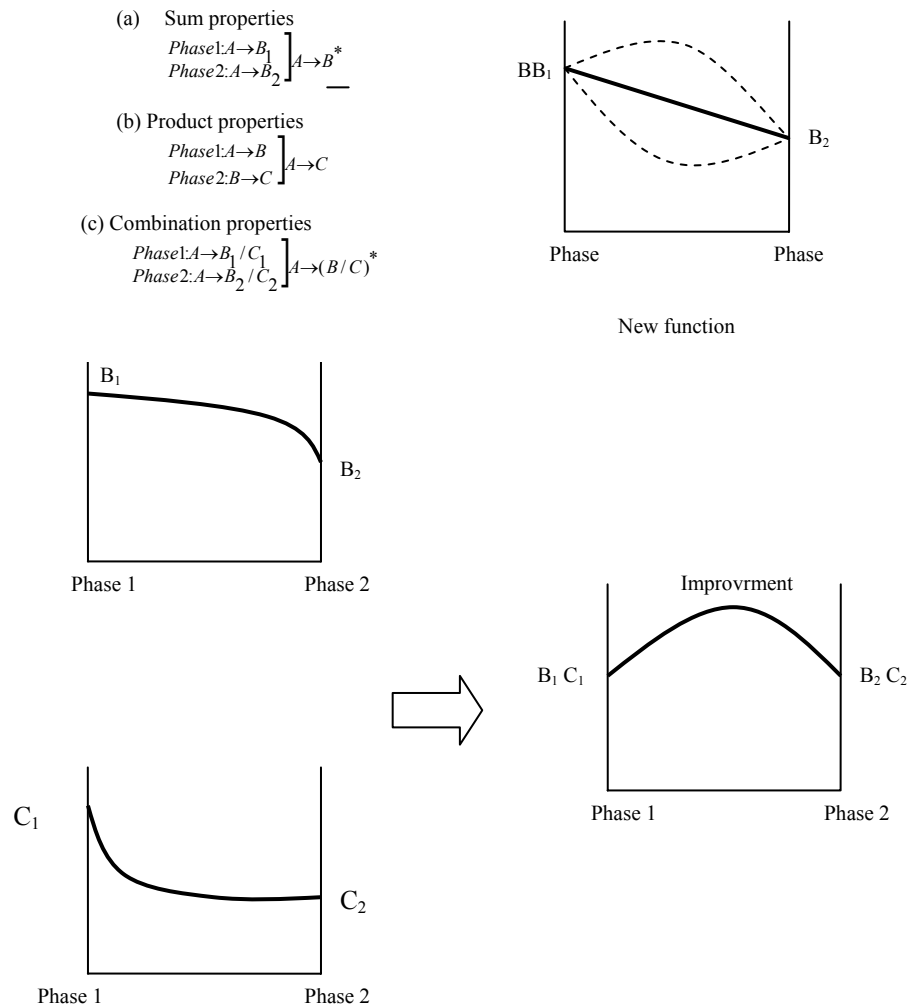


Fig. 2. Composite properties; (a) sum properties, (b) product properties, and (c) combination properties [29].

The basic ideas underlying composite electroceramics can be classified into three categories: (1) sum properties, (2) product properties, (3) combination properties [24, 27-28]. Fig. 2 shows a schematic representation of these properties of a composite [28]. Physical quantities like density and resistivity are sum properties. A more interesting result of a composite structure is the product property, which is reflected in the composite structure but is absent in the individual phases.

In 1978, Boomgaard [29] outlined the conceptual points inherent to the ME effect in composites. These can be summarized as (i) two individual phases should be in equilibrium (ii) mismatching between grains should not be present (iii) magnitude of the magnetostriction coefficient of piezomagnetic or magnetostrictive phase and magnitude of the piezoelectric coefficient of the piezoelectric phase must be greater (iv) accumulated charge must not leak through the piezomagnetic or magnetostrictive phase. But, as mentioned already, composites offer a much higher magnetoelectric coefficient and combining different materials opens many possibilities. A nowadays, often chosen ways are composites based on layers. An example is shown in Fig.3 which shows a sandwich structure between Terfenol-D (magnetostrictive component) and PZT (piezoelectric component) [30].

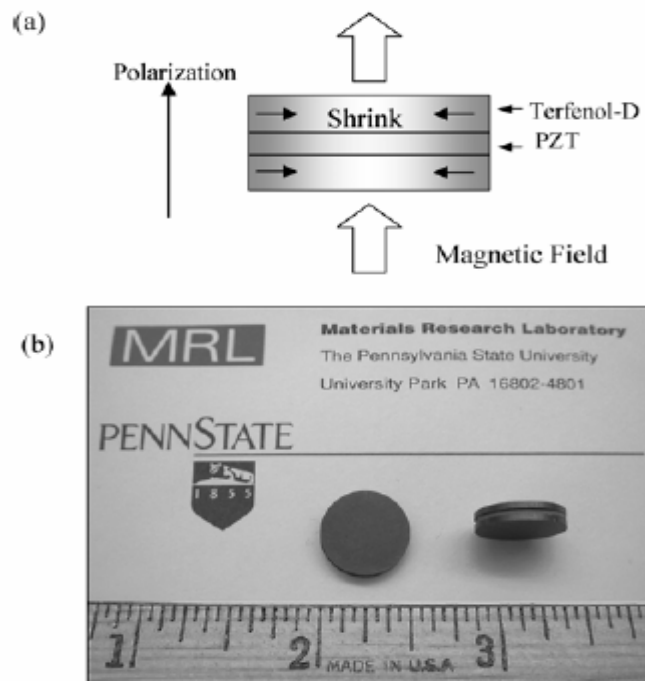


Fig. 3. ME laminate composite using Terfenol-D and PZT disks. (a) schematic structure, and (b) photograph of the device.

The value of the ME voltage coefficient  $dE/dH$  is proportional to  $m_v \times (dS/dH)_{\text{magneto}} \times (1 - m_v) \times (g_{33} C_{33})_{\text{piezo}}$ . Here  $m_v$  is the volume fraction of the magnetostrictive component;  $g_{33}$  and  $C_{33}$  are the piezoelectric voltage and stiffness coefficients, respectively, of the piezoelectric phase,  $T$  is the stress and  $S$  is the strain. Fig. 4 shows the ME-voltage coefficient variation as a function of the d.c. magnetic bias field with three different PZT types. Fig.4 shows very clear that the ME-voltage in the composite is much higher than in a single phase material.

Another interesting type of composite which was suggested from theoretical considerations is a composite which consists of small grains of magnetostrictive compounds such as  $\text{REFe}_2$  ( $\text{RE} = \text{Sm, Tb, \dots}$ ) filled into a ferroelectric polymer matrix [31] – see Fig. 5. A very high magnetoelectric effect was predicted for this type of composite.

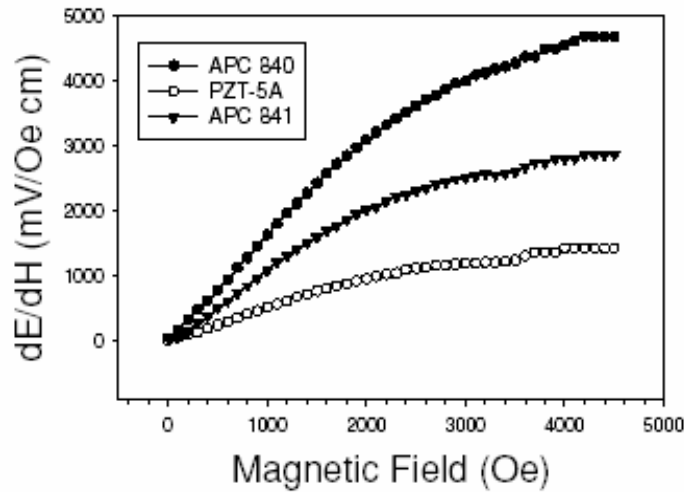


Fig. 4. ME voltage coefficient as a function of applied d.c. magnetic bias field for various PZT disks (APC 840 for high  $g_{33}$ , PZT-5A for high  $d_{33}$ , APC 841 for high  $Q_m$ ) at 1 kHz.

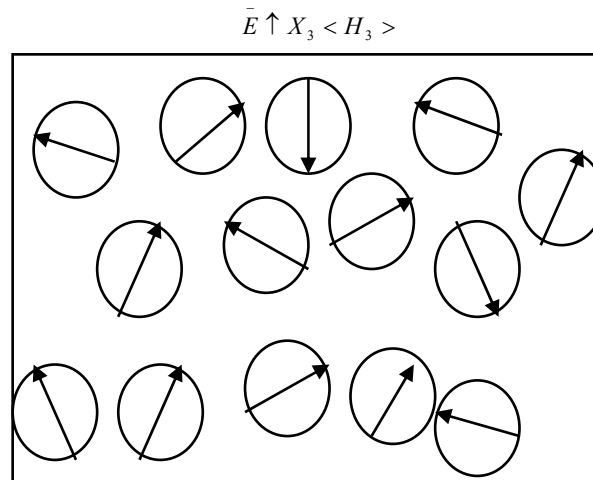


Fig. 5. Schematic illustration of the Terfenol-D particles (denoted by the circles with the arrows representing their orientations) filled P(VDF-TrFE) matrix composite. The polarization direction in the P(VDF-TrFE) is parallel to  $X_3$  axis of the composite, along which an external

Special measuring methods have to be developed for determining the magnetoelectric coefficient. The general method looks as follows: applying a dc-field  $H_0$  allows choosing any working point in the magnetization of the magnetic (magnetostrictive) material; the sample has the thickness  $d$ . This causes at this point some magnetostriction  $\lambda(H_0)$ , which causes a corresponding stress. In the magnetoelectric materials, this stress couples to the piezoelectric component which transfers the stress into a charge. Generally, the exact measurement of charges is difficult. Therefore an ac-method was chosen. Applying now a small ac-field  $h_0$  with a pair of Helmholtz coils causes a small periodically varying charge and consequently a voltage which can be measured with a lock-in amplifier. Fig.6 shows the set-up of such a measuring device as used in our laboratory.

The lock-in amplifier measured voltage,  $V_{out}$ , is proportional to the magneto-electric coefficient:

$$\frac{dE}{dH_0} = \frac{V_{out}}{h_0 d} = \frac{1}{d} \frac{dV}{dH_0}$$

Going over a larger field range delivers naturally contributions which represent the magnetization curve of the magnetostrictive materials. Generally the voltage  $V_{out}$  can then be described by:

$$V_{out} = h_0 (\alpha + 2\beta H_0 + 3\gamma H_0^2 + 4\delta H_0^3 + \dots)$$

In order to demonstrate how this method works, measurements on a sample of 50%CoFe<sub>2</sub>O<sub>4</sub>-50%BaTiO<sub>3</sub> were performed.

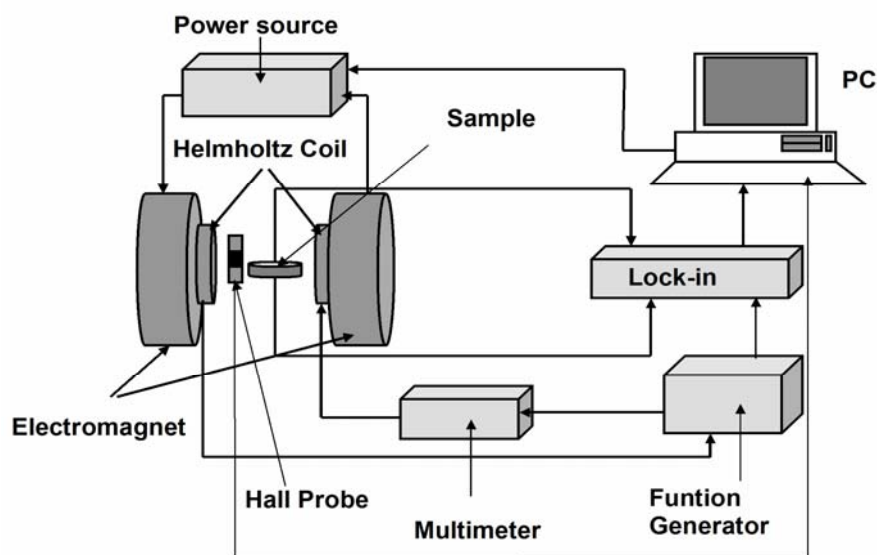


Fig.6. Setup for measuring the magneto-electric coefficient in a constant dc-field produced by an electromagnet. The magneto-electric voltage is measured by the lock-in amplifier.

Barium titanate is a piezoelectric material bellow the  $T_C = 130^\circ\text{C}$ . It has a centrosymmetric perovskite cubic structure above  $T_C$  and a tetragonal non-centrosymmetric bellow  $T_C$ . The longitudinal strain piezoelectric coefficient is  $1.9 \times 10^{-8}$  cm/V. Cobalt ferrite is a magnetostrictive material bellow  $T_C = 520^\circ\text{C}$ . It has a spinel cubic structure. The magnetostriction constant is  $\lambda = -120 \cdot 10^{-6}$

The powders of  $\text{BaTiO}_3$  and  $\text{CoFe}_2\text{O}_4$  were mixed in different proportions and pressed into disk shape of 1.2 cm in diameter and 0.12 in thickness. The disk samples were sintered, electrically poled at  $150^\circ\text{C}$  down to room temperature for 1 hour in an electric field of 5 kV/cm. The disk faces were covered with silver paste for ohmic contacts.

A pulsed field measurement determining the magnetostriction of  $\text{CoFe}_2\text{O}_4$  at room temperature is shown in Fig.7. The measurement was performed using standard strain gauges. In order to demonstrate the measurement of the magneto-electric effect, a room temperature measurement performed on a composite sample of 50%  $\text{BaTiO}_3$ -50% $\text{CoFe}_2\text{O}_4$  is shown in Fig. 8.

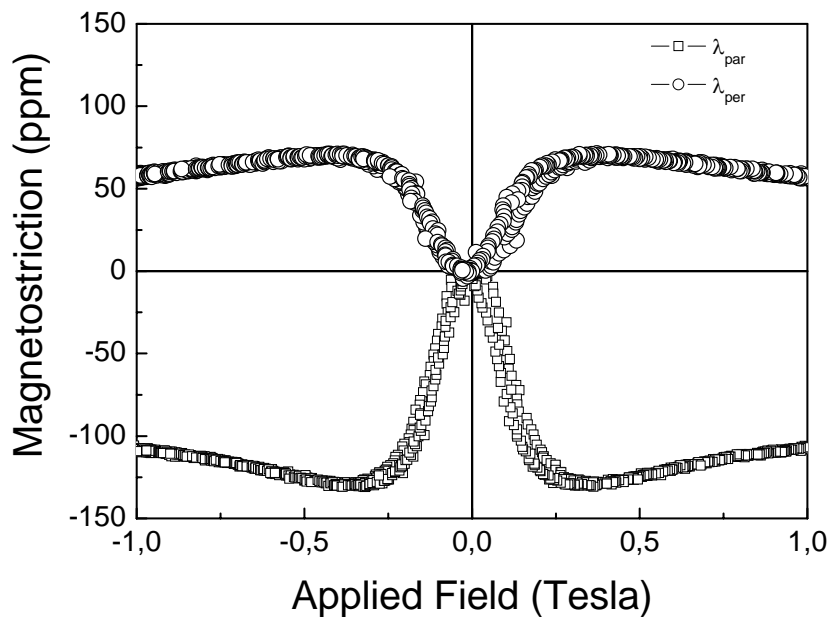


Fig.7. Room temperature parallel and perpendicular magnetostriction,  $\lambda_{\text{par}}$  and  $\lambda_{\text{per}}$ , of polycrystalline  $\text{CoFe}_2\text{O}_4$ .

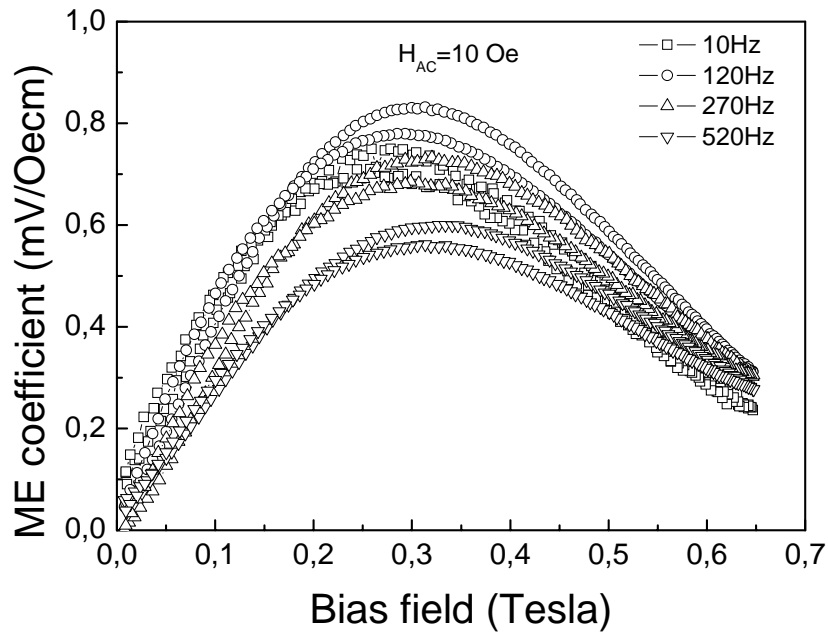


Fig. 8: ME coefficient measured at room temperature on a composite of 50%CoFe<sub>2</sub>O<sub>4</sub>-50% BaTiO<sub>3</sub> (in mass) as function of the bias field under an AC field of 10 Oe at different frequencies.

## Summary

Composites with a high magnetoelectric effect (especially at room temperature) have to be developed. For this purpose compounds with high magnetostriction and high quality piezoelectric materials have to be brought together in a way that a suitable composite is formed. Very important is here the microstructure of the composite which determines the coupling between the components. The microstructure can be adjusted by the technology (heat treatment, application of field etc.) Additionally a deeper understanding of the measurement methods is necessary. Especially dynamic methods have to be developed in order to investigate the time behaviour of the effect.

## References

- [1] P. Curie, J. Physique 3e series, 3 (1894), 393.
- [2] L.D. Landau and E. Lifshitz, Electrodynamics of ContinuousMedia (Addison-Wesley: Translation of a Russian edition of 1958), (1960).
- [3] I.E. Dzyaloshinskii, Sov. Phys.—JETP, 37 (1960), 628.



- [4] D.N. Astrov, *Sov. Phys.—JETP*, 11 (1960) 708.
- [5] G.T. Rado and V.J. Folen, *Phys. Rev. Lett.*, 7 (1961), 310.
- [6] H. Schmid, *Bull. Mater. Sci.*, 17 (1994), 1411.
- [7] T.H. O'Dell, *Electronics and Power*, 11 (1965), 266.
- [8] D.N. Astrov, *Soviet Phys.—JETP*, 13 (1961), 729.
- [9] R.M. Hornreich, *Sol. State Comm.*, 7 (1969), 1081.
- [10] R.M. Hornreich, *J. Appl. Phys.*, 41 (1970), 950.
- [11] E. Fischer, G. Gorodetsky, and R.M. Hornreich, *Sol. StateComm.*, 10 (1972), 1127.
- [12] V.J. Folen, G.T. Rado, and E.W. Stalder, *Phys. Rev. Lett.*, 6 (1961), 607.
- [13] S. Foner and M. Hanabusa, *J. Appl. Phys.*, 34 (1963), 1246.
- [14] L.M. Holmes, L.G. van Uitert, and G.W. Hull, *Sol. State Comm.*, 9 (1971), 1373.
- [15] R.M. Hornreich, *IEEE Trans. Magn.*, MAG-8 (1972), 582.
- [16] R.M. Hornreich, in *Proc. of Symposium on Magnetoelectric Interaction Phenomena in Crystals*, Seattle, May 21–24, 1973, edited by A. Freeman and A. Schmid (Gordon and Breach Science Publishers, New York, 1975), p. 211.
- [17] R.M. Hornreich and S. Shtrikman, *Phys. Rev.*, 161 (1967), 506.
- [18] T.J. Martin and J.C. Anderson, *Phys. Lett.*, 11 (1964), 109.
- [19] T.J. Martin and J.C. Anderson, *IEEE Trans. Magn.*, MAG-2 (1966), 446.
- [20] M. Mercier, in *Proc. of Symposium on Magnetoelectric Interaction Phenomena in Crystals*, Seattle, May 21–24, 1973, edited by A. Freeman and A. Schmid (Gordon and Breach Science Publishers, New York, 1975), p. 99.
- [21] S. Alexander and S. Shtrikman, *Sol. State Comm.*, 4 (1966), 115.
- [22] R.M. Hornreich, *IEEE Trans. Magn.*, MAG-8 (1972), 582.
- [23] R. M. Hornreich and S. Shtrikman, *Phys. Rev.*, 161 (1967), 506.
- [24] J. Van Suchetelene, *Philips Res. Rep.*, 27 (1972), 28.
- [25] L.Fuentes, *Textures and Microstructures* 30 (1998), 167-189.
- [26] L. Fuentes, M. Garcia, J. Matutes-Aquino, D. Rios-Jara; *Journal of Alloys and Compounds* 369 (2004) 10–13.
- [27] R.E. Newnham, *Ferroelectrics*, 68 (1/4) (1986) 1.
- [28] K. Uchino, *Ferroelectric Devices* (Marcel Dekker, New York, 2000), p. 255.
- [29] J. van den Boomgaard and R.A.J. Born, *J. Mater. Sci.*, 13 (1978), 1538.
- [30] Jungho-Ryu, Shashankprya, Kenjiuchinoi, Hyoun-ee Kim, *Journal of Electroceramics*, 8 (2002), 107-119.
- [31] Ce Wen Nan, Ming Li, Xiqiao Feng, Shouwen Yu; *Appl. Phys. Lett.* 78 (2001) 2527.

# Magnetoelectric composites: An overview

Giap V. Duong<sup>1,2,\*</sup>, R.Grössinger<sup>1</sup>

<sup>1</sup>*Institute of Solid State Physics, T.U. Wien, Wiedner Hauptstr. 8-10; A-1040 Vienna, Austria*

<sup>2</sup>*Faculty of Chemical Engineering, Hanoi Uni. Techn., No.1 Dai Co Viet, Hanoi, Vietnam*

To be submitted for publication

---

## Abstract

This paper will give an overview about most important aspects concerning the study of magnetoelectric effect in composites. With intention of giving a wide spectrum of information, it starts with some basic concepts, then follows the development of most important branches of the field, including the sample preparation, measuring techniques, theoretical models and potential applications.

© 2006 Elsevier B.V. All rights reserved

PACS: 75.80.+q; 77.65.-j; 77.84.Lf

Keywords: Magnetoelectric effect, magnetoelectric composite, multiferroics, magnetostriction, piezoelectricity

---

## 1. Introduction

The magnetoelectric effect (ME) is the induction of electric polarization by means of a magnetic field and the induction of magnetization by means of an electric field. In matter, it describes the coupling between electric and magnetic fields. The history of the ME effect started around the last decade of the 19<sup>th</sup> century when Röntgen discovered the electric-field-induced magnetization of a moving dielectric (1888) [1]. The reverse effect, the magnetic-field-induced polarization, was discovered later by Wilson (1905) [2]. Another event which

marked the birth of ME effect was in 1894 when Curie pointed out that it would be possible for an asymmetric molecular body to polarize directionally under the influence of a magnetic field [3]. However, the first experimental observation of the ME effect was much later, in 1960, when Astrov found the electric-field-induced magnetization in Cr<sub>2</sub>O<sub>3</sub> [4, 5]. One year later, the reverse effect in the same system was observed by Rado *et al* [6, 7].

Differently from the history of the ME effect in single phase materials, the ME effect in composite starts much later in the year 1972 when Van Suchetelene introduced the concept of “product properties” and used it to grow successfully the first magnetoelectric composite by unidirectional solidification of a BaTiO<sub>3</sub>-CoFe<sub>2</sub>O<sub>4</sub> eutectic liquid [8]. The product properties refer to those present in the composite, but absent in none of its constituents. For ME composite, the combination of magnetostrictive and piezoelectric materials produces the ME effect which does not exist in either magnetostrictive or piezoelectric phase. The reason is: under a magnetic field, the magnetostrictive constituent will change its length according to the so-called magnetostriction, and this change in length of the magnetostrictive phase is passed into the piezoelectric phase which then causes a stress and produces electric polarization. In a rough description, the ME effect in composite can be written as [9-11]:

$$\underbrace{ME\ effect}_{composite} = \underbrace{\frac{electrical}{mechanical}}_{piezoelectric\ phase} \times \underbrace{\frac{mechanical}{magnetic}}_{magnetostrictive\ phase} \quad (1)$$

However, recently it is found that the origin of the ME effect in composite may be not only due to only the mechanical coupling between the magnetostrictive and piezoelectric phases, but perhaps also due to the direct coupling between magnetic and electric moments [12-13]. If this is true, it will open up a new trend in the study of the ME effect in composites, since it allows to obtain materials which exhibit the intrinsic ME effect like the case of single phase materials, but at room temperature and probably higher order of magnitude.

The scope of this paper is systematically to review the development of the study of the ME effect in composites, ranging from its early time to recent achievements, focusing on most important fundamental and practical aspects of the field, such as: the sample preparation; the measuring techniques; compounds, structure and magnitude; the theory of ME effect in composites, and to point out the open questions and unsolved problems as possible future directions in the development of the field.

## 2. Requirements for ME composite

The requirements for the existence of the ME effect in general is the coexistence of ordered magnetic and electric dipoles. In single phase materials, the coexistence of these two kinds of moments is found due to the importance of the in multiferroic compounds involved 3d-electrons be almost chemically incompatible [14]. This explains why only few materials exhibit the ME effect. In composites, the situation is much easier since the magnetic and electric moments can be introduced into the system by different phases. However, to ensure the ME effect, the composites have to fulfill some requirements which can be summarized as follow [10, 15]: i) mechanical defect and mismatching between grains should not be present, ii) the sample resistivity should be high to prevent the discharging process and to avoid eddy currents in dynamic applications, iii) the magnetostrictive and piezoelectric coefficients of the constituent should be high, iv) the composite should be poled electrically in a proper way.

## 3. Sample preparation

### 3.1 Solid state reaction

Most of the ME composites are prepared by solid state reaction, or conventional ceramics method in the other name. The preparation procedure consists of mixing the initial materials, pressing the powder into pellet and sintering them at high temperature, from 800 to 1300 °C, for 1 to 24 hours, depending on particular system. The samples can also be ground into powders again and the procedure is repeated for several times to get a complete reaction between initial materials or homogenous distribution between constituents. The advantage of this method is: simple, cheap and free choice of the composition of the constituents. Using this method, a large amount of ME composites have been prepared. Examples are:  $\text{CoFe}_2\text{O}_4/\text{PZT}$  [16],  $\text{Ni}_{0.75}\text{Co}_{0.25}\text{Fe}_2\text{O}_4+\text{Ba}_{0.8}\text{Pb}_{0.2}\text{TiO}_3$  [17],  $\text{Ni}_{0.75}\text{Co}_{0.25}\text{Fe}_2\text{O}_4/\text{Ba}_{0.8}\text{Pb}_{0.2}\text{TiO}_3$  [18],  $\text{CuFe}_{1.8}\text{Cr}_{0.2}\text{O}_4-\text{Ba}_{0.8}\text{Pb}_{0.2}\text{Ti}_{0.8}\text{Zr}_{0.2}\text{O}_3$  [19], etc. However, the composites prepared by this method usually give a lower ME coefficient compared to those similar prepared by other methods [20].

### 3.2 Solidification from eutectic liquid

The solidification from eutectic liquid method is for the first time used by Van Suchetelene [8], and then by van den Boomgaard *et al* [21-22]. This method gives the highest ME coefficients for the cobalt ferrite/barium titanate system, reaching 130 mV/cmOe for the  $(\text{BaTiO}_3)_{0.61}-((\text{CoFe}_2\text{O}_4)_{0.47}-(\text{CoTiO}_4)_{0.53})_{0.39}$  system and 1-4 mV/cmOe for other compositions. The disadvantage of this method is: the difficulty in controlling the composition of the system since the initial materials have to be chosen in a proper ratio to give the eutectic composition and the chemical reaction between constituents due to high temperature is used to melt the initial materials.

### 3.3 Spark plasma method

The spark plasma method is used to prepare mixed structure system of  $\text{BaFe}_2\text{O}_4/\text{PZT-5A}$  and  $\text{NiFe}_2\text{O}_4/\text{PZT-5A}$  magnetoelectric composites [23]. These composites have a ME coefficient of about 20 mV/cmOe. Due to the vacuum and the high pressure, high temperature, this method allows to prepare composites with very high density, reaching 99% of the theoretical value [23].

### 3.4 Wet chemical method

Wet chemical method can be used to prepare ME composites with a complex structure such as core-shell structure. Using this method, the  $\text{CoFe}_2\text{O}_4-\text{BaTiO}_3$  system with either  $\text{CoFe}_2\text{O}_4$  or  $\text{BaTiO}_3$  in core has been successfully prepared. It is found that, the core-shell structure composite prepared by wet chemical method gives the highest ME coefficient which is of about 20 times higher compared to those similar sample prepared by the conventional ceramics method [20, 24]. The schema illustrating the preparation procedure of this core-shell structure composite is shown in Fig.1 bellow.

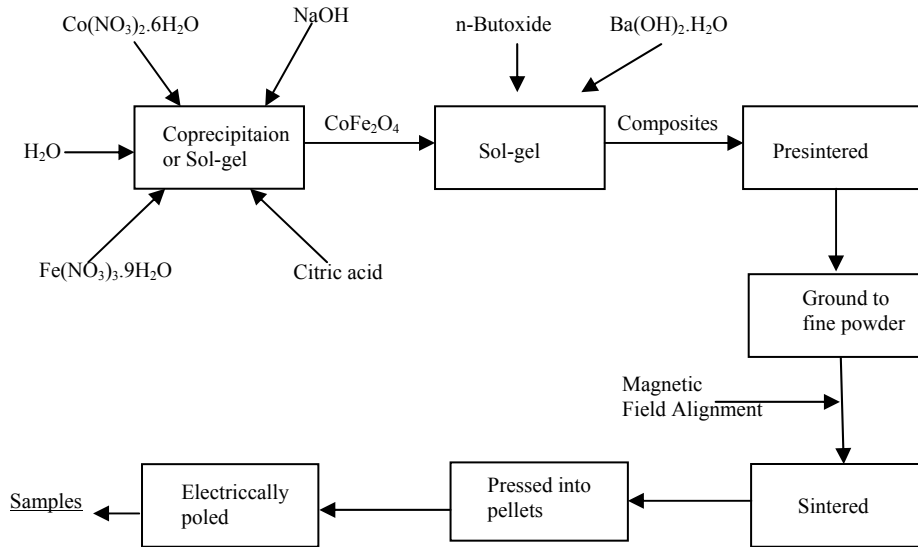


Fig.1. Schema of the procedure for preparing the  $\text{CoFe}_2\text{O}_4\text{-BaTiO}_3$  core-shell structure composite.

### 3.5 Tape casting method

The doctor-blade or tape casting methods is used to prepare multilayer structure ME composites. The initial materials in the form of fine powders, together with solvent and binder, are taped on the moving substrate using doctor-blade technique [25]. Using this method, multilayer ME composites such as  $\text{Ni}_{0.8}\text{Zn}_{0.2}\text{Fe}_2\text{O}_4/\text{PZT}$ ,  $\text{La}_{0.7}\text{Ca}_{0.3}\text{MnO}_3/\text{PZT}$  [26],  $\text{Ni}_{0.9}\text{Zn}_{0.1}\text{Fe}_2\text{O}_4/\text{PbZr}_{0.52}\text{Ti}_{0.48}\text{O}_3$  [27], etc., have been prepared. The ME effect in this kind of multilayer composite is found to be one order of magnitude bigger than those of the similar bulk samples [25].

### 3.6 Hot moulding method

The hot moulding method involves the pressing of the initial powders or mixtures of initial powders with plasticizers or binders into stark layers at elevated temperature. Using this method, an assemble composites of  $\text{PZT}/\text{Terfenol-D}/\text{PZT}$  with poly vinylidene fluoride (PVDF) as binder was produced [28, 29]. The ME coefficients of this composite is about 10-15 mV/cmOe measured at non-resonant conditions.

### *3.7 Stacking method*

The stacking method is used to make multilayer ME composite from separate magnetostrictive and piezoelectric disk. The disks are stacked by epoxy glue, then annealed at low temperature to ensure the bonding between them. Using this method, laminated ME composites of PZT and Terfenol-D which has the highest value of ME coefficient, up to 4.68 V/cmOe has been achieved [11].

The preparation method seems to affect strongly the ME properties of the composites. However, it would be worth to remind that the difference in sample composition, sample microstructure, measuring conditions and measuring techniques make the comparison between reported results very difficult as discussed in details later.

## **4. Measuring methods**

### *4.1 Dynamic method*

The ME effect in composites until now is measured mainly by an AC-method, in which a small AC field is superimposed onto a DC bias field and the ME voltage is measured by means of a lock-in amplifier. This voltage is found to be proportional to the amplitude of the AC field, establishing an analogy to the linear ME effect in single phase materials. In some cases, the ME voltage is measured directly across the sample by the lock-in amplifier, and in other cases, a charge amplifier is used to measure the charge, and its output voltage is measured by the lock-in amplifier. This may cause different results since the charge amplifier will integrate all charges before producing an output voltage whereas a differential preamplifier within the lock-in amplifier does not.

If the voltage due to the ME effect is measured directly across the sample, the magnitude of this voltage is proportional to the charge generated by the ME effect. If a charge sensitive amplifier is used the charge is measured directly. In any case the signal depends on the internal resistance of the sample as well as on the used ac frequency

It is worth to remind that the measuring technique, even for this frequently used dynamic method, is not well established yet, i.e. a commercial measuring system is not available. On the other hand, the measuring conditions also affect seriously the amplitude of

the ME coefficient, e.g. the ME coefficient can be measured at (mechanical) resonance and non-resonance conditions. This gives ME values which differ orders of magnitude. This makes any comparison between reported results from different groups, even on the same sample but measured by different techniques or at different conditions, very difficult. The theory of the dynamic method using lock-in amplifier can be briefly described as follow:

When magnetoelectric materials exposed to a magnetic field  $H$ , a voltage  $V$  appears. Assuming:

$$V = f(H) = Const . + \alpha H + \beta H^2 + \gamma H^3 + \delta H^4 + \dots \quad (2)$$

$$\Rightarrow \frac{dV}{dH} = \alpha + 2\beta H + 3\gamma H^2 + 4\delta H^3 + \dots \quad (3)$$

When a small AC field  $h = h_0 \sin \omega t$  superimposed onto a DC bias field  $H$ , the total field:  $H_{total} = H + h_0 \sin \omega t$ , then:

$$\begin{aligned} V &= Const + \alpha(H + h_0 \sin \omega t) + \beta(H + h_0 \sin \omega t)^2 + \gamma(H + h_0 \sin \omega t)^3 + \delta(H + h_0 \sin \omega t)^4 + \dots \\ &= \frac{1}{8} \left[ (Const + 4\beta h_0^2 + 3\delta h_0^4 + 8\alpha H + 12\gamma h_0^2 H + 8\beta H^2 + 24\delta h_0^2 H^2 + 8\gamma H^3 + 8\delta H^4) \right. \\ &\quad + (8\alpha h_0 + 6\gamma h_0^3 + 16\beta h_0 H + 24\delta h_0^3 H + 24\gamma h_0 H^2 + 32\delta h_0 H^3) \sin \omega t \\ &\quad \left. + (-4\beta h_0^2 - 4\delta h_0^4 - 12\gamma h_0^2 H - 24\delta h_0^2 H^2) \cos 2\omega t + (-2\gamma h_0^3 - 8\delta h_0^3 H) \sin 3\omega t + \delta h_0^4 \cos 4\omega t + \dots \right] \end{aligned} \quad (4)$$

The lock-in amplifier output voltage  $V_{out}$  is:

$$\begin{aligned} V_{out} &= \frac{1}{8} (8\alpha h_0 + 6\gamma h_0^3 + 16\beta h_0 H + 24\delta h_0^3 H + 24\gamma h_0 H^2 + 32\delta h_0 H^3) \\ &= \frac{H^4}{8} \left[ \frac{8\alpha}{H^3} \left( \frac{h_0}{H} \right) + \frac{6\gamma}{H} \left( \frac{h_0}{H} \right)^3 + \frac{16\beta}{H^2} \left( \frac{h_0}{H} \right) + 24\delta \left( \frac{h_0}{H} \right)^3 + \frac{24\gamma}{H} \left( \frac{h_0}{H} \right) + 32\delta \left( \frac{h_0}{H} \right) \right] \end{aligned} \quad (5)$$

Neglecting high order terms in  $\left( \frac{h_0}{H} \right)$  when  $\left( \frac{h_0}{H} \right) \ll 1$ , then:

$$V_{out} = \frac{H^4}{8} \left( \frac{8\alpha}{H^3} + \frac{16\beta}{H^2} + \frac{24\gamma}{H} + 32\delta \right) \left( \frac{h_0}{H} \right) = h_0 (\alpha + 2\beta H + 3\gamma H^2 + 4\delta H^3) = h_0 \left( \frac{dV}{dH} \right) \quad (6)$$

$$\Rightarrow ME \text{ coefficient} = \alpha_E = \frac{dE}{dH} = \frac{1}{d} \frac{dV}{dH} = \frac{V_{out}}{h_0 \times d} \quad (7)$$

where  $d$  is the effective thickness of the sample.

Fig.2 shows a block diagram of the experimental set up of the dynamic method using lock-in technique without [30] charge amplifier used in our laboratory.



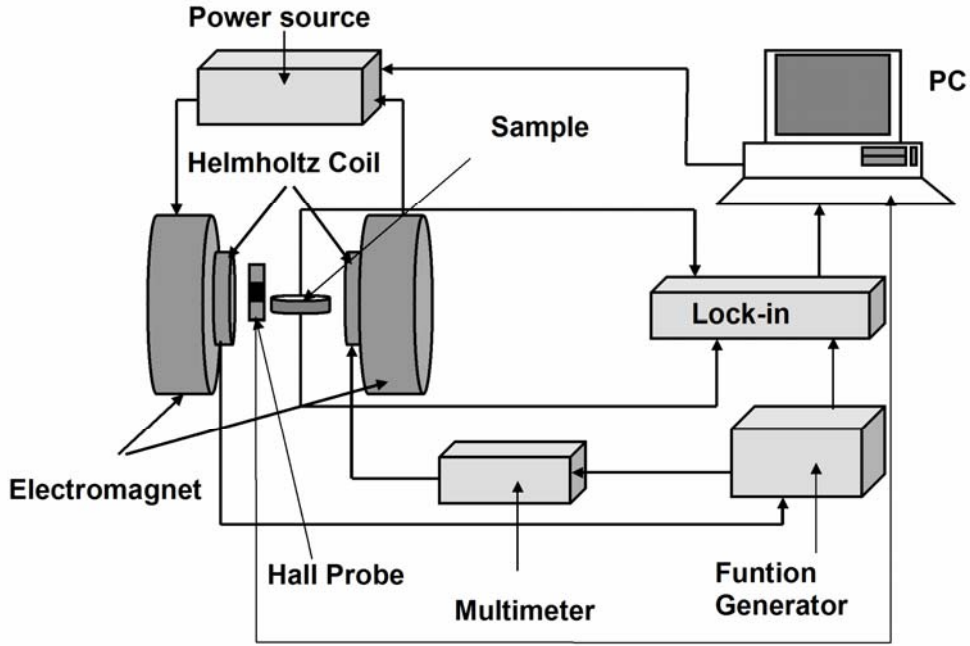


Fig.2. Block diagram of the experimental set-up of the dynamic method using lock-in technique without charge amplifier [30].

#### 4.2 Pulse field method

The magnetic pulse field is a new method which can be used to study the ME effect in composites [31-32]. By applying a magnetic field pulse instead of an AC field, it is claimed that the spectroscopic and dynamic characteristics of the ME effect can be studied within one experimental set-up [32]. The method is based on the excitation of the ME composite with a short magnetic field pulse, followed by the signal registration and a Fourier analysis of the ME response signal. This analysis can give the frequency dependence of the ME signal up to 800 kHz [32].

Another way of using magnetic pulse field to study the ME effect is to measure directly the ME signal across the sample when it is exposed to the magnetic pulse. Using the differential mode of the preamplifier, any induction voltage can be avoided. The ME coefficient is obtained using the equation:

$$ME \text{ coefficient } t = \alpha_E = \frac{V}{d \times H} \quad (8)$$

where  $V$ ,  $d$ ,  $H$  are the ME voltage, the effective thickness of the sample and the applied magnetic field.

Fig.3 below shows a block diagram of the experimental set-up of this direct pulse method used in our laboratory.

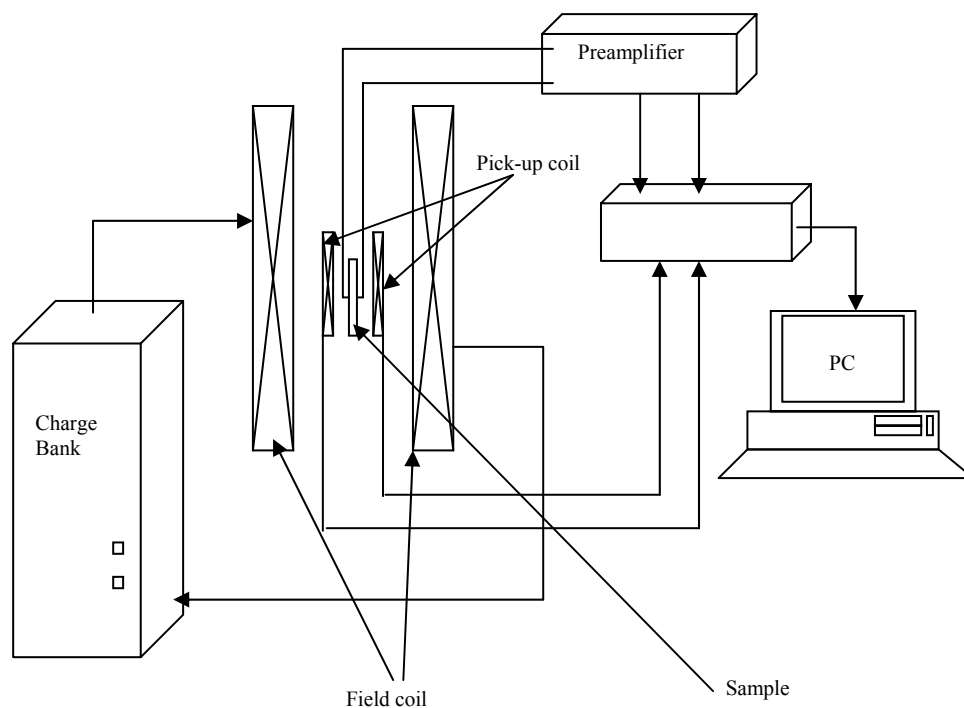


Fig.3. Block diagram of the experimental set-up of the direct magnetic pulse field method.

## 5. Compounds, structures and magnitude

Due to the requirement of a high electrical resistivity to prevent the discharging process, the ME composites are mainly composed by oxides if they are in the form of particulate composite or metallic materials separated by oxide layer if they are in the form of laminated or multilayer ones. The piezoelectric constituents, including lead zirconium titanate (PZT) and barium titanate ( $\text{BaTiO}_3$ ) and their metal-doped derivatives, are usually oxides. Therefore, the problem of high resistivity lays on the magnetostrictive constituents. Usually, the magnetic constituents are ferrites, manganites and their metal-doped derivatives if the composite is in the particulate form. However, due to their low value of magnetostriction, the ME coefficient in these composites is quite low. In laminated or multilayer form, due to the ability to be separated by piezoelectric insulating layer, the magnetic constituents can be metallic. Preference is given to Terfenol-D since it has a very high value of magnetostriction, up to 1500 ppm at room temperature.

### 5.1 Particulate composite

The first synthesized ME composite is in the form the particulate system of cobalt ferrite/barium titanate obtained from the liquid of eutectic composition by unidirectional solidification by Van Suchetelene in Phillips Research Laboratories in 1972 [8]. The ME coefficient depends on the composition, reaching a maximum value of 130 mV/cmOe for a  $(\text{BaTiO}_3)_{0.61}-((\text{CoFe}_2\text{O}_4)_{0.47}-((\text{CoTiO}_4)_{0.53}))_{0.39}$  composite when measured under resonance condition, but varies from 1-4 mV/cmOe for other compositions. Soon after the success of synthesizing the first composite, researchers in the same lab have synthesized and studied different cobalt and nickel ferrite/barium titanate systems:  $\text{CoO}-\text{Fe}_2\text{O}_3-\text{BaO}-\text{TiO}_3$  in eutectic composition by unidirectional solidification from liquid and  $\text{Ni}(\text{Co, Mn})\text{Fe}_2\text{O}_4-\text{BaTiO}_3$  from initial oxides by ceramics method. The maximum value for the nickel ferrite/barium titanate system is 80 mV/cmOe. The researchers also found that excess of a small amount of  $\text{TiO}_2$ , the poling procedure, the grain size of the constituents and the composition affect seriously the ME coefficient.

As mentioned above, the maximum ME coefficient for the  $\text{CoFe}_2\text{O}_3-\text{BaTiO}_3$  system is 130 mV/cmOe at resonance condition achieved already in the earliest experiments. However, for the same system prepared by a very similar procedure, the ME coefficient measured by the dynamic method is only 3-5 mV/cmOe [33], or even worse, 0.2 mV/cmOe if the composite is prepared by conventional ceramics method [34]. The effect of using different measuring technique and sample conditions as discussed above makes any comparison concerning the highest value of the ME coefficient for a particular composite difficult, and in some way impossible.

Beside barium titanate as piezoelectric component in the early time, the recent preference is the PZT as it has larger piezoelectric coefficient and commercial availability [16, 35-36]. The highest ME coefficient in this ferrite/PZT particulate composite is about 100 mV/cmOe [11]. However, the PZT component is usually used in the multilayer structure due to the evaporation of lead at high temperature preventing its use in particulate composites, which are generally sintered at high temperature during sample preparation.

Another main direction in the study of ME particulate composites is the metal-doped ferrite/titanate system. The doping occurs in both magnetostrictive and piezoelectric components. Examples are:  $(x)\text{BaTiO}_3+(1-x)\text{Ni}_{0.92}\text{Co}_{0.03}\text{Cu}_{0.05}\text{Fe}_2\text{O}_4$  [37],  $(x)\text{Ni}_{0.8}\text{Cu}_{0.2}\text{Fe}_2\text{O}_4+(1-x)\text{Ba}_{0.9}\text{Pb}_{0.1}\text{Ti}_{0.9}\text{Zr}_{0.1}\text{O}_3$  [38],  $\text{Ni}_{0.5}\text{Co}_{0.5}\text{Fe}_2\text{O}_4+\text{Ba}_{0.8}\text{Pb}_{0.2}\text{TiO}_3$  [39],  $\text{MnFe}_{1.8}\text{Cr}_{0.2}\text{O}_4-\text{BaTiO}_3$  [40], etc. The doping in titanate phase may enhance the ME effect

while the doping in ferrite phase usually weakens it. The difference in ME coefficient of doped and undoped sample may be one order of magnitude.

Choosing alternative magnetostrictive and piezoelectric constituents other than ferrite and titanate is also a new trend of the investigations in this field. The magnetostrictive component can be metal-doped rare-earth manganite such as  $\text{La}_{0.7}\text{Sr}_{0.3}\text{MnO}_3$ ,  $\text{La}_{0.7}\text{Ca}_{0.3}\text{MnO}_3$  [41] or Terfenol-D [42]. The piezoelectric phase can be polyvinylidene-fluoride [43],  $\text{PbMg}_{1/3}\text{V}_{2/3}\text{O}_3$  [44] and  $\text{PbX}_{1/3}\text{Nb}_{2/3}\text{O}_3\text{-PbTiO}_3$  ( $X = \text{Mg, Zn}$ ) [45]. The ME effect can be bigger in this case, especially when Terfenol-D is used. However, due to the low resistivity, Terfenol-D is preferred in laminated or multilayer structure.

## 5.2 Laminated composite

The ability of using a high magnetostrictive, up to 1500 ppm, but metallic component like Terfenol-D in the laminated composites helps to avoid the robust insulation problem and leads to a new family of ME composites. This started in 2001 when Ryu *et al* reported the high ME coefficient in laminar composite prepared by bonding the Terfenol-D and PZT disks [46-48]. With this laminar structure, not only the insulation problem, but also the reaction between the constituents during preparation is overcome. The highest ME coefficient of this Terfenol-D/PZT/Terfenol-D ME composite is 4.68 V/cmOe which is about 36 times higher than those of particulate composites[11]. This encourages several groups to focus on this type of composite and make it one of the most frequently studied systems [49-57]. Replacing PZT by  $\text{PbMg}_{1/2}\text{Nb}_{2/3}\text{O}_3\text{-PbTiO}_3$  single crystals, a system of sandwiched Terfenol-D disk between this two single crystal disks, the highest value of ME coefficient up to 10.3 V/cmOe has been achieved. Fig. 5 shows the ME coefficient as function of bias field for this laminar composite [58].

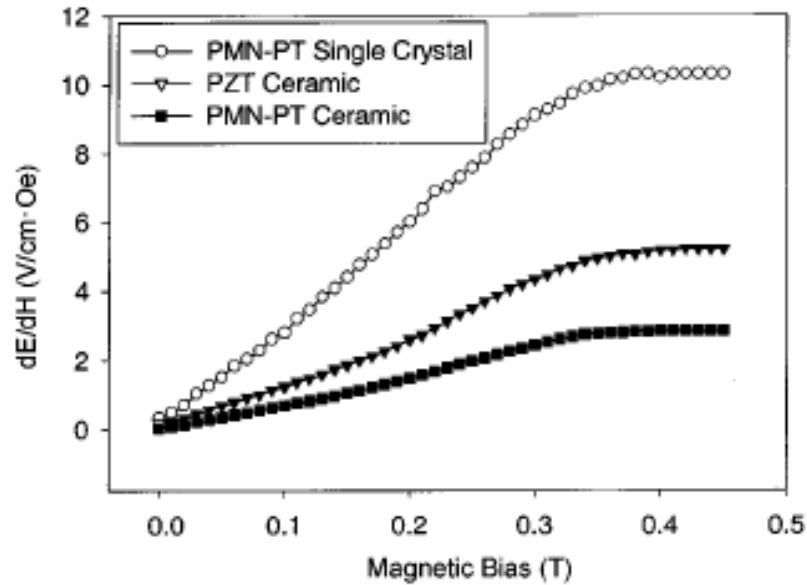


Fig. 4. ME voltage coefficient of laminate composites as a function of an applied dc magnetic bias field with different piezoelectric disks. Data are shown for PZT, PMN-PT ceramic and PMN-PT single crystal disks [58].

Beside the constituents, the stacking parameters such as the thickness ratio between the magnetostrictive and the piezoelectric layers, the bonding between layers and the geometric aspects, i.e. the direction of the sample surface with respect to the applied magnetic or electric field and the relative orientation between the intrinsic magnetization and polarization of the constituents, also affect strongly the ME properties of the composites. The magnitude of the ME signal depends strongly on the frequency of the AC field, in some cases even a resonant behaviour can be observed. The ME coefficient at resonant condition can be as 40 times higher than that of the normal one [42, 59-60]. Details will be skipped here since some excellent reviews on these aspects have been published elsewhere [10-11].

## 6. Theory of ME composites

### 6.1 Particulate composite

Some theoretical models for particulate composite have been reported in literature. In general, these models estimate the ME effect of the composite based on the physical properties and microstructure of the constituents, volume fraction, shape and connectivity of constituents. For the bulk composite of ferrite and barium titanate, assuming that: i) the

dielectric constant of BaTiO<sub>3</sub> is much larger than the dielectric constant of the ferrite, ii) the Young's modulus of both the phases are equal, iii) the coupling between the two phases is perfect, Van den Boomgaard *et al* has derived the ME coefficient as below [61]:

$$\left(\frac{dE}{dH}\right)_{composite} = \left(\frac{dx}{dH}\right)_{composite} \times \left(\frac{dE}{dx}\right)_{composite} = m_v \left(\frac{dx}{dH}\right)_{ferrite} \times \left(\frac{dE}{dx}\right)_{BaTiO_3} \quad (9)$$

where  $(dx/dH)$  is the change in dimension per unit magnetic field,  $(dE/dx)$  is the change in dimension per unit electric field and  $m_v$  is the volume fraction of ferrite. Using the maximum optimistic value of the parameters:

$$(dx/x)/dH = 5.10^{-7} (Oe^{-1}), \quad dE/(dx/x) = 2.10^9 (V/m), \quad m_v = 0.5,$$

the estimated maximum value of the ME coefficient is  $dE/dH = 5$  V/cmOe. This value is orders of magnitude bigger than the experimental value observed for this type of composites. Therefore, Zubkov has modified the expression as [62]:

$$\left(\frac{dE}{dH}\right)_{composite} = m_v \left(\frac{dx}{dH}\right)_{ferrite} \times (1 - m_v) \left(\frac{dE}{dx}\right)_{BaTiO_3}. \quad (10)$$

Since  $dE = dE_3 = g_{33}dT_3$  and  $dS = (dT_3)/C_{33}$  where  $g_{33}$  and  $C_{33}$  are the piezoelectric and stiffness coefficients of the piezoelectric phase, respectively,  $T$  is the stress and  $S$  is the strain, then:

$$\left(\frac{dE}{dH}\right)_{composite} = m_v \left(\frac{dx}{dH}\right)_{ferrite} \times (1 - m_v) (g_{33} \cdot C_{33})_{BaTiO_3}. \quad (11)$$

Using the above parameters, the ME coefficient is found to be 0.92 V/cmOe, still one order of magnitude bigger than the experimental value.

An expression that is believed to describe properly the ME effect in composite need at least six different variables describing the magnetic, electric and elastic properties. Nan *et al* uses this approach to describe the magnetoelctromechanical response of the ME composite as follow [9, 63]:

$$\begin{pmatrix} \sigma \\ D \\ B \end{pmatrix} = \begin{pmatrix} C & -e^T & -q^T \\ e & \varepsilon & \alpha \\ q & \alpha^T & \mu \end{pmatrix} \begin{pmatrix} s \\ E \\ H \end{pmatrix} \quad (12)$$

where  $\sigma$ ,  $s$ ,  $D$ ,  $E$ ,  $B$ ,  $H$ ,  $C$ ,  $\varepsilon$ ,  $\mu$ ,  $e$ ,  $q$  are the stress tensor, strain tensor, electric displacement, electric field intensity, magnetic induction, magnetic field intensity, stiffness tensor, dielectric permeability tensor, magnetic permeability tensor, piezoelectric and piezomagnetic

coefficient tensor, ( $e^T$  and  $q^T$  are the transposes of  $e$  and  $q$ ), respectively. For the composite, these quantities are local values and depend on the spatial position. Therefore, in the mean-field approach, they are chosen as the average values of the constituents. However, the ME coefficient calculated using this expression is still much higher than the experimental value, suggesting that the nature of the coupling between the magnetostrictive and piezoelectric phases is not well understood yet.

In the case of layered structures we are close to theoretical predictions, only in the case of powder composites where the coupling may be very poor and where an optimised microstructure is still open and where the determination of the “true” ME value is still under question we are much smaller than the theoretical predictions!

## 6.2 Laminated composite

The first prediction and calculation of ME effect in laminated composites was made by Harshe *et al* [63-64]. As they assumed an ideal coupling between the magnetostrictive and piezoelectric phases, the difference between calculated and experimental results is very large. To avoid this, Bichurin *et al* introduce a new approach where the non-ideal coupling between the two phases was quantified by the coupling parameter. According to this approach, the polarized piezoelectric phase can be described by the equations [65]:

$$\begin{aligned} {}^p S_i &= {}^p s_{ij} {}^p T_j + {}^p d_{ki} {}^p E_k, \\ {}^p D_k &= {}^p d_{ki} {}^p T_i + {}^p \varepsilon_{kn} {}^p E_n, \end{aligned} \quad (13)$$

where  ${}^p S_i$  and  ${}^p T_j$  are strain and stress tensor component of the piezoelectric phase,  ${}^p E_k$  and  ${}^p D_k$  are the vector component of the electric field and electric displacement,  ${}^p s_{ij}$  and  ${}^p d_{ki}$  are compliance and piezoelectric coefficients, and  ${}^p \varepsilon_{kn}$  is the permittivity matrix. Similarly, the magnetostrictive phase can be described as:

$$\begin{aligned} {}^m S_i &= {}^m s_{ij} {}^m T_j + {}^m q_{ki} {}^m H_k, \\ {}^m B_k &= {}^m q_{ki} {}^m T_i + {}^m \mu_{kn} {}^m H_n, \end{aligned} \quad (14)$$

where  ${}^m S_i$  and  ${}^m T_j$  are strain and stress tensor component of the magnetostrictive phase,  ${}^m H_k$  and  ${}^m B_k$  are the vector component of the magnetic field and magnetic induction,  ${}^m s_{ij}$  and  ${}^m q_{ki}$  are compliance and piezomagnetic coefficients, and  ${}^m \mu_{kn}$  is the permeability matrix.

The non-ideal coupling between the two phases is described by the coupling coefficient  $k$  defined as:

$$k = ({}^p S_i - {}^p S_{i0}) / ({}^m S_i - {}^p S_{i0}), \quad (i = 1, 2) \quad (15)$$

where  ${}^p S_{i0}$  is the strain tensor component with no friction between layers. Finally, the bilayer composite is considered to be homogeneous and described by the equations:

$$\begin{aligned} S_i &= s_{ij} T_j + d_{ki} E_k + q_{ki} H_k, \\ D_k &= d_{ki} T_i + \varepsilon_{kn} E_n + \alpha_{kn} H_n, \\ B_k &= q_{ki} T_i + \alpha_{kn} E_n + \mu_{kn} H_n, \end{aligned} \quad (16)$$

where  $S_i$  and  $T_j$  are strain and stress tensor components,  ${}^k E$ ,  ${}^k D$ ,  $H_k$  and  ${}^m B_k$  are the vector components of the electric field, electric displacement, magnetic field and magnetic induction,  $s_{ij}$ ,  $d_{ki}$ , and  $q_{ki}$  are compliance, piezoelectric and piezomagnetic coefficients, and  $\varepsilon_{kn}$ ,  $\mu_{kn}$  and  $\alpha_{kn}$  are the effective permittivity, permeability and ME coefficient, respectively.

By solving eq.(16) with taking into account the solution of eq.(13) & (14), the longitudinal,  $\alpha_{E,33}$ , and transverse,  $\alpha_{E,31}$ , ME coefficient for the unclamped case are:

$$\alpha_{E,33} = \frac{dE_3}{dH_3} = 2 \times \frac{\mu_0^{k\nu(1-\nu)^P} d_{31}^m q_{31}^m}{\left\{ 2^P d_{31}^{2(1-\nu)+P} \varepsilon_{33} \left[ {}^p s_{11} + {}^p s_{12}(\nu-1) - \nu({}^m s_{11} + {}^m s_{12}) \right] \right\}} \quad (17)$$

$$\times \frac{\left[ ({}^p s_{11} + {}^p s_{12})(\nu-1) - k\nu({}^m s_{11} + {}^m s_{12}) \right]}{\left\{ \left[ \mu_0^{(\nu-1)-m} \mu_{33}^\nu \right] \left[ k\nu({}^m s_{12} + {}^m s_{11}) - ({}^p s_{11} + {}^p s_{12})(\nu-1) + 2^m q_{31}^2 k\nu^2 \right] \right\}},$$

$$\alpha_{E,31} = \frac{dE_3}{dH_1} = \frac{-k\nu(1-\nu)({}^m q_{11} + {}^m q_{21})^P d_{31}}{{}^p \varepsilon_{33} ({}^m s_{12} + {}^m s_{11})k\nu + {}^p \varepsilon_{33} ({}^p s_{11} + {}^p s_{12})(1-\nu) - 2k^P d_{31}^{2(1-\nu)}}, \quad (18)$$

And for the clamped case:

$$\alpha_{E,33} = -\frac{\alpha_{33}(s_{33} + s_{c33}) - d_{33}q_{33}}{\varepsilon_{33}(s_{33} + s_{c33} - d_{33}^2)}, \quad (19)$$

$$\alpha_{E,31} = \frac{\alpha_{33}(s_{33} + s_{c33}) - d_{33}q_{33}}{\varepsilon_{33}(s_{33} + s_{c33} - d_{33}^2)}, \quad (20)$$

where  $\nu = {}^p \nu / ({}^p \nu + {}^m \nu)$  with  ${}^p \nu$  and  ${}^m \nu$  are the volume of piezoelectric and magnetostrictive phase, and the subscript  $c$  in  $s_{c33}$  denotes the  $s_{33}$  of the clamped sample.

Using this approach, the authors found that: i) the magnitude of the ME coefficient decreases with decreasing  $k$ , ii) for different system, the value of  $k$  is different, and  $k$  is close to 1 for NiFe<sub>2</sub>O<sub>4</sub>/PZT, but only 0.1 for CoFe<sub>2</sub>O<sub>4</sub>/PZT system, iii) the strongest and weakest ME coupling is corresponding to the in-plane and out-of-plane longitudinal configuration, and



iv) the transverse ME coefficient is bigger than the longitudinal one. Though this approach seems to be general and can be expanded for multilayer structure, improvements are still needed since the value of  $k$  has to be chosen somewhat randomly to fit the experimental data and the difference between the predicted and experimental values of ME coefficients still exists.

## 7. Applications

Technical applications of the ME materials have been suggested by many researchers. For composite, due to its high ME coefficient compared to that of the single phase materials, the suggested applications become more promising. In general, it is a tool to convert energy from magnetic to electric type and vice versa. And the ability to couple with either the magnetic or the electric polarization offers an extra degree of freedom in the design of conventional actuators, transducer and store devices [11, 14].

The first suggested application was in 1948, more than ten years before the first experimental observation of ME effect, when Tellegen proposed a gyrator using a ME material [66]. In 1973, about ten years after the first observation of the ME effect, Wood and Austin has proposed fifteen different types of applications [67]. Due to the hysteresis nature and the change in sign of the ME effect, the ME materials can find application in memory devices. Multiple-state memory elements or storage media where information is written by magnetic field and read by electric field or vice versa can be designed. Such memory can be an effective read only memory (ROM) since the reading can be done at very high frequency. However, the writing may be difficult since it involves the processing materials at high temperature and high magnetic or electric field [10-11].

The dynamic behaviour of the ME composite, especially the ability to tune both the dielectric and magnetic properties, i.e. the permittivity and permeability, makes the ME composite an ideal candidate for microwave applications. Different frequency ranges can be accessed from electromechanical resonance,  $\sim 100$  kHz, up to antiferromagnetic resonance,  $\sim 100$  GHz. At the resonance frequency, the ME materials can be used as transducer that convert microwave magnetic field to microwave electric field [10, 68]. By changing the bias magnetic or electric field, one can force the ME materials to operate at different working point, leading to a shift in both phase and resonance frequency. Therefore, it can be used as phase shifters or attenuators.

The ME materials can also be used for magnetic field sensor as an alternative of Hall probe. It can be used to detect both DC and AC field since its behaviour changes with its working point determined by the DC bias field and the ME effect is linear with respect to a small AC field. Using proper configuration such as ring-type laminated composite with circumferential polarization and magnetization, the rotating or vortex AC magnetic field can be detected [53, 57, 69]. With a PZT/Terfenol-D laminated ring, an ME response of  $260\text{mVOe}^{-1}$  and a voltage gain of 25 was achieved, which allows one to detect magnetic fields as weak as 1 nT [10].

Another promising application of ME materials is stress sensor. Due to the presence of a piezoelectric constituent, the ME signal may depend sensitively on the applied stress. Therefore, the blood coagulation and chemical liquid curing time measurements can be better implemented using such a material [70].

In conclusion, the possible applications of ME composites are very promising. However, difficulties in sample preparations, especially the control of sample microstructure and sample reproducibility, as well as the lack of fundamental understanding of the materials, both experimentally and theoretically, may be the reason that practical applications are not yet commercially available.

## **Conclusion**

The development as well as some most important aspects of the research on the ME effect in composites have been reviewed. The origin of the ME effect has been discussed. Practical problems in the sample preparation, measuring techniques and applications have been shown. Theoretical models for both particulate and laminated composites have been described. The open questions and unsolved problems that prevent the understanding of composite materials have been demonstrated. More work on both experiment and theory, from very basic concept like the ME coefficient for finding new materials and structures, controlling the materials properties and reproducibility, measuring techniques, coupling nature between magnetic and electric domains, formulating the phenomenon to an equivalent electric circuit, have still to be done to get a proper understanding of the materials and to proceed it for applications.

## Acknowledgement

This work is supported by the FWF Proj. Nr. P16500-N02, Proj. Nr. P15737 and the Austrian Exchange Service (ÖAD).

## References

1. W.C. Röntgen, *Ann. Phys.* 35 (1888) 264.
2. H.A. Wilson, *Phil. Trans. R. Soc. A* 204 (1905) 129.
3. P. Curie, *J. Physique* 3 (1894) 393.
4. D.N. Astrov, *Sov. Phys.—JETP* 11 (1960) 708.
5. D.N. Astrov, *Sov. Phys.—JETP* 13 (1961) 729.
6. G.T. Rado, V.J. Folen, *Phys. Rev. Lett.* 7 (1961) 310.
7. V.J. Folen, G.T. Rado, E.W. Stalder, *Phys. Rev. Lett.* 6 (1961) 607.
8. J. Van Suchetelene, *Philips Res. Rep.* 27 (1972) 28.
9. C.W. Nan, *Phys. Rev. B* 50 (1994) 6082.
10. Manfred Fiebig, *J. Phys. D: Appl. Phys.* 38 (2005) R123–R152.
11. Jungho-Ryu, Shashankprya, Kenjiuchinoi, Hyoun-ee Kim, *J. Electroceramics* 8 (2002), 107-119.
12. H. Zheng et al, *Science* 303 (2004) 661.
13. Giap V. Duong, R. Groessinger, “Evidence of Magneto-Electric Moment Interactions in  $\text{CoFe}_2\text{O}_4\text{-BaTiO}_3$  Composites”, *Technical Digest, IEEE Int. Magn. Conference 2006 (Intermag 2006) AF-02*.
14. N.A. Hill, *J. Phys. Chem. B* 104 (2000) 6694-6709.
15. J. van den Boomgaard, R.A.J. Born, *J. Mater. Sci.* 13 (1978) 1538.
16. Jun Yi Zhai, Ning Cai, Li Liu, Yuan Hua Lin and Ce Wen Nan, *Mater. Sci. Eng. B* 99 (2003) 329-331.
17. S.L. Kadam, K.K. Patankar, V.L. Mathe, M.B. Kothale, R.B. Kale, B.K. Chougule, *Mater. Chem. Phys.* 78 (2003) 684-690.
18. M.B. Kothale, K.K. Patankar, S.L. Kadam, V.L. Mathe, A.V. Rao, B.K. Chougule, *Mater. Chem. Phys.* 77(2003) 691-696.
19. K.K. Patankar, R.P. Nipankar, V.L. Mathe, R.P. Mahajan, S.A. Patil, *Ceramics Int.* 27 (2001) 853-858.

20. Giap V. Duong, R. Groessinger, R. Sato Turtelli, Magnetoelectric Properties of CoFe<sub>2</sub>O<sub>4</sub>-BaTiO<sub>3</sub> Core-Shell Structure Composite, *Trans. Magn.*, in press.
21. J. van den Boomgard, D.R. Terrell, R.A.J. Born, H.F.J.I. Giller, *J. Mater. Sci.* 9 (1974) 1705.
22. A.M. J.G. van Run, D.R. Terrell, J.H. Scholing, *J. Mater. Sci.* 9 (1974) 1710.
23. Q.H. Jiang, Z.J. Shen, J.P. Zhou, Z. Shi, Ce-Wen Nan, *J. European Ceramic Society*, in press.
24. Giap V. Duong, R. Groessinger, R. Sato Turtelli, Effect of Structure on Magnetoelectric Properties of CoFe<sub>2</sub>O<sub>4</sub>-BaTiO<sub>3</sub> Multiferroic Composites, accepted for publication.
25. Srinivasan, E.T. Rasmussen, J. Gallegous, R. Srinivasan, Y.I. Bukhan, V.M. Laletin, *Phys. Rev. B* 64 (2001) 214408.
26. Y.K. Fetisov, A.A. Bush, K.E. Kamentsev, G. Srinivasan, *Solid State Comm.* 132 (2004)319-324.
27. Y.K. Fetisov, K.E. Kamentsev, A.Y. Ostashchenko, *J. Magn. Magn. Mater.* 272-276 (2004) 2064-2066.
28. N. Cai, J. Zhai, C.W. Nan, Y. Lin, Z. Shi, *Phys. Rev. B* 68 (2003) 224103.
29. N. Cai, C.W. Nan, J.Y. Zhai, Y.H. Lin, *Appl. Phys. Lett.* 84 (2004) 3516.
30. Giap V. Duong, R. Groessinger, The Lock-in Technique for Studying Magnetoelectric Effect, accepted for publication.
31. Giap V. Duong. R. Groessinger, The Magnetic Pulse Field Method for Studying Magnetoelectric Effect, in preparation.
32. Y.K. Fetisov, K.E. Kamentsev, A.Y. Ostashchenko, G. Srinivasan, *Solid State Comm.* 132 (2004) 13-17.
33. S. Mazuder, G.S. Bhattacharyya, *Ceramics Int.* 30 (2004) 389-392.
34. R.P. Mahajan, K.K. Patankar, M.B. Kothale, S.C. Chaudhari, V.L. Mathe, S.A. Patil, *Pramana-J. Phys.* 58 (2002) 1115.
35. S.R. Kulkarni, C.M. Kanamadi, B.K. Chougule, *Mater. Res. Bull.* 40 (2005) 2064-2072.
36. S.R. Kulkarni, C.M. Kanamadi, B.K. Chougule, *J. Phys. Chem. Solids* 67 (2006) 1607-1611.
37. R.S. Devan, S.A. Lokare, D.R. Patil, S.S. Chougule, Y.D. Kolekar, B.K. Chougule, *J. Phys. Chem. Solids* 67 (2006) 1524-1530.
38. C.M. Kanamadi, L.B. Pujari, B.K. Chougule, *J. Magn. Magn. Mater.* 295 (2005) 139-144.
39. S.L. Kadam, C.M. Kanamadi, K.K. Patankar, B.K. Chougule, *Mater. Lett.*, 59 (2005) 215-219.

40. K.K. Patankar, R.P. Nipankar, V.L. Mathe, R.P. Mahajan, S. A. Patil, *Ceramics Int.* 27 (2001) 853-858.
41. G. Srinivasan, E.T. Rasmussen, B.J. Levin, R. Hayes, *Phys. Rev. B* 65 (2002) 134402.
42. Tongle Li, Siu Wing Or, Helen Lai Wa Chan, *J. Magn. Mater.* 304 (2006) 442-444.
43. K. Mori, M. Wuttig, *Appl. Phys. Lett.* 81 (2002) 100.
44. V.L. Mathe, K.K. Patankar, U.V. Jadhav, A.N. Patil, S.D. Lotake, S.A. Patil, *Ceram. Int.* 27 (2001) 531.
45. S.X. Dong, J.F. Li, D. Viehland, *Appl. Phys. Lett.* 83 (2003) 2265.
46. J. Ryu, Ph.D Thesis, Seoul National University, Seoul, Korea, Aug. 2001.
47. J. Ryu, A. Vazquez Carazo, K. Uchino, H.E. Kim, *Jpn. J. Appl. Phys.* 40 (2001) 4948.
48. J. Ryu, S. Priya, A. Vazquez Carazo, K. Uchino, H.E. Kim, *J. Am. Ceram. Soc.* 84 (2001) 2905.
49. J.G. Wan, J.M. Liu, H.L.W. Chand, C.L. Choy, G.H. Wang, C.W. Nan, *J. Appl. Phys.* 93 (2003) 9916.
50. S.X. Dong, J.F. Li, D. Viehland, *IEEE Trans. Ultrason. Ferroelectr. Frequency Control* 50 (2003) 1253.
51. S.X. Dong, J.R. Cheng, J.F. Li, D. Viehland, *Appl. Phys. Lett.* 83 (2003) 4812.
52. S.X. Dong, J.F. Li, D. Viehland, *J. Appl. Phys.* 95 (2004) 2625.
53. J.F. Li, D. Viehland, *Appl. Phys. Lett.* 84 (2004) 4188.
54. M. Zeng, J.G. Wan, Y. Wang, H. Yu, J.M. Liu, X.P. Jiang, C.W. Nan, *J. Appl. Phys.* 95 (2004) 8069.
55. S.X. Dong, J.F. Li, D. Viehland, *IEEE Trans. Ultrason. Ferroelectr. Frequency Control* 51 (2004) 794.
56. N. Nersessian, S.W. Or, G.P. Carman, *IEEE Trans. Magn.* 40 (2004) 2646.
57. S.X. Dong, J.F. Li, D. Viehland, *J. Appl. Phys.* 96 (2004) 3382.
58. Jungho Ryu, Shashank Priya, Kenji Uchino, Hyoun-Ee Kim, Dwight Viehland, *J. Kor. Ceramic Soc.*, 39 (2002). 813-817.
59. N. Cai, J. Zhai, C.W. Nan, Y. Lin, Z. Shi, *Phys. Rev. B* 68 (2003) 224103.
60. N. Cai, C.W. Nan, J.Y. Zhai, Y.H. Lin, *Appl. Phys. Lett.* 84 (2004) 3516.
61. J. van den Boomgaard, A.M.J.G. Van Run, J. Van Suchetelene, *Ferroelectrics*, 10 (1976) 295.
62. A.S. Zubkov, *Elektrichestvo*, 10 (1978) 77.
63. G. Harshe, PhD Thesis, 1991, Pennsylvania State University.

64. G. Harshe, J.P. Dougherty, R.E. Newnham, *Int. J. Appl. Electromagn. Mater.* 4 (1993) 145.
65. M.I. Bichurin, D.A. Filippov, V.M. Petrov, V.M. Laetsin, N. Paddubnaya, G. Srinivasan, *Phys. Rev. B* 68 (2003) 054402.
66. B.D.H. Tellegen, *Philips Res. Rep.*, 3 (1948) 81.
67. V.E. Wood, A.E. Austin, *Int. J. Magn.* 5 (1973)303.
68. M.I. Bichurin, V.M. Petrov, Y.V. Kiliba, G. Srinivasan, *Phys. Rev. B* 66 (2002) 134404.
69. S.X. Dong, J.F. Li, D. Viehland, *Appl. Phys. Lett.* 85 (2004) 2307.
70. Evangelos Hristoforou, Aphrodite Ktena, Magnetostriction and magnetostrictive materials for sensing applications, III Joint European Magnetic Symposia, June 26-30<sup>th</sup>, San Sebastian, Spain.

*...measure what is measurable and make measurable what is not yet so...*

G. Galileo

## **Experiment**

*The sample preparation and measuring techniques used to characterize the physical properties of the studied materials will be discussed in this chapter.*

## Sample preparation

All chemicals used to prepare the sample were in analytical purity grade (PA). Details are list in Table 1 below:

Table 1. Information concerning chemicals used to prepare studied samples.

Name of chemicals	Chemical formula	Purity grade	Supplier
Aluminium nitrate 9-hydrate	$\text{Al}(\text{NO}_3)_3 \cdot 9\text{H}_2\text{O}$	>98.5%	Merck
Barium nitrate	$\text{Ba}(\text{NO}_3)_2$	>99%	Merck
Barium hydroxide	$\text{Ba}(\text{OH})_2$	PA	Merck
Calcium nitrate tetrahydrate	$\text{Ca}(\text{NO}_3)_2 \cdot 4\text{H}_2\text{O}$	PA	Merck
Cobalt nitrate hexahydrate	$\text{Co}(\text{NO}_3)_2 \cdot 6\text{H}_2\text{O}$	>99%	Acros Organics
Cooper nitrate trihydrate	$\text{Cu}(\text{NO}_3)_2 \cdot 3\text{H}_2\text{O}$	PA	Merck
Iron nitrate 9-hydrate	$\text{Fe}(\text{NO}_3)_3 \cdot 9\text{H}_2\text{O}$	98-101%	J. T. Baker
Manganese nitrate tetrahydrate	$\text{Mn}(\text{NO}_3)_2 \cdot 4\text{H}_2\text{O}$	PA	Merck
Magnesium nitrate hexahydrate	$\text{Mg}(\text{NO}_3)_2 \cdot 6\text{H}_2\text{O}$	PA	Merck
Nickel nitrate hexahydrate	$\text{Ni}(\text{NO}_3)_2 \cdot 6\text{H}_2\text{O}$	PA	Merck
Strontium nitrate	$\text{Sr}(\text{NO}_3)_2$	99.97%	Alfa Aesar
Zinc nitrate hexahydrate	$\text{Zn}(\text{NO}_3)_2 \cdot 6\text{H}_2\text{O}$	99-101%	J. T. Baker
Ammonium 25%	$\text{NH}_3$	PA	Merck
Citric acid	$\text{C}_6\text{H}_8\text{O}_7$	99%	Merck
Acetic acid	$\text{C}_2\text{H}_4\text{O}_2$	PA	Merck
Titanium Butylate (n-Butoxide)	$\text{C}_{16}\text{H}_{36}\text{O}_4\text{Ti}$	PA	Research Org/inor. Chem.

All samples studied within this thesis were prepared by wet chemical methods. They include co-porecipitation (CP), forced hydrolysis (FH), citrate-gel (CG) and sol-gel techniques (SG). Table 1 below shows the list of sample and their preparation conditions.



Table 2. Samples and their preparation conditions

Samples	Preparation method	Pressure	Temperature & Duration	Remarks	Notes
$\text{Co}_{1-x}\text{Zn}_x\text{Fe}_2\text{O}_4$ ( $x = 0-0.4$ )	FH		160 °C-5 h 100 °C-12 h	D~3 nm	D~12 nm after heat treatment
$\text{CoFe}_2\text{O}_4$	CP		70 °C	D~10 nm	Presented at 450 °C for 3 h
$\text{CoFe}_2\text{O}_4$	CG		1000 °C-5h	D~40 nm	Presented at 450 °C for 3 h
$\text{Co}_{0.7}\text{Zn}_{0.3}\text{Fe}_2\text{O}_4$	CG		1000 °C-5h	D~53 nm	Presented at 450 °C for 3 h
$\text{BaTiO}_3$	SG		1000 °C-5h	D~41 nm	Presented at 450 °C for 3 h
$\text{CoFe}_2\text{O}_4\text{-BaTiO}_3$	CP+SG	3-7.5 tone/cm <sup>2</sup>	1000-1250 °C, 1-20 h	Poled at 7500 V/cm	Core-shell structure
$\text{CoFe}_2\text{O}_4\text{-BaTiO}_3$	CP+SG	6 tone/cm <sup>2</sup>	1250 °C-12 h	Poled at 7500 V/cm	Mixed structure
$\text{CoFe}_2\text{O}_4\text{-BaTiO}_3$	CP+SG	6 tone/cm <sup>2</sup>	1250 °C-12 h	Poled at 7500 V/cm	Layer structure
$\text{Co}_{0.7}\text{Zn}_{0.3}\text{Fe}_2\text{O}_4$ - $\text{BaTiO}_3$	SG	6 tone/cm <sup>2</sup>	1250 °C-12 h	Poled at 7500 V/cm	Core-shell structure

Further details about the preparation procedure can be found in the papers in next chapters. For imagination, they can be briefly described as follow:

## 1. Preparation of the ferrites and barium titanate

### 1.1 Coprecipitation method

This method is used to prepare nanocrystalline  $\text{CoFe}_2\text{O}_4$  with average grain size of about 10 nm. The precursor salts:  $\text{Co}(\text{NO}_3)_2 \cdot 6\text{H}_2\text{O}$ ,  $\text{Fe}(\text{NO}_3)_3 \cdot 9\text{H}_2\text{O}$ , all with analytical purity, were added to 150 ml deionized water and stirred to get the homogeneous solution and heated to 70 °C. The stirring speed was kept constantly at 3000 rpm. Metal ions in the solution were coprecipitated using sodium solution. To be completely coprecipitated, a 50% extra amount of the necessary sodium was used. The precipitated materials were washed by deionized water for several times, dried naturally at room temperature for 24 hours before carrying out measurements or further heat treatments.

### 1.2 Forced hydrolysis

This method is used to prepared nanocrystalline  $\text{Co}_{1-x}\text{Zn}_x\text{Fe}_2\text{O}_4$  ( $x = 0-0.4$ ) with average grain size of 3 nm. The starting mixture containing the precursor salts,  $\text{Fe}(\text{NO}_3)_3 \cdot 9\text{H}_2\text{O}$ ,  $\text{Zn}(\text{NO}_3)_2 \cdot 6\text{H}_2\text{O}$  and  $\text{Co}(\text{CH}_3\text{COO})_2 \cdot 4\text{H}_2\text{O}$ , all with analytical purity, were added to 250 ml of 1,2-propanediol in stoichiometric ratio. The total metal concentration was 0.3 mol/l. The hydrolysis ratio (molar ratio between water and total metal ions) and the acetate ratio (molar ratio between acetate and metal ions) were fixed to 9 and 3, respectively. The starting mixture containing the salts, deionized water, sodium acetate and 1,2-propanediol was heated to 160 °C with a heating rate of 10 °C/min. A black colloidal suspension achieved after refluxing the mixture for 5h was kept at 100 °C in air for 12 h. The particles, separated from the suspension by centrifugation, were washed for several times with water and ethanol. The resultant powders were then dried at 50 °C in air and used as samples for measurements.

The as-prepared nanocrystalline  $\text{Co}_{1-x}\text{Zn}_x\text{Fe}_2\text{O}_4$  can also be heat treated at 500 °C for 3 hours in air. After heat treatment, the grain size of ferrites increase up to 12 nm.

### 1.3 Citrate gel technique

This method is used to prepared nanocrystalline  $\text{CoFe}_2\text{O}_4$  with average grain size of about 40 nm. The precursor salts,  $\text{Fe}(\text{NO}_3)_3 \cdot 9\text{H}_2\text{O}$ ,  $\text{Co}(\text{NO}_3)_2 \cdot 6\text{H}_2\text{O}$  and citric acid, all with analytical purity, were added to 150 ml of deionized water in stoichiometric ratio. The total

metal concentration was 1 mol/l. The molar ratio between total metal ions and citric acid was fixed to 1. The starting mixture containing the salts, deionized water and citric acid was stirred to get homogeneous solution and heated to 80 °C with a heating rate of 5 °C/min using a hot plate magnetic stirrer. The pH of the solution was adjusted to 6 by dropping ammonia (NH<sub>3</sub> 25%). The sol was formed during stirring. Increasing the temperature of the hot plate up to 200 °C and keep stirring constantly, the water in the solution was evaporated and a viscous gel was formed. Keeping heating, the gel is dried and burnt as being ignited to form loose powder. The powder was pressed into pellet under a pressure of 4.5 tones/cm<sup>2</sup> and sintered at 1000 °C for 5 hours. After naturally cooling down to room temperature, it was cut in to pieces of 2x4x6 mm and used as sample for measurements.

#### *1.4 Sol-gel technique*

This method is used to prepare BaTiO<sub>3</sub>. First, Ba(OH)<sub>2</sub> was dissolved by acetic acid to get barium acetate. A 50% extra amount of Ba(OH)<sub>2</sub> was used to ensure the completeness of the reaction. Then n-butoxide was introduced to the solution while keeping stirring constantly. The solution was heated up to 80 °C with a heating rate of 5 °C/min using a hot plate magnetic stirrer. Keeping heating and stirring, the solvent was evaporated and the sol was formed. The gel was formed from the sol by gelation process. The gel was dried at 120 °C for 12 hours before annealing at 1000 °C for 5 hours.

## **2. Preparation of the ferrite-barium titanate composites**

### *2.1 Core-shell structure composite with CoFe<sub>2</sub>O<sub>4</sub> in core*

The sample was synthesized using coprecipitation and sol-gel method. All chemicals are in analytic pure grade. CoFe<sub>2</sub>O<sub>4</sub> powder obtained from appropriate solution containing Co(NO<sub>3</sub>)<sub>2</sub>.6H<sub>2</sub>O and Fe(NO<sub>3</sub>)<sub>3</sub>.9H<sub>2</sub>O and co-precipitating at 75°C using NaOH solution. To obtain CoFe<sub>2</sub>O<sub>4</sub>-BaTiO<sub>3</sub> core-shell structure composite, the co-precipitated CoFe<sub>2</sub>O<sub>4</sub> powder, calculated to get a composite containing 50% in mass of each constituent, was introduced into a solution of acetic acid, barium hydroxide and titanium (IV) n-Butoxide, which is then gelled on the surface of the CoFe<sub>2</sub>O<sub>4</sub> grains or particles during heating and stirring. The obtained material is dried, pre-sintered at 700°C for 2 hours, ground into fine powder, then pressed under a pressure of 6 tones/cm<sup>2</sup> to obtain a sample in shape of a disc of 10 mm in

diameter and 1.5 mm thick. This sample is sintered at 1250°C for 12 hours to get a core-shell structure composite. After heat treatment, due to shrinkage, the diameter and thickness of the sample are 8.7 and 1.3mm, respectively. The sample was painted by silver paste for electric contacts, then poled electrically under an electric field of 7500V/cm (field direction is perpendicular to the surface of the sample) in silicon oil from 150°C down to room temperature.

### *2.2 Core-shell structure composite with BaTiO<sub>3</sub> in core*

For the core-shell structure with BaTiO<sub>3</sub> in core and CoFe<sub>2</sub>O<sub>4</sub> as shell, the BaTiO<sub>3</sub> was first synthesized by sol-gel method as mentioned above, then introduced to a solution containing cobalt nitrate, iron nitrate, citric acid, all in stoichiometric. Stirring and heating were kept constantly to evaporate the solvent. The gelation process occurs on the surface of BaTiO<sub>3</sub> particle to form the core-shell structure. Other procedures were performed similarly to those described above.

### *2.3 Mixed structure composite*

The mixed structure composite was obtained simply by mixing the two constituents previously prepared by methods listed above. The mixed powder was ground to get homogenous distribution, then pressed into pellets. The preparing conditions, including the pressure, annealing temperature and duration, poling procedure, etc., were kept similar to those of the core-shell structure composite.

### *2.4 Layer structure composite*

The layer structure composite was prepared by casting the powders, which are prepared previously by method described above, into the matrix. The powder was slightly pressed before casting the other layers, then the whole powders in the matrix were pressed under a pressure of 6 tones/cm<sup>2</sup>.

All other procedures, including the heat treatment and poling procedure, are similar to those of the core-shell structure samples.

Relevant information about the above sample preparation methods can also be found in some references listed below.

**References:**

- [1] T. Pannaparayil and S. Komarneni. IEEE Trans. Magn. 25 (1989), 4233.
- [2] Yeong Il Kim, Don Kim and Choong Sub Lee, Physica B: Cond. Matter 337 (2003) 42-51.
- [3] San Che, Jun Wang, Qianwang Chen, J.Phys.: Condens. Matter. 15 (2003) L335.
- [5] S. Ammar et al.J. Mater. Chem. 11 (2001) 186.
- [6] N. Hanh, O. K. Quy, N. P. Thuy, L. D. Tung and L. Spinu, Physica B: Cond. Matter, 327 (2003) 382.
- [7] V. Corral-Flores\_ and D. Bueno-Baques, D. Carrillo-Flores, J. A. Matutes-Aquino, J.Appl. phys. 99 (2006) 08J503
- [8] R. N. Panda, J. C. Shih and T. S. Chin, J. Magn. Magnetic Mate. 257 (2003) 79-86.

# Structural Characterization

The structure characterization of the studied samples, including phase purity analysis and grain size determination, was carried out by means of X-ray diffraction in two different diffractometer. The first one (Siemens Kristalloflex 4 Diffraktometer) uses  $\text{CoK}_\alpha$  radiation and performed automatically by the computer program KF4 (*Kristalloflex 4*). The second one uses synchrotron radiation available at the Synchrotron ELETTRA, Trieste, Italy. The diffraction profiles were measured by a special double crystal diffractometer with negligible instrumental broadening [1]. A fine focus rotating copper anode was operated as a line focus at 36 kV and 50 mA ( $\lambda=0.15406$  nm). Using a Ge monochromator and a slit, the  $\text{K}_\beta$  as well as the  $\text{K}_{\beta\beta}$  component was removed. The scattered radiation was registered in reflection by a linear position sensitive X-ray detector of type OED-50 (Braun, Munich) installed at distance of 450 mm from the sample.

## Phase analysis

The phase analysis, including crystal structure, phase purity and lattice constant, was determined from the diffraction patterns. For a particular lattice with distant  $d$  between planes, the diffraction pattern can be calculated from Bragg equation:

$$n\lambda = 2d_{hkl} \sin \theta$$

The diffraction pattern was performed using the LAZY PULVERIX program. By comparing the calculated pattern with the experimental one, the information about phases in the studied sample was obtained. Similarly to the diffraction pattern calculation, the lattice constant was calculated by the GIKO v1.0 program.

## Grain size determination

The average grain size was determined using the Scherrer equation for the full-width at half maximum (FWHM) of the strongest reflection [2]:

$$D = K\lambda / \beta \cos \theta ,$$

where  $D$  is the crystallite size,  $K$  is the shape function for which a value of 0.9 is used [2],  $\beta$  is the width of the pure diffraction profile and  $\theta$  is the angle of incidence.

### Grain size distribution determination

The grain size distribution is determined by Convolutional Multiple Whole Profile (CMWP) fitting. In kinematical theory of X-ray diffraction, a physical profile of a Bragg reflection is given by the convolution of the size and the distortion profiles [3]:

$$A(L) = A^S(L)A^D(L)$$

where  $A(L)$  are the absolute values of the Fourier coefficients of the physical profiles,  $A^S$  and  $A^D$  are the size and the distortion Fourier coefficients,  $L$  is the Fourier variable.

In bulk nanostructured materials, the crystallite-size distribution can be described by a log-normal function [4]. If  $\sigma$  is the variance and  $m$  is the median of the log-normal size distribution function, the arithmetic, the area- and the volume-weighted mean crystallite sizes are obtained as :

$$\langle x \rangle_{arit} = m.e^{0.5\sigma^2}, \langle x \rangle_{area} = m..e^{2.5\sigma^2}, \langle x \rangle_{vol} = m..e^{3.5\sigma^2}$$

For the successful investigation of nanostructured materials, a numerical procedure was used for fitting the Fourier transforms of the product of the theoretical functions of size and strain to the experimental profiles [5]. The procedure has five fitting parameters for cubic crystals:  $m$  and  $\sigma$  describing the size distribution of the coherently scattering domains,  $\sigma$  and  $M$  corresponding to strain broadening and  $q$  corresponding to the strain anisotropy.

### References:

- [1] J. Gubicza, J. Szépövolgyi, I. Mohai, L. Zsoldos, T. Ungár, *Mater. Sci. Eng. A* 280 (2000) 263.
- [2] H.G. Jiang, M. Rühle and E.J. Lavernia *J. Mater. Res.* 14, 2 (1999), 549.
- [3] B. E. Warren, *Progr. Metal Phys.* 8 (1959) 147.
- [4] C.E. Krill, R. Birringer, *Phil. Mag. A* 77 (1998) 621.
- [5] G. Ribárik, J. Gubicza, T. Ungár, *Mater. Sci. Eng. A* 387-389 (2004) 343.

# Magnetic Characterization

## Hysteresis loops and temperature dependent magnetization

The hysteresis loops and temperature dependent magnetization of the studied samples were measured using different magnetometer such as: Parallel Field Vibrating Sample Magnetometer (VSM), Model 150A, Princeton Research Applied, in the temperature range from 4.2K up to room temperate, under static field produced by a superconducting coil up to 7 Tesla; Superconducting Quantum Interference Device (SQUID) Magnetometer (Quantum Design MPMS XL7) in the temperature range 3-400 K with maximum magnetic field of 6.5 Tesla; Physical Property Measurement System (PPMS-9T, Quantum Design) in the temperature range of 1.9-400 K with maximum magnetic field of 9 Tesla; Pulse Field Magnetometer (lab made) with maximum magnetic field of 35 Tesla (PFM) in the temperature range from 4.2 K to room temperature, with a pulse duration up to 20 ms. The sketch of this lab made pulse field magnetometer is given below:

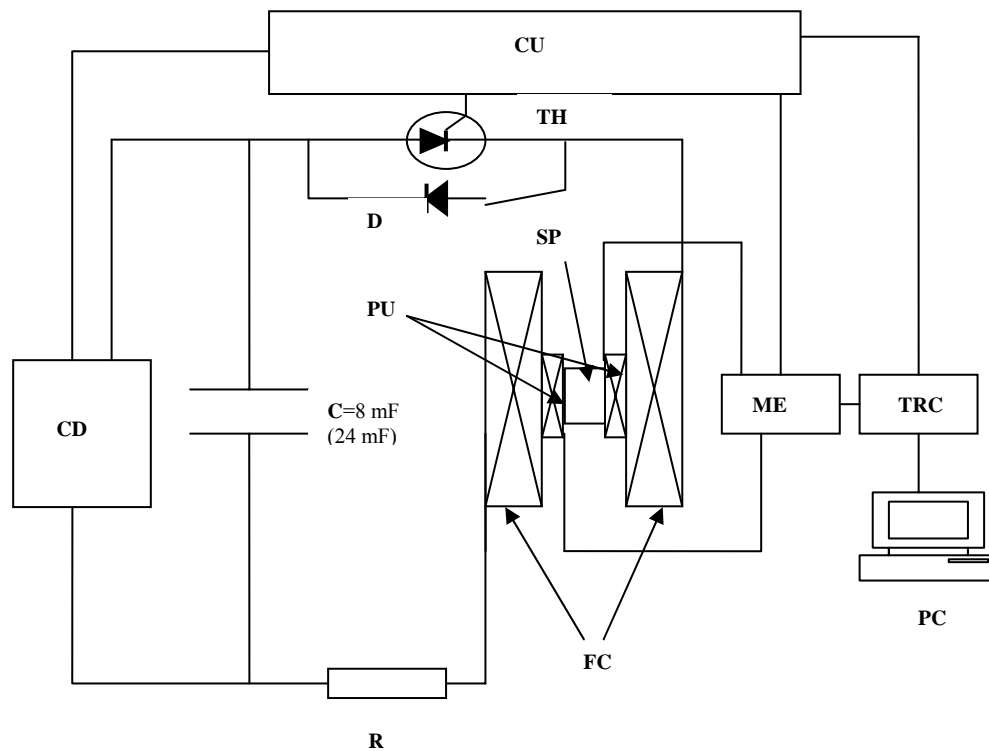


Fig. 1. Schema of the PFM: C: Condenser battery, CD: Charge device, CU: Control unit, D: Diode, FC: Field coil, ME: Measuring electronics, PC: Personal computer, PU: Pick-up system; R: Resistance, SP: Sample space, TH: Thyristor, TRC: Transient recorder.



The charge device (CD) uses to charge the capacitor bank which consists of many 40  $\mu\text{F}$  capacitances up to the desired voltage (maximum 2150 V). The capacitances were connected in two different configurations that lead to a total capacitance of 8 and 24 mF. When starting measurement, the control unit (CU) starts the charge device which forced the capacitor bank charge up the chosen voltage, then a trigger signal is sent to the measurement electronics (ME) and the transient recorder (TRC). After a short delay, the thyristor opens and a current flow through the field coil (FC) to produce the magnetic field. To have the full wave, the diode (D) must be connected. Due to experiencing the magnetic field, the magnetization of the sample changes, causing an induction voltage between in the pick-up system. This induction voltage is processed by measurement electronics and collected by the transient recorder. After that, it is read by computer using a LABVIEW interfere program.

### **AC susceptibility**

AC susceptibility measurement was carried out on an AC Susceptometer, Model 710, Lake Shore Cryotronics, with frequency of 1kHz and field amplitude of 200A/m, also from 4.2K up to room temperature. From AC susceptibility measurement, information about blocking temperature of the non-interacting magnetic nanoparticles, Curie temperature, magnetic phase transition, etc. can be obtained.

### **Magnetostriction**

Linear magnetostriction was measured by strain gauge method using a 50 kHz bridge (HBM Type KWS 85.A1). The strain gauge (US-Type 1,5/120XY91) was mounted on the surface of the sample using a special glue. The sample was then place in a pulse magnetic field up to 5 Tesla with pulse duration of 40 or 58 ms (Hirst PFM 11). The change in length of the sample under magnetic field causes a change in strain gauge resistance, leading to a change of the output voltage of the bridge which is proportional to the linear magnetostriction. This voltage was measured automatically by computer using a LABVIEW program. The sensitivity of this method is  $\pm 1$  ppm.

# Magnetolectric Characterization

The magnetolectric coefficient of the samples was measured by lock-in technique and pulse field method that are developed as one of the aim of this dissertation. Details on these measuring techniques were discussed in the papers of the next chapters. However, for short description will be given as below.

## Lock-in Technique

This method needs a DC field in order to chose the working point of the material and a superimposed small AC-field for generating due to the ME effect an ac-voltage which can be measured using a lock-in amplifier. This DC magnetic bias field up to 15 kOe is produced by an electromagnet. The slowly with time in- and decreasing DC field can be achieved by a programmable DC power source (Siemens NTN 35000-200). To measure the DC field, a Hall probe (PT1486) is employed. The AC field is produced by a Helmholtz coil (100 turns with a diameter of 50 mm) which is driven by an AC current generated by a function generator (Siemens 17A). The amplitude of the AC field is calculated from the driving current which is measured by a multimeter (Keithley 2000). The sample is placed in the magnetic field (DC + AC) with its surface perpendicular or parallel to the DC-field direction, according to the longitudinal and transverse measurement, respectively. The voltage across the sample which is proportional to the ME coefficient was measured using a lock-in amplifier (EG&G model 5210) with an input resistance and capacitance of 100 M $\Omega$  and 25 pF, respectively. To avoid noise as well as zero signal problem, the lock-in amplifier must be operated in the differential mode. Data acquisition was performed by a computer using a Labview interference program.

The magnetolectric coefficient,  $\alpha_E$ , was determined using equation:

$$\alpha_E = \frac{V_{out}}{h_0 \times d}$$

where  $V_{out}$  is the output voltage of the lock-in amplifier,  $h_0$  is the amplitude of the AC field and  $d$  is the effective thickness of the studied sample.

A special sample holder containing gold contact was design to measure the magnetolectric coefficient. All measurements were carried out in room temperature and ambient pressure.

Fig.2 & 3 show the block diagram and the picture of the Lock-in technique measuring system.

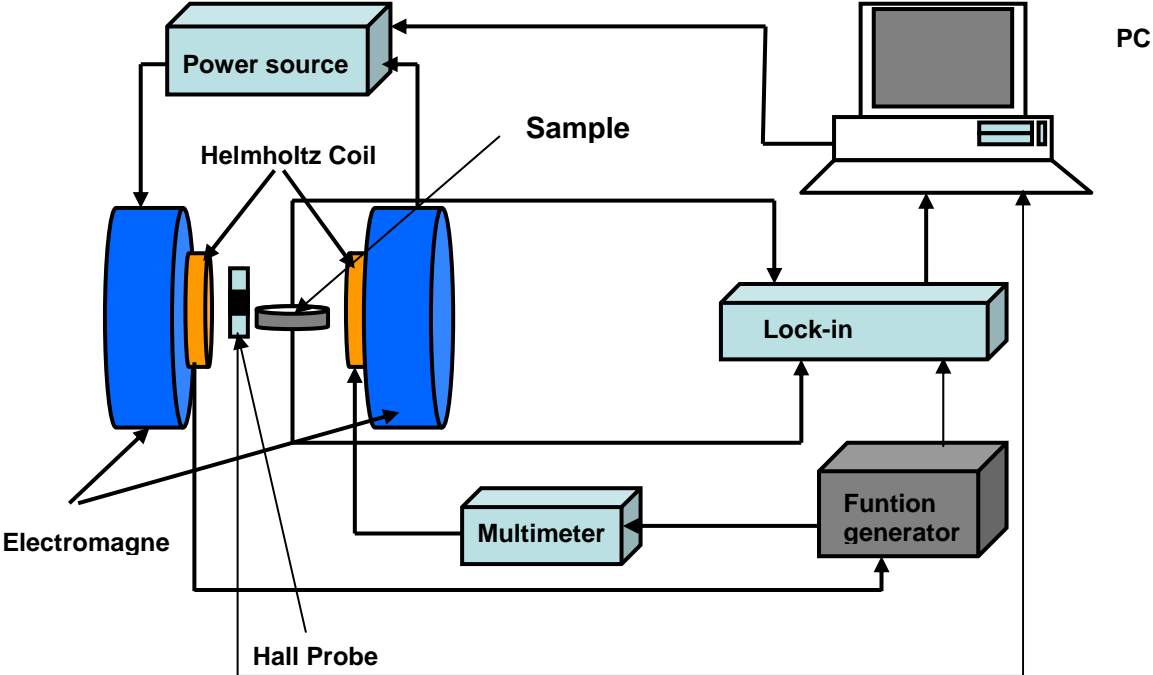


Fig.2. Schema of the Lock-in technique measuring set-up.

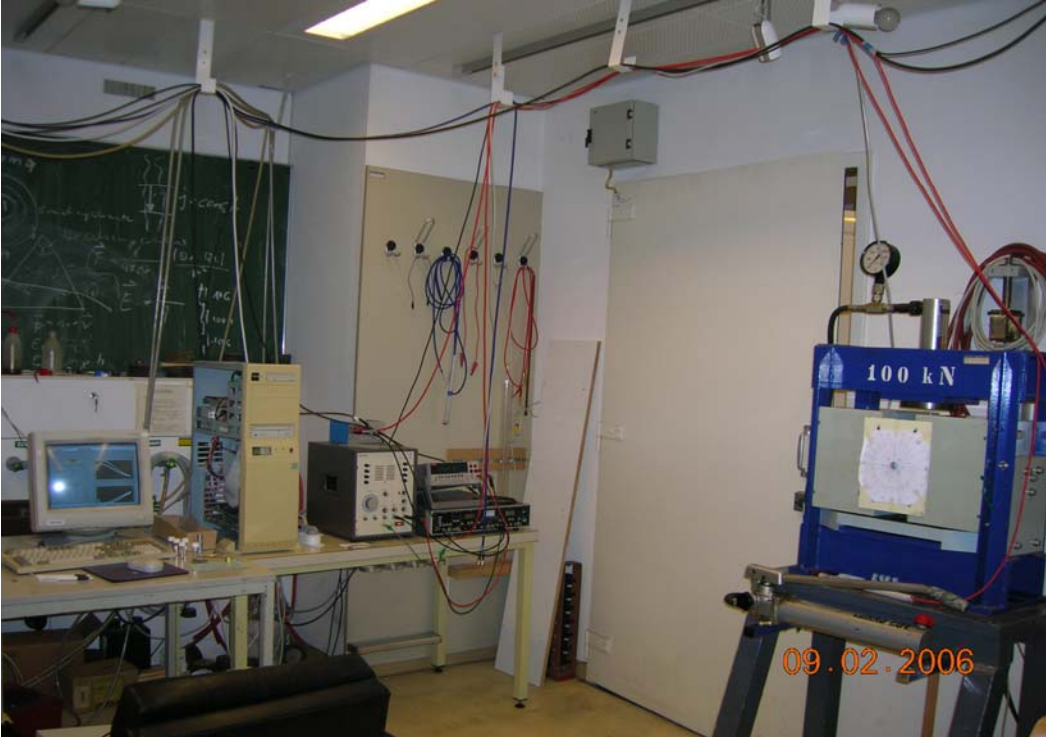


Fig.3. The Lock-in technique measuring system.

**Pulse Filed Method**

Here a pulsed magnetic field with a pulse duration between 4 and 50 ms can be applied on the ME sample. The magnetoelectric coefficient can be measured directly by registrating the voltage which appears across the sample when it is exposed to the pulsed magnetic field. The maximum field is 5 Tesla (Hirst, PMF 11). The pulse duration is 40 or 58 ms. To avoid any induction voltage, the magnetoelectric signal is processed using an preamplifier (Stanford Research Systems, Model SR 560; input resistance 100 M $\Omega$ ) operated in the differential mode. The output voltage of the preamplifier is registrated by a fast ADC (14 bit 5Msample/s two channel ADC card; Datel model: PCI-416N) measuring card by computer using a LABVIEW program.

The magnetoelectric coefficient,  $\alpha_E$ , was determined using equation:

$$\alpha_E = \frac{V}{H \times d}$$

where  $V$  is the voltage across the sample,  $H$  is the applied magnetic field and  $d$  is the effective thickness of the studied sample.

Fig.4 & 5 show the block diagram and the picture of the Pulse Field Method measuring system.

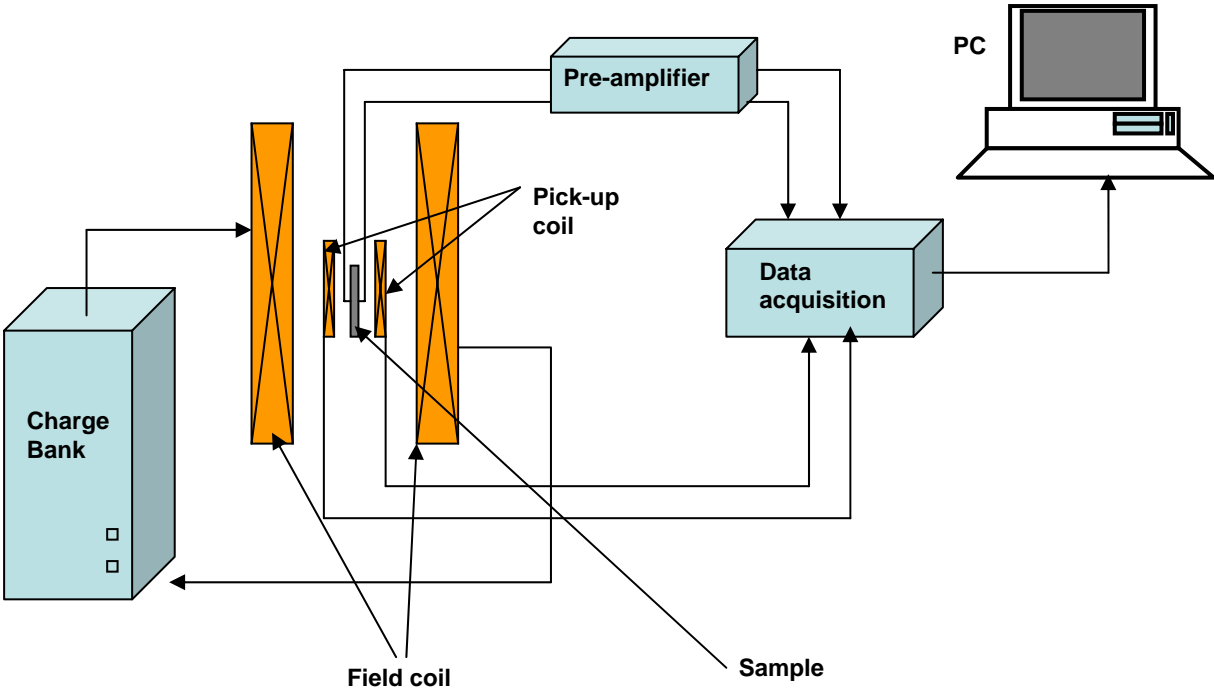


Fig.4. The block diagram of pulse field method measuring set-up.

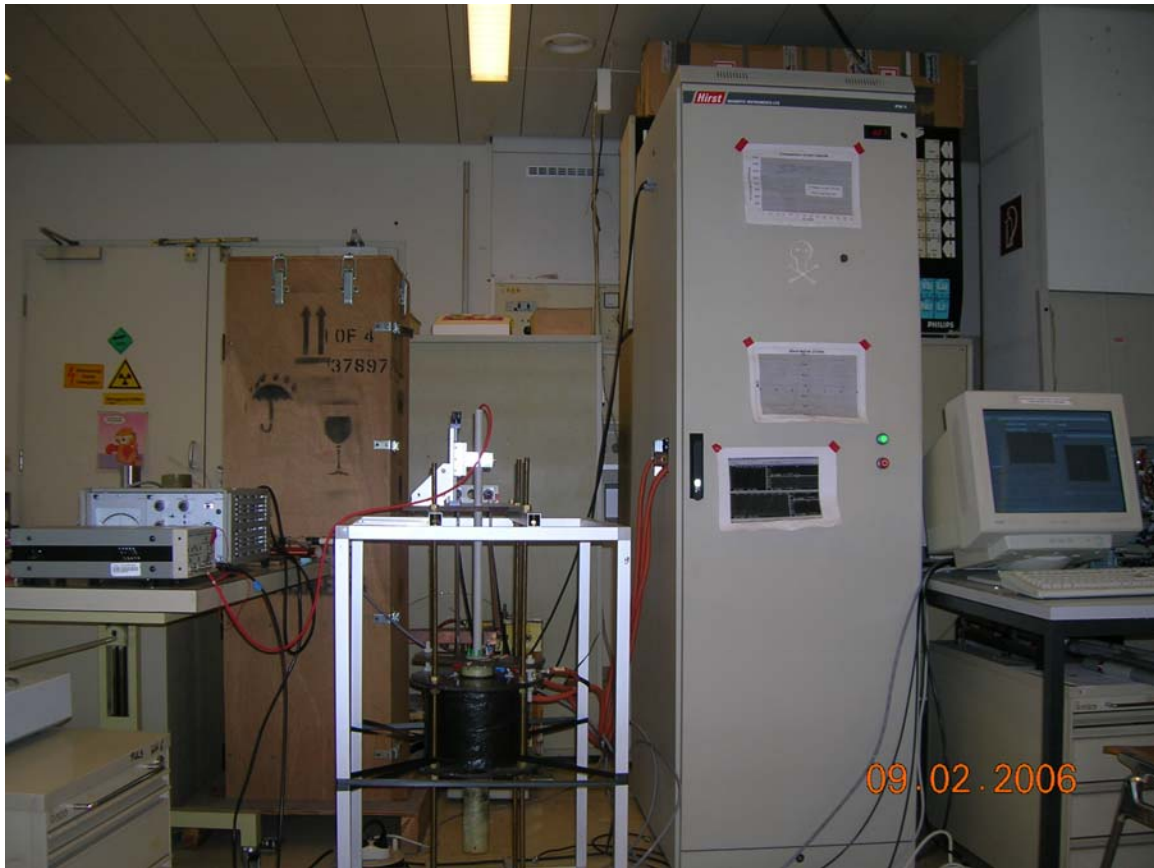


Fig.5. The pulse field method measuring system.

## Other Experiments

### Pressing sample

The powders were pressed into pellets using a hydrostatic pressure up to 1000 bar (OMCN ART-156). The diameter of the die is 10, 12 or 14 mm.

### Annealing sample

The samples were annealed using a high temperature furnace (Heraeus, Typ. ROS 4/50) in the temperature range of room temperature up to 1300°C for different annealing duration. The heating speed is in the range of 10-20 °C/min.

### Electrical poling

Electrical poling was carried out in an electric field of 7.5 KV/cm produce by a high voltage DC power supplier (Heizinger HCNs 3500-100). The maximum voltage is 3 kV. The distance between electrodes varies from 1-3 mm. Poling procedure was carried out from 150 °C to room temperature in atmosphere or silicon oil media.

### Magnetic field alignment

The magnetic field alignment was carried out in a static field of 1.5 Tesla produced by a water cool electromagnet. The distance between magnetic poles is 53 mm. The high DC voltage power supplier is NTN 35000-200 from Siemens.

### FT-IR spectroscopy:

The organic impurities on the surface of the samples were investigated using a Fourier Transform Infrared (FT-IR) Spectroscopy (Perkin-Elmer 16 PC) in the absorption band of 4000-450  $\text{cm}^{-1}$ . For a good signal-to-noise ratio, 64 scans were summed.

## **Transmission Electron Microscopy**

The sample microstructure, including the powder morphology as well as grain size was also investigated using a High-Resolution Transmission Electron Microscope, (JEOL 2000FX) equipped with an Electron Selected Area Diffractometer (SAD).

## **Mössbauer spectroscopy**

The  $^{57}\text{Fe}$  Mössbauer measurements were carried out in transmission geometry at 4.2 K and at room temperature using a constant acceleration type spectrometer with a  $^{57}\text{Co}(\text{Rh})$  source with an activity of about 20 mCi ( $7.4 \cdot 10^8$  Bq). The data were analyzed applying a fitting routine assuming a discrete superposition of sextets (doublets). The isomer shift values are given relative to the source material, their magnitude differing from those relative to the reference material  $\alpha$  Fe by  $-0.12$  mm/s.

*...those who control materials will control the future...*

Material Scientist

## **Results and Discussion**

*The most important results of the thesis will be shown in the form of individual but related articles in this chapter.*



*...one is all and vice versa...*

## **Structural & Magnetic Studies**

*Magnetic properties of the magnetostrictive components that play the key role for the magnetoelectric effect of composites will be discussed here.*

# Monodispersed Nanocrystalline $\text{Co}_{1-x}\text{Zn}_x\text{Fe}_2\text{O}_4$ Particles by Forced Hydrolysis: Synthesis and Characterization

Giap V. Duong<sup>a,\*</sup>, N. Hanh<sup>a</sup>, D. V. Linh<sup>a</sup>, R. Groessinger<sup>b</sup>, P. Weinberger<sup>c</sup>,  
E. Schafler<sup>d</sup>, M. Zehetbauer<sup>d</sup>

<sup>a</sup>*Faculty of Chemical Engineering, Hanoi University of Technology,  
No.1 Dai Co Viet, Hanoi, Vietnam*

<sup>b</sup>*Institute of Solid State Physics, Vienna University of Technology,  
Wiedner Hauptstrasse 8-10, A-1040, Wien, Austria*

<sup>c</sup>*Institute of Applied Synthetic Chemistry, Vienna University of Technology,  
Getreidemarkt 9/163, A-1060, Wien, Austria*

<sup>d</sup>*Department of Materials Physics, Faculty of Physics, University of Vienna,  
Boltzmannngasse 5, A-1090, Vienna, Austria*

Accepted July 24<sup>th</sup>, 2006.

---

## Abstract

Zinc-substituted cobalt ferrites,  $\text{Co}_{1-x}\text{Zn}_x\text{Fe}_2\text{O}_4$ , were for the first time successfully prepared by forced hydrolysis method. The obtained materials are single phase, monodispersed nanocrystalline with an average grain size of about 3 nm. These materials are superparamagnetic at room temperature and ferrimagnetic at temperature lower than the blocking temperature. When the zinc substitution increases from  $x = 0$  to  $x = 0.4$ , at 4.2 K, the saturation magnetization increases from 72.1 emu/g to 99.7 emu/g. The high saturation magnetization of these samples suggests that this method is suitable for preparing high quality nanocrystalline magnetic ferrites for practical applications.

© 2006 Elsevier B.V. All rights reserved

PACS: 75.50.Tt; 75.60.Ej; 75.75.+a; 61.16.Bg

Keywords: Nanocrystalline, Ferrite, superparamagnetism, forced hydrolysis method, Zinc substitution, hysteresis loops.

---

## 1. Introduction

Nanocrystalline magnetic particles are attractive due to many important applications such as ferrofluids, magnetic drug delivery, hyperthermia for cancer treatment, etc. [1-3]. Among them, cobalt ferrite,  $\text{CoFe}_2\text{O}_4$ , is a good candidate for such applications due to the remarkable properties observed in the bulk sample: high saturation magnetization,  $M_s$ , high coercivity,  $H_c$ , strong anisotropy along with good mechanical hardness and chemical stability [4].

Zinc substitution may improve magnetic properties of nanocrystalline ferrites since it is well known that substituting  $\text{M}^{2+}$  metal ions in inverse spinel M-ferrite by non-magnetic  $\text{Zn}^{2+}$  ions will cause an increase of saturation magnetization in bulk ferrite samples [5].

Recently, a novel method, namely: forced hydrolysis, has been developed to synthesize high quality nanocrystalline  $\text{CoFe}_2\text{O}_4$  [6-7]. The materials obtained by this method have a higher degree of crystallinity compared to those prepared by other methods, such as: co-precipitation [8], mechano-chemical [9], micro-emulsion [10], sol-gel [11], etc., leading to a higher saturation magnetization [6-7]. However, this method is reported only for the Co-Fe-O, a two metal element system. No work reports on the substitution of Co by Zn, or other metal element, using this promising synthesis technique. Therefore, the purpose of this work is to synthesize zinc substituted nanocrystalline cobalt ferrites,  $\text{Co}_{1-x}\text{Zn}_x\text{Fe}_2\text{O}_4$  ( $x=0, 0.2, 0.4$ ) by forced hydrolysis method and to study the structure, morphology as well as magnetic properties of the obtained materials.

## 2. Experimental Methods

### 2.1. Sample preparation

The precursor salts,  $\text{Fe}(\text{NO}_3)_3 \cdot 9\text{H}_2\text{O}$ ,  $\text{Zn}(\text{NO}_3)_2 \cdot 6\text{H}_2\text{O}$  and  $\text{Co}(\text{CH}_3\text{COO})_2 \cdot 4\text{H}_2\text{O}$ , all with analytical purity, were added to 250 ml of 1,2-propanediol in stoichiometric ratio. The total metal concentration was 0.3 mol/l. The hydrolysis ratio (molar ratio between water and total metal ions) and the acetate ratio (molar ratio between acetate and metal ions) were fixed to 9 and 3, respectively. The starting mixture containing the salts, deionized water, sodium acetate and 1,2-propanediol was heated to 160 °C with a heating rate of 10 °C/min. A black colloidal suspension achieved after refluxing the mixture for 5h was kept at 100 °C in air for 12 h. The particles, separated from the suspension by centrifugation, were washed for several

times with water and ethanol. The resultant powders were then dried at 50 °C in air and used as samples for measurements.

## 2.2. Characterization

The crystal structure was studied by means of an X-ray diffractometer (XRD). The diffraction profiles were measured by a special double crystal diffractometer with negligible instrumental broadening [12]. A fine focus rotating copper anode was operated as a line focus at 36 kV and 50 mA ( $\lambda=0.15406$  nm). Using a Ge monochromator and a slit, the  $K_{\alpha}$  as well as the  $K_{\beta}$  component was removed.

The scattered radiation was registered in reflection by a linear position sensitive X-ray detector of type OED-50 (Braun, Munich) installed at distance of 450 mm from the sample.

In kinematical theory of X-ray diffraction, a physical profile of a Bragg reflection is given by the convolution of the size and the distortion profiles [13]:

$$A(L) = A^S(L)A^D(L) \quad (1)$$

where  $A(L)$  are the absolute values of the Fourier coefficients of the physical profiles,  $A^S$  and  $A^D$  are the size and the distortion Fourier coefficients,  $L$  is the Fourier variable.

The method of X-ray Bragg profile analysis frequently applied in the characterization of nanostructured materials of different type [14-15], especially the quantification of microstrains due to lattice defects as well as the size of the coherently scattering domains.

In bulk nanostructured materials, the crystallite-size distribution can be described by a log-normal function [16]. If  $\sigma$  is the variance and  $m$  is the median of the log-normal size distribution function, the arithmetic, the area- and the volume-weighted mean crystallite sizes are obtained as :

$$\langle x \rangle_{arit} = m.e^{0.5\sigma^2}, \langle x \rangle_{area} = m..e^{2.5\sigma^2}, \langle x \rangle_{vol} = m..e^{3.5\sigma^2} \quad (2)$$

For the successful investigation of nanostructured materials, a numerical procedure was used for fitting the Fourier transforms of the product of the theoretical functions of size and strain to the experimental profiles [17]. The procedure has five fitting parameters for cubic crystals:  $m$  and  $\sigma$  describing the size distribution of the coherently scattering domains,  $\square$  and  $M$  corresponding to strain broadening and  $q$  corresponding to the strain anisotropy.

The powder morphology as well as grain size was also investigated using a High-Resolution Transmission Electron Microscope, (JEOL 2000FX) equipped with an Electron Selected Area Diffractometer (SAD).

The organic impurities on the surface of the samples were investigated using a Fourier Transform Infrared (FT-IR) Spectrometer (Perkin-Elmer 16 PC) in the absorption band of 4000-450  $\text{cm}^{-1}$ . For a good signal-to-noise ratio, 64 scans were summed.

The temperature dependence of the magnetization and the hysteresis loops were measured by means of a Parallel Field Vibrating Sample Magnetometer (VSM), (Model 150A, Princeton Research Applied) in the temperature range from 4.2 to 300 K with maximum applied field of  $\mu_0 H = 7$  T. The blocking temperature was determined from the temperature dependence of the initial ac-susceptibility,  $\chi_i$ . Measurements of  $\chi_i$  were carried out at temperatures between 4.2 and 300 K in an ac-magnetic field of 200 A/m with a frequency of 1 kHz, using a AC Susceptometer (Model 710, Lake Shore Cryotronics). The  $^{57}\text{Fe}$  Mössbauer measurements were carried out in transmission geometry at 4.2 K and at room temperature using a constant acceleration type spectrometer with a  $^{57}\text{Co}(\text{Rh})$  source with an activity of about 20 mCi ( $7.4 \cdot 10^8$  Bq). The data were analyzed applying a fitting routine assuming a discrete superposition of discrete sextets. The isomer shift values are given relative to the source material.

### 3. Results and Discussion

The XRD pattern of the as-prepared  $\text{CoFe}_2\text{O}_4$  sample at room temperature is shown in Fig. 1. Very similar patterns are obtained for the other samples. The lattice constant of  $\text{CoFe}_2\text{O}_4$  sample calculated from our RXD pattern is 8.362 Å which is slightly smaller compared to the value of 8.38 Å for bulk sample reported in literature [5]. As can be seen in Fig.1, all peaks are characteristics for the cubic structure and spinel-type lattice of cobalt ferrite. The absence of extra lines in the diffraction patterns confirm the phase purity. The peaks are relatively broad indicating that the materials exhibit a very small average particles size. Using the Convolutional Multiple Whole Profile (CMWP) fitting, the grain-size distribution is described by a log-normal function [16-17]. A very narrow size distribution as shown in Fig.2 was obtained suggesting a monodispersed nanocrystalline system with  $m = 2.4$  nm and  $\sigma = 0.39$ , resulting in an average area-weighted grain size of 3.5 nm. which is in good correspondence with the TEM investigations, suggesting that one particle is only one grain and do not contain any detectable crystal defects.

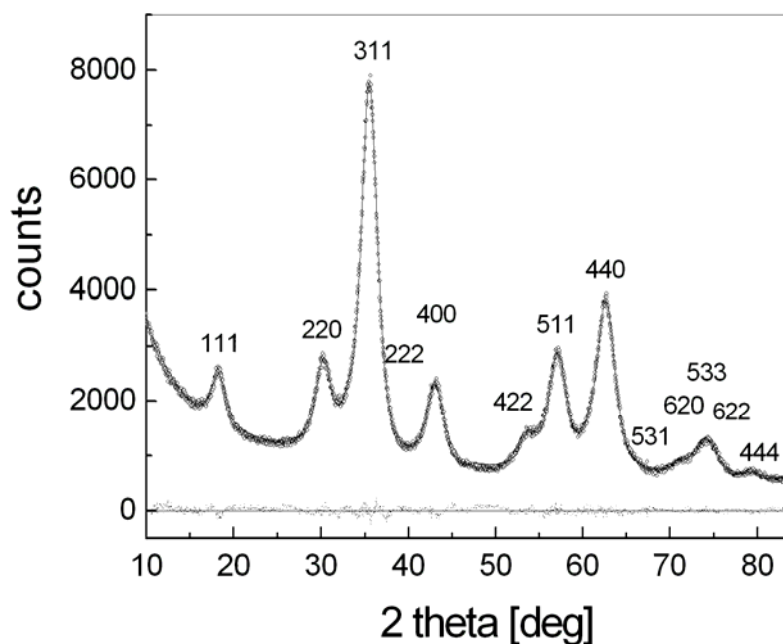


Fig.1. XRD pattern of the as-synthesized  $\text{CoFe}_2\text{O}_4$  sample at room temperature.

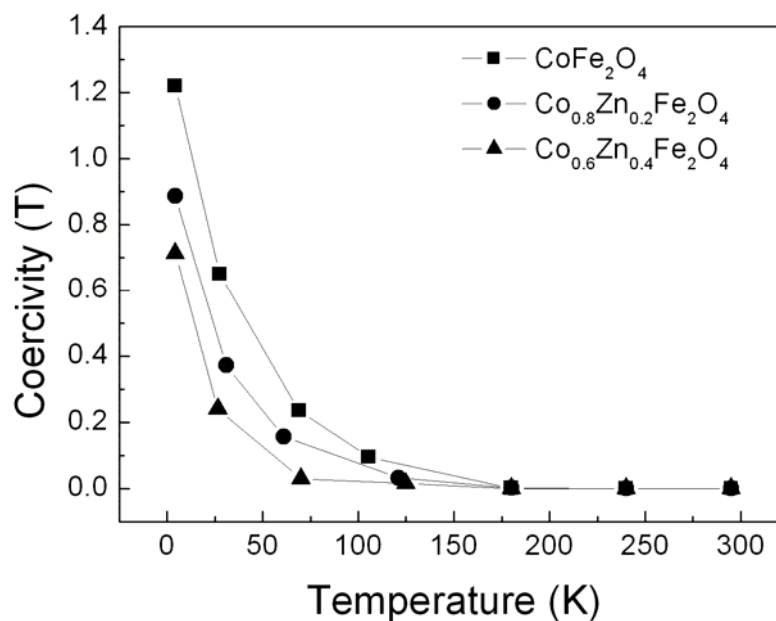


Fig.2. Area-weighted grain size distribution of the as-synthesized  $\text{CoFe}_2\text{O}_4$  sample.

A TEM image of the  $\text{Co}_{0.8}\text{Zn}_{0.2}\text{Fe}_2\text{O}_4$  sample is shown in Fig. 3. It is clear that the size of most particles is  $\sim 3$  nm. The particle sizes determined from TEM are not so far from that obtained from the XRD measurements, suggesting that each particle here is a single nanocrystallite. The electron diffraction pattern of this sample was shown in Fig.4. The clear and

broaden rings in the diffraction pattern suggest a very small particle size of a typical nanocrystalline sample.

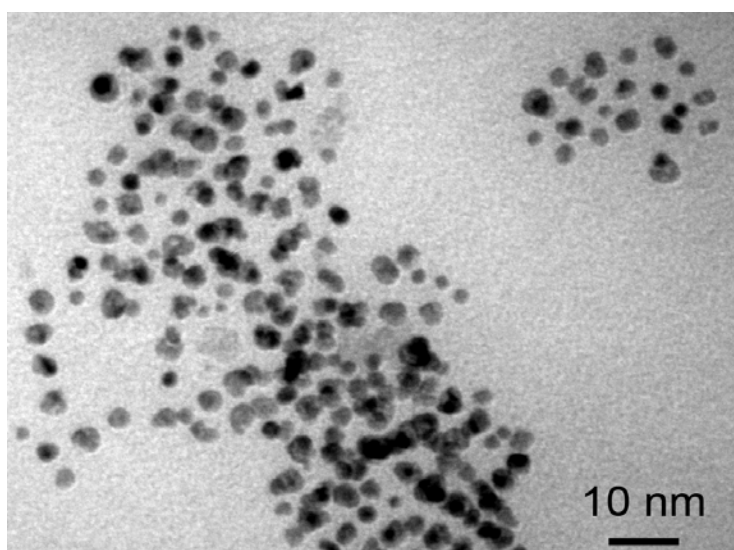


Fig.3. TEM image of the as-synthesized  $\text{Co}_{0.8}\text{Zn}_{0.2}\text{Fe}_2\text{O}_4$  sample.

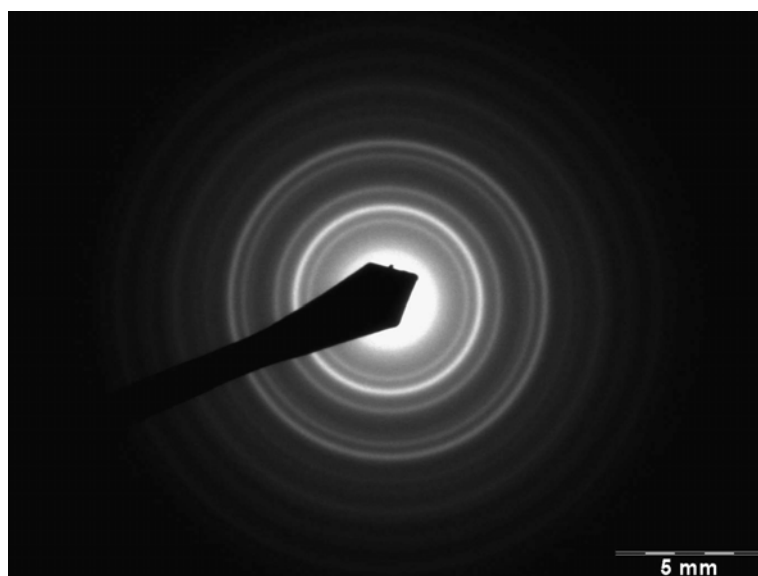


Fig.4. Electron diffraction pattern of the as-synthesized  $\text{Co}_{0.8}\text{Zn}_{0.2}\text{Fe}_2\text{O}_4$  sample.

The FT-IT spectra of all samples revealed the existence of some organic impurities on the surface of the particles. The main adsorbed organic species are acetate ion and 1,2-propanediol, both coming from the organic media used when preparing and washing the samples. These species seem to be strongly bonded (chemisorbed) to the oxide surface [6].

Under heat treatment at 500°C for 3 hours, most of the organic species was removed as evidenced by the disappearance of the absorption peaks in the FT-IR spectra. .

From Moessbauer spectroscopy studies at room temperature, a quadrupole doublet is obtained, indicating that the material at this temperature is superparamagnetic, which is in agreement with magnetic hysteresis measurements. At 4.2 K, the spectra can be fitted as the overlapping of two six-lines patterns with hyperfine fields  $H = 51.11$  and  $53.10$  Tesla, corresponding to  $\text{Fe}^{3+}$  ions in A (tetrahedral) and B (octahedral) spinel sites, respectively. The isomer shift ( $\delta$ ) and quadrupole splitting ( $\Delta$ ) for the A and B site are:  $\delta_A = 0.28$  mm/s,  $\Delta_A = -0.01$  mm/s and  $\delta_B = 0.37$  mm/s,  $\Delta_B = 0.09$  mm/s. These results are in agreement with those reported in literature [6], [18]. Zinc substitution showed only a minor influence on the quadrupole interaction, leading only to a slight asymmetry patterns of the Zn substituted samples.

The saturation magnetization  $M_s$  of  $\text{CoFe}_2\text{O}_4$ ,  $\text{Co}_{0.8}\text{Zn}_{0.2}\text{Fe}_2\text{O}_4$  and  $\text{Co}_{0.6}\text{Zn}_{0.4}\text{Fe}_2\text{O}_4$  determined from extrapolating the  $M$  (at 7 T) vs.  $1/H$  curve to  $1/H = 0$  are 72.1, 89.7 and 99.7 emu/g, respectively. The reason for the increase of  $M_s$  when increasing Zn substitution from  $x=0$  to  $x=0.4$  is:  $\text{Zn}^{2+}$  ions with zero magnetic moment replace ions on the tetrahedral A-sites, causing the decrease of magnetic moment in this sublattice,  $M_A$ , resulting in the increase of the total magnetic moment,  $M$ , since  $M = M_B - M_A$  where  $M_B$  is the magnetic moment of the sublattice formed by the octahedral B-sites [5]. On the other hand, the saturation magnetization of all three samples is smaller than that of the bulk sample with the same composition. For example, a  $\text{CoFe}_2\text{O}_4$  bulk sample prepared by citrate gel method has an  $M_s$  of  $\sim 80$  emu/g. The reduction of  $M_s$  may be related to the organic impurities absorbed on the surface of the particles which are seen by FT-IR spectra and the formation of a surface layer  $S_A$  of particles in which magnetic moments do not contribute to the magnetization in the applied field. However, the determined  $M_s$  value of  $\text{CoFe}_2\text{O}_4$  is still quite higher than that previously reported for nanoparticles of  $\text{CoFe}_2\text{O}_4$ , even with a bigger grain size, prepared by other methods: 45 emu/g at 20 K for  $\text{CoFe}_2\text{O}_4$  with average grain size of 5 nm [10], and 15 emu/g at 5 K for the average grain size of 4.7 nm [19]. This indicates that the samples prepared by the forced hydrolysis route might have a thinner  $S_A$ , e.g. a higher crystallinity or better quality, than those prepared by other methods.

The hysteresis loops measured at different temperatures indicate that at low temperature, all samples are ferrimagnetic, and at room temperature, they are superparamagnetic. Fig. 5 showed the hysteresis loops for the  $\text{Co}_{0.8}\text{Zn}_{0.2}\text{Fe}_2\text{O}_4$  sample. Similar loops were found for the other two samples. Both saturation magnetization and coercivity



decrease with the increasing temperature. Fig. 6 and Fig.7 show the temperature dependence of saturation magnetizations and coercivities of all samples, respectively.

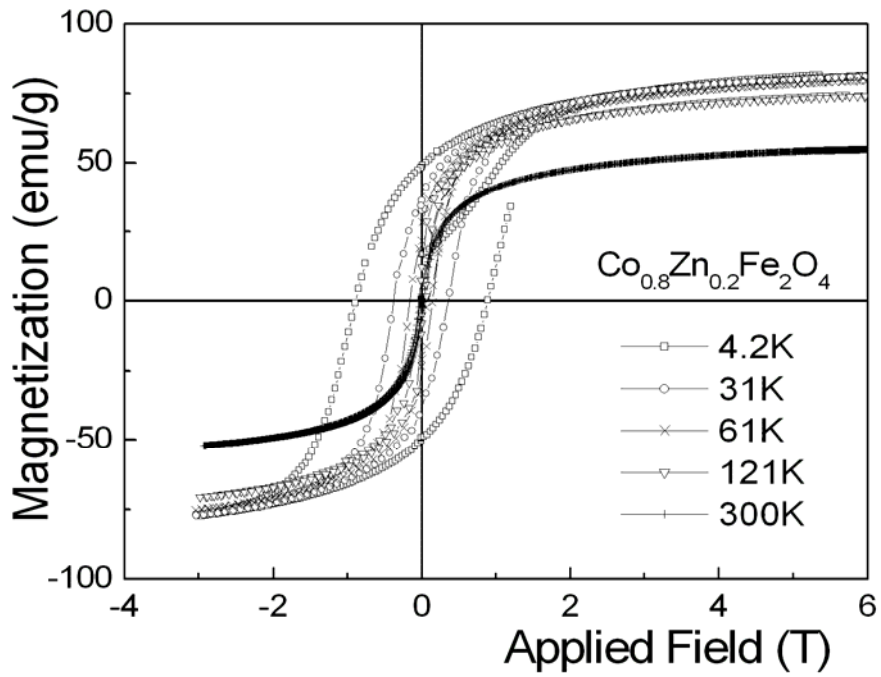


Fig.5. Hysteresis loops of the as-synthesized  $\text{Co}_{0.8}\text{Zn}_{0.2}\text{Fe}_2\text{O}_4$  sample measured at different temperatures.

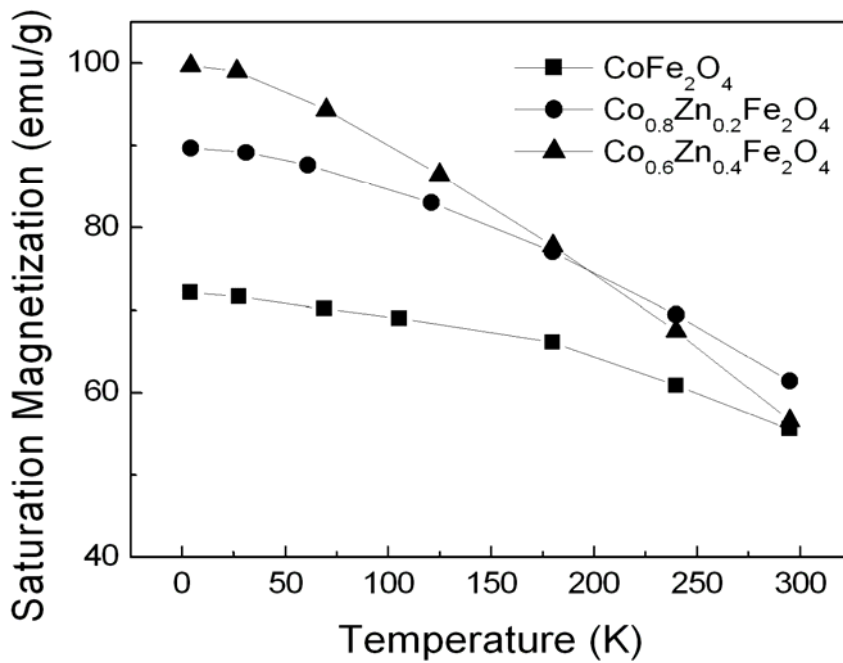


Fig.6. Temperature dependence of saturation magnetizations.

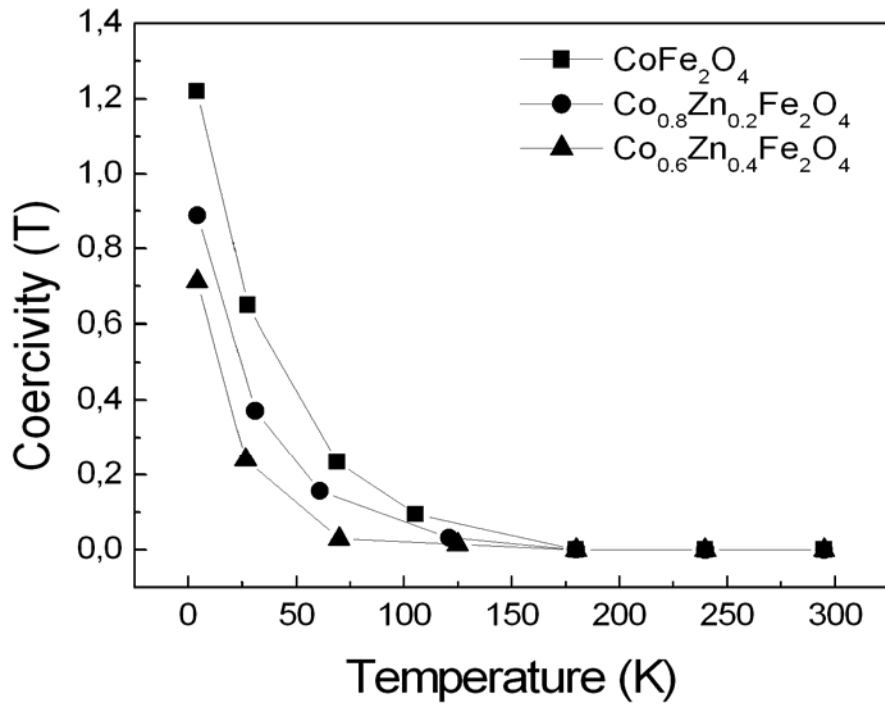


Fig.7. Temperature dependence of coercivities.

The saturation magnetizations at lower temperatures increase with increasing Zn substitution level. However, at room temperature, the  $M_s$  of the sample with  $x = 0.4$  becomes smaller than that of the sample with  $x = 0.2$ . The reason may be attributed to the spin canting effect in the Zn-rich sample [20], the decrease of Curie temperature,  $T_C$ , when increasing Zn substitution [21] and the faster decrease of the magnetization due to the lower blocking temperature in the sample with  $x=0.4$  as shown by the temperature dependent of ac-susceptibilities.

The blocking temperatures,  $T_B$ , were determined by the maxima of the in-phase components of the ac-susceptibility curves as function of temperature,  $\chi'$ .  $T_B$  becomes smaller with increasing Zn substitution. The maxima of the out-phase components,  $\chi''$ , correspond approximately to the inflection point of  $\chi'$ . The values of  $T_B$  for  $\text{CoFe}_2\text{O}_4$ ,  $\text{Co}_{0.8}\text{Zn}_{0.2}\text{Fe}_2\text{O}_4$  and  $\text{Co}_{0.6}\text{Zn}_{0.4}\text{Fe}_2\text{O}_4$  are 221, 202 and 142 K, respectively. As mentioned above, the smaller  $T_B$ , the spin canting effect [20] and the lower  $T_C$  [21] lead to the faster decrease of  $M_s$  in the Zn-rich sample, appearing as smaller  $M_s$  of the sample with  $x=0.4$  compared to that of the sample with  $x=0.2$ .

Let  $V_A$  be the volume of the magnetic disorder layers on the surface of the particle,  $V$  be the volume of the magnetic core,  $M_{s,n}$  and  $M_{s,b}$  be the saturation magnetization of the nanocrystalline and bulk samples, respectively, one can assume:

$$\frac{V_A}{V_A + V} = \frac{M_{s,n}}{M_{s,b}} \quad (3)$$

Using the grain size of 3 nm from our structural investigations, the thickness of the magnetic disorder surface layers is estimated to be about 0.12 nm for all samples. This value is smaller than one lattice constant, indicating that only part of the surface is magnetically disturbed by symmetry broken which leads to spin canting effect.

The coercive field  $H_c$  the cubic crystals of the non-interacting single-domain nanoparticles with a magnetic anisotropy  $K$  at temperatures below  $T_B$  is given by the well-known equation:

$$H_c = \alpha \frac{3K}{2\mu_0 M_s} \left[ 1 - \left( \frac{T}{T_B} \right)^{1/2} \right] \quad (4)$$

where  $\mu_0 M_s$  is the saturation magnetization and the constant  $\alpha = 1$ , if the particle easy axes are aligned or  $\alpha = 0.48$  if they are randomly oriented. Then, the coercive field of such assembly is expected to decay linear with the square root of temperature if  $K$  and  $M_s$  are constants, reaching zero in thermal equilibrium at  $T_B$ .

Using the experimental values of  $H_c$ ,  $M_s$  and  $T_B$ , the anisotropy constant  $K$  found to be  $8.01 \times 10^5$ ,  $7.79 \times 10^5$  and  $7.12 \times 10^5$  J/m<sup>3</sup>, for the samples with  $x = 0$ , 0.2 and 0.4, respectively. This decrease of anisotropy constant may explain the decrease of blocking temperature from 221 to 142 K when increasing Zn substitution level from  $x=0$  to  $x=0.4$ .

## 5. Conclusion

For the first time, zinc substituted cobalt ferrites,  $\text{Co}_{1-x}\text{Zn}_x\text{Fe}_2\text{O}_4$  ( $x=0, 0.2, 0.4$ ) with an average grain size of about 3 nm and a very narrow size distribution, were successfully synthesized by the forced hydrolysis method. The morphology, crystal structure and magnetic properties of the obtained materials have been studied. The high quality of these materials, e.g. monodispersed nanocrystallites, no detectable crystal defect, high saturation magnetization, suggests that this method is a promising route for preparing high quality nanocrystalline spinel ferrites which can be used for many practical applications such as ferrofluids, magnetic separation, magnetic drug delivery, hyperthermia, nanocatalyst.

## Acknowledgment

Many thanks to J. Fidler, H. Michor, M. Reissner, G. Wiesinger and R. Sato Turtelli for their kind help in experiments and fruitful discussions. This work is partly supported by the projects: Proj. 81.2004, FWF Proj. Nr. P16500-N02 and the Technology Grant Southeast Asia Program (ÖAD).

## References

- [1] K. Raj, R. Moskowitz, R. Casciari, J. Magn. Mater. 149 (1995) 174.
- [2] U. Häfelli, W. Schütt, J. Teller M. Zborowski, Scientific and Clinical Applications of Magnetic Carriers Plenum, New York, (1997).
- [3] M. H. Kryder, MRS Bull. 21 (1996) 917.
- [4] R. Valenzuela, Magnetic ceramics, Cambridge University Press, Cambridge (1984) 191-212.
- [5] Soshin Chikazumi, Physics of Ferromagnetism, 2<sup>nd</sup> edition, Oxford Science Publications (1997) 202-203.
- [6] S. Ammar, A. Helfen, M. Jouini, F. Fiévet, I. Rosenman, F. Villain, P. Molinié, M. Danot, J. Mater. Chem. 11 (2001) 186.
- [7] N. Hanh, O.K. Quy, N.P. Thuy, L.D. Tung, L. Spinu, Physica B: Condensed Matter. 327 (2003) 382.
- [8] T. Pannaparayil, S. Komarneni, IEEE Trans. Magn. 25 (1989) 4233.
- [9] F. Congiu, G. Concas, G. Ennas, A. Falqui, D. Fiorani, G. Marongiu, S. Marras, G. Spano, A.M. Alberto, M. Testa, J. Magn. Mater. 272-276 (2004) 1561.
- [10] N. Moumen, P. Veillet, M.P. Pileni. J. Magn. Mater. 149 (1995) 67.
- [11] F.X. Cheng, Z.Y. Peng, C.S. Liao, Z.G. Xu, S.Gao and C.H. Yan, Solid State Commun. 107 (1996) 471.
- [12] J. Gubicza, J. Szépövolgyi, I. Mohai, L. Zsoldos, T. Ungár, Mater. Sci. Eng. A280 (2000) 263.
- [13] B. E. Warren, Progr. Metal Phys. 8 (1959) 147.
- [14] J. Gubicza, J. Szépövolgyi, I. Mohai, G. Ribárik and T. Ungár, J. Mater. Sci., 35 (2000) 3711-3717.
- [15] J. Gubicza, N. H. Nam, L. Balogh, R. J. Hellmig, V. V. Stolyarov, Y. Estrin and T. Ungár, J. Alloys Compd. 378 (2004) 248-252.

- [16] C.E. Krill, R. Birringer, *Phil. Mag. A* 77 (1998) 621.
- [17] G. Ribárik, J. Gubicza, T. Ungár, *Mater. Sci. Eng. A* 387-389 (2004) 343.
- [18] N. Moumen, P. Bonville and M. P. Pileni, *J. Phys. Chem.* 100 (1996) 14410.
- [19] M. Grigorova, H.J. Blythe, V. Blaskov, V. Rusanov, V. Petkov, V. Masheva, D. Nihtianova, L.I.M. Martinez, J.S. Muñoz, M. Mikhov, *J. Magn. Magn. Mater.* 183 (1998) 163.
- [20] Y. Yafet, C. Kittel, *Phys. Rev.* 87 (1952) 290.
- [21] R. Arulmurugan, G. Vaidyanathan, S. Sendhilnathan and B. Jeyadevan, *J. Magn.* 303 (2006) 131.

## Magnetic properties of nanocrystalline $\text{Co}_{1-x}\text{Zn}_x\text{Fe}_2\text{O}_4$ prepared by forced hydrolysis method.

Giap.V. Duong<sup>a,b</sup>, R. Sato Turtelli<sup>b</sup>, N. Hanh<sup>a</sup>, D.V. Linh<sup>a</sup>, M. Reissner<sup>b</sup>,  
H. Michor<sup>b</sup>, J. Fidler<sup>b</sup>, G. Wiesinger<sup>b</sup>, R. Grössinger<sup>b</sup>

<sup>a</sup>*Faculty of Chemical Engineering, Hanoi University of Technology,  
No.1 Dai Co Viet, Hai Ba Trung, Hanoi, Vietnam*

<sup>b</sup>*Institute of Solid State Physics, Vienna University of Technology  
Wiedner Hauptstrasse 8-10, A-1040, Vienna, Austria*

Received 5 December 2005, received in revised form 24 March 2006,

Available online 19<sup>th</sup> May 2006.

---

### Abstract

Nanocrystalline zinc-substituted cobalt ferrite powders,  $\text{Co}_{1-x}\text{Zn}_x\text{Fe}_2\text{O}_4$  ( $x = 0; 0.2; 0.4$ ), were for the first time prepared by forced hydrolysis method. Magnetic and structural properties in these specimens were investigated. The average crystallite size is about 3.0 nm. When the zinc substitution increases from  $x = 0$  to  $x = 0.4$ , at 4.2K, the saturation magnetization increases from 72.1 to 99.7 emu/g and the coercive field decreases from 1.22 to 0.71 T. All samples are superparamagnetic at room temperature and ferrimagnetic at temperatures below the blocking temperature. The high value of the saturation magnetization and the very thin thickness of the disorder surface layer of all samples suggest that this forced hydrolysis method is suitable not only for preparing two metal element systems but also for three or more ones.

© 2006 Elsevier B.V. All rights reserved

PACS: 75.50.Tt; 75.60.Ej, 75.75.+a; 61.16.Bg

Keywords: Fine particles, Ferrite, superparamagnetism, forced hydrolysis method, hysteresis loops.

---

## 1. Introduction

There is an increasing interest in magnetic nanoparticles, due to both the broad practical applications in several important technological fields such as ferrofluids, magnetic drug delivery, high-density information storage [1-3], and fundamental understanding of unusual properties of nanoparticles compared to those of bulk samples. Among these materials, nanocrystalline  $\text{CoFe}_2\text{O}_4$  receives much attention due to remarkable properties observed in bulk samples, such as high saturation magnetization,  $M_s$ , high coercivity,  $H_c$ , strong anisotropy along with good mechanical hardness and chemical stability [4].

Many methods have been developed to prepare nanocrystalline  $\text{CoFe}_2\text{O}_4$ , namely: co-precipitation [5], mechano-chemical [6], combustion [7], micro-emulsion [8], redox process [9], ion exchange [10], hydrothermal [11], sol-gel [12], forced hydrolysis [13, 14]. Among them, the forced hydrolysis method seems to be one of the best methods since it allows the preparation of nanocrystalline  $\text{CoFe}_2\text{O}_4$  with an equiaxial shape and narrow size distribution with high saturation magnetization and coercivity [13, 14]. However, all studies concerning forced hydrolysis reported until now are limited to one or two metal element systems. No papers on three metal element systems have been reported yet. Therefore, in this work we investigate magnetic and structural properties of zinc-substituted nanocrystalline cobalt ferrites, which are three metal element systems, prepared by forced hydrolysis method. The obtained ferrites consist of particles with an average size of 3.0 nm. At very low temperatures, an increase in saturation magnetization with Zn content was observed.

## 2. Experimental Methods

### 2.1. Sample preparation

The precursor salts,  $\text{Fe}(\text{NO}_3)_3 \cdot 9\text{H}_2\text{O}$ ,  $\text{Zn}(\text{NO}_3)_2 \cdot 6\text{H}_2\text{O}$  and  $\text{Co}(\text{CH}_3\text{COO})_2 \cdot 4\text{H}_2\text{O}$ , all with analytical purity, were added to 250 ml of 1,2-propanediol in stoichiometric ratio. The total metal concentration was 0.3 mol/l. The hydrolysis ratio (molar ratio between water and metal ions) and the amount of acetate (molar ratio between acetate and metal ions) were fixed to 9 and 3, respectively. The starting mixture containing the salts, deionized water, sodium acetate and 1,2-propanediol was heated to 160 °C with a heating rate of 10 °C/min. A black colloidal suspension achieved after refluxing the mixture for 5h was kept at 100 °C in air for

12 h. The particles, separated from the suspension by centrifugation, were washed for several times with water and ethanol. The resultant powders were then dried at 50 °C in air.

## 2.2. Structural and magnetic characterization

X-ray diffraction (XRD) patterns of the as-prepared powders were obtained using  $\text{CoK}_\alpha$  radiation. To estimate the crystallite size, the Scherrer equation for the full-width at half maximum (FWHM) of the strongest reflection was employed [15]:

$$D = K\lambda / \beta \cos\theta, \quad (1)$$

where  $D$  is the crystallite size,  $K$  is the shape function for which a value of 0.9 is used [15],  $\beta$  is the width of the pure diffraction profile and  $\theta$  is the angle of incidence.

The powder morphology was also investigated using a high-resolution transmission electron microscope, (JEOL 2000FX).

The blocking temperature was determined from the temperature dependence of the initial ac-susceptibility,  $\chi_i$ . Measurements of  $\chi_i$  were carried out at temperatures between 4.2 and 300 K in an ac-magnetic field of 200 A/m with a frequency of 1 kHz. The temperature dependence of the magnetization and the hysteresis loops were measured by means of a VSM magnetometer with maximum applied field of  $\mu_0 H = 7$  T. The  $^{57}\text{Fe}$  Mössbauer measurements were carried out in transmission geometry at 4.2 K and at room temperature using a constant acceleration type spectrometer with a  $^{57}\text{Co}(\text{Rh})$  source with an activity of about 20 mCi ( $7.4 \cdot 10^8$  Bq). The data were analyzed applying a fitting routine assuming a discrete superposition of discrete sextets (doublets). The isomer shift values are given relative to the source material.

## 3. Results

XRD patterns of prepared samples obtained at room temperature are shown in Fig. 1. All peaks are characteristics for the cubic structure and spinel-type lattice of cobalt ferrite. The absence of extra lines in the diffraction patterns ensures the phase purity. The peaks are relatively broad indicating that the materials exhibit a very small average particles size. Using Equation (1) and the width of the strongest peak, average grain size is estimated obtaining a value of  $3.5 \pm 0.5$  nm for all samples.



A TEM image of the  $\text{Co}_{0.8}\text{Zn}_{0.2}\text{Fe}_2\text{O}_4$  sample is shown in Fig. 2. It is clear that the size of most particles is in the range of  $D = 2 - 3.1$  nm, resulting in a narrow size distribution with an average particle size of about 2.7 nm. Particles sizes determined from TEM are not so far from those obtained from the XRD measurements, suggesting that the materials are single nano-particles and can exhibit superparamagnetic behavior.

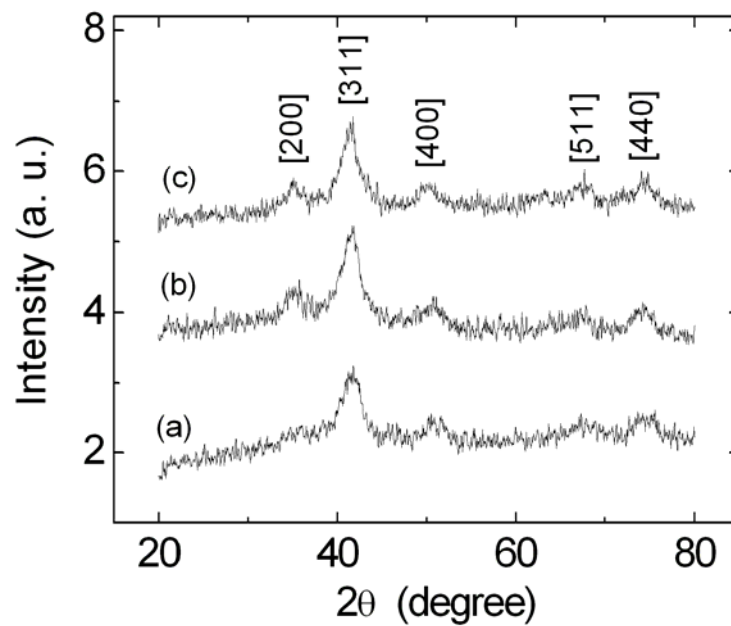


Fig.1. XRD patterns obtained at room temperature on powders of: (a)  $\text{CoFe}_2\text{O}_4$ ; (b)  $\text{Co}_{0.8}\text{Zn}_{0.2}\text{Fe}_2\text{O}_4$  and (c)  $\text{Co}_{0.6}\text{Zn}_{0.4}\text{Fe}_2\text{O}_4$ .

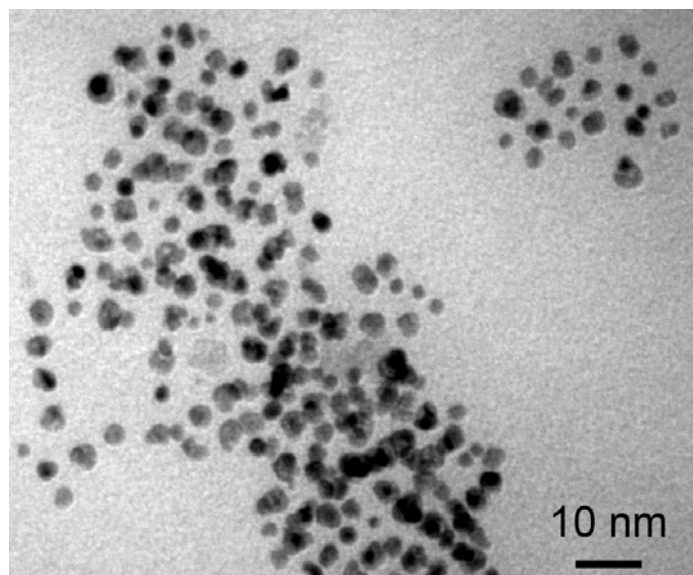


Fig.2. TEM image of  $\text{Co}_{0.8}\text{Zn}_{0.2}\text{Fe}_2\text{O}_4$  sample.

Fig. 3 shows the temperature dependence of the ac-susceptibility measured on the samples with  $x = 0, 0.2$  and  $0.4$ . The in-phase component  $\chi'$ , represented by full symbols, of all samples exhibits a maximum at a certain temperature  $T_B$  (blocking temperature). The position of  $T_B$  changes to lower temperatures with increasing Zn concentration. The maximum of the out-phase component  $\chi''$  (open symbols) corresponds approximately to the inflection point of  $\chi'$ . The values of  $T_B$  for  $\text{CoFe}_2\text{O}_4$ ,  $\text{Co}_{0.8}\text{Zn}_{0.2}\text{Fe}_2\text{O}_4$  and  $\text{Co}_{0.6}\text{Zn}_{0.4}\text{Fe}_2\text{O}_4$  are 221, 202 and 142 K, respectively. The  $T_B$  value of  $\text{CoFe}_2\text{O}_4$  reported by S. Ammar et al [13] at 300 K is higher probably due to larger grain size.

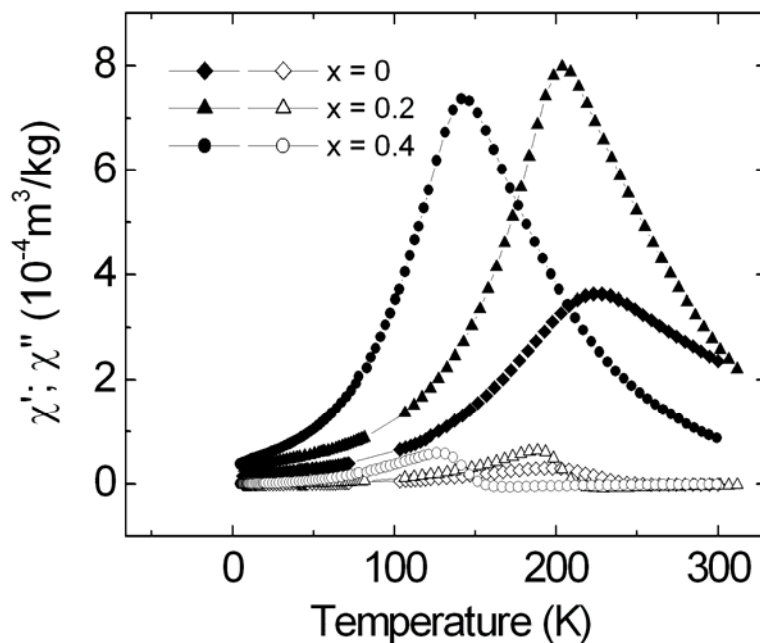


Fig.3. Temperature dependence of  $\chi'$  (full symbols) and  $\chi''$  (open symbols) measured on the  $\text{Co}_{1-x}\text{Zn}_x\text{Fe}_2\text{O}_4$  samples with  $x = 0, 0.2$  and  $0.4$ .

Typical hysteresis loops measured at different temperatures are shown in Fig. 4 for sample  $\text{Co}_{0.6}\text{Zn}_{0.4}\text{Fe}_2\text{O}_4$ . Similar loops were found for the other two samples. In fact, the magnetization curves measured at temperatures above  $T_B$  present superparamagnetic behavior.

The temperature dependencies of the magnetization measured in applied magnetic field of 7 T are shown in Fig. 5. In fact, the magnetization at lower temperatures increases with increasing Zn content. However, at room temperature, the magnetization of the sample with  $x = 0.4$  becomes smaller than that of the sample with  $x = 0.2$ . As can be seen in Fig. 5, the decrease of the magnetization with increasing temperature is much faster in

$\text{Co}_{0.6}\text{Zn}_{0.4}\text{Fe}_2\text{O}_4$  (which exhibits a smaller  $T_B$ ) than that in other samples, which results in the smaller magnetization at higher temperatures.

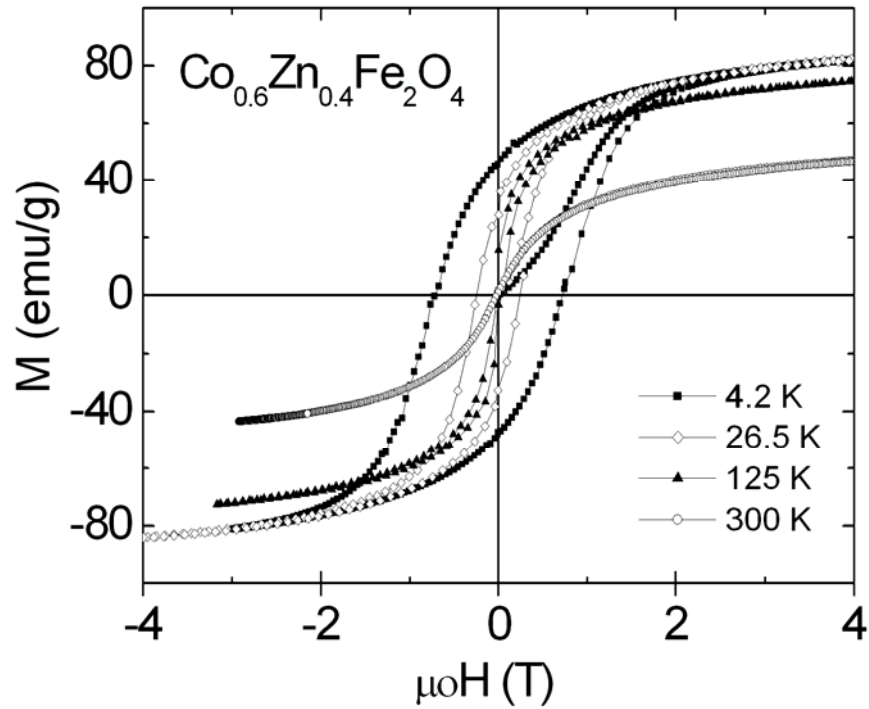


Fig.4. Hysteresis loops of the sample with  $x = 0.4$  measured at different temperatures.

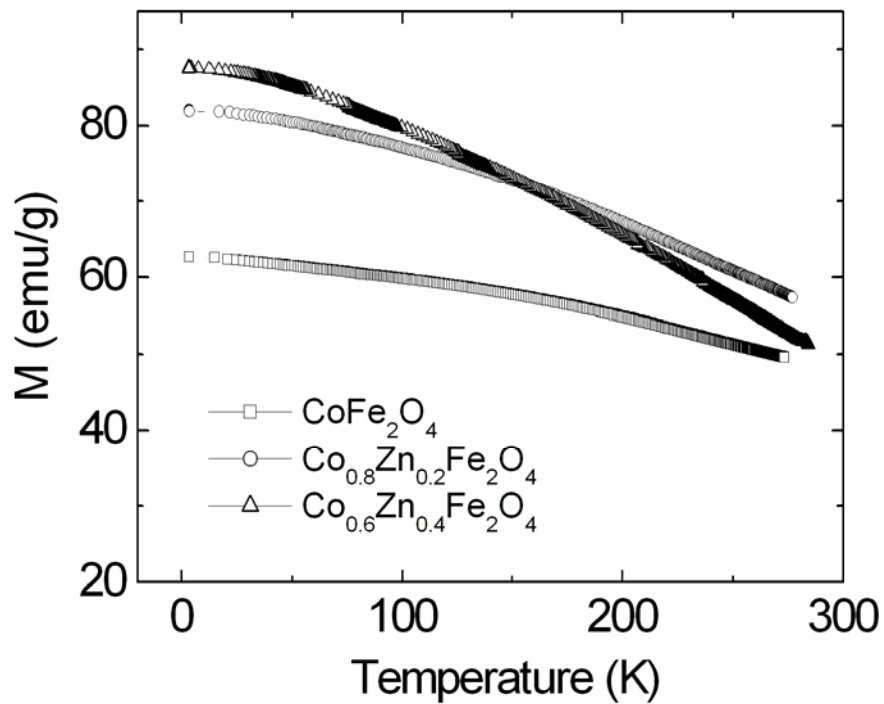
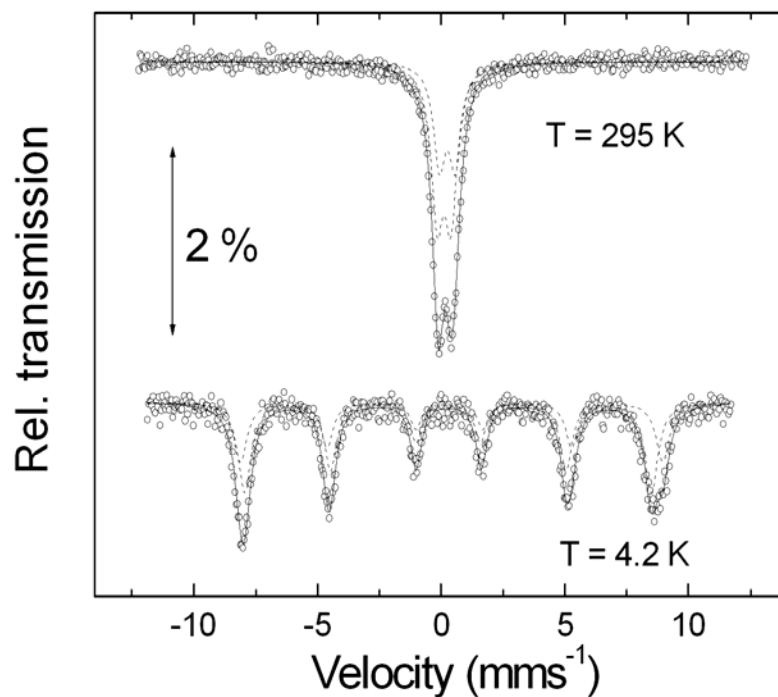


Fig.5. Temperature dependence of the magnetization measured with applied field of 7 T.

Mössbauer spectra, taken from the compound  $\text{Zn}_{0.2}\text{Co}_{0.8}\text{Fe}_2\text{O}_4$ , are displayed in Fig. 6. At room temperature a quadrupole doublet is obtained, indicating that the material at this temperature is superparamagnetic, which is in agreement with magnetic hysteresis measurements. If the present spectrum is compared with those displayed in [16], only a minor influence of Zn-doping on the quadrupole interaction is seen, leading only to a slight asymmetry of the pattern. As already shown in [16], a successful fit can be performed using an area ratio of 2:3 for the (tetrahedral) A site to the (octahedral) B site. If the absorption areas were allowed to vary, only weak changes were observed for the hyperfine parameters and the area ratio. Despite the presence of two lattice sites the Mössbauer pattern recorded at liquid helium temperature does not show a distinct splitting of the utmost lines. It resembles the spectrum recorded from  $\text{CoFe}_2\text{O}_4$  with a particle size of 5 nm [16]. Most probably the reduced resolution must be attributed to the influence of the varying local environment of the Mössbauer nucleus upon the nuclear Zeeman effect due to Zn doping which is more sensitive than the electrostatic quadrupole interaction. Since the reduction of the hyperfine field is below the resolution of the experiment, it manifests itself by a significant line broadening. The magnetic hyperfine fields are essentially unchanged compared to the undoped compound with a particle size of 5 nm [16] (table 1).



Fi.g. 6.  $^{57}\text{Fe}$  Moessbauer spectrum of  $\text{Co}_{0.8}\text{Zn}_{0.2}\text{Fe}_2\text{O}_4$  sample.

Table I. Hyperfine parameters (isomer shift  $\delta$ , quadrupole splitting  $\Delta$ , hyperfine field  $B_{\text{hf}}$ ) of  $\text{Co}_{0.8}\text{Zn}_{0.2}\text{Fe}_2\text{O}_4$  sample.

Temperature (K)	$\delta_A$ (mm/s)	$\delta_B$ (mm/s)	$\Delta_A$ (mm/s)	$\Delta_B$ (mm/s)	$B_{\text{hf}A}$ (T)	$B_{\text{hf}B}$ (T)
4.2	0.28	0.37	- 0.01	0.09	51.11	53.10
295	0.12	0.25	0.46	0.64	-	-

#### 4. Discussion

At room temperature, all samples behave as superparamagnetic materials. Below the blocking temperatures they show ferrimagnetic ordering [14].

As was mentioned before, at 4.2 K, the magnetization at 7 T increases with increasing Zn concentration. The saturation magnetization  $M_s$  of  $\text{CoFe}_2\text{O}_4$ ,  $\text{Co}_{0.8}\text{Zn}_{0.2}\text{Fe}_2\text{O}_4$  and  $\text{Co}_{0.6}\text{Zn}_{0.4}\text{Fe}_2\text{O}_4$  determined from extrapolating the  $M$  (at 7 T) vs.  $1/H$  curve to  $1/H = 0$  are 72.1, 89.7 and 99.7 emu/g, respectively. The phenomenon of an increasing  $M_s$  in Co, Mn or Ni ferrites, when small quantities of Zn are added, is already well known [17].  $\text{Zn}^{2+}$  ions with zero moment replace ions on the tetrahedral A-sites. However, in this work, the expected variation of lattice constant and hyperfine field could not be detected by means of the XRD and Mössbauer experiments, respectively. It seems that these variations are below the resolution of the experiments.

On the other side, the saturation magnetization of all three samples is smaller than that of the bulk ones of the same composition. Using Sol-gel process, we obtained  $M_s$  values of 86 and 125 emu/g for  $\text{CoFe}_2\text{O}_4$  and  $\text{Co}_{0.7}\text{Zn}_{0.3}\text{Fe}_2\text{O}_4$ , respectively. The reduction of  $M_s$  may be related to the formation of a surface layer  $S_A$  of particles in which magnetic moments do not contribute to the magnetization in the applied field. However, the determined  $M_s$  value of  $\text{CoFe}_2\text{O}_4$  is still quite higher than that previously reported for nanoparticle of  $\text{CoFe}_2\text{O}_4$  prepared by other methods, e. g., 45 emu/g at 20 K [8], and 15 emu/g at 5 K [18]. This indicates that the samples prepared by the forced hydrolysis might have a thinner  $S_A$  than that prepared by other methods.

Generally, the magnetic behavior of noninteracting single-domain nanoparticles with a magnetic anisotropy  $K$  is understood on the basis of the well-known Néel relaxation relation

$$\tau = \tau_0 e^{KV/k_B T}, \quad (2)$$

where  $V$  is the particle volume,  $k_B$  the Boltzmann constant and  $\tau_0$  is an intrinsic time constant of the order of  $10^{-9} - 10^{-12}$  s.  $KV$  represents the energy barrier between two easy directions. For identical, isolated and mono-domain particles, a critical temperature, called the blocking temperature  $T_B$  is predicted:

$$T_B = \frac{KV}{\ln\left(\frac{t}{\tau_0}\right)k_B}, \quad (3)$$

where  $t$  is the characteristic time of the experiment. Above  $T_B$ , the magnetization reversal changes from blocked (showing hysteresis) to superparamagnetic-type behavior. Within this framework, for temperatures below  $T_B$ , the coercive field of cubic crystals is given by the well-known relation

$$H_c = \alpha \frac{3K}{2\mu_0 M_s} \left[ 1 - \left( \frac{T}{T_B} \right)^{1/2} \right], \quad (4)$$

where  $\mu_0 M_s$  is the saturation magnetization and the constant  $\alpha = 1$ , if the particle easy axes are aligned or  $\alpha = 0.48$  if they are randomly oriented. Then, the coercive field of such assembly is expected to decay linear with the square root of temperature (if  $K$  and  $M_s$  are constants), reaching zero in thermal equilibrium at  $T_B$ .

Coercive field as function of the square root of  $T$  is shown in Fig. 7. For  $T < T_B/3$  where the saturation magnetization with the temperature is almost constant (see Fig. 5), the linearity between  $H_c$  and  $T^{1/2}$  can be assumed, although few hysteresis loops were measured between 4.2 and  $T_B$ . Then, assuming that  $H_c$  is proportional to  $T^{1/2}$  at very low temperatures, the anisotropy constant of each specimen was determined from the linear coefficient of the equation (4). As result, we obtain  $K$  decreasing with increasing zinc content, namely:  $8.01 \times 10^5$ ,  $7.79 \times 10^5$  and  $7.12 \times 10^5$  J/m<sup>3</sup>, for the samples with  $x = 0, 0.2$  and  $0.4$ , respectively.

From equations (3) and (4) one can see that blocking temperature and coercive field of nano-materials depend on both intrinsic and extrinsic factors. From our structural investigations, we can assume that the thickness of  $S_A$  (about 0.12 nm, estimated from the ratio between the volume of magnetic core and the total volume of the particle being equal to the ratio between the measured saturation magnetization of nano-particles and that  $M_s$  of the bulk sample, and assuming spherical particles) and the particles shape and size of all three samples are similar. Consequently, the variation of the blocking temperature with the substitution of cobalt by zinc may arise from magnetocrystalline anisotropy change.

The blocking temperature as function of the anisotropy is given in Fig. 8. A linearity between  $T_B$  and  $K$  is found, indicating that in our investigations we can really consider that all samples exhibit similar particles in the size and shape.

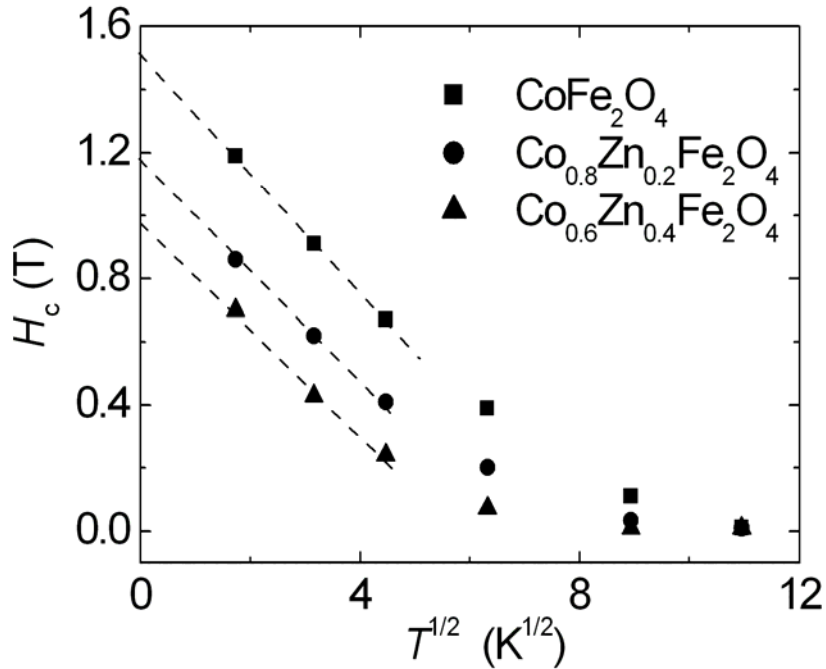


Fig.7. Coercivity as function of the square root of temperature obtained in  $\text{CoFe}_2\text{O}_4$ ,  $\text{Co}_{0.8}\text{Zn}_{0.2}\text{Fe}_2\text{O}_4$  and  $\text{Co}_{0.6}\text{Zn}_{0.4}\text{Fe}_2\text{O}_4$ .

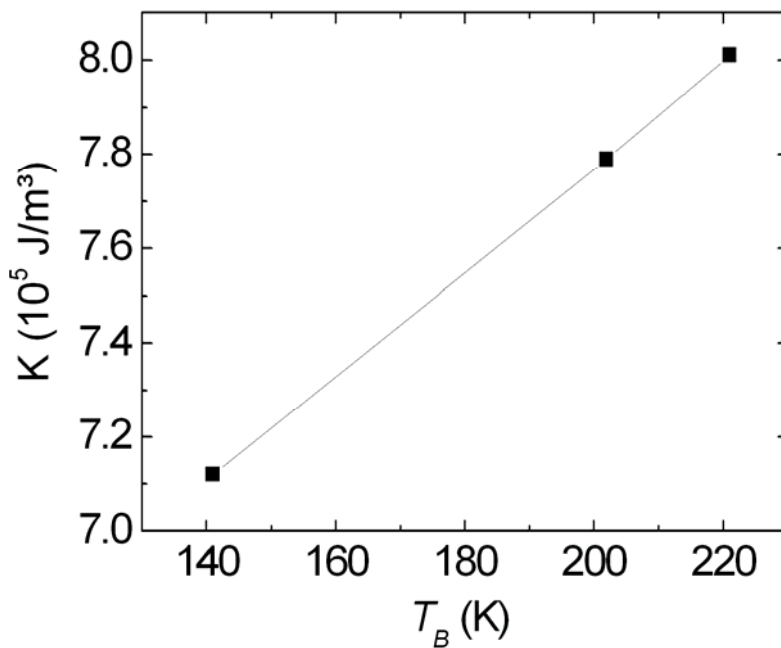


Fig.8. Magnetocrystalline anisotropy  $K$  dependence of the blocking temperature of the samples with  $x = 0, 0.2$  and  $0.4$ .

## 5. Conclusion

For the first time, zinc substituted cobalt ferrites were synthesized by forced hydrolysis method. This suggests that this method is suitable not only to synthesize two metal systems but also systems containing three metals. All samples show a well nano-crystallized state, with an average particle size of around 3.1 nm. When substituting cobalt by zinc, the magnetization increases, but the coercivity, the blocking temperature and the anisotropy constant decrease with increasing substitution level.

## Acknowledgments

The Austrian Exchange Service (ÖAD) is grateful for financial supporting one of the authors.

## References

1. K. Raj, R. Moskowitz, R. Casciari, *J. Magn. Magn. Mater.* 149 (1995) 174.
2. U. Häfelli, W. Schütt, J. Teller M. Zborowski, *Scientific and Clinical Applications of Magnetic Carriers* Plenum, New York, (1997).
3. M. H. Kryder, *MRS Bull.* 21 (1996) 917.
4. R. Valenzuela, *Magnetic ceramics*, Cambridge University Press, Cambridge, (1984), p. 212.
5. T. Pannaparayil, S. Komarneni, *IEEE Trans. Magn.* 25 (1989), 4233.
6. F. Congiu, G. Concas, G. Ennas, A. Falqui, D. Fiorani, G. Marongiu, S. Marras, G. Spano, A.M. Alberto, M. Testa, *J. Magn. Magn. Mater.* 272-276 (2004) 1561.
7. C.H. Yan, Z.G. Xu, F.X. Cheng, Z.M. Wang, L.D. Sun, C.S. Liao and J.T. Jia, *Solid State Commun.* 111 (1999) 287.
8. N. Moumen, P. Veillet, M.P. Pileni. *J. Magn. Magn. Mater.* 149 (1995), 67.
9. M. Rajendran, R.C. Pullar, A.K. Bhattacharya, D. Das, S.N. Chintalapudi, C.K. Majumdar, *J. Magn. Magn. Mater.* 232 (2001) 71.
10. R.F. Ziolo, E.P. Giannelis, B.A. Weinstein, M.P. O'Horo, B.N. Ganguly, V. Mehrotra, M.W. Russell, D.R. Huffman, *Science* 257 (1992) 5067.
11. L.J. Cote, A.S. Teja, A.P. Wilkinson, Z. John Zhang, *Fluid Phase Equilibria* 210, (2003), 307.



12. F.X. Cheng, Z.Y. Peng, C.S. Liao, Z.G. Xu, S.Gao and C.H. Yan, *Solid State Commun.* 107 (1996) 471.
13. S. Ammar, A. Helfen, M. Jouini, F. Fiévet, I. Rosenman, F. Villain, P. Molinié, M. Danot, *J. Mater. Chem.* 11 (2001) 186.
14. N. Hanh, O.K. Quy, N.P. Thuy, L.D. Tung, L. Spinu, *Physica B: Condensed Matter* 327, (2003) 382.
15. H.G. Jiang, M. Rühle, E.J. Lavernia, *J. Mater. Res.* 14, 2 (1999), 549.
16. N. Moumen, P. Bonville, M.P. Pileni, *J. Phys. Chem.* 100 (1996) 14410.
17. Soshin Chikazumi, *Physics of Ferromagnetism*, 2<sup>nd</sup> edition, Oxford Science Publications (1997) 197-221.
18. M. Grigorova, H.J. Blythe, V. Blaskov, V. Rusanov, V. Petkov, V. Masheva, D. Nihtianova, L.I.M. Martinez, J.S. Muñoz, M. Mikhov, *J. Magn. Magn. Mater.* 183 (1998) 163.

# Ultrafine $\text{Co}_{1-x}\text{Zn}_x\text{Fe}_2\text{O}_4$ particles synthesized by forced hydrolysis: Effect of thermal treatment and its relationship with magnetic properties

Giap V. Duong<sup>1,2</sup>, R. Sato Turtelli<sup>1</sup>, W. Nunes<sup>3</sup>, E. Schafler<sup>4</sup>, N. Hanh<sup>2</sup>,  
R. Grössinger<sup>1</sup>, M. Knobel<sup>3</sup>

<sup>1</sup>*Instut. F. Festkörperphysik, T.U. Wien, Wiedner Hauptstr. 8-10, A-1040, Wien, Austria*

<sup>2</sup>*Faculty of Chemical Engineering, Hanoi Uni. Techn., 1 Dai Co Viet, Hanoi, Vietnam*

<sup>3</sup>*Instituto de Física - Universidade Estadual de Campinas, CP 6165, Campinas, Brasil*

<sup>4</sup>*Dept. Mater. Phys., Faculty of Phys., Uni. Vienna, Boltzmannng. 5, 1090, Vienna, Austria*

Accepted September 12<sup>th</sup>, 2006.

---

## Abstract

$\text{Co}_{1-x}\text{Zn}_x\text{Fe}_2\text{O}_4$  ( $x = 0, 0.2$  and  $0.4$ ) fine powders with particles size of 3 nm were prepared by hydrolysis method. The powders were annealed at 500 °C for 3 h. With heat treatment, the average particles size increased to 12 nm with corresponding increase in blocking temperature, saturation magnetization and reduced remanence. A significant increase in coercive field was found only for the pure  $\text{CoFe}_2\text{O}_4$ .

*PACS codes:* 75.50.Tt; 75.60.Ej; 75.75.+a

*Keywords:* Magnetic materials; nanocrystalline; forced hydrolysis; cobalt ferrite; zinc substitution; thermal treatment

---

Co ferrite,  $\text{CoFe}_2\text{O}_4$  is an oxide with a spinel structure and exhibits a very high cubic magnetocrystalline anisotropy and a reasonable saturation magnetization,  $M_s$ . The effect of  $\text{Co}^{2+}$  ions is great because the orbital angular momentum in octahedral sites is not fully quenched by the electric crystal field. Their moments are hence coupled strongly to the trigonal [111] axis of the crystal field producing a strong uniaxial anisotropy superposed on the weak cubic anisotropy. High anisotropy and high  $M_s$  make  $\text{CoFe}_2\text{O}_4$  a promising material for isotropic permanent magnet, magnetic recording and magnetic fluids. When a small quantity of Zn substitutes Co atoms in  $\text{CoFe}_2\text{O}_4$ , the  $M_s$  increases and the coercivity,  $H_c$ , decreases [1]. Then, the use of  $\text{Co}_{1-x}\text{Zn}_x\text{Fe}_2\text{O}_4$  system allows the tailoring of the magnetic properties by changing the cobalt content, which can be very useful in applications. For such applications it is necessary to produce stable single-domain particles.

Ultra fine  $\text{CoFe}_2\text{O}_4$  particles have been produced by a variety of synthesis methods: forced hydrolysis [2], micro-emulsion [3], calcinations [4], and combustion [5], etc. The results suggest that the magnetic characteristics depend not only on the particle size but also on the method of preparation. Significantly better magnetic properties have been in ferrites synthesized by forced hydrolysis than that prepared by the other methods, where the fine particles exhibit a thin disordered surface layer,  $SL$ . [2].

Recently, the ultra-fine particles of three metal element systems of  $\text{Co}_{1-x}\text{Zn}_x\text{Fe}_2\text{O}_4$  ( $x = 0.2; 0.4$ ), for the first time, were produced by forced hydrolysis method by us [1]. The average grain size  $D$  is of 3 nm and the particles behave superparamagnetically at room temperature. At temperatures  $T < T_B$  (blocking temperature), the  $M_s$  of ferrimagnetic phase increases from 72.1 to 99.7 emu/g and the  $H_c$  decreases from 1.22 to 0.71 T, as Zn content varies from  $x = 0$  to  $x = 0.4$ . The reduced remanence,  $M_r$ , lied around 0.6 [1]. These values are still low in comparison with the bulk material. Therefore, the aim of the present work is to investigate magnetic properties of the annealed  $\text{Co}_{1-x}\text{Zn}_x\text{Fe}_2\text{O}_4$  ( $x = 0; 0.2; 0.4$ ) powders consisting of fine particles with an increased average grain size to  $\sim 12$  nm. The magnetic properties will be compared to the results found in the as-produced samples.

The  $\text{Co}_{1-x}\text{Zn}_x\text{Fe}_2\text{O}_4$  with  $x = 0, 0.2$  and  $0.4$  particles with  $D = (3 \pm 0.5)$  nm were prepared by forced hydrolysis method as described elsewhere [1]. To modify the grain size of the nanoparticles, the powders were thermally treated at  $500^\circ\text{C}$  for 3 hours. Structural characterizations of the samples were performed recording X-ray diffraction patterns from a double crystal diffractometer with negligible instrumental broadening. A fine focus rotating cobalt anode (Nonius FR 591) was operated as a line focus at 36 kV and 50 mA ( $\lambda=0.1789$

nm). Using a Ge monochroator and a slit the  $K_\beta$  as well as the  $K_{\alpha 2}$  component were removed. The scattered radiation was registered in reflection by a linear position sensitive X-ray detector of type OED-50 (Braun, Munich) installed at distance of 450 mm from the sample. The average grain sizes and the grain-size distribution were estimated by fitting the Fourier transforms of the theoretical functions of size and strain to the experimental profiles [6].

Magnetization ( $M$ ) loops with maximum applied field of 63 kOe were performed in a commercial superconducting quantum interference device (SQUID) magnetometer (quantum Design MPMS XL7) in the temperature range 3 - 300 K.

Figure 1 shows X-ray pattern obtained for annealed (AN) sample of  $\text{CoFe}_2\text{O}_4$ . Very similar patterns were obtained for the other two samples. The measured pattern is represented by open circles and the fitting by a solid curve. The estimated  $D$  for all AN samples was of  $(12.0 \pm 0.5)$  nm.

The temperature dependence of the coercive field,  $H_c(T)$ , measured for all samples is shown in Fig. 2. After a thermal treatment, a significant increase of  $H_c$  at 3 K was found only for the nanocrystalline  $\text{CoFe}_2\text{O}_4$  exhibiting a value of  $H_c = 1.87$  T. The  $H_c$  value of the as-produced (AP) sample is 1.2 T. At 3 K, with annealing, no change in the  $H_c$  value was found for  $\text{Co}_{0.8}\text{Zn}_{0.2}\text{Fe}_2\text{O}_4$ , keeping a value of  $H_c = 0.86$  T. On the other hand, the annealing has caused a significant decrease of the  $H_c$  in the sample with  $x = 0.4$ , changing from 0.7 T (before annealing) to 0.44 T (after annealing). However, at 300 K, all AN samples exhibit magnetic hysteresis

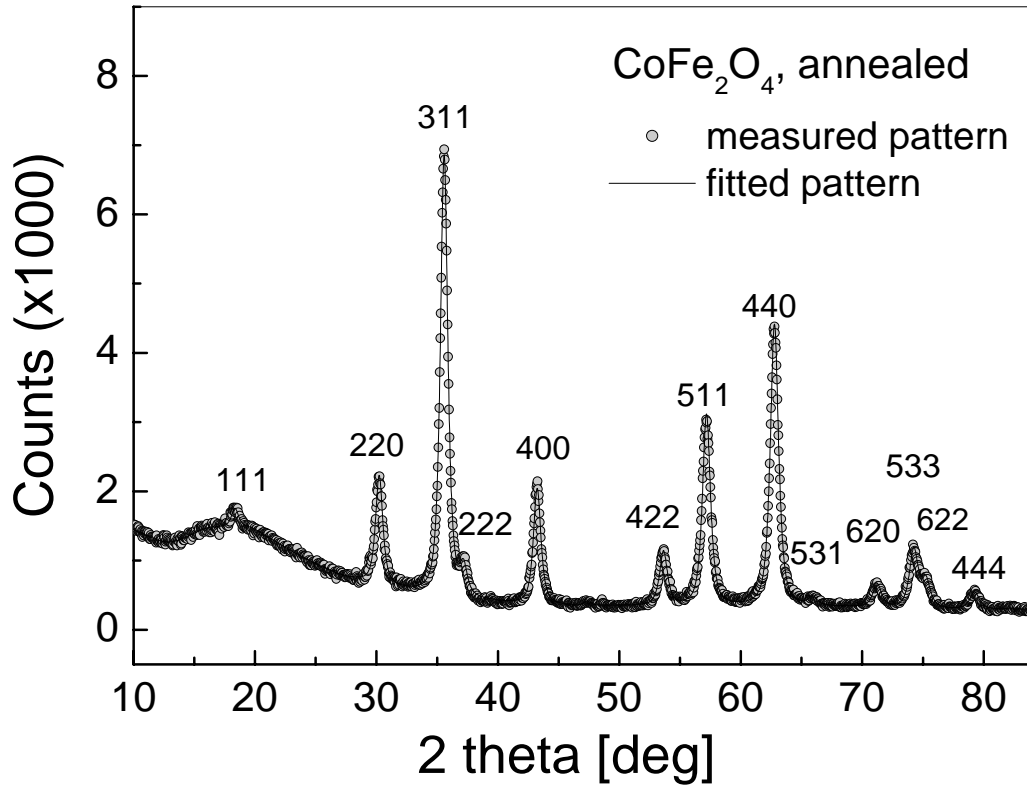


Fig. 1. X-ray pattern obtained for annealed sample of  $\text{CoFe}_2\text{O}_4$ . The open circles are experimental data and the solid curve was obtained by Fourier analysis.

In contrast with our results previously reported in [1] for the AP samples, for the AN samples (except for the powder with  $x = 0.4$ ), the  $H_c(T)$  does not behave as systems of identical non-interacting particles with random anisotropy axes. These results could be related to (i) the system exhibiting a mixture of superparamagnetic and ferrimagnetic phases; ii) the existence of the distribution of particle sizes; iii) the small particles exhibiting exchange coupling due to very thin surface layer; iv) the formation of finite clusters with different size and associated relaxation distribution as in polycrystalline materials [7].

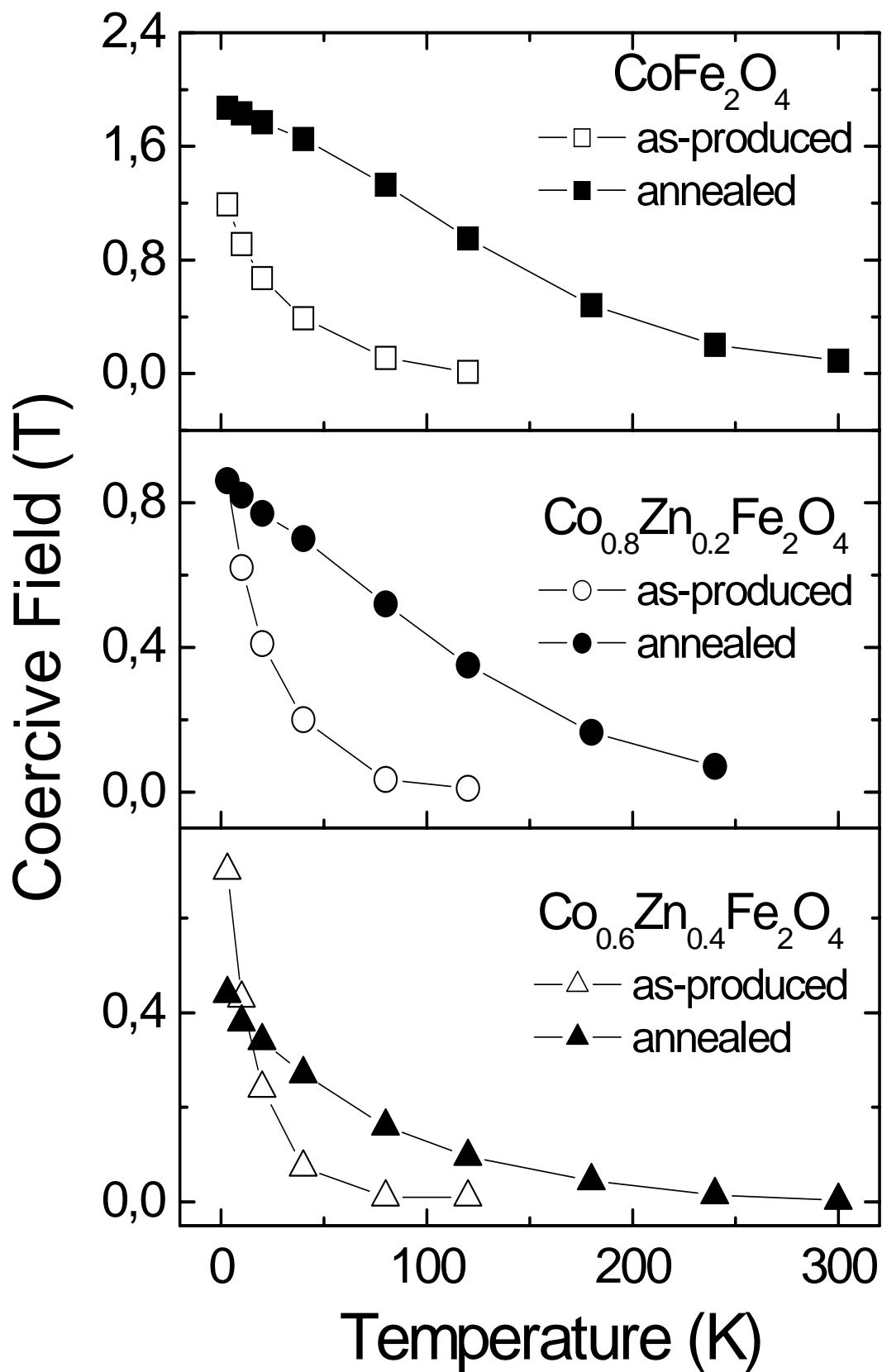


Fig. 2. Temperature dependence of the coercive field measured for all samples.

The following conclusions can be partially drawn from the  $M$  vs.  $T$  and reduced remanence vs.  $T$  shown in Fig. 3(a) and Fig. 3(b), respectively. The saturation magnetization of the AN powders approach those of the bulk samples (e.g. for  $\text{CoFe}_2\text{O}_4$  and  $\text{Co}_{0.6}\text{Zn}_{0.3}\text{Fe}_2\text{O}_4$ ,  $M_s$  values at 3 K are 88 and 133 emu/g, respectively) indicating that larger particles exhibit a thinner  $SL$ .

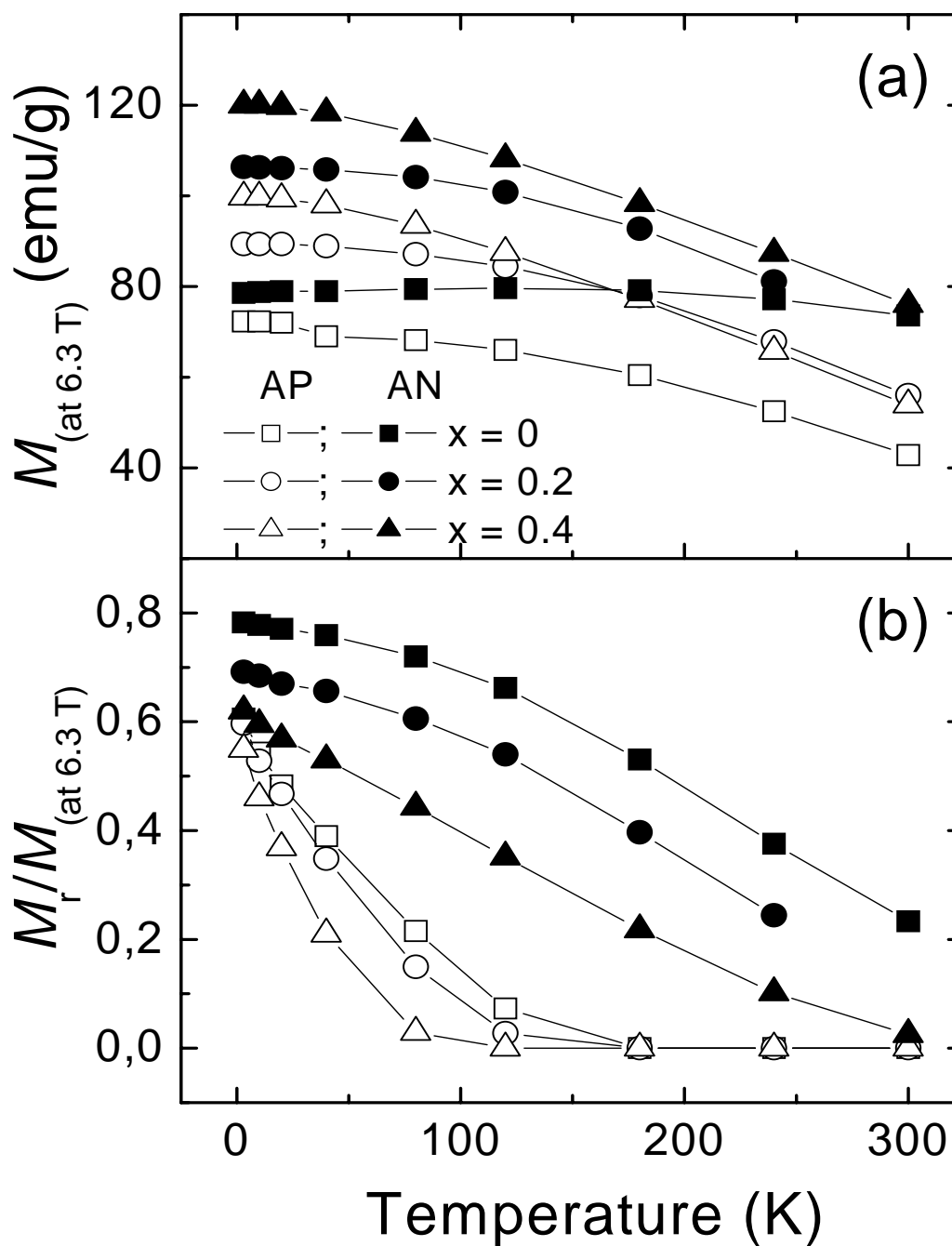


Fig. 3. Temperature dependence of the magnetization at 6.3 T (a) and reduced remanence (b) determined from the hysteresis loops measurements.

Small decrease in  $M$  (at 6.3 T) found in annealed  $\text{CoFe}_2\text{O}_4$  with decreasing  $T$  may be related to the lack of saturation  $M$  up to 6.3 T due to the high anisotropy and possible local canting of magnetic moments. The increase of  $H_c$ ,  $M_s$  and  $M_r$  in  $\text{CoFe}_2\text{O}_4$  can be attributed to the exchange-coupling phenomenon. At 300 K,  $H_c$  and  $M_r$  of all samples are somewhat lower than the expected values, in fact that may be related to the presence of superparamagnetic particles or formation of finite clusters.

The combination of  $H_c$  decreasing and  $M_r$  increasing with increase of particle size, as observed for  $\text{Co}_{0.6}\text{Zn}_{0.4}\text{Fe}_2\text{O}_4$ , is rather unusual. From the  $H_c$  vs.  $T^{0.5}$  curve (not shown here) of this sample, one can conclude that the particles are still non-interacting single domains [1], however exhibiting  $T_B > 300$  K. The as-produced single-domain samples may exhibit higher internal strains leading to the existence of uniaxial magnetic anisotropy in addition to the cubic magnetocrystalline anisotropy. Thus, the magnetic behavior of the system is far from the one of the behaviour expected for non-interacting single-particles with cubic anisotropy. In the thermal treated sample the decrease of uniaxial anisotropy may occur due to the relief of the internal strains and their anisotropy approaches the cubic type value resulting thus in a decrease of  $H_c$  accompanied of in an increase of  $M_r$ .

This work was partly supported by FWF Proj. Nr. P16500-N02 and a Tecnology Grant Southeast Asia from the ÖAD.

## References

- [1] Giap V. Duong, R. Sato Turtelli, N. Hanh, D.V. Linh, M. Reissner, H. Michor, J. Fidler, G. Wiesinger, R. Grössinger, in print in *J. Magn. Magn. Mater.*
- [2] S. Ammar, A. Helfen, M. Jouini, F. Fiévet, I. Rosenman, F. Villain, P. Molinié, M. Danot, *J. Mater. Chem.* 11 (2001) 186.
- [3] N. Moumen, P. Bonville, M.P. Pileni, *J. Phys. Chem.* 100 (1996) 14410.
- [4] M. Grigorova, H.J. Blythe, V. Blaskov, V. Rusanov, V. Petkov, V. Masheva, D. Nihtianova, L.I.M. Martinez, J.S. Muñoz, M. Mikhov, *J. Magn. Magn. Mater.* 183 (1998) 163.
- [5] C.H. Yan, Z.G. Xu, F.X. Cheng, Z.M. Wang, L.D. Sun, C.S. Liao and J.T. Jia, *Solid State Commun.* 111 (1999) 287.
- [6] G. Ribárik, J. Kubicza, T. Ungár, *Mater. Sci. Eng. A* 387-389 (2004) 343.



[7] R.N. Bhowmik, R. Ranganathan, J. Magn. Magn. Mater 248 (2002) 101.

## Magnetic properties of nanocrystalline $\text{CoFe}_2\text{O}_4$ synthesized by modified citrate-gel method

Giap V. Duong<sup>1,2</sup>, R. Grössinger<sup>1</sup>, R. Sato Turtelli<sup>1</sup>, W. Nunes<sup>3</sup>, M. Knobel<sup>3</sup>

<sup>1</sup>*Institute of Solid State Physics, Vienna Uni. Techn., Wiedner Hauptstr. 8-10, A-1040, Vienna, Austria*

<sup>2</sup>*Faculty of Chemical Engineering, Hanoi Uni. Techn., No.1 Dai Co Viet, Hanoi, Vietnam*

<sup>3</sup>*Instituto de Física, Universidade Estadual de Campinas, CP 6165, Campinas (SP), Brasil*

To be submitted for publication.

---

### Abstract

Nanocrystalline  $\text{CoFe}_2\text{O}_4$  with average grain size of 40 nm was successfully prepared by modified citrate gel method. The saturation magnetization is among the highest ever achieved value for this kind of nanocrystalline materials: 89 emu/g at 3 K and 83 emu/g at 300 K under a magnetic field of 7 T. When changing temperature from 3 to 300 K, the saturation magnetization experiences an unusual minimum at about 50 K and a maximum at about 155 K. The coercivity is typical for bulk  $\text{CoFe}_2\text{O}_4$ : 0.43 T at 3 K which decreases linearly with increasing temperature up about 200 K and reaches 0.07 T at 300 K. The magnetostriction is higher than that of the bulk sample: -130 and 70 ppm for parallel and perpendicular measurements, respectively. The high value of saturation magnetization and magnetostriction as well as typical value of coercivity lead to conclusion that this simple, economic modified citrate gel method can be used to synthesize high quality nanocrystalline  $\text{CoFe}_2\text{O}_4$ , especially in a large scale.

© 2006 Elsevier B.V. All rights reserved

PACS: 75.50.Tt; 75.60.Ej, 75.75.+a; 61.16.Bg, 75.80.+q

Keywords: Cobalt ferrite, nanocrystalline, hysteresis loops, magnetostriction, citrate gel

---

## 1. Introduction

Magnetic oxides of spinel structure,  $A^{2+}B_2^{3+}O_4$ , have received much attention due to its large range of applications in several important technological fields, such as: information and communication devices, high-density information storage, ferrofluids, magnetic drug delivery, catalysis, etc. [1-5]. Among them,  $CoFe_2O_4$  is attractive due to its remarkable properties: strong magnetocrystalline anisotropy, high coercivity, high saturation magnetization, high Curie temperature (up to 793 K), non-toxic, good mechanical hardness along with excellent chemical stability [6].

There are several methods used for preparing  $CoFe_2O_4$ : solid state reaction [7], co-precipitation [8], mechano-chemical [9], combustion [10], micro-emulsion [11], redox process [12], ion exchange [13], hydrothermal [14], sol-gel [15], forced hydrolysis [16], citrate precursor [17], etc. However, it is found that the magnetic properties of  $CoFe_2O_4$ , especially in the nanocrystalline state, seriously depend on the preparation methods. For example, saturation magnetization,  $M_s$ , reported for  $CoFe_2O_4$  with particle size of about 5 nm prepared by different methods is: 6 emu/g at 2K by micro-emulsion (reverse micelles at 300 K) [18], 45 emu/g at 20 K by micro-emulsion (oil-in-water micelles at 300 K) [11], 15 emu/g at 5K by co-precipitation (along with calcinations at 600K) [19], 85.1 emu/g at 5 K by forced hydrolysis (in polyol at 433 K) [16]. On the other hand, most of the above methods concerns expensive materials or high processing cost due to the requirements of special starting materials or processing procedures.

Recently, we are successful in preparation of high quality nanocrystalline  $Co_{1-x}Zn_xFe_2O_4$  by forced hydrolysis method [20]. However, to have a large scale production is very difficult. Therefore, to find a simple and economic route which allows the preparation of a large amount of high quality nanocrystalline  $CoFe_2O_4$  is necessary and will benefit to practical applications of this interesting material.

This work will report on the synthesis and characterization, both structurally and magnetically, of nanocrystalline  $CoFe_2O_4$  by modified citrate gel, a simple, non-grinding, economic and large scale production method.

## 2. Experiment

### 2.1. Sample preparation

The precursor salts,  $\text{Fe}(\text{NO}_3)_3 \cdot 9\text{H}_2\text{O}$ ,  $\text{Co}(\text{NO}_3)_2 \cdot 6\text{H}_2\text{O}$  and citric acid, all with analytical purity, were added to 150 ml of deionized water in stoichiometric ratio. The total metal concentration was 1 mol/l. The molar ratio between total metal ions and citric acid was fixed to 1. The starting mixture containing the salts, deionized water and citric acid was stirred to get homogeneous solution and heated to 80 °C with a heating rate of 5 °C/min using a hot plate magnetic stirrer. The pH of the solution was adjusted to 6 by dropping ammonia ( $\text{NH}_3$  25%). The sol was formed during stirring. Increasing the temperature of the hot plate up to 200 °C and keep stirring constantly, the water in the solution was evaporated and a viscous gel was formed. Keeping heating, the gel is dried and burnt as being ignited to form loose powder. The powder was pressed into pellet under a pressure of 4.5 tones/cm<sup>2</sup> and sintered at 1000 °C for 5 hours. After naturally cooling down to room temperature, it was cut in to pieces of 2x4x6 mm and were used as samples for measurements.

Differently from reported literatures, here we did not use chelating agent such as ethylene glycol and also did not dry the gel but forcing it auto-combusted by keeping heating after gelating the sol. This will make the process more simple and economic for prepare large amount of sample.

### 2.2. Structural and magnetic characterization

The crystal structure of the obtained material was studied by X-ray diffraction (XRD) using  $\text{CoK}_\alpha$  radiation. To estimate the crystallite size, the Scherrer equation for the full-width at half maximum (FWHM) of the strongest reflection was employed [21]:

$$D = K\lambda / \beta \cos \theta, \quad (1)$$

where  $D$  is the crystallite size,  $K$  is the shape function for which a value of 0.9 is used [21],  $\beta$  is the width of the pure diffraction profile and  $\theta$  is the angle of incidence.

The hysteresis loops and temperature dependence of magnetization were measured by means of a commercial superconducting quantum interference device (SQUID) and a vibrating sample magnetometer in the temperature range of 3–300 K with maximum magnetic field of 7 Tesla. Linear magnetostriction was measured at room temperature using strain gauge method with a 50 kHz bridge (HBM Type KWS 85.A1).

### 3. Results and Discussion

The XRD pattern of the sample was shown in Fig.1. The clear and sharp peaks indicate a well-crystallized sample. All peaks are characteristics for  $\text{CoFe}_2\text{O}_4$  in cubic spinel-type structure. The absence of foreign diffraction lines suggests the phase purity. From the XRD pattern, the determined lattice constant is of 8.38 Å, a typical value for cobalt ferrite. Using equation (1), we obtained an average grain size of about 40 nm.

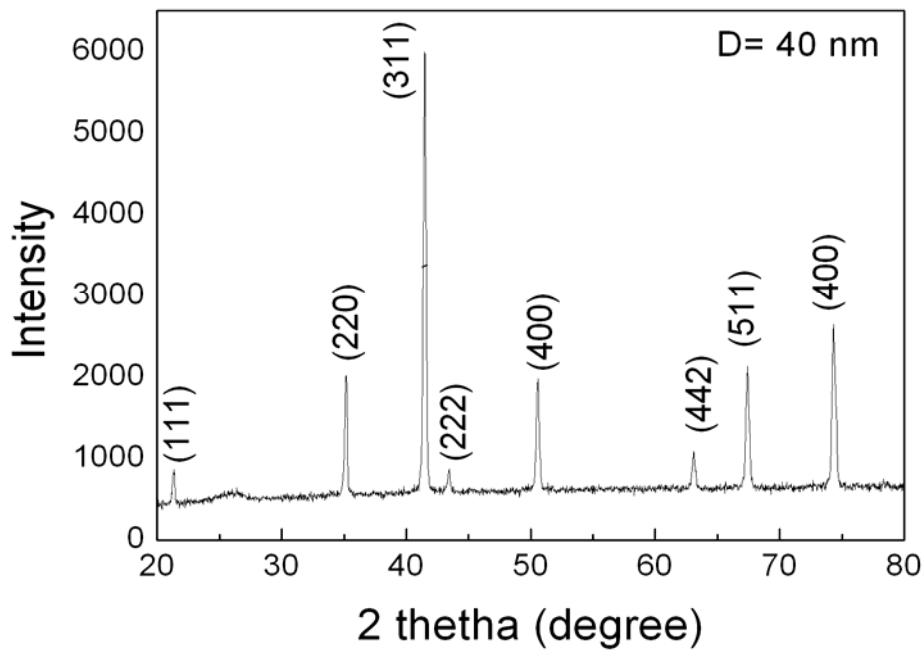


Fig.1. XRD pattern of the studied sample.

Fig.2 showed the hysteresis loops of the studied sample measured at 3 and 300 K. Very similar loops were obtained for other temperatures. At 3 K, the magnetization,  $M$ , measured under a magnetic field,  $H$ , of 7 T is 89 emu/g and the coercivity,  $H_C$ , is about 0.43 T. Extrapolated from the  $M-1/H$  curve when  $1/H \rightarrow 0$ , a saturation magnetizations of 94 emu/g is obtained. Reminding that the anisotropy field of  $\text{CoFe}_2\text{O}_4$  is about 0.6 T [6], and the magnetic field here is about 12 times higher than this anisotropy field, however it cannot saturate the sample magnetically as shown in Fig.2.

The magnetization and coercivity measured at 300 K under the same magnetic field are 82.8 emu/g and 0.07 T, respectively. Extrapolating from the  $M-1/H$  curve when  $1/H \rightarrow 0$ , a  $M_s$  value of 84 emu/g is obtained. Differently from the case of 3 K, the sample here is very closed to magnetic saturation.

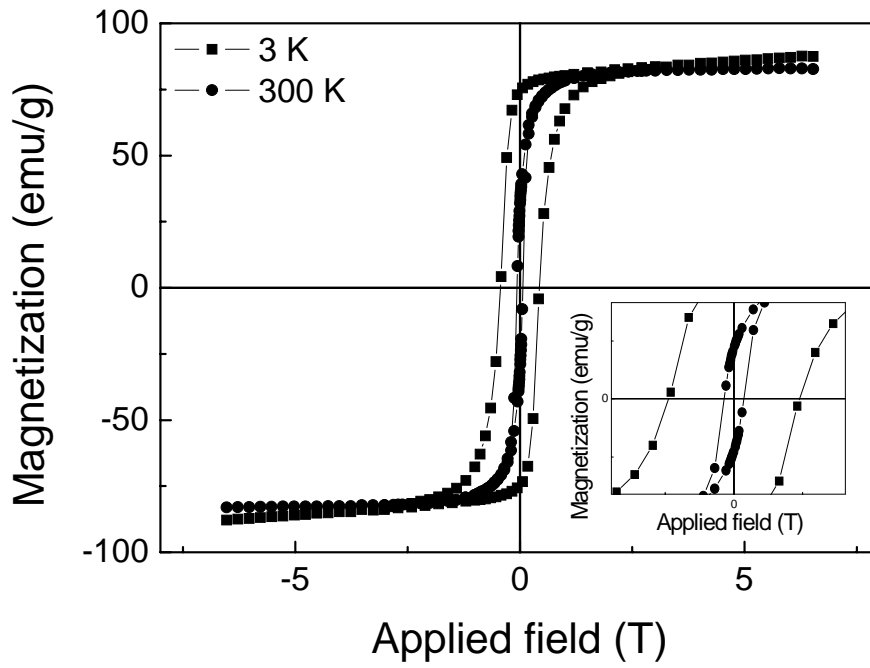


Fig.2. Hysteresis loops of the studied sample at 3 K and 300 K.  
Inset is the hysteresis loops around the oercivity.

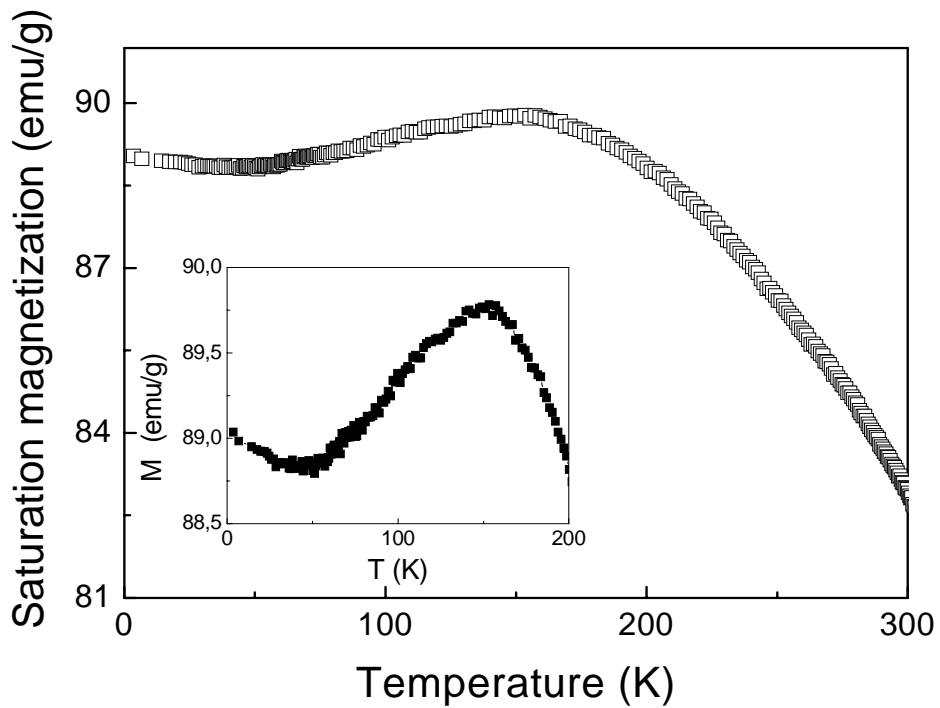


Fig.3. Saturation magnetization as function of temperature. Inset is the close look of magnetization in the temperature range of 3-200 K.

The temperature dependence of magnetization measured under a magnetic field of 7 T is shown in Fig.3. An unusual minimum and a maximum are found in the magnetization curve. The temperature where the minimum and maximum occur,  $T_{min}$  and  $T_{max}$ , are about 50 and 155 K, respectively. The minimum  $M_s$  at 50 K is about 0.5% smaller and the maximum  $M_s$  at 155 K is about 1% bigger compared to the  $M_s$  at 3 K. However, they are absolutely obvious as shown in the inset of Fig.3.

The reason why these minimum and maximum appear is until now not clear. However, reminding that the anisotropy field of cobalt ferrite is only about 0.6 T [6], and the applied magnetic field here is almost 12 times higher than the anisotropy field, so the change in magnetization is not concerned the magnetocrystalline anisotropy. On the other hand, the change in magnetization is smooth and less than 1%, it therefore cannot be attributed to the change in crystal structure, which is first order phase transition and usually causes a sharp jump in magnetization. One also cannot attribute it to the affect of surface layers in nanocrystalline particles since this behavior is observed only for sample with grain size larger than 3 nm.

The higher saturation magnetization compared to those reported for nanocrystalline  $\text{CoFe}_2\text{O}_4$  with similar grain size is attributed to the suitability of the preparation method. For example, at room temperature,  $M_s$  of nanocrystalline  $\text{CoFe}_2\text{O}_4$  prepared by co-precipitation method with average grain size of 33.5 and 47.4 nm, are  $M_s=21.3$  and 29.5 emu/g [22].

For crystalline  $\text{CoFe}_2\text{O}_4$ , the temperature dependence of saturation magnetization is given by the expression [23]:

$$M_s(T) = 93.9 \times (1 - 1.576 \times 10^{-6} \times T^2) \text{ emu/g} \quad (2)$$

According to this expression, at 3 and 300 K, the saturation magnetization is 93.9 and 80.6 emu/g, respectively. These values are similar to our data. Our values of saturation magnetization are among the highest ones ever achieved for nanocrystalline  $\text{CoFe}_2\text{O}_4$ . The reason is: the modified citrate gel method here allows to mix the metal ions at atomic scale using stirring and to combine them through metal-citric gel network, leading to a perfect reaction between ions to form cobalt ferrite when annealing. This suggests that the modified citrate gel method is very effective to prepared high quality nanocrystalline  $\text{CoFe}_2\text{O}_4$ , especially in a large scale.

Fig.4 showed the temperature dependence of the remanence,  $M_r$ , and the squareness ratio,  $S$ . Both  $M_r$  and  $S$  decrease when increasing temperature. At 3 K, the remanence is about 75 emu/g and the squareness ratio is 0.847. However, they decrease to 31.2 emu/g and 0.375

at 300 K, respectively. For random distribution of easy axes of particles with cubic magnetocrystalline anisotropy, the squareness ratio is expected to be equal to 0.83 at 0 K [11]. In the low temperature range, the squareness ratio of the studied sample is bigger than 0.5 and quite closed to the value of 0.83, indicating that the cubic magnetocrystalline anisotropy is the dominant. At high temperature range, S becomes closed to 0.5. The reason is the fast decrease of cubic anisotropy constant that leads to the prominence of uniaxial anisotropy which found to be coexisted in cobalt ferrite system [24].

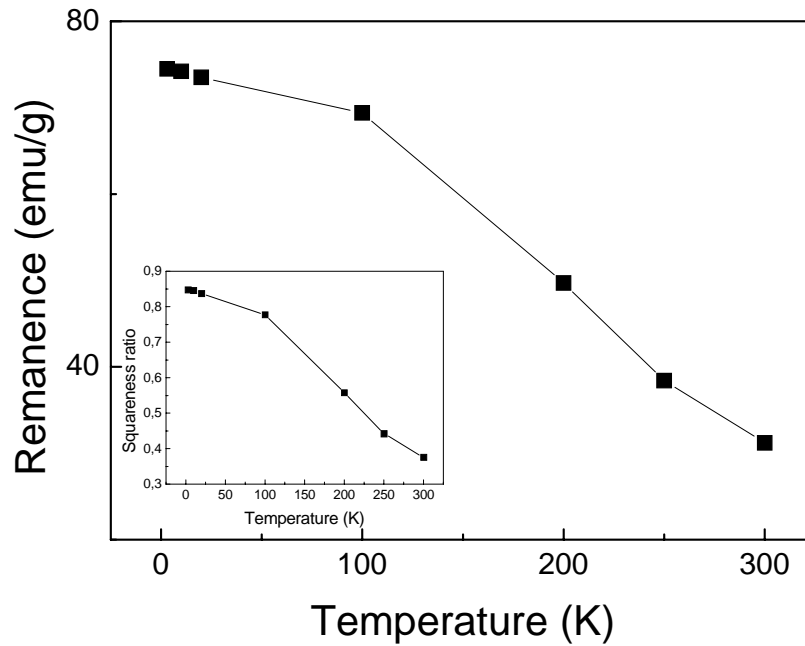


Fig.4. Magnetic remanence and squareness ratio (inset) as function of temperature.

The temperature dependence of coercivity is shown in Fig. 5. It decreases linearly with increasing temperature up about 200 K. At 300 K,  $H_C$  is about 0.07 T (700 Oe), which is typical for bulk cobalt ferrite, 750-980 Oe at room temperature [25]. For non-interacting single domain nanoparticles, the relationship between  $H_C$  and  $K$  at temperature below blocking temperature,  $T_B$ , is given by the well-known equation:

$$H_C = \frac{3K}{2\mu_0 M_s} \left[ 1 - \left( \frac{T}{T_B} \right)^{1/2} \right] \quad (2)$$

where  $\mu_0 M_s$  is the saturation magnetization and the constant  $\alpha=1$ , if the particle easy axes are aligned or  $\alpha=0.48$ , if they are randomly oriented.

If the coercivity obeys equation (2), at low temperature when  $K$  and  $M_s$  are considered



to be constant,  $H_C$  will linearly decrease with respect to  $T^{1/2}$ . However, this is not the case. Here  $H_C$  decreases linearly with respect to  $T$  as shown in Fig.5. The reason is the strong interactions between magnetic nanoparticles which drives the system far away from the superparamagnetic state.

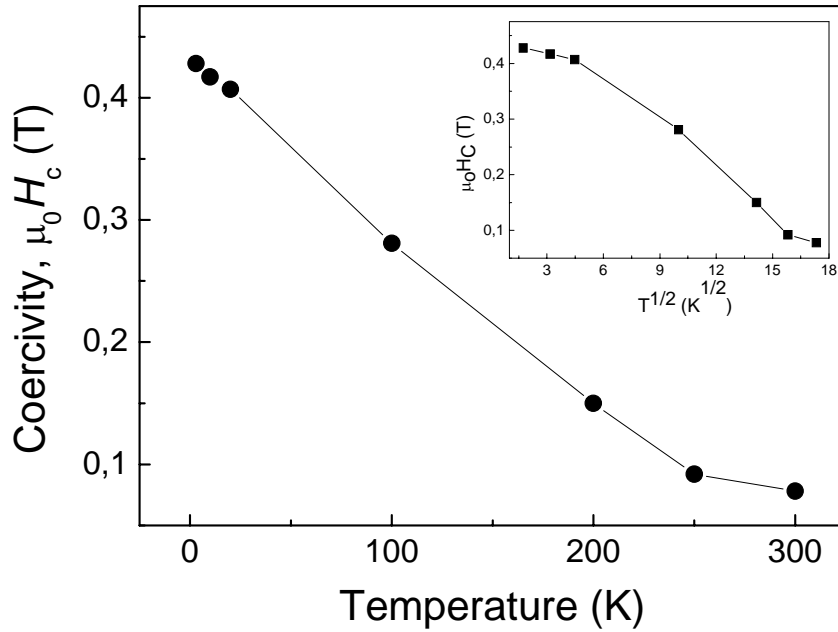


Fig.5. Coercivity as function of temperature. Inset is the  $\mu_0H_C-T^{1/2}$  curve.

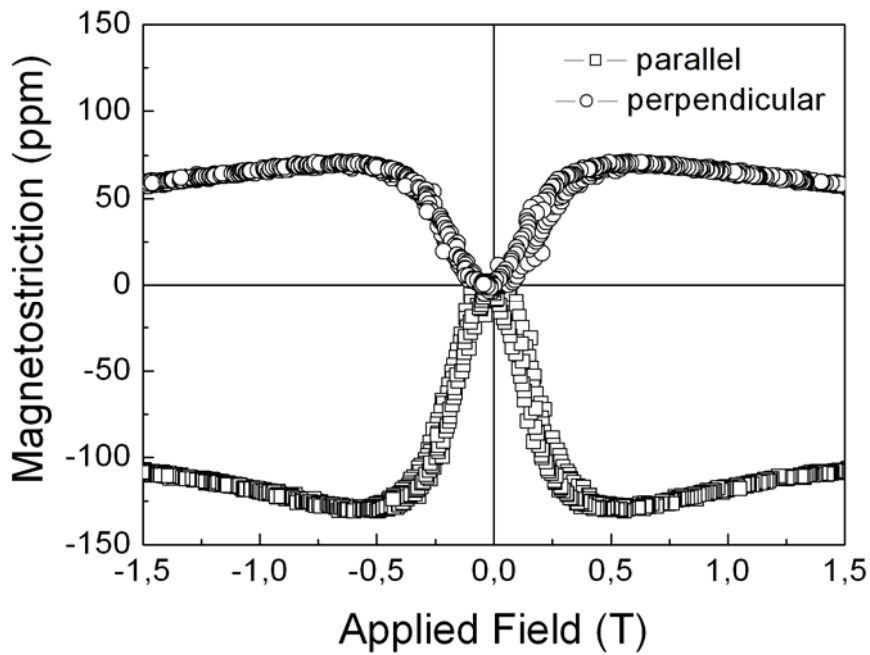


Fig.5. Magnetostriction of the studied sample at room temperature.

The linear magnetostriction  $\lambda$  measured by strain gauge method gave a value of -130 and 70 ppm for parallel and perpendicular measurements, respectively. These values are slightly higher compared to those of polycrystalline samples: e.g., -110 ppm for parallel magnetostriction [6]. This is reasonable as in the nanocrystalline, the atoms are easier to move due to less rigidity of the crystal. It is also true for the thermal expansion  $\delta$ , i.e. nanoparticles have anomaly large thermal expansion coefficient. It can be one order of magnitude greater than that of bulk samples [26]. Since  $\lambda$  and  $\delta$  have a close relationship: the higher  $\delta$  the higher  $\lambda$ . Therefore, a higher magnetostriction in nanoparticles compared to that of bulk sample is expected, and in fact, it is evidenced in our magnetostriction measurements.

The magnetic field where  $\lambda$  gets maximum is about 0.5 T. This is according to the coercive field of cobalt ferrite. At higher field, the linear magnetostriction decreases. This is due to the fact that volume magnetostriction starts to approach saturation.

#### **4. Conclusion**

In conclusion, nanocrystalline  $\text{CoFe}_2\text{O}_4$  has been successfully synthesized by modified citrate gel method along with annealing. The obtained sample has a average grain size of 40 nm and shows very high saturation, typical coercivity and high magnetostriction, suggesting that this simple, economic method can be use to prepared high quality nanocrystalline  $\text{CoFe}_2\text{O}_4$ , especially in a large scale.

#### **Acknowledgement**

This work is supported by the FWF Proj. Nr. P16500-N02, Proj. Nr. P15737 and the Austrian Exchange Service (ÖAD).

#### **References**

- [1] Soshin Chikazumi, Physics of Ferromagnetism, 2nd edition, Oxford Science Publications, 1997, 197-221.
- [2] M. H. Kryder, MRS Bull., 21 (1996) 917.
- [3] K. Raj, R. Moskowitz and R. Casciari, J. Magn. Magn. Mater., 149 (1995) 174.
- [4] U. Häfelli, W. Schütt, J. Teller and M. Zborowski, Scientific and Clinical Applications of Magnetic Carriers Plenum, New York, (1997).
- [5] C.G. Ramankutty, S. Sugunan, Applied Catalysis A: General 218 (2001) 39–51

- [6] R. Valenzuela, *Magnetic ceramics*, Cambridge University Press, Cambridge, 1984, 137-191.
- [7] Juliana B. Silva, Walter de Brito and Nelcy D.S. Mohallem, *Mate. Sci. Eng. B*, 112 (2004) 182.
- [8] T. Pannaparayil and S. Komarneni. *IEEE Trans. Magn.* 25 (1989), 4233.
- [9] Francesco Congiu, Giorgio Concas, Guido Ennas, Andrea Falqui, Dino Fiorani, Giaime Marongiu, Sergio Marras, Giorgio Spano and A.M.Alberto M. Testa, *J. Magn. Magn. Mater*, 272-276 (2004) 1561.
- [10] C. H. Yan, Z. G. Xu, F. X. Cheng, Z. M. Wang, L. D. Sun, C. S. Liao and J. T. Jia, *Solid State Commun.*, 111 (1999) 287.
- [11] N. Moumen, P. Veillet and M.P. Pileni. *J. Magn. Magn. Mater.* 149 (1995), 67.
- [12] M. Rajendran, R.C. Pullar, A.K. Bhattacharya, D. Das, S.N. Chintalapudi and C.K. Majumdar. *J. Magn. Magn. Mater.* 232 (2001) 71.
- [13] R.F. Ziolo, E.P. Giannelis, B.A. Weinstein, M.P. O'Horo, B.N. Ganguly, V. Mehrotra, M.W. Russell and D.R. Huffman. *Science* 257 (1992) 5067.
- [14] Linda J. Cote, Aryn S. Teja, Angus P. Wilkinson and Z. John Zhang, *Fluid Phase Equilibria*, Vol. 210, Iss. 2, 15 August 2003, 307.
- [15] F. X. Cheng, Z. Y. Peng, C. S. Liao, Z. G. Xu, S. Gao and C. H. Yan, *Solid State Commun.*, 107 (1996) 471.
- [16] S. Ammar et al. *J. Mater. Chem.* 11 (2001) 186.
- [17] R. N. Panda, J. C. Shih and T. S. Chin, *J. Magn. Magnetic Mate.* 257 (2003) 79-86.
- [18] C. T. Seip, E. E. Carpenter and C. J. O'Connor, *IEEE Trans. Magn.*, 34 (1998) 41111.
- [19] M. Grigorova, H.J. Blythe, V. Blaskov, V. Rusanov, V. Petkov, V. Masheva, D. Nihtianova, L.I.M. Martinez, J.S. Muñoz and M. Mikhov, *J. Magn. Magn. Mater.* 183 (1998), p. 163.
- [20] Giap.V. Duong, R. Sato Turtelli, N. Hanh, D.V. Linh, M. Reissner, H. Michor, J. Fidler, G. Wiesinger, R. Grössinger, *Magnetic properties of nanocrystalline  $\text{Co}_{1-x}\text{Zn}_x\text{Fe}_2\text{O}_4$  prepared by forced hydrolysis method*, *J. Magn. Magn. Mater.*, in press.
- [21] H.G. Jiang, M. Rühle and E.J. Lavernia, *J. Mater. Res.* 14 (1999) 549.
- [22] Yuqiu Qu, Haibin Yang, Nan Yang, Yuzun Fan, Hongyang Zhu, Guangtian Zou, *Mater. Lett.* (2006), in press.
- [23] R. Pauthenet, *Ann. Phys.* 7 (1952) 710.
- [24] V. Blaskov, V. Petkov, V. Rusanov, L.I. M. Martinez, B. Martinez, J. S. Muñoz and M. Mikhov, *J. Magn. Magn. Mater.* 162 (1996) 331-337.

[25] D.J. Craik, *Magnetic Oxides, Part 2*, Wiley, London, 1975, pp. 703.

[26] V.I. Nikolaev, A.M. Shipilin, *Fizika Tverdogo Tela (Solid State Physics, Russia)* 42 (2000)109–110.

# Magnetic properties of nanocrystalline cobalt ferrite in CoFe<sub>2</sub>O<sub>4</sub>-BaTiO<sub>3</sub> core-shell structure composite

Giap V. Duong<sup>1,2</sup>, R. Grössinger<sup>1</sup>, R. Sato Turtelli, M. Reissner<sup>1</sup>

<sup>1</sup>*Institute of Solid State Physics, Vienna Uni. Techn., Wiedner Hauptstr. 8-10, A-1040, Vienna, Austria*

<sup>2</sup>*Faculty of Chemical Engineering, Hanoi Uni. Techn., No.1 Dai Co Viet, Hanoi, Vietnam*

To be submitted for publication.

---

## Abstract

The 50%CoFe<sub>2</sub>O<sub>4</sub>-50%BaTiO<sub>3</sub> (in mass) core-shell structure composite has been successfully prepared by wet chemical method. The grain size of the starting CoFe<sub>2</sub>O<sub>4</sub> constituent is about 10 nm, but increases up to 20.5 nm in the composite after heat treatment. The magnetic study showed that the nanocrystalline CoFe<sub>2</sub>O<sub>4</sub> constituent has a saturation magnetization, extrapolated from the  $1/H$ - $M$  curve, and coercivity of 76.5 emu/g and 2000 Oe at 4.2 K, but decrease to 51.5 emu/g and 265 Oe at 380 K, respectively. Temperature dependence of saturation magnetization showed an upturn at 50 K. The coercivity is found to decrease linearly up to 220 K. Magnetostriction measurements revealed the strong mechanical coupling between the two constituents. Low field temperature dependent magnetization of the CoFe<sub>2</sub>O<sub>4</sub> constituent showed a huge difference when the BaTiO<sub>3</sub> component is in ferroelectric or paraelectric state, suggesting a strong direct coupling between magnetic and electric domains.

© 2006 Elsevier B.V. All rights reserved

PACS: 75.50.Tt; 75.60.Ej; 75.75.+a; 75.80.+q; 77.65.-j; 77.84.Lf

Keywords: Cobalt ferrite, barium titanate, magnetic properties, magnetoelectric effect, magnetoelectric composite.

---

## 1. Introduction

Magnetoelectric materials become magnetized when exposed to an electric field and electrical polarized when exposed to a magnetic field. In single phase materials, this kind of materials shows a coexistence of magnetic and electric moments. In composites, these moments are introduced independently from magnetostrictive and piezoelectric constituents. The magnetoelectric property is a “product property” of this combination.

To have a high magnetoelectric coefficient, the magnetic phase should have high magnetostrictive coefficient and high electric resistance to avoid discharging process. Among magnetic materials, cobalt ferrite is a good candidate to be constituent of magnetoelectric composite since it is an insulator and has the highest magnetostriction among ferrites. Using  $\text{CoFe}_2\text{O}_4$  as magnetostrictive constituent, many magnetoelectric composites such as  $\text{CoFe}_2\text{O}_4$ - $\text{BaTiO}_3$  [1-4],  $\text{BaO-TiO-FeO-CoO}$  system [1, 3, 5], etc. have been prepared. However, magnetic properties of the  $\text{CoFe}_2\text{O}_4$  constituent in this composite were not well studied yet.

Recently we successfully prepared 50%- $\text{CoFe}_2\text{O}_4$ -50% $\text{BaTiO}_3$  (in mass) core-shell structure composite [6]. Magnetoelectric measurements using the lock-in technique [7] showed that this core-shell structure composite has a magnetoelectric coefficient of about 18 times higher than that of mixed structure composite with the same composition. The reason is the better coupling between the two phases in the core-shell structure compared to that of the mixed structure. In this work, the magnetic properties of the  $\text{CoFe}_2\text{O}_4$  core in this core-shell structure composite will be study to evidence the coupling between these two phases.

## 2. Experiment

### 2.1. Sample preparation

The starting materials,  $\text{Fe}(\text{NO}_3)_3 \cdot 9\text{H}_2\text{O}$ ,  $\text{Co}(\text{NO}_3)_2 \cdot 6\text{H}_2\text{O}$ , all with analytical purity, were added to 200 ml of deionized water in stoichiometric ratio, then stirred to get homogenous solution. The concentration of metal ions is 2 M. The solution the was heated to 70 °C and stirred at 3000 rpm, and co-precipitated by NaOH 2 M solution while keeping stirring constant. To ensure the co-precipitation, a 50 % extra amount of NaOH was used. The obtained product was washed by deionized water several time until pH of the outlet solution is 7, then dried naturally at room temperature for 24 hours to get the nanocrystalline  $\text{CoFe}_2\text{O}_4$  powder.

To prepare the core-shell structure composite, the co-precipitated  $\text{CoFe}_2\text{O}_4$  powder, calculated to get a composite containing 50% in mass of each constituent, was introduced into

a solution of acetic acid, barium hydroxide and titanium (IV) n-Butoxide, which is then gelated on the surface of the  $\text{CoFe}_2\text{O}_4$  grains or particles during heating and stirring. The obtained material is dried, pre-sintered at  $700^\circ\text{C}$  for 2 hours, ground into fine powder, then pressed under a pressure of 6 tones/ $\text{cm}^2$  to obtain a sample in shape of a disc of 10 mm in diameter and 1.5 mm thick. This disk is sintered at  $1250^\circ\text{C}$  for 12 hours to get a core-shell structure composite, then cut into pieces of  $1.5 \times 1.5 \times 1$  mm and used as sample for magnetic measurements.

## 2.2. Structural and magnetic characterization

The crystal structure of the obtained material was studied by X-ray diffraction (XRD) using  $\text{CoK}_\alpha$  radiation. To estimate the crystallite size, the Scherrer equation for the full-width at half maximum (FWHM) of the strongest reflection was employed [8]:

$$D = K\lambda / \beta \cos \theta, \quad (1)$$

where  $D$  is the crystallite size,  $K$  is the shape function for which a value of 0.9 is used [8],  $\beta$  is the width of the pure diffraction profile and  $\theta$  is the angle of incidence.

The magnetic properties were measured by means of a Physical Property measurement System (PPMS-9T, Quantum Design) with maximum field of 9 T in a temperature range of 4.2-400 K. Linear magnetostriction was measured at room temperature using strain gauge method with a 50 kHz bridge (HBM Type KWS 85.A1).

## 3. Results and Discussion

The XRD pattern of the studied composite as well as its pure constituents was shown in Fig.1. The composite contains only two single phases:  $\text{CoFe}_2\text{O}_4$  and  $\text{BaTiO}_3$ ; no intermediate phase was detected by means of XRD characterization. Using equation (1) above for the strongest reflection at low angle, the grain size of the  $\text{CoFe}_2\text{O}_4$  powder after co-precipitation is about 10 nm. In the composite, after heat treatment, the grain size of this constituent increases to 20.5 nm.

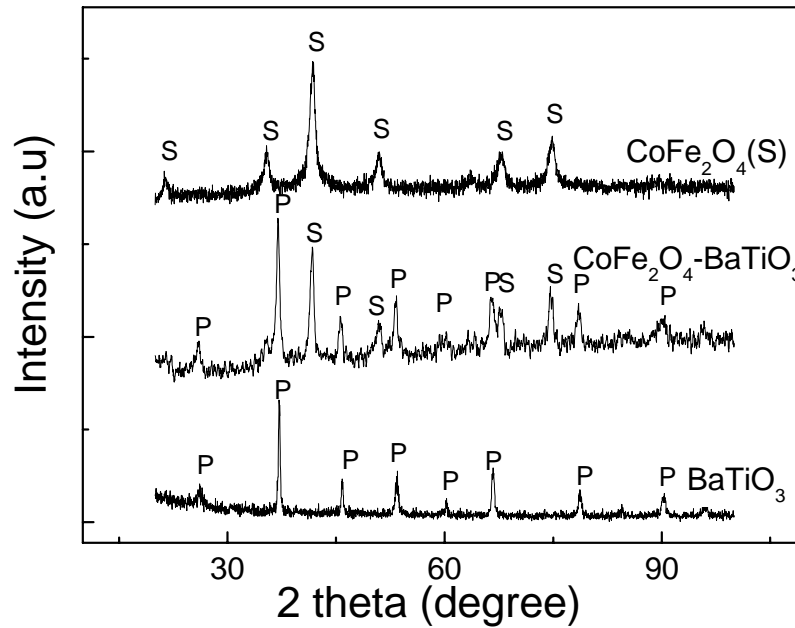


Fig.1. XRD pattern of the composite and its pure constituents.

Fig.2 showed the hysteresis loops of the  $\text{CoFe}_2\text{O}_4$  constituent measured at 77 and 380 K. Very similar loops were obtained for other temperatures. At 4.2 K, the magnetization,  $M$ , measured under a magnetic field,  $H$ , of 9 T is 69.5 emu/g and the coercivity,  $H_C$ , is about 2000 Oe. Extrapolated from the  $M-1/H$  curve when  $1/H \rightarrow 0$ , at 4.2 K, a saturation magnetizations of 76.5 emu/g is obtained. Reminding that the anisotropy field of  $\text{CoFe}_2\text{O}_4$  is about 0.5 T, and the magnetic field here is about 18 times higher than this anisotropy field, however it cannot saturate the sample magnetically as shown in Fig.2, giving hint that another magnetic contribution than that of the pure ferrimagnetic  $\text{CoFe}_2\text{O}_4$  may exist. Some anomalous feature is also seen in the temperature dependence of magnetization and will be discuss in more details later.

The magnetization and coercivity measured at 380 K under the same magnetic field (9 T) are 48.5 emu/g and 265 Oe, respectively. Extrapolating from the  $M-1/H$  curve when  $1/H \rightarrow 0$ , a  $M_s$  value of 51.5 emu/g is obtained. Differently from the case at 4.2 K, the sample here is very close to magnetic saturation.

The temperature dependence of the magnetization measured under a magnetic field of 9 T is shown in Fig.3. In general, the magnetization decreases from 68.5 to 46.5 emu/g when the temperature increases from 4.2 to 400 K, however it shows an upturn below about 50 K.



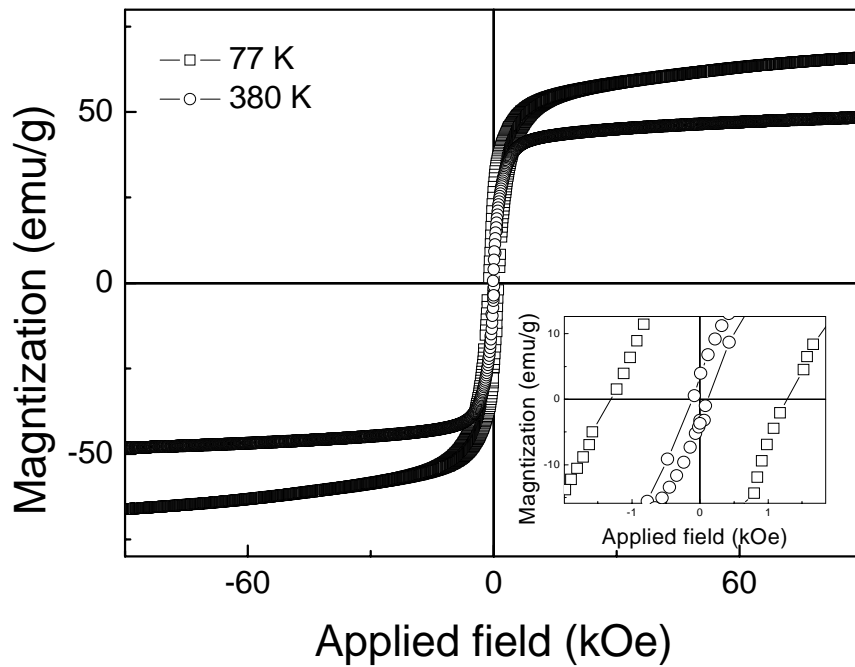


Fig.2. Hysteresis loops of the composite at 77 and 380 K.

The saturation magnetization of the  $\text{CoFe}_2\text{O}_4$  constituent here is about 15% smaller than that of the bulk cobalt ferrite. A possible reason may be spin canting at the surface of the small grains, forming a magnetic disordered layer, leading to a decrease of the total saturation magnetization. However, this value is still higher than that of nanocrystalline  $\text{CoFe}_2\text{O}_4$  prepared by the same method, but without further heat treatment, e.g. nanocrystalline  $\text{CoFe}_2\text{O}_4$  with average grain size of 33.5 and 47.4 nm has  $M_s=21.3$  and 29.5 emu/g,  $H_C=1281$  and 1180 Oe at room temperature, respectively [9]. This suggests that the heat treatment here has reduced the magnetic disordered layers by perfecting its crystal structure.

The origin of the upturn at low temperature range of the temperature dependent magnetization curve is until now not clear. In pure nanocrystalline  $\text{CoFe}_2\text{O}_4$  with average grain size of 40 nm, also a slightly increase of saturation magnetization at 50 K was observed [10]. However, different from that case, here no maximum in the magnetization at 155 K was found. The anomalous upturn at low temperature is proposed to be due to a new magnetic phase which becomes ordered at low temperature. However, more experiments need to be carried out to confirm and characterize the existence and nature of this new phase.

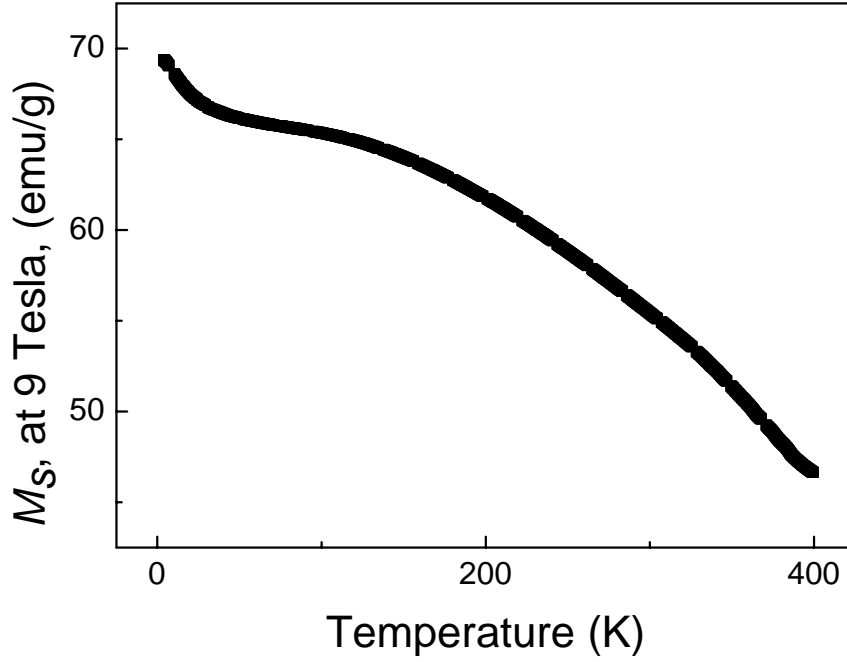


Fig.3. Saturation magnetization of the composite as function of temperature.

The temperature dependence of the coercivity is shown in Fig. 4. At 4.2 K,  $H_C$  is 2000 Oe. However, it decreases linearly with increasing temperature up about 220 K. At 300 K,  $H_C$  is about 396 Oe, which is smaller than that of bulk cobalt ferrite, 750-980 Oe at room temperature [11].

For non-interacting single domain nanoparticles, the relationship between  $H_C$  and  $K$  at temperatures below the blocking temperature,  $T_B$ , is given by the well-known equation:

$$H_C = \frac{3K}{2\mu_0 M_s} \left[ 1 - \left( \frac{T}{T_B} \right)^{1/2} \right] \quad (2)$$

where  $\mu_0 M_s$  is the saturation magnetization and the constant  $\alpha=1$ , if the particle easy axes are aligned or  $\alpha=0.48$ , if they are randomly oriented.

If the studied sample obeys equation (2), at low temperature when  $K$  and  $M_s$  are considered to be constant,  $H_C$  will linearly decrease with respect to  $T^{1/2}$ . However, this is not the case. Here  $H_C$  decreases linearly with respect to  $T$  as shown in Fig.4. This means the nanoparticles here, even separated by BaTiO<sub>3</sub> shell, still have some magnetic interaction and do not behave like a superparamagnetic system.

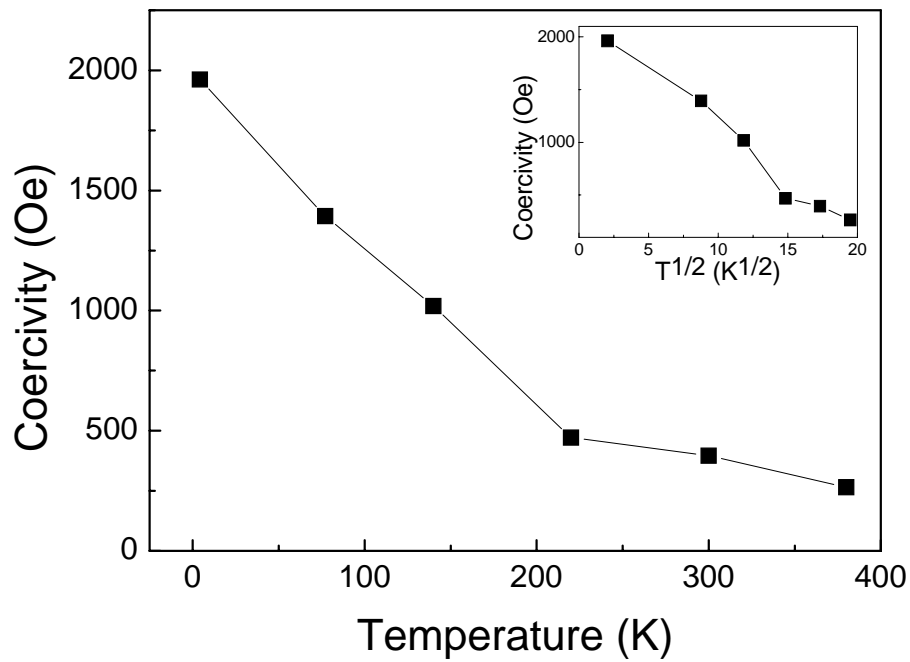


Fig.4. Coercivity as function of temperature. Inset is the  $\mu_0 H_C - T^{1/2}$  and  $\mu_0 H_C - T^2$  curves.

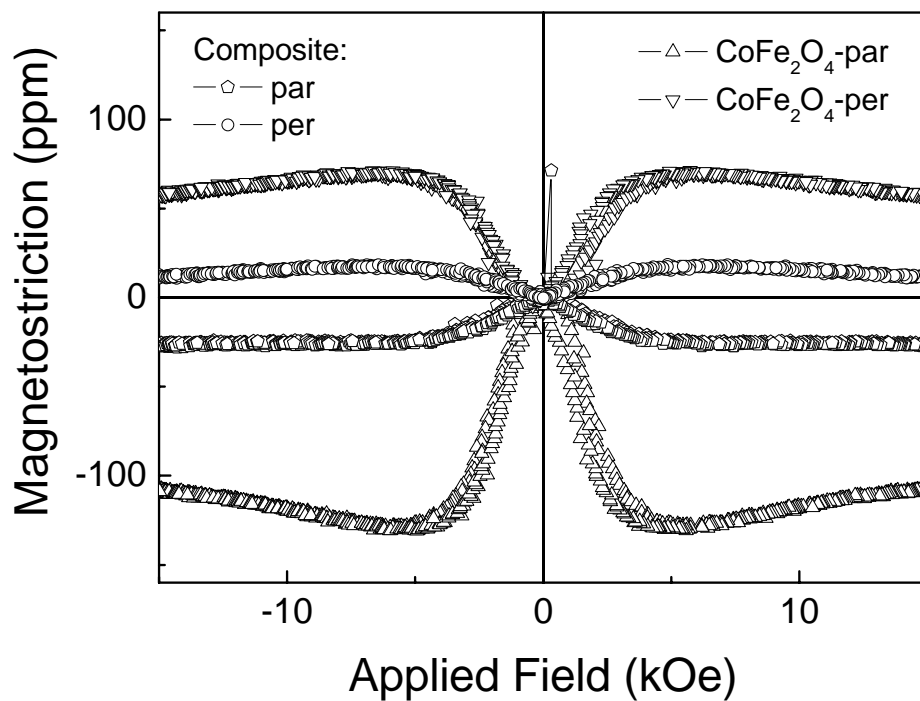


Fig.5. Magnetostriction of the composite and pure  $\text{CoFe}_2\text{O}_4$  at room temperature.

The linear magnetostriction  $\lambda$  measured by strain gauge method gave a value of -26 and 17 ppm for parallel and perpendicular measurements, respectively. For comparison, the magnetostriction of pure  $\text{CoFe}_2\text{O}_4$  prepared by citrate method has a linear magnetostriction of -130 and 70 ppm for parallel and perpendicular measurement, respectively, see Fig.5. The magnetostriction of the 50% $\text{CoFe}_2\text{O}_4$ - $\text{BaTiO}_3$  composite is much smaller than the expected value, i.e about half the value of the pure  $\text{CoFe}_2\text{O}_4$ , suggesting that part of the “effective” strain produced by  $\text{CoFe}_2\text{O}_4$  is reduced either by the different elastic constants of the components or by the interface between the magnetostrictive and piezoelectric constituent.

The low field temperature dependence of the magnetization is shown in Fig. 6. It reveals a huge change in the magnetization of the  $\text{CoFe}_2\text{O}_4$  constituent when the alignment of the electric dipoles in  $\text{BaTiO}_3$  constituent is destroyed by increasing temperature to its ferroelectric Curie point (393 K). When increasing the temperature from 300 to 400 K, the part A-B, the magnetization of the  $\text{CoFe}_2\text{O}_4$  constituent in the electrically poled sample, i.e the electric dipoles of the  $\text{BaTiO}_3$  constituent are aligned, decreasing from 7.6 to 5.25 emu/g. After that, decreasing the temperature from 400 to 300 K, the magnetization increases to only 6.2 emu/g, which is about 18.4 % smaller than its initial value. This huge difference proposed result from the difference in the alignment of the electric dipoles of the  $\text{BaTiO}_3$  constituent. In the first case, all electric dipoles were almost parallel at 300 K due to electrical poling of the sample. These parallel electric dipoles will interact with the magnetic moments of the  $\text{CoFe}_2\text{O}_4$  constituent, acting as an “additional field”. When the temperature reached 400 K which is slightly higher than the Curie temperature of  $\text{BaTiO}_3$ , the electric dipoles are vanishing. On the way cooling back to 300 K, the part B-C, the electric dipoles raised again, however, in a random distribution, making the total electric polarization of the  $\text{BaTiO}_3$  constituent almost zero. Therefore, the “additional field” causing by the interaction between electric dipoles and magnetic moments in this case is also almost zero, resulting in a smaller “total field” compared to that of the first case, leading to a smaller magnetization as shown in Fig. 6. Increasing again the temperature from 300 to 400 K, the part C-D, as well as decreasing it from 400 to 4.2 K and increasing up to 400 K, the part D-E and E-F, causes almost no change in the magnetization since the electric dipoles in these cases were already randomly distributed, giving no “additional field” as when all electric dipoles are parallel alignment.

The nature of the interaction between magnetic and electric moments or more probable domains, i.e some kind of direct magneto-electric coupling, in this composite is not understood yet. In matter, the electromagnetic field will act on both magnetic and electric

domains, leading to a direct coupling between these domains on a nanoscale, especially when the distance between them is very small as is the case of single phase ME materials or the ME nanocomposite studied here.

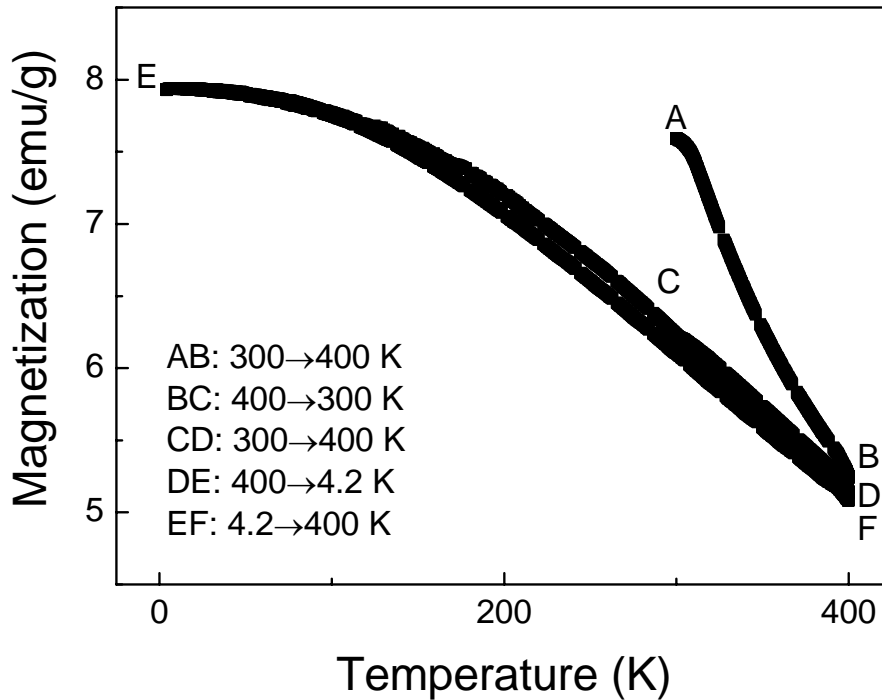


Fig.6 : Temperature-dependent magnetization of the cobalt ferrite constituent in  $\text{CoFe}_2\text{O}_4\text{-BaTiO}_3$  core-shell structure composite under a magnetic field of 100 Oe.

#### 4. Conclusion

Magnetic properties of the nanocrystalline cobalt ferrite in  $\text{CoFe}_2\text{O}_4$  core-shell structure composite have been studied. An unusual upturn in the magnetization at low temperatures was observed. The reduced magnetostriction in the composite is attributed to differences of the elastic constants or interfaces within the substituents, leading to a mechanical coupling between the magnetostrictive and piezoelectric phases which can be increased by optimizing the microstructure. The huge difference in low field temperature dependent magnetization of  $\text{CoFe}_2\text{O}_4$  constituent, when  $\text{BaTiO}_3$  is in ferroelectric or paraelectric state, gives evidence of strong direct coupling between magnetic and electric domains.

## Acknowledgement

This work is supported by the FWF Proj. Nr. P16500-N02, Proj. Nr. P15737 and the Austrian Exchange Service (ÖAD).

## References

- [1] J. Van Suchetelene, Philips Res. Rep. 27 (1972) 28.
- [2] J. van den Boomgaard and R.A.J. Born, J. Mater. Sci., 13 (1978) 1538.
- [3] J. van den Boomgaard, A.M.J.G. Van Run, and J. Van Suchetelene, Ferroelectrics, 10 (1976) 295.
- [4] J. van den Boomgaard, D.R. Terrell, R.A.J. Born, and H.F.J.I. Giller, J. Mater. Sci., 9 (1974) 1705.
- [5] A.M.J.G. Van Run, D.R. Terrell, and J.H. Scholing, J. Mater. Sci., 9 (1974) 1710.
- [6] S.Mazuder, G.S. Bhattacharyya, Ceramics Int. 30 (2004) 389-392.
- [7] Giap V. Duong, R. Groessinger, R. Sato Turtelli, Magnetolectric Properties of CoFe<sub>2</sub>O<sub>4</sub>-BaTiO<sub>3</sub> Core-Shell Structure Composite, IEEE Transactions on Magnetics, in press.
- [8] Giap V. Duong, R. Groessinger, M. Schoenhardt, D. Bueno-Basques, The Lock-in Technique for Studying Magnetolectric Effect, J. Magn. Mater., accepted for publication.
- [9] H.G. Jiang, M. Rühle, E.J. Lavenia J. Mater. Res. 14, 2 (1999) 549.
- [10] Yuqiu Qu, Haibin Yang, Nan Yang, Yuzun Fan, Hongyang Zhu, Guangtian Zou, Mater. Lett. (2006), in press.
- [11] Giap V. Duong, R. Grössinger, R. Sato Turtelli, M. Knobel, Magnetic properties of nanocrystalline CoFe<sub>2</sub>O<sub>4</sub> synthesized by modified citrate-gel method, submitted for publication.
- [12] D.J. Craik, Magnetic Oxides, Part 2, Wiley, London, 1975, pp. 703.

*...they are different aspects of the same thing...*

## **Magnetoelectric Studies**

*Magnetoelectric properties of the studied composites will be discussed in this part.*

## The Lock-in Technique for Studying Magnetolectric Effect

Giap V. Duong<sup>1,2</sup>, R. Groessinger<sup>1</sup>, M. Schoenhardt<sup>1</sup>, D. Bueno-Basques<sup>3</sup>

<sup>1</sup>*Institute for Solid State Physics, Vienna Uni. Tech., Wiedner Hauptstr. 8-10, 1040, Vienna, Austria*

<sup>2</sup>*Faculty of Chemical Engineering, Hanoi Uni. Techn., 1- Dai Co Viet, Hai Ba Trung, Hanoi, Vietnam*

<sup>3</sup>*CIMAV, Miguel de Cervantes, 120<sup>o</sup>, 31109, Chihuahua, Mexico*

Accepted June 22<sup>nd</sup>, 2006.

---

### Abstract

Measuring techniques for studying the magnetolectric effect are not established yet. In this work, we report about a lock-in technique for studying the magnetolectric effect in magnetolectric-multiferroic composites. The philosophy as well as the theory of measurement is discussed. The advantages and disadvantages of this method are described. Details on our experimental set-up in which an AC field with frequencies ranging from 1 to 10 kHz and amplitudes from 1 to 20 Oe are superimposed onto a DC bias field up to 15 kOe are shown. Treatments of the zero signal and operation modes are demonstrated. Magnetolectric investigations on  $\text{CoFe}_2\text{O}_4\text{-BaTiO}_3$  composites are discussed in details.

© 2006 Elsevier B.V. All rights reserved

*PACS:* 75.80.+q; 77.65.-j; 77.84.Lf; 83.85.-c

*Keywords:* Magnetolectric effect, Lock-in technique; Measuring technique; Dynamic method; Multiferroic composite

---



## 1. Introduction

The magnetoelectric (ME) effect - the induction of magnetization by means of an electric field and the induction of polarization by means of a magnetic field - is on the way of renaissance [1]. The possibility of mutual control of magnetic and electric properties is attractive due to both important potential applications and fundamental understanding of material physics [2]. However, measuring techniques for studying the ME effect are not established yet. Commercial measurement systems are not available. Different groups use different techniques to study the ME effect. This leads to a situation that results obtained by different research groups, even on similar materials, are difficult to compare. For example, ME coefficients in  $\text{CoFe}_2\text{O}_4\text{-BaTiO}_3$  composites are scattering in the range from 0.19mV/cmOe in ref. [3] to 130mV/cmOe in ref. [4]. Therefore a well established and reliable measuring technique for studying ME effect is urgently needed.

There are basically three direct methods to measure ME effect, namely: static, quasi-static and dynamic method. In the static method, the ME signal is measured as function of increasing magnetic field using a high input impedance electrometer. While poling and measuring, the charge is produced and may accumulate at the grain boundaries which then move towards the electrode during the experiments. This may lead to erroneous conclusion [5]. For the quasi-static case, the ME signal is measured as a function of time using a high input impedance electrometer while the applied DC magnetic field is varied with time [6]. However, this quasi-static method cannot solve the problem of charge accumulation, especially for polycrystalline samples. Recently a dynamic technique has been developed to study ME effect [7]. However, the theory of measurement, treatment of zero signal, operation modes, advantages and disadvantages of this method, especially the discharging process, have not been fully discussed. This motivated us to build-up an experiment set-up and to study all details on the measuring technique as well as the theory behind it. A case study of  $\text{CoFe}_2\text{O}_3\text{-BaTiO}_3$  core-shell structure composite will be discussed in details.

## 2. Experimental Set-up

The experiment set-up to measure the ME effect using lock-in technique is shown in Fig.1. The DC magnetic bias field up to 15 kOe is produced by an electromagnet. The time varying DC field is achieved by a programmable DC power source (Siemens NTN 35000-200). To measure the DC field, a Hall probe (PT1486) is employed. Additionally an AC magnetic field up to 20 Oe with frequencies from 1 to 10 kHz is superimposed onto the DC

field. The AC field is produced by a Helmholtz coil (100 turns with a diameter of 50 mm) which is driven by an AC current generated by a function generator (Siemens 17A). The amplitude of the AC field is calculated from the driving current which is measured by a multimeter (Keithley 2000). The sample is placed in the magnetic field with its surface perpendicular or parallel to the field direction, according to the longitudinal and transverse measurement, respectively. The ME signal was measured using a lock-in amplifier (EG&G model 5210) with input resistance and capacitance of 100 MΩ and 25 pF, respectively. Data acquisition was performed by computer using a Labview interference program.

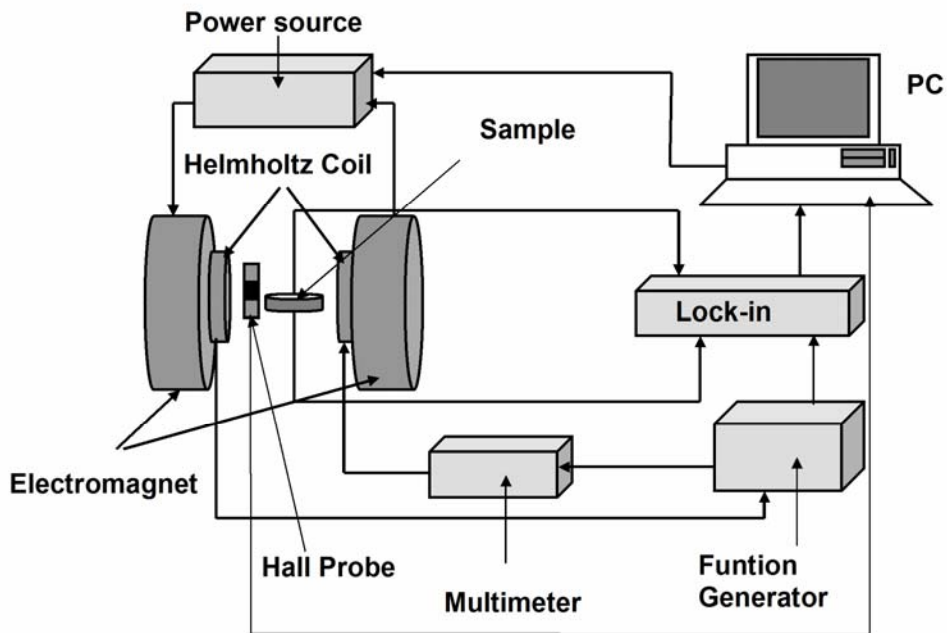


Fig.1: Schema of experiment set-up

### 3. Theory of Measurement

When magnetoelectric materials exposed to a magnetic field  $H$ , a voltage  $V$  appears. Assuming:

$$V = f(H) = Const. + \alpha H + \beta H^2 + \gamma H^3 + \delta H^4 + \dots$$

$$\Rightarrow \frac{dV}{dH} = \alpha + 2\beta H + 3\gamma H^2 + 4\delta H^3 + \dots$$

When a small AC field  $h = h_0 \sin \omega t$  superimposed onto a DC bias field  $H$ , the total field:  $H_{total} = H + h_0 \sin \omega t$ . Then:

$$\begin{aligned}
V &= Const. + \alpha(H + h_o \sin \omega t) + \beta(H + h_o \sin \omega t)^2 \\
&+ \gamma(H + h_o \sin \omega t)^3 + \delta(H + h_o \sin \omega t)^4 + \dots \\
&= \frac{1}{8} \left[ \left( Const. + 4\beta h_o^2 + 3\delta h_o^4 + 8\alpha H + 12\gamma h_o^2 H + 8\beta H^2 \right. \right. \\
&\quad \left. \left. + 24\delta h_o^2 H^2 + 8\gamma H^3 + 8\delta H^4 \right) + \left( 8\alpha h_o + 6\gamma h_o^3 \right. \right. \\
&\quad \left. \left. + 16\beta h_o H + 24\delta h_o^3 H + 24\gamma h_o H^2 + 32\delta h_o H^3 \right) \sin \omega t \right. \\
&\quad \left. + \left( -4\beta h_o^2 - 4\delta h_o^4 - 12\gamma h_o^2 H - 24\delta h_o^2 H^2 \right) \cos 2\omega t \right. \\
&\quad \left. + \left( -2\gamma h_o^3 - 8\delta h_o^3 H \right) \sin 3\omega t + \delta h_o^4 \cos 4\omega t + \dots \right]
\end{aligned}$$

The lock-in amplifier out put voltage  $V_{out}$  is:

$$\begin{aligned}
V_{out} &= \frac{1}{8} \left( 8\alpha h_o + 6\gamma h_o^3 + 16\beta h_o H + 24\delta h_o^3 H \right. \\
&\quad \left. + 24\gamma h_o H^2 + 32\delta h_o H^3 \right) \\
&= \frac{H^4}{8} \left[ \frac{8\alpha}{H^3} \left( \frac{h_o}{H} \right) + \frac{6\gamma}{H} \left( \frac{h_o}{H} \right)^3 + \frac{16\beta}{H^2} \left( \frac{h_o}{H} \right) + 24\delta \left( \frac{h_o}{H} \right)^3 \right. \\
&\quad \left. + \frac{24\gamma}{H} \left( \frac{h_o}{H} \right) + 32\delta \left( \frac{h_o}{H} \right) \right]
\end{aligned}$$

Neglecting high order terms in  $\left( \frac{h_o}{H} \right)$  when  $\left( \frac{h_o}{H} \right) \ll 1$ :

$$\begin{aligned}
V_{out} &= \frac{H^4}{8} \left( \frac{8\alpha}{H^3} + \frac{16\beta}{H^2} + \frac{24\gamma}{H} + 32\delta \right) \left( \frac{h_o}{H} \right) \\
&= h_o \left( \alpha + 2\beta H + 3\gamma H^2 + 4\delta H^3 \right) = h_o \left( \frac{dV}{dH} \right)
\end{aligned}$$

$$ME \text{ coefficient} = \frac{dE}{dH} = \frac{1}{d} \frac{dV}{dH} = \frac{V_{out}}{h_o d}$$

where  $d$  is the effective thickness of the piezoelectric phase.

Looking in the equations above one can recognize that the philosophy of this technique is to measure the effective value of the small AC ME voltage ( $V_{out}$ ) appeared across the sample when applying a small AC magnetic field instead of measuring the ME charge or voltage as in the static method. This method also allows one to measure the phase shift of the signal. However, this phase shift is approximately constant during varying the bias field measurements. By changing the DC magnetic bias field, one can explore the ME effect at different working points of the sample. And by changing the frequency of the AC field, one can study the response of the sample under different time scale. Since the ME signal in this method has a well defined frequency (determined by the driving current) and is measured by a lock-in amplifier, the noise is dramatically reduced and the problem of charge accumulation is

avoided. These are the advantages of this method. However, due to the assumption that the AC field is much smaller than the DC one ( $h_o/H \ll 1$ ), this method will give information about the ME effect at low AC magnetic field but at different working points of the magnetostrictive component.

Another weak point of this method is the discharging process which may occur under the periodic condition during measurements. If low frequencies are employed, the discharge may happen through the resistance of the sample. At high frequencies, the discharge will occur through the capacitance formed by the two surface of the sample. So this method may give a smaller ME coefficients as compared to those measured by other method.

Since an AC magnetic field is employed, an induction voltage always exists, contributing as zero signal. To avoid it, the lock-in amplifier has to work in differential mode to subtract the common mode induction contribution. Using this mode, not only the zero signal problem is solved, but also the calibration is not needed, since with good cable (well shielded, low capacity) and good connection, the ME signal is zero without sample or with a non-magnetoelectric samples.

#### 4. Results and discussion

Using the experiment set-up above, the ME effect of the 50%CoFe<sub>2</sub>O<sub>4</sub>-50%BaTiO<sub>3</sub> (in mass) core-shell structure ME composite has been studied. The preparation procedure has been described elsewhere [8]. Fig.2 shown the longitudinal and transverse ME coefficient at room temperature of this sample.

The ME coefficient vs. DC bias field curves,  $\alpha_E-H_{DC}$ , shown maxima at DC bias field of 1-2.5 kOe, depending on the condition of measurement (longitudinal or transverse). The maximum ME coefficient is 3.4 mV/cmOe, which is similar to those reported in ref. [9] (3.0081 to 5.5886 mV/cmOe for CoFe<sub>2</sub>O<sub>4</sub>-BaTiO<sub>3</sub> composite prepared by in situ solid state reactions), smaller than the one reported in ref. [4] (130mV/cmOe for (BaTiO<sub>3</sub>)<sub>0.61</sub>-((CoFe<sub>2</sub>O<sub>4</sub>)<sub>0.47</sub>(CoTiO<sub>4</sub>)<sub>0.53</sub>)<sub>0.39</sub> composite prepared by unidirectional solidification (measuring in resonance condition), but 1-4 mV/cmOe for other compositions) and bigger than the one reported in ref. [3] (0.19 mV/cmOe for 50%CoFe<sub>2</sub>O<sub>4</sub>-50%BaTiO<sub>3</sub> (in mass) mixed structure composite prepared by solid state reaction). The wide range scattering of the ME coefficients may be attributed to the difference in composition, structure of the composites or the different measuring methods.

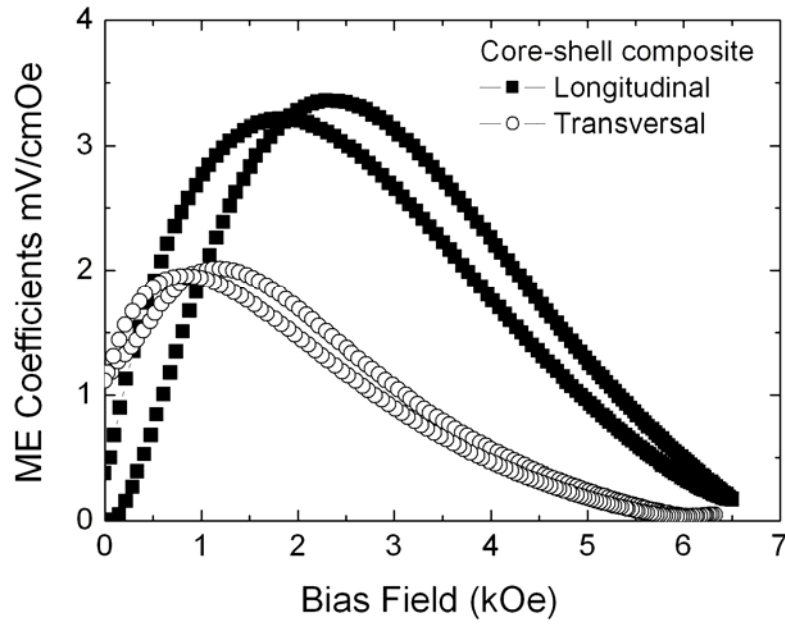


Fig.2: Longitudinal and transvers ME coefficients of  $\text{CoFe}_2\text{O}_4\text{-BaTiO}_3$  core-shell structure composite, AC magnetic field: 270 Hz, 10 Oe.

The DC bias field  $H_{max}$ , where maximum ME coefficient occurs, is not the coercive field as supposed by some researchers [10], but the one where maximum linear magnetostriction occurs [8]. When changing the measuring condition from longitudinal to transverse, this  $H_{max}$  change due to the different demagnetizing field.

The  $\alpha_E\text{-}H_{DC}$  has a hysteretic nature due to the hysteresis behavior of the constituents. A remanence is also observed. The reason is the polarization remanence of the  $\text{BaTiO}_3$  component and the charge accumulation on the grain boundaries of the sample [5]. The irreversibility in the  $\alpha_E\text{-}H_{DC}$  curve measured when increasing and decreasing DC bias field may be attributed to the irreversible behavior of the constituents. The curves do not depend on the sweep rate of the DC bias field.

The frequency dependence of  $\alpha_E$  at room temperature is shown in Fig.3. For our sample, the optimum frequency is about 200 Hz. This is not the resonant frequency since it is quite small as compared to those reported in literature [10], and the change of  $\alpha_E$  is just about 20%. Below this frequency, the discharging process occurs through the sample resistance, but above this one, it occurs through the capacitance as mentioned above. Our experiments with different input resistances and capacitances confirm this phenomenon.

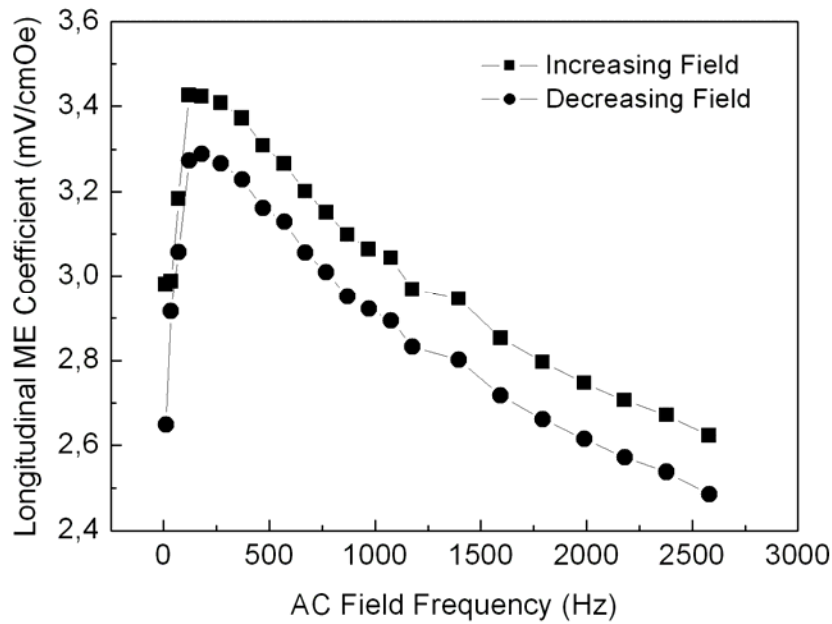


Fig.3: Frequency dependent of longitudinal ME coefficient.

## 5. Conclusion

An experiment set-up using lock-in technique to study the ME effect has been developed. The theory of measurement as well as the advantages and disadvantages of this technique have been discussed. During measurement, the discharging process may occur due to the finite impedances of the sample and the lock-in amplifier.

## Acknowledgment

This work was partly supported by FWF Proj. Nr. P16500-N02 and a Technology Grant Southeast Asia from the ÖAD.

## References

- [1] Nicola A. Spaldin and Manfred Fiebig, Science 309 (2005) July 15.
- [2] Bas V. Van Aken et al, Nature, Vol.3 (2004) March.
- [3] R.P. Mahajan, K.K. Patankar, M.B. Kothale, S.C. Chaudhari, V.L. Mathe, S.A. Patil, Pramana-J. Phys. 58 (2002) 1115.
- [4] J. van Suchetelene, Philips Res. Rep., 27, 28 (1972).

- [5] R. S. Singh, T. Bhimasankaram, G. S. Kumar and S. V. Suryanarayana, *Solid State Commun.* 91 (1994) 567.
- [6] J.P. Rivera, *Ferroelectrics* 161 (1994) 165.
- [7] M. Mahesh Kumar, A. Srinivas, S. V. Suryanarayana, G. S. Kumar, T. Bhimasankaram, *Bull. Mater. Sci.* Vol.21 No.3 (1998) 251
- [8] Giap V. Duong, R. Groessinger, R. Sato Turtelli, *Magnetoelectric Properties of CoFe<sub>2</sub>O<sub>4</sub>-BaTiO<sub>3</sub> Core-Shell Structure Composite*, submitted for publication.
- [9] S. Mazumder, G.S. Bhattacharyya, *Ceram. Int.* vol.30 no.3 (2004) 389.
- [10] Manfred Fiebig, *J. Phys. D: Appl. Phys.* 38 (2005) R123–R152.

# Magnetoelectric Properties of CoFe<sub>2</sub>O<sub>4</sub>-BaTiO<sub>3</sub> Core-Shell Structure Composite

Giap V. Duong, Roland Groessinger, Reiko Sato Turtelli

Accepted June 19<sup>th</sup>, 2006.

*Abstract*—The CoFe<sub>2</sub>O<sub>4</sub>-BaTiO<sub>3</sub> core-shell structure composite has been successfully synthesized by wet chemical method. X-ray characterization showed that the composite consisted of two single phases: CoFe<sub>2</sub>O<sub>4</sub> and BaTiO<sub>3</sub>. The saturation magnetization of the CoFe<sub>2</sub>O<sub>4</sub> component in composite was found to be similar to those of the bulk sample. It was observed that the longitudinal and transverse magnetoelectric coefficients of the core-shell structure are 18 times higher than those of the mixed structure.

*Index Terms*—Barium titanate, Cobalt ferrite, Magnetoelectric effect, Multiferroics.

## I. INTRODUCTION

MAGNETOELECTRIC (ME) materials become magnetized when placed in an electric field and electrically polarized when placed in a magnetic field. Thus an effective conversion between electric and magnetic energy becomes possible. They can be realized as single phase and composite materials. The number of single phase ME materials is limited due to the primary requirement that magnetic and electric dipoles have to coexist in an asymmetric structure. The ME coefficient,  $\alpha_E = (\partial E / \partial H)_T$ , where  $E$  is the induced electrical field in an applied magnetic field  $H$ , in single phase materials is small, the working temperature is low and they involve expensive materials and processing techniques. These limitations can be overcome when

---

Manuscript received March 13, accepted June 19, 2006. This work was supported by the ÖAD (Technology Grant Southeast Asia) and FWF Proj. Nr. P16500-N02.

Giap V. Duong is with the Faculty of Chemical Engineering, Hanoi University of Technology, No.1 Dai Co Viet, Hai Ba Trung, Hanoi, Vietnam, and the Institute of Solid State Physics, Vienna University of Technology, Wiedner Hauptstrasse 8-10, 1040, Vienna, Austria (phone: +43 1 58801 13152; fax: +43 1 58801 13899; e-mail: giap@ifp.tuwien.ac.at).

Roland Groessinger is with the Institute of Solid State Physics, Vienna University of Technology, Wiedner Hauptstrasse 8-10, 1040, Vienna, Austria (e-mail: rgroess@ifp.tuwien.ac.at)

Reiko Sato Turtelli is with the Institute of Solid State Physics, Vienna University of Technology, Wiedner Hauptstrasse 8-10, 1040, Vienna, Austria (e-mail: reiko.sato@ifp.tuwien.ac.at).



shifting to composites, which usually consist of magnetostrictive and piezoelectric phases. Multilayer or laminate composites of ferrite and piezoelectric thick layers show a large ME effect [1]-[3]. The ME effect in such structure originates from “product properties” of the constituent phases and can reach a maximum ME coefficient of  $5900 \text{ mV.cm}^{-1}.\text{Oe}^{-1}$  [1]. However, in the  $\text{CoFe}_2\text{O}_4\text{-BaTiO}_3$  systems, the ME coefficients vary in a wide range, from 0.19 in ref. [4] to  $130 \text{ mV.cm}^{-1}.\text{Oe}^{-1}$  in ref. [5]. The highest value is for the  $(\text{BaTiO}_3)_{0.61}\text{-}((\text{CoFe}_2\text{O}_4)_{0.47}\text{-}(\text{CoTiO}_4)_{0.53})_{0.39}$  composite (eutectic composition with alternate layers prepared by unidirectional solidification method). For other composition, the ME coefficients vary from 1-4  $\text{mV.cm}^{-1}.\text{Oe}^{-1}$ . Differences in the sample characteristics (constituent, composition, microstructure, size, impedance, etc.), measuring techniques (static, quasi-static, pulse, resonant, etc.) and measuring conditions (input impedance of instruments, field direction, frequency of the AC field, etc.) make a conclusion what is the highest possible ME effect for a certain material up to now impossible.

The motivation of this work is to synthesize a  $\text{CoFe}_2\text{O}_4\text{-BaTiO}_3$  core-shell structure composite and to study its ME properties. The core-shell structure was chosen believing that this can cause a better coupling between the two phases.  $\text{CoFe}_2\text{O}_4$  and  $\text{BaTiO}_3$  were chosen not only due to its good magnetic and piezoelectric properties but also its high electrical resistance that can help to prevent the discharging process during the measurements. Additionally, its chemical and mechanical stability and non-toxic properties are important for environment and health in applications.

## II. EXPERIMENTAL

The sample was synthesized using wet chemical method. All chemicals are in analytic pure grade.  $\text{CoFe}_2\text{O}_4$  powder obtained from appropriate solution containing  $\text{Co}(\text{NO}_3)_2.6\text{H}_2\text{O}$  and  $\text{Fe}(\text{NO}_3)_3.9\text{H}_2\text{O}$  and co-precipitating at  $75^\circ\text{C}$  using  $\text{NaOH}$  solution. To obtain  $\text{CoFe}_2\text{O}_4\text{-BaTiO}_3$  core-shell structure composite, the co-precipitated  $\text{CoFe}_2\text{O}_4$  powder, calculated to get a composite containing 50% in mass of each constituent, was introduced into a solution of acetic acid, barium hydroxide and titanium (IV) n-Butoxide, which is then gelled on the surface of the  $\text{CoFe}_2\text{O}_4$  grains or particles during heating and stirring. The obtained material is dried, pre-sintered at  $700^\circ\text{C}$  for 2 hours, ground into fine powder, then pressed under a pressure of 6 tones/ $\text{cm}^2$  to obtain a sample in shape of a disc of 10 mm in diameter and 1.5 mm thick. This sample is sintered at  $1250^\circ\text{C}$  for 12 hours to get a core-shell structure composite. After heat treatment, due to shrinkage, the diameter and thickness of the sample

are 8.7 and 1.3mm, respectively. The sample was painted by silver paste for electric contacts, then poled electrically under an electric field of 7500V/cm (field direction is perpendicular to the surface of the sample) in silicon oil from 150°C down to room temperature. For comparison, a sample with similar composition was produced by mixing the CoFe<sub>2</sub>O<sub>4</sub> and BaTiO<sub>3</sub> powders following by the same heat treatment and poling procedure.

The crystalline structures of single phase materials as well as composites were investigated by X-ray diffractometer (XRD) using Co-K<sub>α</sub> radiation. The hysteresis loops were measured at room temperature using a pulse field magnetometer which generates field up to 5T with a typical pulse duration of 50 ms. The magnetostriction was measured using strain gauge method with a 50 kHz bridge (HBM Type KWS 85.A1).

The ME coefficient was measured using lock-in technique employing an AC field with frequencies from 1 Hz to 4 kHz and amplitudes from 0.1 Oe to 20 Oe superimposed onto a DC magnetic field (generated by an electromagnet) up to 6.5 kOe,  $H_{DC}$  [6]. The input resistance and capacitance of the lock-in (EG&G model 5210) is 100 MΩ and 25 pF, respectively. The measurements of the ME voltage were performed for two different field orientations with respect to the sample plane to obtain the transverse and longitudinal ME coefficients. The absolute values of the voltage may depend on the ratio between the resistances of the samples and the lock-in amplifier. The ME coefficient,  $\alpha_E$ , was determined using the equation  $\alpha_E = (\partial E / \partial H)_T = V / (d \cdot H_{AC})$ , where  $V$  is the voltage measured with the lock-in amplifier,  $d$  is the effective thickness of the piezoelectric phase (in this work it was considered 47% of the thickness of the sample since the density of CoFe<sub>2</sub>O<sub>4</sub> and BaTiO<sub>3</sub> are 5.3 and 6.08 g/cm<sup>3</sup>, respectively) and  $H_{AC}$  is the amplitude of the applied AC field [6]. The schema showing the ME transverse ( $E$  perpendicular to  $H$ ) and longitudinal ( $E$  parallel to  $H$ ) measurements are represented in Fig. 1. All measurements were carried out at room temperature and ambient pressure.

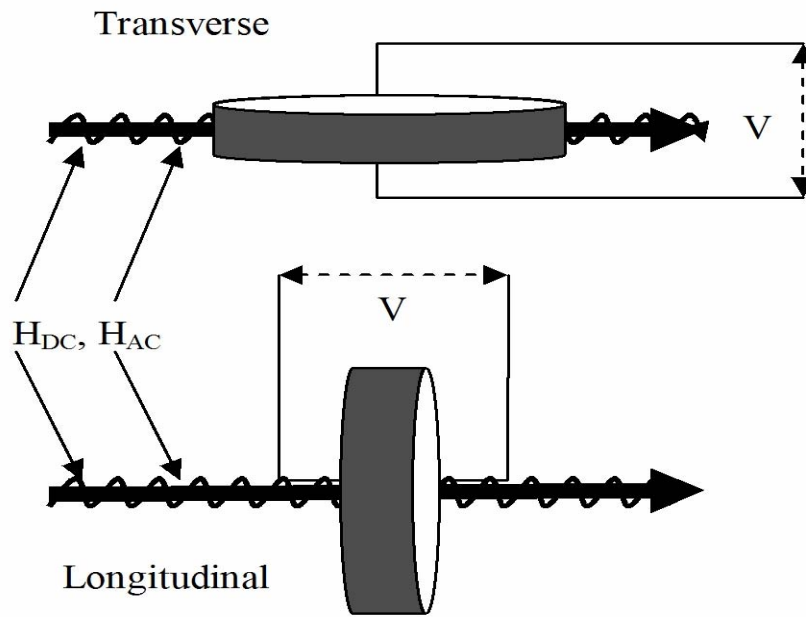


Fig. 1. Schema of the longitudinal and transverse ME coefficient measurements

### III. RESULTS AND DISCUSSIONS

The XRD patterns in Fig. 2 suggest that the composites consist of two single phases only:  $\text{CoFe}_2\text{O}_4$  and  $\text{BaTiO}_3$ . The particle size of the as-coprecipitated  $\text{CoFe}_2\text{O}_4$  evaluated using Scherrer equation [7] for the full-width at half maximum is about 10 nm. The saturation magnetization and coercive field of the as-coprecipitated  $\text{CoFe}_2\text{O}_4$  is of 53 emu/g and 310 Oe, respectively. However, the saturation magnetization of the magnetostrictive component ( $\text{CoFe}_2\text{O}_4$ ) in the core-shell structure composite increases to 72 emu/g and the coercive field of the composite is similar to that of co-precipitated ferrite. This increase of the saturation magnetization may be attributed to the less spin canted surface layers due to heat treatment. To have a comparison, the bulk  $\text{CoFe}_2\text{O}_4$  prepared by sol-gel method presents a saturation magnetization of 78 emu/g, but a coercivity of 825 Oe.

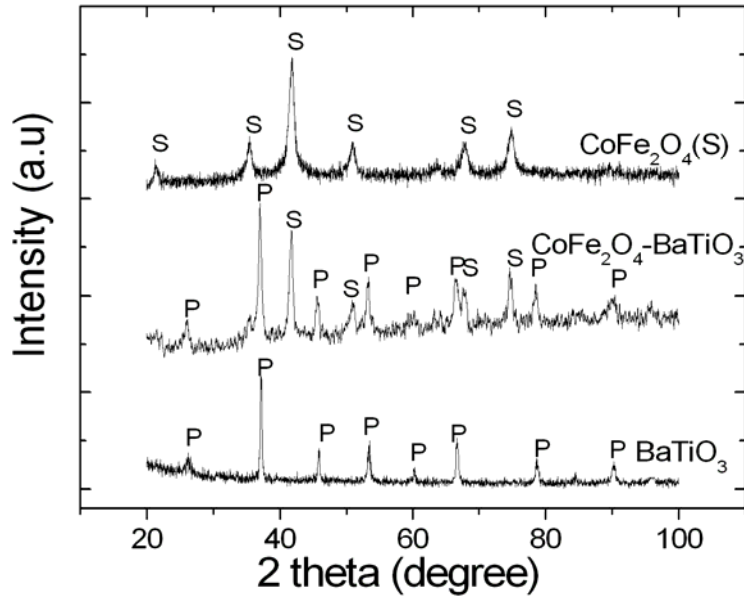


Fig. 2. XRD patterns of  $\text{CoFe}_2\text{O}_4$  (spinel structure),  $\text{BaTiO}_3$  (perovskite structure) and  $\text{CoFe}_2\text{O}_4$ - $\text{BaTiO}_3$  composite

Fig. 3 and 4 show the longitudinal and transverse ME coefficients as function of the bias field,  $\alpha_E(H_{DC})$ , measured on the core-shell structure and mixed structure composites, respectively, under an AC field of 10 Oe with a frequency of 270 Hz. The  $\alpha_E(H_{DC})$  curves show hysteresis, remanence and maximum, where the values and positions of the maxima depend on the samples and field orientations. As the bias field is increased from zero, in core-shell composite, for the longitudinal  $\alpha_E$  vs.  $H_{DC}$  curve, the maximum of  $\alpha_E$  occurs at 2.2 kOe with a value of  $3.4 \text{ mV}\cdot\text{cm}^{-1}\cdot\text{Oe}^{-1}$ , and in the transverse case, at 1.4 kOe with a value of  $2.0 \text{ mV}\cdot\text{cm}^{-1}\cdot\text{Oe}^{-1}$ . These values are smaller compared to those in ref. [5] ( $130 \text{ mV}\cdot\text{cm}^{-1}\cdot\text{Oe}^{-1}$  for the  $(\text{BaTiO}_3)_{0.61}-(\text{CoFe}_2\text{O}_4)_{0.47}-(\text{CoTiO}_4)_{0.53})_{0.39}$  composition) but bigger than those in ref. [4] ( $0.19 \text{ mV}\cdot\text{cm}^{-1}\cdot\text{Oe}^{-1}$  for  $\text{CoFe}_2\text{O}_4$ - $\text{BaTiO}_3$  sintered composite). The reason may be due to the difference in the sample compositions and the actual microstructures.

The bias field where the maximum occurs in case of the longitudinal is larger than the transverse case. The reason is: the demagnetizing field in the longitudinal case (magnetic field parallel to the sample plane) is bigger than that of the transverse (magnetic field perpendicular to the sample plane), which can be seen clearly in Fig. 5.

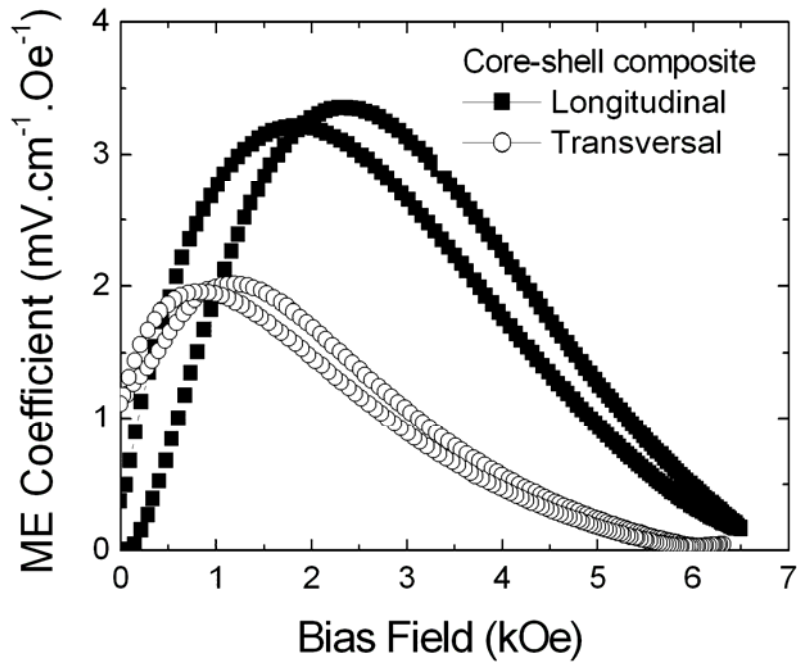


Fig. 3. Bias field dependent of  $\alpha_E$  measured on  $\text{CoFe}_2\text{O}_4$ - $\text{BaTiO}_3$  core-shell structure composite.

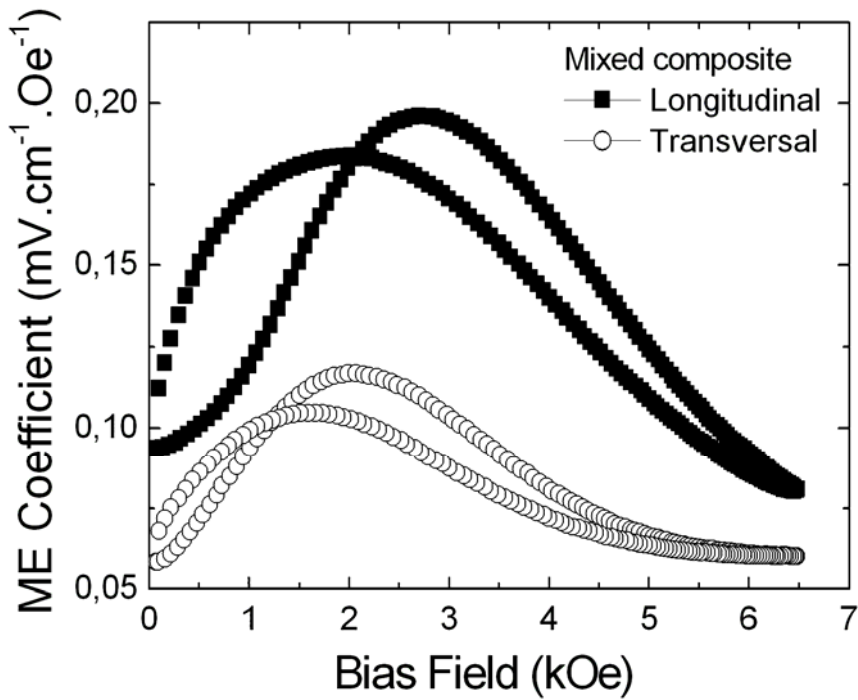


Fig. 4. Bias field dependent of  $\alpha_E$  measured on  $\text{CoFe}_2\text{O}_4$ - $\text{BaTiO}_3$  mixed structure composite.

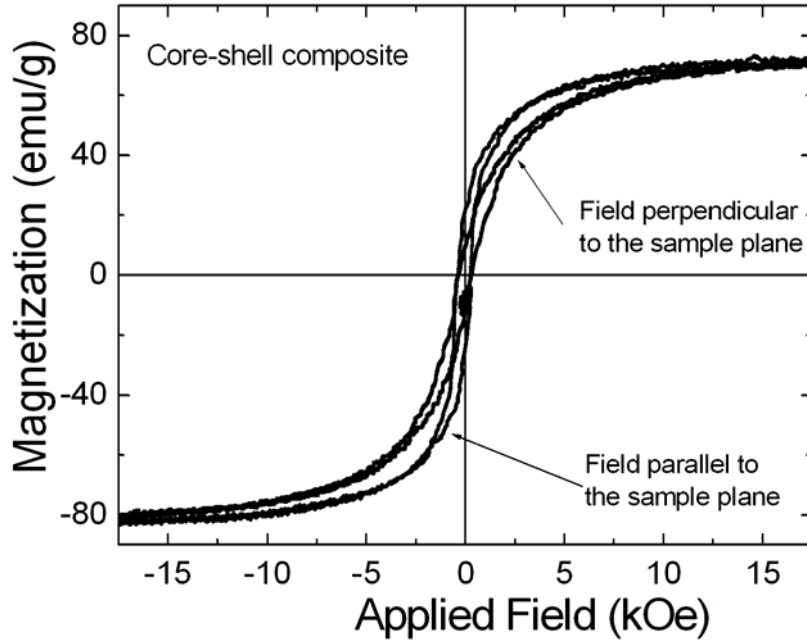


Fig. 5. Hysteresis loops of  $\text{CoFe}_2\text{O}_4$  component measured parallel and perpendicular to the sample plane

As reported in [3], the  $\alpha_E(H_{DC})$  tracks roughly the strength of piezomagnetic coupling  $q=d\lambda/dH$  where  $\lambda$  is the magnetostriction of the ferrite. As can be seen in Fig. 6 which shows the field dependence of  $\lambda$  ( $\lambda_{\text{par}}$  is the longitudinal magnetostriction and  $\lambda_{\text{per}}$  is transverse magnetostriction), the maximum  $d\lambda/dH$  occurs at around 1-3 kOe, where the maximum  $dM/dH$  in the magnetization curve occurs, too (see magnetic hysteresis loops in Fig. 5). The longitudinal and transverse  $\alpha_E$  are almost 18 times higher as compared to those found in the mixed structure composite (see Fig. 4). Our results obtained in the mixed structure composite are in agreement with the results reported in [4]. One can deduce that the coupling between the two phases in the core-shell structure is much better than in the mixture. In this work, in both cases, the longitudinal ME coefficient is bigger than the transverse one. This is different from results reported in literature [3]: the transverse ME coefficient is bigger than the transverse one. However, our results actually suggest that the  $\alpha_E(H_{DC})$  curve follows the strength of the  $H$  dependent of  $\lambda$ , that is,  $\lambda_{\text{par}} > \lambda_{\text{per}}$ , see Fig.6. The decrease in ME coefficient at higher bias field may be attributed to the saturated state of the magnetization and total magnetostriction that weaken the piezomagnetic coupling.

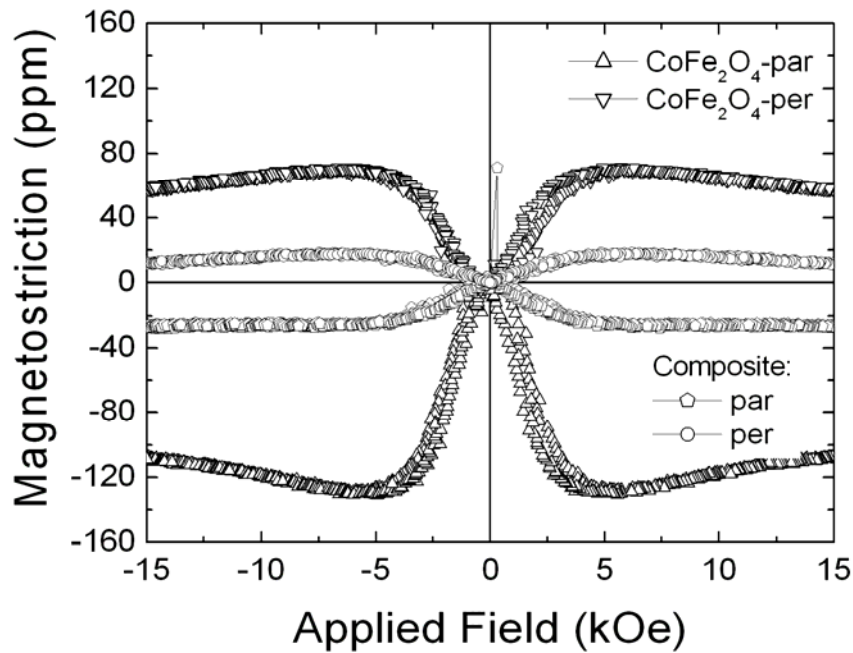


Fig. 6. Magnetostriction of  $\text{CoFe}_2\text{O}_4$  and  $\text{CoFe}_2\text{O}_4$ - $\text{BaTiO}_3$  core-shell structure composite at room temperature

#### IV. CONCLUSION

Composite with core-shell structure of 50%  $\text{CoFe}_2\text{O}_4$  and 50%  $\text{BaTiO}_3$  in mass has been successfully synthesized. The magnetoelectric properties of the composite have been studied at room temperature and ambient pressure. The coupling between the magnetostrictive and piezoelectric phases in the core-shell structure composite is much better than that in the mixed structure, resulting in a ME coefficient which is about 18 times bigger in the former as compared to those in the later. In our work,  $\alpha_E$  vs.  $H_{DC}$  curve tracks roughly the strength of piezomagnetic coupling  $q = d\lambda/dH$ .

#### REFERENCES

- [8] Jungho Ryu, Shashank Priya, Kenji Uchino & Hyoun-Ee Kim, "Magnetoelectric Effect in Composites of Magnetostrictive and Piezoelectric Materials", *J. Electroceramics*, **8**, 107–119, 2002.
- [9] Manfred Fiebig, "Revival of the magnetoelectric effect", *J. Phys. D: Appl. Phys.* **38**, R123–R152, 2005.

- [10] G. Srinivasan, E. T. Rasmussen and R. Hayes, “Magnetolectric effects in ferrite-lead zirconate titanate layered composites: The influence of zinc substitution in ferrites”, *Phys. Rev. B*, **67** 014418, 2003.
- [11] R.P. Mahajan, K.K. Patankar, M.B. Kothale, S.C. Chaudhari, V.L. Mathe, S.A. Patil “Magnetolectric effect in cobalt ferrite-barium titanate composites and their electrical properties”, *Pramana-J. Phys.*, **58**, 1115, 2002.
- [12] J. Van Suchetelene, *Philips Res. Rep.*, **27**, 28, 1972.
- [13] Giap V. Duong, R. Groessinger, M. Schoenhart, D. Bueno-Basques, “The Lock-in technique for studying magnetolectric effect”, *J. Magn. Magn. Mater.*, to be published.
- [14] H.G. Jiang, M. Rühle and E.J. Lavernia, “On the applicability of the X-ray diffraction line profile analysis in extracting grain size and microstrain in nanocrystalline materials”, *J. Mater. Res.* **14**, iss.2, 544-549, 1999.



# Effect of Preparation Conditions on Magnetoelectric Properties of $\text{CoFe}_2\text{O}_4\text{-BaTiO}_3$ Magnetoelectric Composites

Giap V. Duong<sup>1,2</sup>, R. Groessinger<sup>1</sup>

<sup>1</sup>*Institute for Solid State Physics, Vienna Uni. Techn., Wiedner Hauptstr. 8-10, 1040, Vienna, Austria*

<sup>2</sup>*Faculty of Chemical Engineering, Hanoi University of Technology, Dai Co Viet, Hai Ba Trung, Hanoi, Vietnam*

Accepted June 22<sup>nd</sup>, 2006.

---

## Abstract

The preparation conditions affect the microstructure of the samples and influence the coupling between the magnetostrictive and piezoelectric phases in magnetoelectric composites. In this work, the optimum conditions for preparing  $\text{CoFe}_2\text{O}_4\text{-BaTiO}_3$  core-shell structure magnetoelectric composites were investigated. For pressing the composite powders, an optimum pressure of 6 tones/cm<sup>2</sup> was found. For the sintering process, to sinter the sample at 1250°C for 4 hours were best suited. By changing the preparation conditions, the ME coefficients of the studied samples may change 20 times, from 0.18 to 3.53 and 0.1 to 2.23 mV/cmOe for longitudinal and transverse measurements, respectively. This shows that the preparation conditions which mean the microstructure play an important role for the magnetoelectric effect in  $\text{CoFe}_2\text{O}_4\text{-BaTiO}_3$  magnetoelectric composites.

© 2006 Elsevier B.V. All rights reserved

PACS: 75.80.+q; 77.65.-j; 77.84.Lf

**Keywords:** Magnetoelectric effect; Multiferroic composite; Preparation conditions; Barium titanate; Cobalt ferrite

---

## 1. Introduction

The magnetoelectric effect (ME) is generally the induction of magnetization by applying an electric field and/or the induction of an electric polarization by means of a magnetic field. In composites, the origin of ME effect is due to the interactions between a magnetostrictive and a piezoelectric phases through mechanical coupling [1-2]. So the preparation conditions which affect the microstructure of the samples play an important role in the coupling between these two phases. An investigation of a lead zirconate titanate/Ni-ferrite composites showed that the sintering temperature influences considerably the ME properties of the samples [3]. For  $\text{CoFe}_2\text{O}_4$ - $\text{BaTiO}_3$  composites, the ME coefficient scattered in a wide range, from 0.19 to 130 mV/cmOe [1], [4-5] depending on the preparation method suggesting that the microstructure influences strongly the ME properties of the samples. Until now the interplay between the preparation conditions which affect directly the microstructure of the samples and consequently the ME properties of  $\text{CoFe}_2\text{O}_4$ - $\text{BaTiO}_3$  composites is not understood.

Recently a  $\text{CoFe}_2\text{O}_4$ - $\text{BaTiO}_3$  composite with the so-called core-shell structure was prepared by us [6]. In this work, we report on the effect of preparation conditions including pressure, sintering temperature and sintering duration on the ME effect of the 50% $\text{CoFe}_2\text{O}_4$ -50% $\text{BaTiO}_3$  (in mass) core-shell structure composite to demonstrate the effect of microstructure on its ME properties.

## 2. Experiments

The samples were prepared by wet chemical method followed by a proper heat treatment and poling procedure. Details have been described elsewhere [6]. In brief description, the  $\text{CoFe}_2\text{O}_4$  powder with average particle size of 10 nm prepared by co-precipitation method were used as core and introduced into a solution of acetic acid, barium hydroxide and titanium (IV) n-Butoxide, which is then gelled on the surface of the  $\text{CoFe}_2\text{O}_4$  particles during heating and stirring. The obtain materials were dried, presintered, pressed into pellets (1.5 mm thick and 10 mm in diameter), annealed at high temperature, painted by silver paste for electric contact and poled electrically (electric field is 7.5 kV/cm, perpendicular to the surface of the sample). The crystalline structures of single phase materials as well as composites were investigated by X-ray diffractometer (XRD) using  $\text{Co-K}_\alpha$  radiation. The magnetic properties were studied using a pulse field magnetometer with a magnetic field up 50 kOe. The ME voltages were measured using a lock-in technique where a small AC field

(amplitude of 1-20 Oe, frequency of 1-10 kHz) was superimposed onto a DC bias field (up to 15 kOe) as described in ref. [7]. The ME coefficient,  $\alpha_E$ , was determined using the equation  $\alpha_E = (\partial E / \partial H)_T = V / (d \cdot H_{AC})$ , where  $V$  is the voltage measured with the lock-in amplifier,  $d$  is the effective thickness of the piezoelectric phase (in this work it was considered 47% of the thickness of the sample since the density of  $\text{CoFe}_2\text{O}_4$  and  $\text{BaTiO}_3$  are 5.3 and 6.08 g/cm<sup>3</sup>, respectively) and  $H_{AC}$  is the amplitude of the applied AC field. Longitudinal or transverse measurements were carried out when the surface of the sample is perpendicular or parallel to the magnetic field direction, respectively. All measurements were carried out at room temperature.

### 3. Results and Discussion

The XRD patterns of the sample sintered at 1250°C for 12 hours demonstrate that the composite consist of two single phases only:  $\text{CoFe}_2\text{O}_4$  and  $\text{BaTiO}_3$  [6]. The particle size of the as-coprecipitated  $\text{CoFe}_2\text{O}_4$  evaluated using Scherrer equation [8] for the full-width at half maximum is about 10 nm. The saturation magnetization and coercive field of the as-coprecipitated  $\text{CoFe}_2\text{O}_4$  is 53 emu/g and 310 Oe, respectively. Sintering this sample at 1250°C for 12 hours leads to a saturation magnetization of 72 emu/g of the  $\text{CoFe}_2\text{O}_4$  in the core-shell structure composite whereas the coercive field is about 460 Oe. This increase of the saturation magnetization may be attributed to a curing of the disturbed surface layer due to heat treatment. To have a comparison, a bulk  $\text{CoFe}_2\text{O}_4$  sample prepared by sol-gel method presents a saturation magnetization of 78 emu/g and a coercivity of 825 Oe.

The effect of varying pressure (P), sintering temperature (T) and sintering duration (t) on the density of the samples is shown in Fig.1. In general, the sample density increases when increasing P, T and t.

The ME coefficient vs. DC bias field curve,  $\alpha_E$ - $H_{DC}$ , of the sample pressed at 6 tones/cm<sup>2</sup> and annealed at 1250°C for 12 hours is shown in Fig.2. The curves show a maximum at a DC bias field of 1-2.5 kOe, depending on the condition of measurement (longitudinal or transverse). The maximum ME coefficient is 3.4 mV/cmOe, which is similar to those reported in ref. [4] (3.0081 to 5.5886 mV/cmOe for an in situ  $\text{CoFe}_2\text{O}_4$ - $\text{BaTiO}_3$  composite prepared by solid state reactions), but smaller than those reported in ref. [1] (130mV/cmOe for  $(\text{BaTiO}_3)_{0.61}((\text{CoFe}_2\text{O}_4)_{0.47}(\text{CoTiO}_4)_{0.53})_{0.39}$  composite prepared by unidirectional solidification and measured in resonance, 1-4 mV/cmOe for other compositions) and bigger than that one reported in ref. [5] (0.19 mV/cmOe for 50% $\text{CoFe}_2\text{O}_4$ -

50%BaTiO<sub>3</sub> (in mass) mixed structure composite prepared by solid state reaction). The shapes of the curves are similar to that one in ref. [1] where the maximum, the hysteresis behavior and the remanence were observed, but different from those in ref. [4] and [5] where these maxima, hysteresis and remanence were not observed or not clearly obvious. The reason may be due to differences in the sample impedance, composition and microstructure. Differences in the used measuring techniques and measuring conditions have to be considered. However, it is worth to remind that both theoretical (definition of  $\alpha_E$ ) and experimental (measuring techniques) background of the ME effect, especially in composites, are not established [6-7], hence the comparison between reported values for  $\alpha_E$  becomes very difficult.

The DC bias field  $H_{max}$ , where maximum ME coefficient occurs, is not the coercive field as supposed [9], but close to the field where a maximum magnetostriction and magnetization occur. When changing the measuring condition from longitudinal to transverse, this  $H_{max}$  changes due to difference in the demagnetizing field.

The  $\alpha_E$ - $H_{DC}$  curve has a hysteretic nature due to the hysteresis behavior of the constituents. The existence of the remanence is due to the polarization remanence of the BaTiO<sub>3</sub> component and the charge accumulation on the grain boundaries of the samples [10].

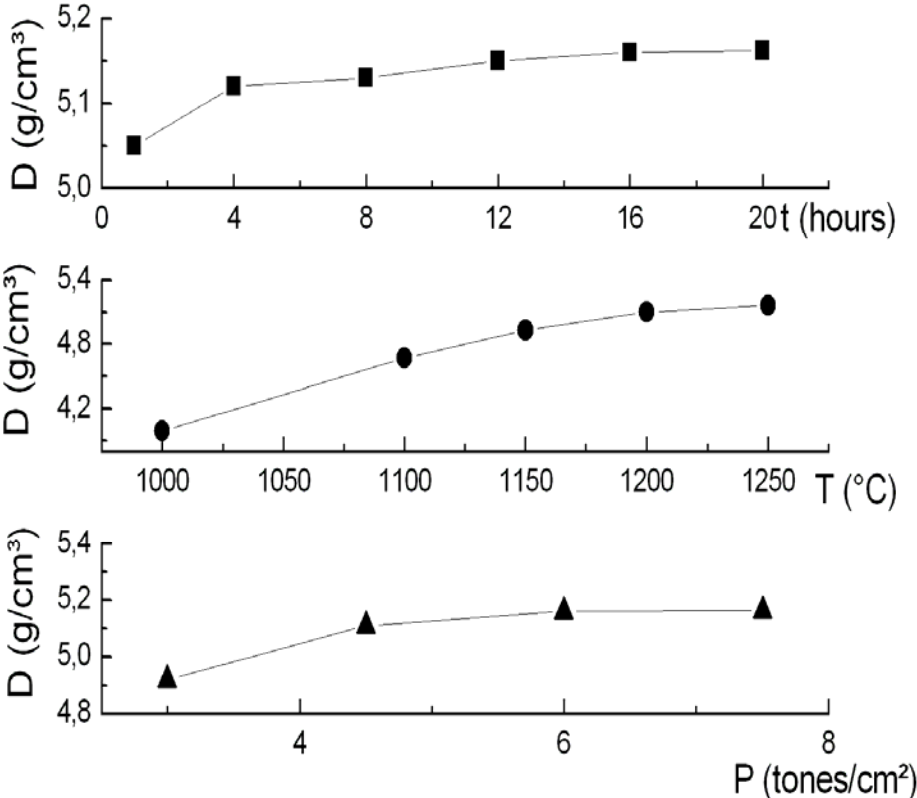


Fig.1. The density of the sample as function of the used pressure P, sintering temperature T and sintering duration t.

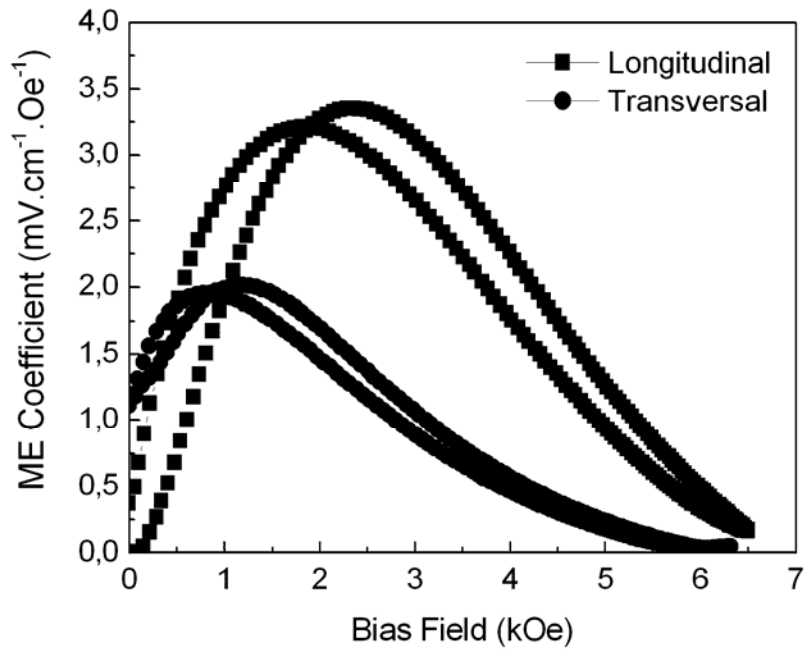


Fig.2. ME coefficients of sample pressed at 6 tones/cm<sup>2</sup> and sintered at 1250°C for 12 hours.

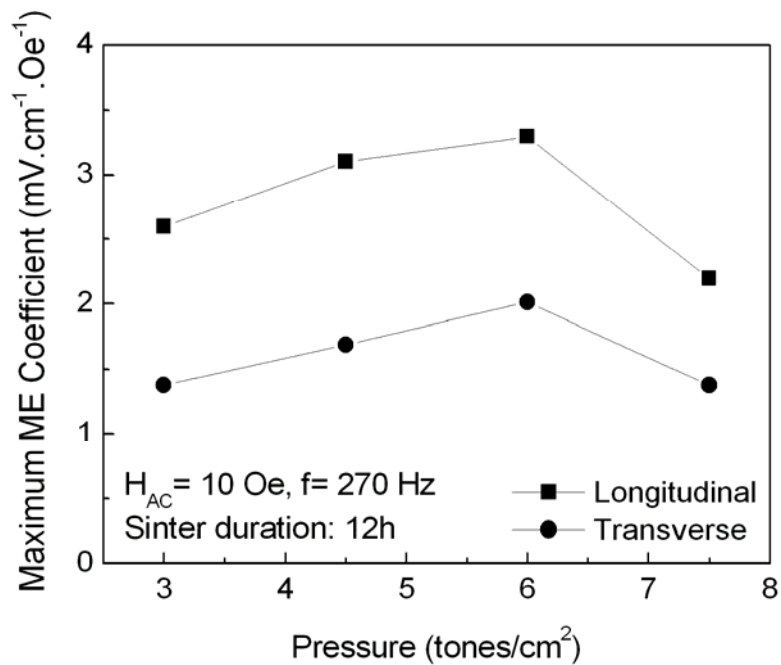


Fig.3. Effect of the used pressure on the ME coefficients of samples sintered at 1250°C for 12 hours.

The effect of the used pressure on  $\alpha_E$  is shown in Fig.3. When increasing pressure,  $\alpha_E$  increases but experiences a maximum. The optimum pressure in our case is 6 tones/cm<sup>2</sup>.

Below this pressure, the compactness of the samples is not good, appearing as low density as presented in Fig.1, leading to a bad mechanical coupling between the two phases in the composites. However, at high pressure, cracks inside the sample may occur which then lower the ME properties of the samples. The cracks can be seen by naked eyes and cause the sample broken when a pressure higher than 8 tones/cm<sup>2</sup> was employed.

The effect of the sintering temperature on the ME coefficient of the composites is shown in Fig.4. For samples pressed at 6 tones/cm<sup>2</sup>, and keeping the sintering duration constant at 12 hours, but increasing the sintering temperature from 1000 to 1250°C, the ME coefficient increases about 20 times from 0.18 to 3.53 and 0.1 to 2.23 mV/cmOe for longitudinal and transversal measurements, respectively. The reason is that at high temperature, the mechanical coupling between the two phases was enhanced, evidenced by the increase of sample density when sintering at high temperature, see Fig.1. This phenomenon is also found in literature [3]. However, in our case, the decrease in  $\alpha_E$  when further increasing the temperature is not observed.

Keeping the sintering temperature constant at 1250°C, the longitudinal ME coefficient increases from 2.25 to 3.87 mV/cmOe when increasing the annealing duration from 1 to 4 hours but decrease for annealing duration longer than 4 hours, see Fig.5 though the sample density is slightly increased, see Fig.1. The reason may be the increase of particle size when increasing the sintering duration, leading to the decrease of interface contact which then lowers the coupling between the two phases, leading to a decrease in the ME coefficients.

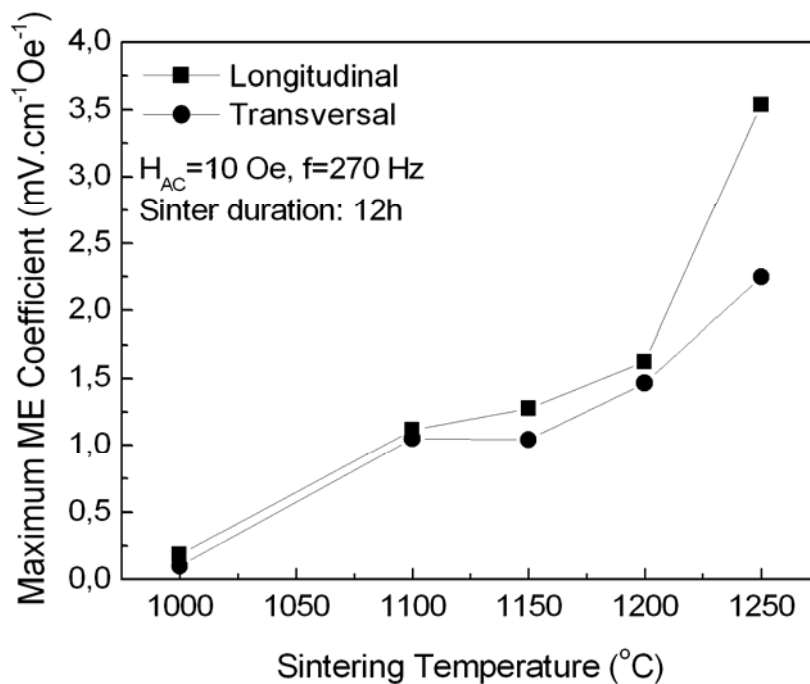


Fig.4. Effect of sintering temperature on the ME coefficients of samples pressed under a pressure of 6 tones/cm<sup>2</sup> and sintered for 12 hours.

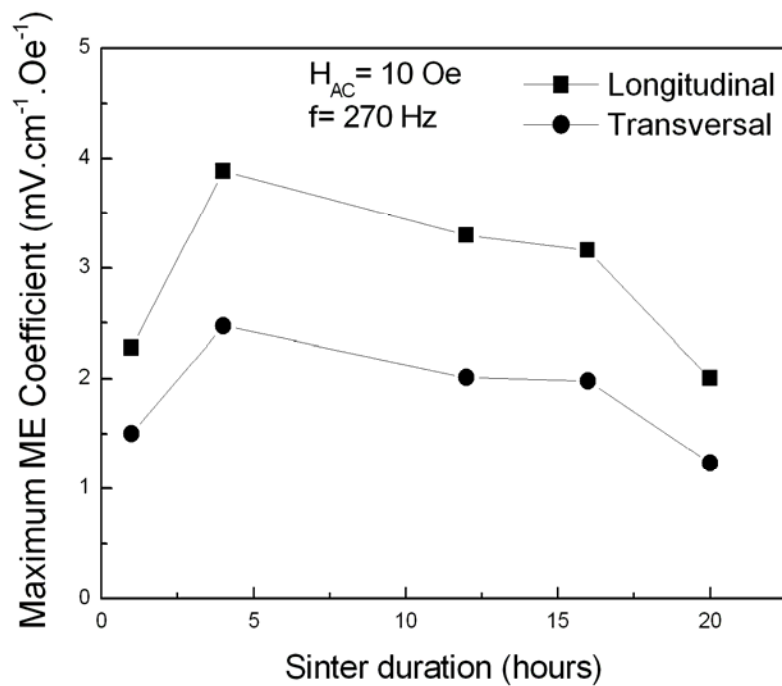


Fig.5. Effect of sintering duration on ME coefficient of sample pressed under a pressure of 6 tone/cm<sup>2</sup> and sintered at 1250°C for 12 hours.

#### 4. Conclusion

The effect of preparation conditions to ME effect of CoFe<sub>2</sub>O<sub>4</sub>-BaTiO<sub>3</sub> ME composites shows that the sample microstructure is sensitive and plays an important role for ME effect in composites.

#### Acknowledgment

This work was partly supported by FWF Proj. Nr. P16500-N02 and a Technology Grant Southeast Asia from the ÖAD.

#### References

- [1] J. Van Suchetelene, Philips Res. Rep. 27 (1972) 28.
- [2] H. Zheng et al, Science 303 (2004) 661.

- [3] Jungho Ryu, Alfredo Vazquez Crazo, Kenji Uchino, Hyoun-Ee Kim, J. Electroceramics 7 (2001) 17-24.
- [4] S.Mazuder, G.S. Bhattacharyya, Ceramics Int. 30 (2004) 389-392.
- [5] R.P. Mahajan, K.K. Patankar, M.B. Kothale, S.C. Chaudhari, V.L. Mathe, S.A. Patil, Pramana-J. Phys. 58 (2002) 1115.
- [6] Giap V. Duong, R. Groessinger, R. Sato Turtelli, Magnetolectric Properties of  $\text{CoFe}_2\text{O}_4$ - $\text{BaTiO}_3$  Core-Shell Structure Composite, IEEE Transactions on Magnetism, in press.
- [7] Giap V. Duong, R. Groessinger, M. Schoenhart, D. Bueno-Basques, The Lock-in Technique for Studying Magnetolectric Effect, accepted for publication.
- [8] H.G. Jiang, M. Rühle, E.J. Lavenia J. Mater. Res. 14, 2 (1999) 549.
- [9] Manfred Fiebig, J. Phys. D: Appl. Phys. 38 (2005) R123-R152.
- [10] R. S. Singh, T. Bhimasankaram, G. S. Kumar and S. V. Suryanarayana, Solid State Commun. 91 (1994) 567.



# Effect of Structure on Magnetoelectric Properties of CoFe<sub>2</sub>O<sub>4</sub>-BaTiO<sub>3</sub> Multiferroic Composites

Giap V. Duong<sup>a,b</sup>, R. Groessinger<sup>a</sup>, R. Sato Turtelli<sup>a</sup>

<sup>a</sup>*Institute of Solid State Physics, Vienna Uni. Techn., Wiedner Hauptstr. 8-10, 1040, Vienna, Austria*

<sup>b</sup>*Faculty of Chemical Engineering, Hanoi University of Technology, No.1 Dai Co Viet, Hanoi,  
Vietnam*

Accepted August 14<sup>th</sup> 2006.

---

## Abstract

The 50%CoFe<sub>2</sub>O<sub>4</sub>-50%BaTiO<sub>3</sub> (in mass) composites with four different building structures, namely: CoFe<sub>2</sub>O<sub>4</sub>-BaTiO<sub>3</sub> core-shell structure with CoFe<sub>2</sub>O<sub>4</sub> in core, BaTiO<sub>3</sub>-CoFe<sub>2</sub>O<sub>4</sub> core-shell structure with BaTiO<sub>3</sub> in core, CoFe<sub>2</sub>O<sub>4</sub>-BaTiO<sub>3</sub> mixed structure, and BaTiO<sub>3</sub>-CoFe<sub>2</sub>O<sub>4</sub>-BaTiO<sub>3</sub> layer structure, have been synthesized and studied. The core-shell structures give higher ME coefficients compared to the other structures. When using CoFe<sub>2</sub>O<sub>4</sub> as core, the ME coefficient is highest, reaching 3.4 mV.cm<sup>-1</sup>.Oe<sup>-1</sup> for the sample pressed at 6 tones/cm<sup>2</sup> and sintered at 1250°C for 12 hours.

© 2006 Elsevier B.V. All rights reserved

PACS: 75.80.+q; 77.65.-j; 77.84.Lf

*Keywords:* Magnetoelectric effect; Multiferroic composite; Effect of structure; Barium titanate; Cobalt ferrite

---

The origin of the magnetoelectric (ME) effect in ME composites is the coupling between the magnetostrictive and piezoelectric phases [1]. So the micro-structure of the composites which affects the interactions between the two phases as well as some physical properties such as electrical resistance, dielectric constant may play an important role in ME composites. In this work, 50%CoFe<sub>2</sub>O<sub>4</sub>-50%BaTiO<sub>3</sub> (in mass) composites with four different building structures, namely: CoFe<sub>2</sub>O<sub>4</sub>-BaTiO<sub>3</sub> core-shell structure with CoFe<sub>2</sub>O<sub>4</sub> in core, BaTiO<sub>3</sub>-CoFe<sub>2</sub>O<sub>4</sub> core-shell structure with BaTiO<sub>3</sub> in core, CoFe<sub>2</sub>O<sub>4</sub>-BaTiO<sub>3</sub> mixed structure, and BaTiO<sub>3</sub>-CoFe<sub>2</sub>O<sub>4</sub>-BaTiO<sub>3</sub> layer structure, have been synthesized and studied.

The core-shell structure samples were prepared by wet chemical method as described elsewhere [2]. In general, the core was prepared by co-precipitation (CoFe<sub>2</sub>O<sub>4</sub>, average grain size of about 10 nm) or sol-gel (BaTiO<sub>3</sub>, average grain size of about 42 nm) technique, then introduced to the homogeneous solution containing chelating agent and elements that form the shell. This solution evaporated and gelled on the surface of the core during heating and stirring. The obtained products were pre-sintered at 450 °C for 3 hours, pressed into pellets under a pressure of 3-7.5 tones/cm<sup>2</sup>, sintered at 1000-1250 °C for 1-20 hours, then cooled down naturally to room temperature (RT).

The mixed structure was prepared by simply mixing the two initial powders: CoFe<sub>2</sub>O<sub>4</sub> (average grain size of 10 nm) and BaTiO<sub>3</sub> (average grain size of 40 nm), then pressed into pellets under a pressure similar to those for the core-shell structure samples. The layer structure was prepared by casting the powder into the matrix, slightly pressed before casting the other layers, then the whole powders in the matrix were pressed under a pressure of 6 tones/cm<sup>2</sup>. The heat treatment of the mixed and layer structure is similar to that of the core-shell structure samples. After heat treatment, all samples were poled under an electric field of 7500 V/cm and painted by silver paste for electrical contacts.

X-ray diffraction characterization showed that all composites consisted of two single phases only: CoFe<sub>2</sub>O<sub>4</sub> and BaTiO<sub>3</sub>. Magnetic studies showed that the magnetic properties of the CoFe<sub>2</sub>O<sub>4</sub> component are similar to those of the bulk sample: saturation magnetization ( $M_s$ ) of 72 emu/g and coercivity ( $H_c$ ) of 460 Oe at RT. For reference, a CoFe<sub>2</sub>O<sub>4</sub> bulk sample prepared by citrate gel method at RT has  $M_s$  of 78 emu/g,  $H_c$  of 825 Oe and magnetostriction  $\lambda$  of -130 and 70 ppm for parallel and perpendicular measurements, respectively. Very similar values are obtained for the other samples.

The ME effect was measured using a lock-in technique as described in ref. [3]. Fig.1 shows the ME coefficient as function of the DC bias field ( $\alpha_E-H_{DC}$ ) of the sample with CoFe<sub>2</sub>O<sub>4</sub> in core using an AC field of 10 Oe, 270 Hz. This sample is formed by pressing the

powder under a pressure of 6 tone/cm<sup>2</sup>, then sintered at 1250 °C for 12 hours. It is clear that the curves experience a maximum and show remanence as well as hysteresis behaviour. The maximum ME coefficient is 3.4 mV.cm<sup>-1</sup>.Oe<sup>-1</sup> for longitudinal measurement and 2.0 mV.cm<sup>-1</sup>.Oe<sup>-1</sup> for transverse case.

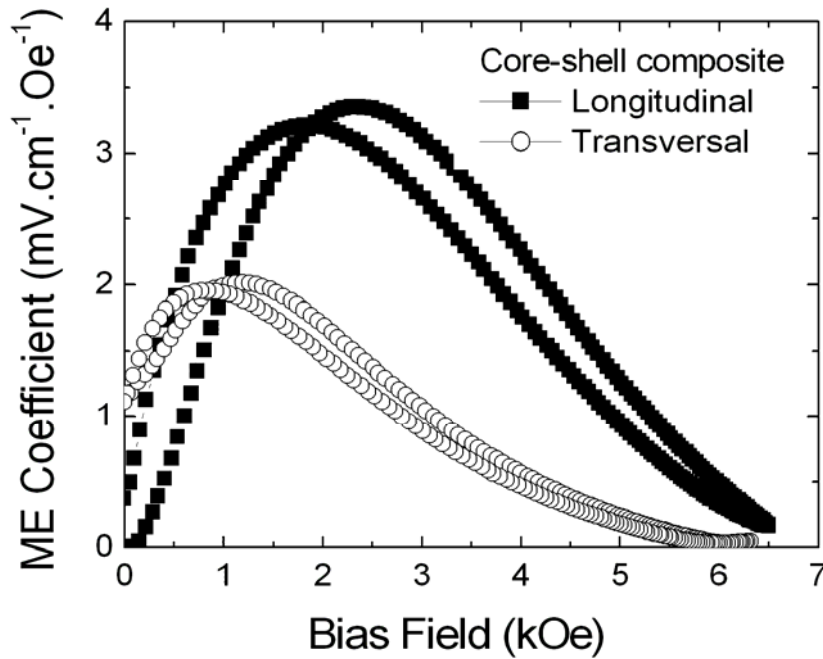


Fig.1: The  $\alpha_E-H_{DC}$  curves of the CoFe<sub>2</sub>O<sub>4</sub>-BaTiO<sub>3</sub> composite with CoFe<sub>2</sub>O<sub>4</sub> in core at RT (sample preparation: pressed at 6 tones/cm<sup>2</sup> and sintered at 1250 °C for 12 hours).

The effect of structure on ME coefficient is shown in Fig.2. It was found that the CoFe<sub>2</sub>O<sub>4</sub>-BaTiO<sub>3</sub> core-shell structure with CoFe<sub>2</sub>O<sub>4</sub> in core has the highest ME coefficient: 1.62 mV.cm<sup>-1</sup>.Oe<sup>-1</sup> for sample annealed at 1200 °C for 16 hours, which is of about 4.2, 8.1 and 11 times higher than that of the BaTiO<sub>3</sub>-CoFe<sub>2</sub>O<sub>4</sub> core-shell structure with BaTiO<sub>3</sub> in core, CoFe<sub>2</sub>O<sub>4</sub>-BaTiO<sub>3</sub> mixed structure, BaTiO<sub>3</sub>-CoFe<sub>2</sub>O<sub>4</sub>-BaTiO<sub>3</sub> layer structure, prepared under the same conditions, respectively. The higher ME coefficient of the core-shell structure may be attributed to the better coupling between the two phases due to its larger interface area. Additionally, the higher measured ME coefficients when CoFe<sub>2</sub>O<sub>4</sub> was used as core compared to the case of BaTiO<sub>3</sub> in core may be understood also as the discharging effect in the former was lesser. The reason is: the electrical resistance of BaTiO<sub>3</sub> is higher than that of CoFe<sub>2</sub>O<sub>4</sub> which is confirmed by electrical resistance measurements on shape normalized samples at RT: 330 MΩ for sample with CoFe<sub>2</sub>O<sub>4</sub> in core, 50 MΩ for sample with BaTiO<sub>3</sub> in core, 80 MΩ for mixed structure, >2000 MΩ for layer structure.

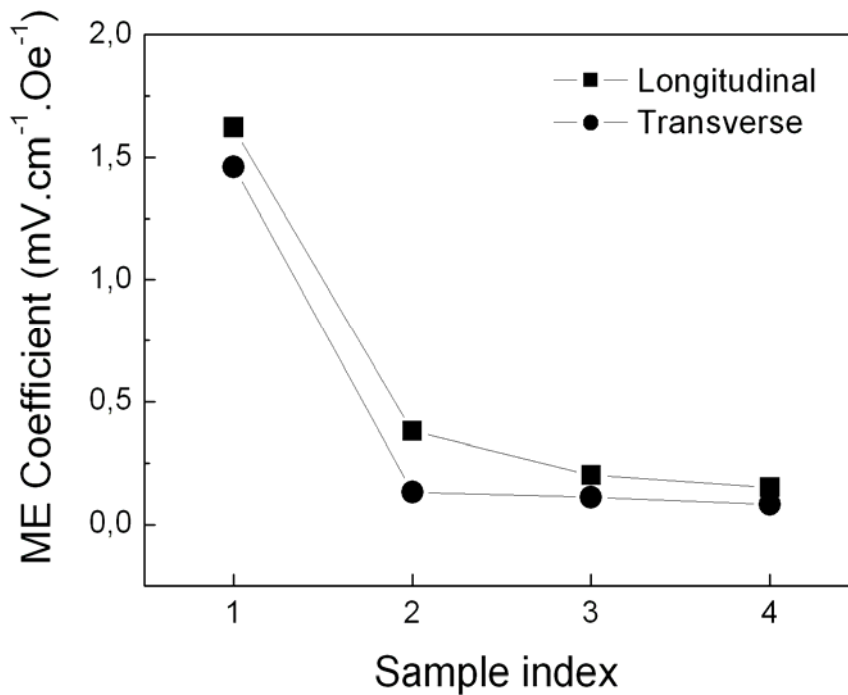


Fig.2: Effect of structure on  $\alpha_E$  at RT. Sample index:

1-CoFe<sub>2</sub>O<sub>4</sub> as core and BaTiO<sub>3</sub> as shell; 2-BaTiO<sub>3</sub> as core and CoFe<sub>2</sub>O<sub>4</sub> as shell; 3-mixed structure; 4-BaTiO<sub>3</sub>-CoFe<sub>2</sub>O<sub>4</sub>-BaTiO<sub>3</sub> layer structure. Preparation of samples: pressed at 6 tones/cm<sup>2</sup> and sintered at 1250 °C for 16 hours.

It is also worth to remind that, beside the physical properties such as electric resistance, the microstructure of the sample also affects seriously on the ME coefficient. When changing the sintering temperature and duration from 1250 °C and 12 hours to 1200 °C and 16 hours, the longitudinal  $\alpha_E$  of the sample with CoFe<sub>2</sub>O<sub>4</sub> in core decreases from 3.4 to 1.62 mV.cm<sup>-1</sup>.Oe<sup>-1</sup> as can be seen in Fig.1 & 2. The reason is the changes in sample microstructure which is now under investigation. For different structures, the optimum preparation conditions are different, e.g. for the core-shell with CoFe<sub>2</sub>O<sub>4</sub> in core, pressed under 6 tones/cm<sup>2</sup> and sintered at 1250°C for 4 hours suited best (max  $\alpha_E = 3.88$  mV.cm<sup>-1</sup>.Oe<sup>-1</sup>), but when BaTiO<sub>3</sub> used as core, the optimum is to press at 3 tones/cm<sup>2</sup> and sintered at 1150 °C for 8 hours (max  $\alpha_E = 0.63$  mV.cm<sup>-1</sup>.Oe<sup>-1</sup>) as shown in Fig.3. These values are in the range of those reported for particulate composites: 0.43 mV.cm<sup>-1</sup>.Oe<sup>-1</sup> in 15%Ni<sub>0.8</sub>Cu<sub>0.2</sub>Fe<sub>2</sub>O<sub>4</sub> +85%Ba<sub>0.9</sub>Pb<sub>0.1</sub>Ti<sub>0.9</sub>Zr<sub>0.1</sub>O<sub>3</sub> (in mole) [4], 3.0-5.58 mV.cm<sup>-1</sup>.Oe<sup>-1</sup> in BaO-TiO-FeO-CoO [5] and 0.19 mV.cm<sup>-1</sup>.Oe<sup>-1</sup> in 50%CoFe<sub>2</sub>O<sub>4</sub>-50%BaTiO<sub>3</sub> (in mass) mixed composite [6].

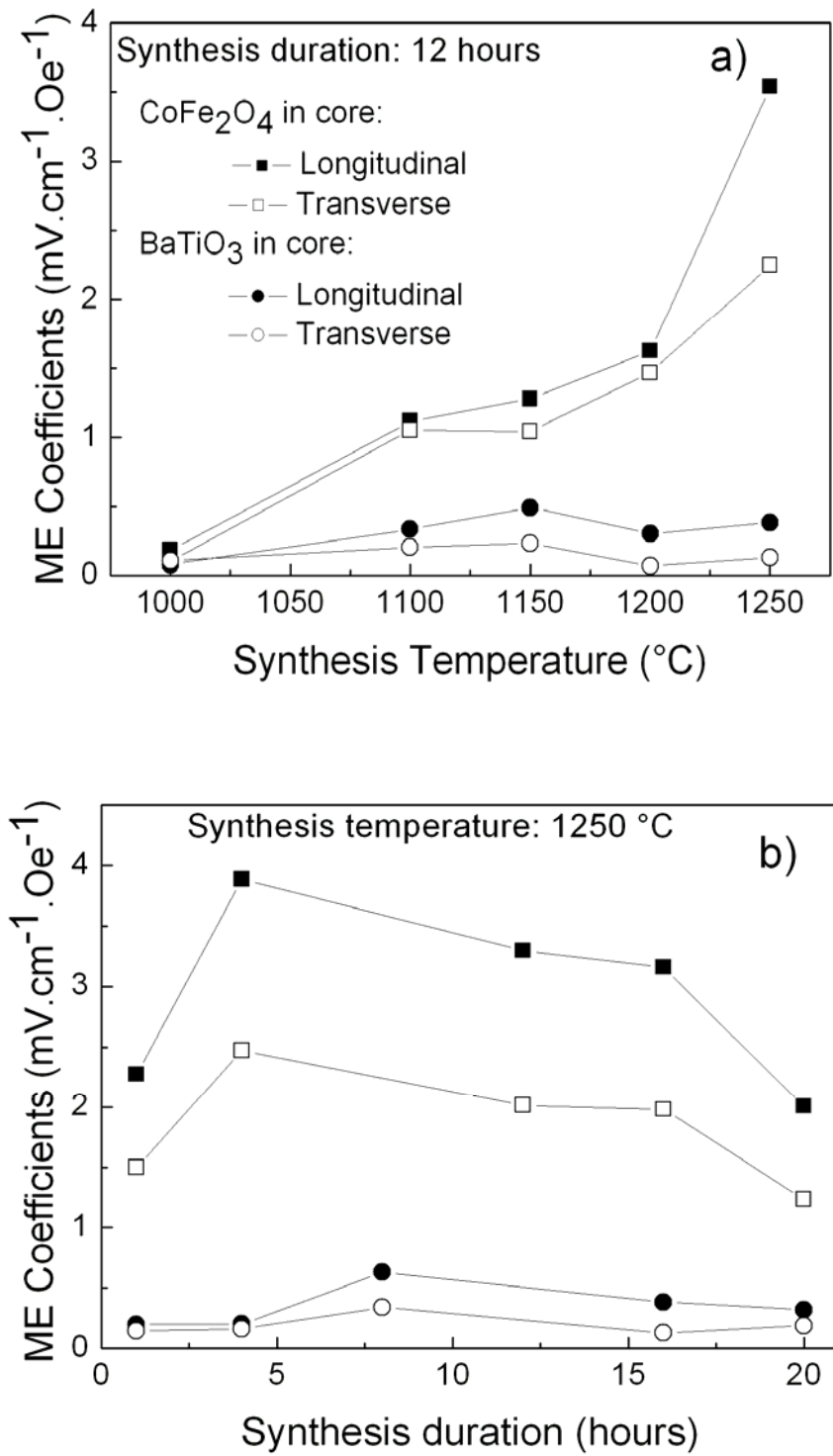


Fig.3: Effect of synthesis temperature (a) and duration (b) on the ME coefficient of core-shell structure composites.

This work is supported by the FWF Proj. Nr. P16500-N02, Proj. Nr. P15737 and the Austrian Exchange Service (ÖAD).

## References

- [15] J. Van Suchetelene, Philips Res. Rep., 27 (1972) 28.
- [16] Giap V. Duong, R. Groessinger, R. Sato Turtelli, “Magnetoelectric Properties of  $\text{CoFe}_2\text{O}_4\text{-BaTiO}_3$  Core-Shell Structure Composite”, IEEE Trans. Magn., to be published.
- [17] Giap V. Duong, R. Groessinger, M. Schoenhart, D. Bueno-Basques, “The Lock-in technique for Studying Magnetoelectric Effect”, J. Magn. Magn. Mater., to be published.
- [18] C.M. Kanamadi, L.B. Pujari and B.K. Chougule, J. Magn. Magn. Mater. 295 (2005) 139.
- [19] S.Mazuder, G.S. Bhattacharyya, Ceramics Int. 30 (2004) 389.
- [20] R.P. Mahajan, K.K. Patankar, M.B. Kothale, S.C. Chaudhari, V.L. Mathe, S.A. Patil, Pramana-J. Phys. 58 (2002) 1115.

# Driving Mechanism for Magnetoelectric Effect in CoFe<sub>2</sub>O<sub>4</sub>-BaTiO<sub>3</sub> Multiferroic Composite

Giap V. Duong<sup>a,b</sup>, R. Groessinger<sup>a</sup>, R. Sato Turtelli<sup>a</sup>

<sup>a</sup>*Institute of Solid State Physics, Vienna Uni. Techn., Wiedner Hauptstr. 8-10, 1040, Vienna, Austria*

<sup>b</sup>*Faculty of Chemical Engineering, Hanoi University of Technology, No.1 Dai Co Viet, Hanoi,  
Vietnam*

Accepted August 15<sup>th</sup> 2006.

---

## Abstract

The magnetoelectric effect in the CoFe<sub>2</sub>O<sub>4</sub>-BaTiO<sub>3</sub> core-shell structure composite prepared by wet chemical method occurs mainly due to a coupling between the magnetostrictive and piezostrictive phases. The driving mechanism is attributed to the mechanical coupling through the magnetostriction of the magnetostrictive constituent. The ME coefficient is found to be proportional to an efficiency factor  $k_0$  and a coupling coefficient  $k$ , defined as  $k = \lambda \cdot \partial \lambda / \partial H$  where  $\lambda$  is the linear magnetostriction.

© 2006 Elsevier B.V. All rights reserved

*PACS:* 75.80.+q; 77.65.-j; 77.84.Lf

*Keywords:* Magnetoelectric effect; Multiferroic composite; Driving mechanism; Barium titanate; Cobalt ferrite

---

Magnetoelectric (ME) materials become magnetized when placed in an electric field and electrically polarized when placed in a magnetic field. For single phase ME materials, the primary requirement to observe the ME effect is the coexistence of magnetic and electric dipoles in an asymmetric structure. For ME composites, a combination of magnetostrictive and piezoelectric phases can result in a ME effect as product property of this combination [1]. However, the mechanism causing the ME effect in composites is not well understood yet.

Recently we successfully prepared a composite of 50%CoFe<sub>2</sub>O<sub>4</sub>-50%BaTiO<sub>3</sub> (in mass) exhibiting the core-shell structure which has a ME coefficient of about 18 times higher than those of the mixed structure with the same composition and measured using the same technique [2]. This work therefore will focus in investigating the driving mechanism for the ME effect in this composite. The sample was prepared by wet chemical method, followed by proper heat treatment and poling procedure as described elsewhere [2], except the CoFe<sub>2</sub>O<sub>4</sub> constituent is prepared using citrate gel method. X-ray diffraction showed that the sample consisted of two single phases: CoFe<sub>2</sub>O<sub>4</sub> and BaTiO<sub>3</sub>. Magnetic measurements revealed that magnetic properties of the magnetostrictive component are similar to those of the bulk sample [2]. To investigate the ME effect, an experimental set-up using the lock-in technique has been developed [3]. The ME coefficient,  $\alpha_E$ , was calculated using the equation:  $\alpha_E = V/(d.H_{AC})$ , where  $V$  is the output voltage of the lock-in,  $d$  is the effective thickness of the piezoelectric phase and  $H_{AC}$  is the amplitude of the AC field.

Figure 1 shows the longitudinal ME coefficient vs. DC bias field curve ( $\alpha_E$ - $H_{DC}$ ) of the CoFe<sub>2</sub>O<sub>4</sub>-BaTiO<sub>3</sub> core-shell structure composite measured at room temperature and ambient pressure. The curve shows a maximum at a DC bias field of about 2.5 kOe. The maximum ME coefficient is 3.4 mV/cm.Oe, which is in the range of reported values [1, 4-5]. The shape of the curve is similar to that one in ref. [1], but different from those in ref. [4] and [5] where the maxima, hysteresis and remanence were not observed or not clearly obvious.

The DC bias field  $H_{max}$  where maximum ME coefficient occurs is not the coercive field as supposed [6], but close to the field where a maximum magnetostriction occurs. When changing the measuring condition from longitudinal to transverse, this  $H_{max}$  changes due to difference in the demagnetizing field, see Fig.1. The  $\alpha_E$ - $H_{DC}$  curve has a hysteretic nature due to the hysteresis behavior of the constituents. The existence of the remanence is due to the polarization remanence of the BaTiO<sub>3</sub> constituent.



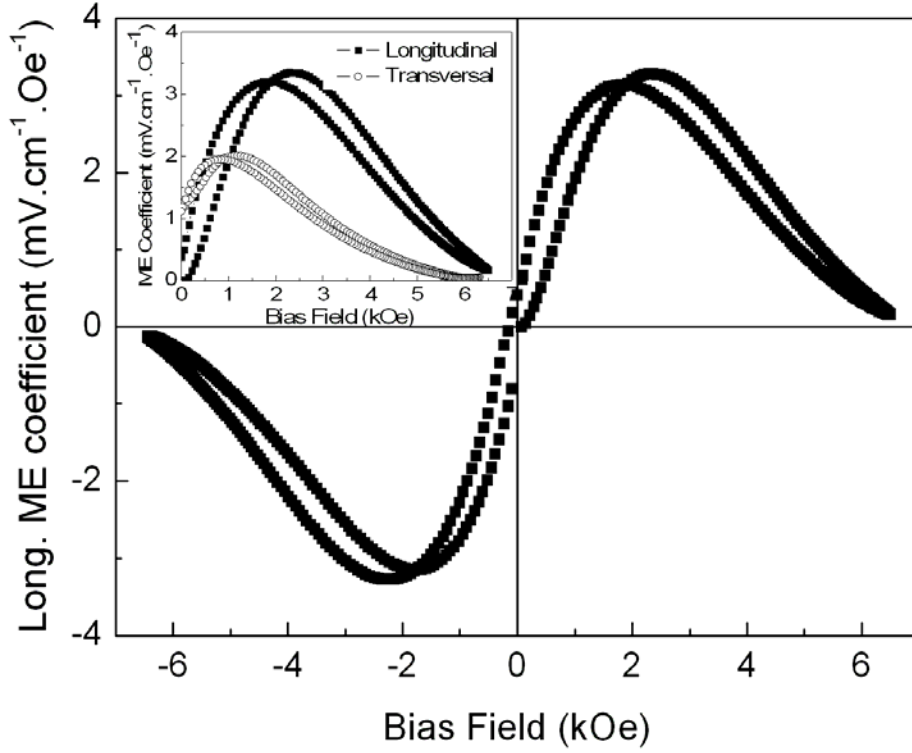


Fig.1: Longitudinal ME coefficient of the  $\text{CoFe}_2\text{O}_4\text{-BaTiO}_3$  core-shell structure composite. Inset is the longitudinal and transverse ME coefficients as function of the DC bias field.

To investigate the mechanical coupling between the magnetostrictive and piezoelectric phases, the magnetostriction  $\lambda$  of the pure  $\text{CoFe}_2\text{O}_4$  and the composite have been measured using a strain gauge method, see Fig.2. The magnetostriction of the 50% $\text{CoFe}_2\text{O}_4$ -50% $\text{BaTiO}_3$  (in mass) composite is smaller than the according to the 50%  $\text{CoFe}_2\text{O}_4$  expected value which is a hint that the strain produced by the  $\text{CoFe}_2\text{O}_4$  component may be partly absorbed by the  $\text{BaTiO}_3$  phase.

The longitudinal ME coefficient is bigger than the transverse one. This is opposite to the results reported in literature [6], where the longitudinal ME coefficient is the smaller. However, our results match the fact that the longitudinal magnetostriction which is responsible for the longitudinal ME coefficient,  $\lambda_{par}$ , is bigger than the transverse one,  $\lambda_{per}$ , suggesting that  $\alpha_E$  depends not only on the piezomagnetic coupling strength  $q=d\lambda/dH$  as reported [6], but also on the absolute value of the linear magnetostriction,  $\lambda$ . Therefore, a new parameter called coupling coefficient  $k$ , defined as  $k = \lambda \cdot d\lambda/dH$ , is introduced. Then the ME coefficient  $\alpha_E$  is found to be proportional to the coupling coefficient  $k$ :  $\alpha_E = k_0 \cdot k$ , where  $0 \leq k_0 \leq 1$  which describes the efficiency of the coupling, characterized by the micro-structure

and possibly a direct coupling between M and E of the sample. For this  $\text{CoFe}_2\text{O}_4\text{-BaTiO}_3$  core-shell structure composite, a value  $k_0 = 0.35$  is obtained. Fig.3 showed the coupling coefficient  $k_{par} = \lambda_{par} \cdot d\lambda_{par}/dH$  (in charge for the longitudinal  $\alpha_E$ ) as function of the applied field  $H$  for the pure  $\text{CoFe}_2\text{O}_4$  and composite when increasing or decreasing the applied field. The shape of the  $k_{par}\text{-}H$  curves is very similar to the longitudinal  $\alpha_E\text{-}H_{DC}$  curve, including the maxima, the hysteresis behavior and the decrease at high bias field, confirming that the ME coefficient  $\alpha_E$  is proportional to the coupling coefficient  $k$ . At a bias field of about 6500 Oe,  $\lambda$  gets maximum, however  $\alpha_E$  reaches zero and changes its sign with a further increase of DC field according to the change in sign of  $\partial\lambda/\partial H$ . The change in sign of  $\alpha_E$  when reverse the bias field is also due to the change in sign of  $\partial\lambda/\partial H$ .

To confirm the role of linear magnetostriction and the difference of  $k_0$  for different sample, a  $\text{Co}_{0.7}\text{Zn}_{0.3}\text{Fe}_2\text{O}_4\text{-BaTiO}_3$  core-shell structure composite was prepared under similar conditions. The  $\text{Co}_{0.7}\text{Zn}_{0.3}\text{Fe}_2\text{O}_4$  component has a saturation magnetization and maximum  $\lambda$  of 125 emu/g and 35 ppm compared to those of 72 emu/g and 130 ppm of  $\text{CoFe}_2\text{O}_4$  bulk sample. As compared to the  $\text{CoFe}_2\text{O}_4\text{-BaTiO}_3$  sample, in the Zn-substituted case, the maximum  $\alpha_E$  is smaller due to the smaller magnetostriction. However, the maximum  $\lambda$  decrease 3.5 times while the maximum  $\alpha_E$  decreases only 2.4 times. The reason is: the Zn-substituted sample has a bigger  $k_0$  (0.51 by calculation) since it is believed Zn substitution enhances the strength of interface coupling [6].

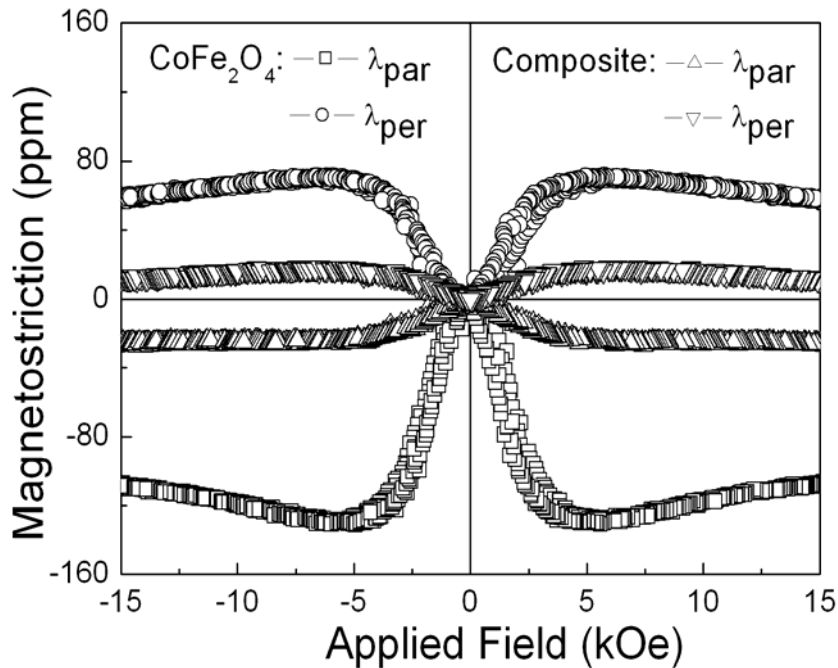


Fig. 2: Magnetostriction of the pure  $\text{CoFe}_2\text{O}_4$  and  $\text{CoFe}_2\text{O}_4\text{-BaTiO}_3$  core-shell structure composite

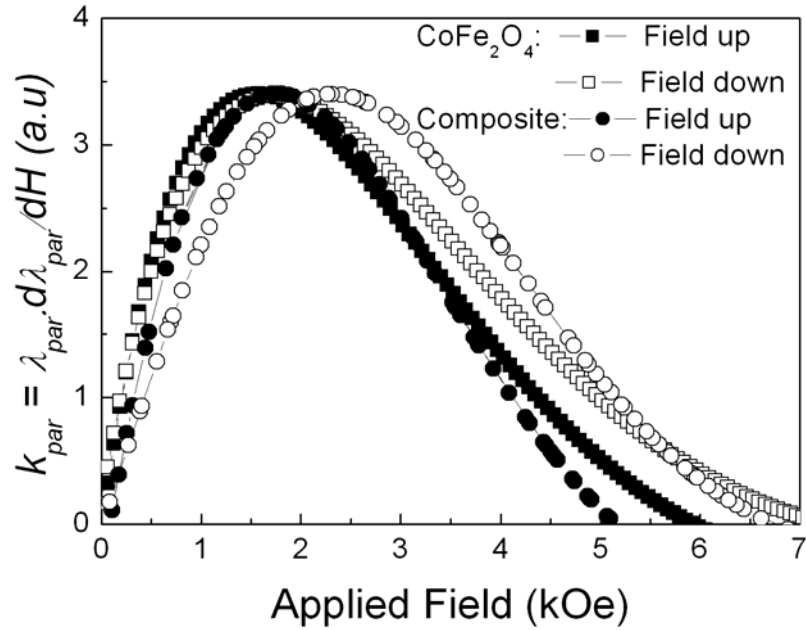


Fig.3: Coupling coefficient  $k$  as function of applied field  $H$

In conclusion, the ME effect in  $\text{CoFe}_2\text{O}_4\text{-BaTiO}_3$  is mainly caused by the mechanical coupling between the magnetostrictive and piezoelectric phases through magnetostriction, and the ME coefficient is found to be proportional to the efficiency factor  $k_o$  and the coupling coefficient  $k$ , defined as  $k = \lambda \cdot \partial \lambda / \partial H$ .

This work is supported by the FWF Proj. Nr. P16500-N02 and the Austrian Exchange Service (ÖAD).

## References

- [1] J. Van Suchetelene, Philips Res. Rep. 27 (1972) 28.
- [2] Giap V. Duong, R. Groessinger, R. Sato Turtelli, Magnetolectric Properties of  $\text{CoFe}_2\text{O}_4\text{-BaTiO}_3$  Core-Shell Structure Composite, presented at Intermag2006, May 8-12, San Diego, California, accepted for publication.
- [3] Giap V. Duong, R. Groessinger, M. Schoenhart, D. Bueno-Basques, The Lock-in Technique for Studying Magnetolectric Effect, submitted for publication.
- [4] S. Mazuder, G.S. Bhattacharyya, Ceramics Int. 30 (2004) 389
- [5] R.P. Mahajan, K.K. Patankar, M.B. Kothale, S.C. Chaudhari, V.L. Mathe, S.A. Patil, Pramana-J. Phys. 58 (2002) 1115.
- [6] G. Srinivasan, E. T. Rasmussen and R. Hayes, Phys. Rev. B 67 (2003) 014418.

# Evidence of direct magneto-electric dipole interaction in CoFe<sub>2</sub>O<sub>4</sub> – BaTiO<sub>3</sub> core-shell structure composite

Giap V. Duong<sup>1,2</sup>, R. Groessinger<sup>1</sup>

<sup>1</sup>*Institute for Solid State Physics, Vienna University of Technology  
Wiedner Hauptstrasse 8-10, A-1040, Vienna, Austria*

<sup>2</sup>*Faculty of Chemical Engineering, Hanoi University of Technology  
1 Dai Co Viet, Hai Ba Trung, Hanoi, Vietnam*

Part of this work was orally presented at the IEEE International Magnetics Conference,  
May 8-12<sup>th</sup>, San Diego, California. To be submitted for publication.

---

## **Abstract:**

For the first time, evidence of direct magneto-electric moment coupling has been observed in CoFe<sub>2</sub>O<sub>4</sub>-BaTiO<sub>3</sub> magnetoelectric core-shell structure nanocomposites. This opens a new trend in the study of magnetoelectric effect since it allows to make a quasi-single phase composite which exhibit the ME properties similar to those of the rare single phase ME materials, and benefit to both fundamental understanding of materials physics, i.e the nature of coupling between magnetic and electric orders, and important technological applications, e.g it may help overcome the superparamagnetism problem which sets the upper bound for current high density storage devices sine with magnetoelectric materials one can write the information by magnetic field and read it from electric field and vice versa.

*PACS:* 75.80.+q; 77.65.-j; 77.84.Lf

*Keywords:* Magnetoelectric effect, magnetoelectric interaction, magnetoelectric composite, magnetostriction, piezoelectricity, cobalt ferrite, barium titanate.

---

## 1. Introduction

Magnetoelectric (ME) effect—the induction of electric polarization by means of a magnetic field and the induction of magnetization by means of an electric field—was predicted as early as 1894, when Curie pointed out that it would be possible for an asymmetric molecular body to polarize directionally under the influence of a magnetic field [1]. Later, Landau and Lifshitz [2] showed that such linear ME effect only exists in a time-asymmetric media such as in long range magnetic order materials [2]. Subsequently, based on the theoretical analysis, Dzyaloshinskii for the first time suggested the existence of such time-asymmetric media in a particular compound,  $\text{Cr}_2\text{O}_3$ , and predicted the linear ME response of this system [3], which was one year later confirmed experimentally by observing the electric-field-induced magnetization [4] and magnetic-field-induced polarization [5].

The primary requirement to observe the ME effect is the coexistence of magnetic and electric dipoles. However, such coexistence is found to be chemically incompatible due to the diametric conditions for the involved 3d-levels [6]. This explains why only few magnetic single phase ferroelectrics exist. On the other hand, the magnetoelectric effect in single phase materials is usually small and occurs generally at low temperatures, inhibiting them in practical applications. These limitations can be overcome when shifting to composites where the magnetic and electric dipoles are introduced from two different magnetostrictive and piezoelectric phases. The ME effect is resulting as a product property of the combination of these two phases. By choosing proper constituents, the ME effect in composites can exhibit at room temperature [7].

The mechanical coupling between the magnetostrictive and piezoelectric phases is believed to be most important for the ME effect in composites. In brief description, when exposing a magnetoelectric composite to a magnetic field, a strain is produced in the magnetostrictive phase which is then passed into the piezoelectric phase through mechanical coupling, causing a stress, and as a result of it, producing an electric polarization in the piezoelectric constituent. However, recently Zheng *et al* found a drop in low field temperature-dependent magnetization of a composite consisting of  $\text{CoFe}_2\text{O}_4$  nanopillars embedded in a  $\text{BaTiO}_3$  matrix at the ferroelectric Curie temperature [8]. This can be a result of a pure mechanical effect due to the phase transition of  $\text{BaTiO}_3$  or a hint of a hidden direct coupling between magnetic and electric dipoles. If this direct coupling is confirmed to exist, it will open up a new area in the study of the ME effect in composites, since it allows to obtain materials which exhibit the ME effect similar as in the case of single phase materials, but at

room or elevated temperature. This will benefit both fundamental understanding of the material physics, e.g. the nature of the coupling between magnetic and electric dipoles, and important technological applications, such as new kind of transducers, sensors, actuators, storage devices, etc. For high density information storage, it may help to solve the problem of superparamagnetism which sets an upper limit of the current magnetic storage media since with magnetoelectric materials, one can write by magnetic field and read by electric field or vice versa. Therefore, the motivation of this work is to investigate if really a direct coupling between magnetic and electric dipoles exist in composites of magnetostrictive and piezoelectric phases like  $\text{CoFe}_2\text{O}_4\text{-BaTiO}_3$  by studying its ME properties, AC susceptibility, low field temperature-dependent magnetization and angle dependence of the ME coefficient.

## 2. Experimental

The samples were synthesized using wet chemical method as described elsewhere [9]. The crystalline structure of single phase materials as well as composites were investigated by X-ray diffractometer (XRD). Magnetic properties were studied using a pulse field magnetometer (Hirst, PFM 11) and a Physical Property Measurement System (PPMS-9T, Quantum Design). Magnetostriction was measured using a strain gauge method with a 50 kHz bridge (HBM Type KWS 85.A1). AC susceptibility and ME coefficient were investigated using lock-in technique in which AC fields with frequencies from 1Hz to 10 kHz and amplitude from 0,1Oe to 20 Oe superimposed onto a DC field up to 6500 Oe were employed [10]. Input resistance and capacitance of the lock-in are 100M $\Omega$  and 25 pF. All measurements were carried out at room temperature and ambient pressure.

## 3. Results and Discussions

The XRD pattern shown in Fig.1 suggested that the composite consists two single phases:  $\text{CoFe}_2\text{O}_4$  and  $\text{BaTiO}_3$ . Line broadening analysis showed that the grain size of the  $\text{CoFe}_2\text{O}_4$  core before sintering is about 10 nm. Magnetic measurements proved that the magnetic properties of the magnetostrictive component in the composite are similar to that of the bulk sample. ME coefficient,  $\alpha_E$ , was determined using the equation  $\alpha_E = V/(d.H_{AC})$  where  $V$  is output voltage of the lock-in amplifier,  $d$  is the effective thickness of the sample and  $H_{AC}$  is the amplitude of the AC field [10]. The ME coefficient-Bias field curves,  $\alpha_E - H_{DC}$ , has a

hysteretic nature, and a remenance of 15-50% of the maximum ME coefficient, depending on the conditions of measurement as shown in Fig.2.

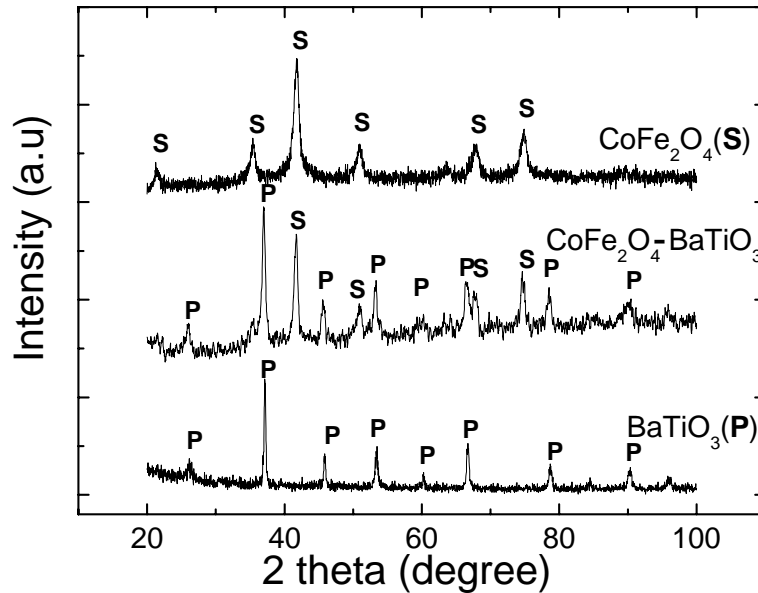


Fig. 1. XRD patterns of  $\text{CoFe}_2\text{O}_4$  (S),  $\text{BaTiO}_3$  (P) and  $\text{CoFe}_2\text{O}_4\text{-BaTiO}_3$  composite

ME measurements on two composites with two different microstructures, mixed and core-shell, showed that the core-shell structure composite has a ME coefficient which is 18 times higher than that of the mixed structure, see Fig.2. A further comparison of the ME coefficients of the mixed  $\text{CoFe}_2\text{O}_4\text{-BaTiO}_3$  composites reported in [11] shows that the ME coefficients in our core-shell  $\text{CoFe}_2\text{O}_4\text{-BaTiO}_3$  is about 15 times larger. It can be concluded that the coupling between the magnetostrictive and piezoelectric phases in the core-shell structure composite is much better than that of the mixed structure. On the other hand, in core-shell structure composite, the longitudinal ME coefficient is bigger than the transversal one. This is opposite to those reported for laminated or multilayer composites [12], suggesting that the coupling mechanism depends strongly on the microstructure of the sample.

The bias field at which the maximum ME coefficient occurs,  $H_{max}$ , is around 2000-3000 Oe, depending on the condition of measurements, which is about six times higher than the coercivity field determined from magnetization measurement, suggesting that the shape of the field dependence of the ME coefficient here is not related to the coercivity field as proposed by many other researchers [12]. The maximum of the ME effect occurs in the field range where the maximum magnetostriction and magnetization occurs. The bias field at

which the ME coefficient gets maximum in the transversal measurement is smaller than that of the longitudinal. The reason for this is may be the demagnetizing field which is in the transversal case smaller than in the longitudinal situation which is also visible in the low field slope of the hysteresis loops shown in Fig.3.

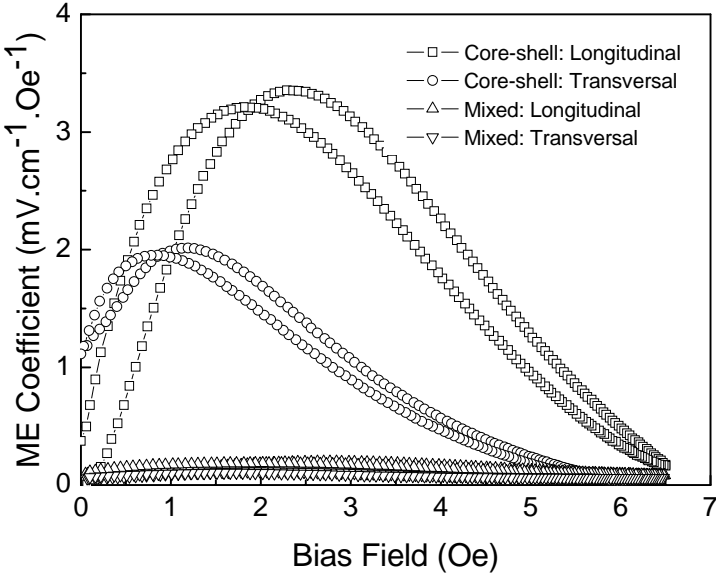


Fig.2. ME coefficients of CoFe<sub>2</sub>O<sub>4</sub>-BaTiO<sub>3</sub> core-shell and mixed structure composites as a function of DC bias field. The employed AC field is: 10 Oe, 270 Hz.

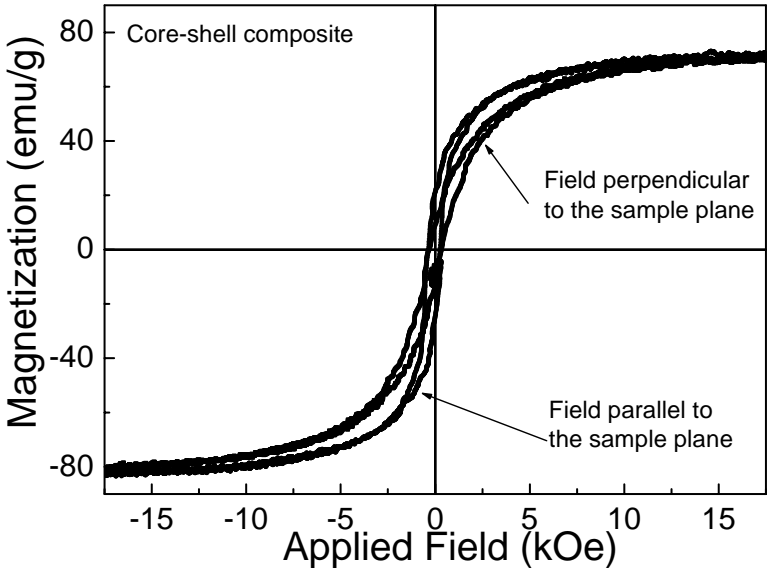


Fig.3. Hysteresis loops of CoFe<sub>2</sub>O<sub>4</sub> constituent measured in longitudinal and transversal position.



Magnetostriction measurements showed that the magnetostriction value in a 50%  $\text{CoFe}_2\text{O}_4$ -50%  $\text{BaTiO}_3$  (in mass) composite is not half that of a bulk  $\text{CoFe}_2\text{O}_4$  sample as expected, which may be explained that the strain produced by the magnetostrictive phase has been adsorbed partly by the piezoelectric phase due to different elastic constants as well as due to the local microstructure which affects the mechanical coupling [9].

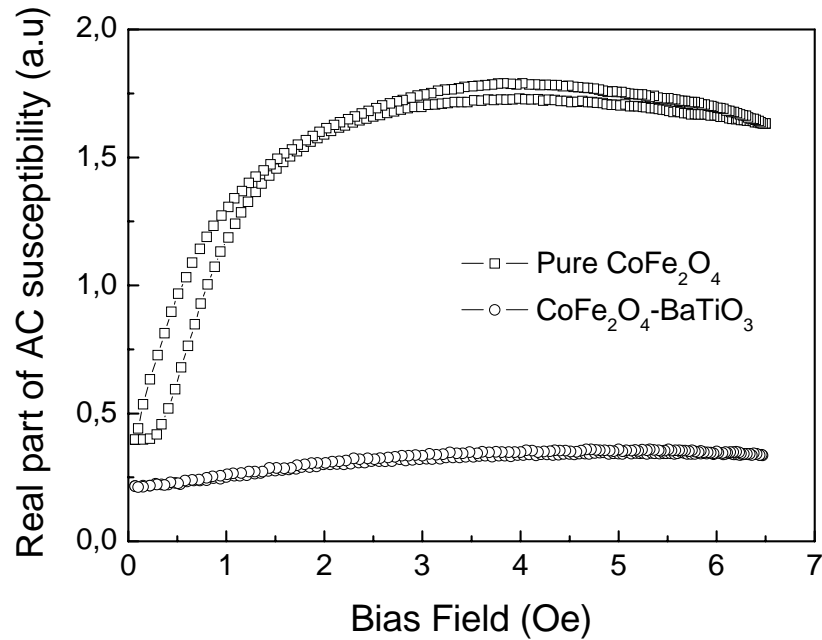


Fig.4. AC susceptibilities in DC bias field of pure  $\text{CoFe}_2\text{O}_4$  and  $\text{CoFe}_2\text{O}_4$ - $\text{BaTiO}_3$  core-shell composite at room temperature.

Differential AC susceptibilities  $\chi$  measured in a similar condition of ME measurement, i.e. in a DC bias field superimposed by an small AC field, showed that the value of the bias field where the maximum  $\chi$  occurs for pure  $\text{CoFe}_2\text{O}_4$ , with average grain size of 10 nm, are lower than that of the magnetic constituent in  $\text{CoFe}_2\text{O}_4$ - $\text{BaTiO}_3$  composite, with average egrain size of 20 nm. The value and the shape of the  $\chi$  versus H curve in the composite case is smaller and significantly different to that of pure  $\text{CoFe}_2\text{O}_4$ , suggesting that the magnetic domains in the composite are less free than those of pure  $\text{CoFe}_2\text{O}_4$ , see Fig.4. This gives evidence about a direct coupling between magnetic and electric dipoles of the domains in the composite, leading to the conclusion that the coupling between magnetostrictive and piezoelectric phases is not only mechanical coupling as believed, but also the direct coupling between dipoles of the magnetic and electric domains. Measurements in a pulse system showed that for a pulse duration smaller than 4ms, equal to a frequency of

250Hz, a phase shift between the field and ME signals occur, indicating that the coupling between magnetic and electric dipole may depend on  $dH/dt$ .

The angle  $\theta$  between the magnetic field vector and the direction of the electric polarization also influences the behaviour of the material. With increasing  $\theta$ , both  $\alpha_E$  and  $H_{max}$  decrease until  $\theta = 45^\circ$ , then increases again with increasing  $\theta$ , see Fig.5. The change in the ME coefficients is up to 400% when changing this  $\theta$  angle. Since the sample is polycrystalline, and the maximum change in magnetostriction when  $\theta$  change from 0 to  $90^\circ$ , i.e. changing the sample from parallel to perpendicular to the magnetic field, is about 100%, this huge change in ME coefficients cannot be understood by means of mechanical coupling between the two phases through magnetostriction. By changing the sample direction with respect to the magnetic field, one changes the direction of the alignment of magnetic moments. If assuming a direct coupling between magnetic and electric dipoles exists, the change in direction of the magnetic moments will cause a change in the direction of the alignment of electric dipoles, leading to a change in electric polarization which appears as the change of ME coefficient. To test this assumption, we align the sample before sintering in a DC magnetic field of 1.5 Tesla to change the magnetic moment alignment, the ME coefficient of this aligned sample increases up to 86 %. This gives again evidence of the existence of a vectorial coupling between the magnetic and electric dipoles inside the composites.

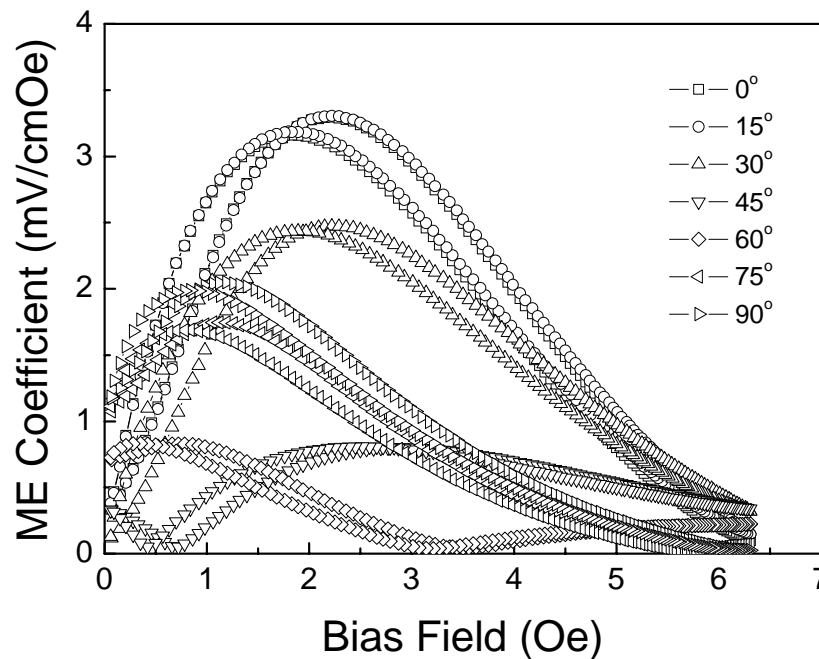


Fig.5. Angular dependence of the ME coefficient of  $\text{CoFe}_2\text{O}_4\text{-BaTiO}_3$  core-shell structure composite.

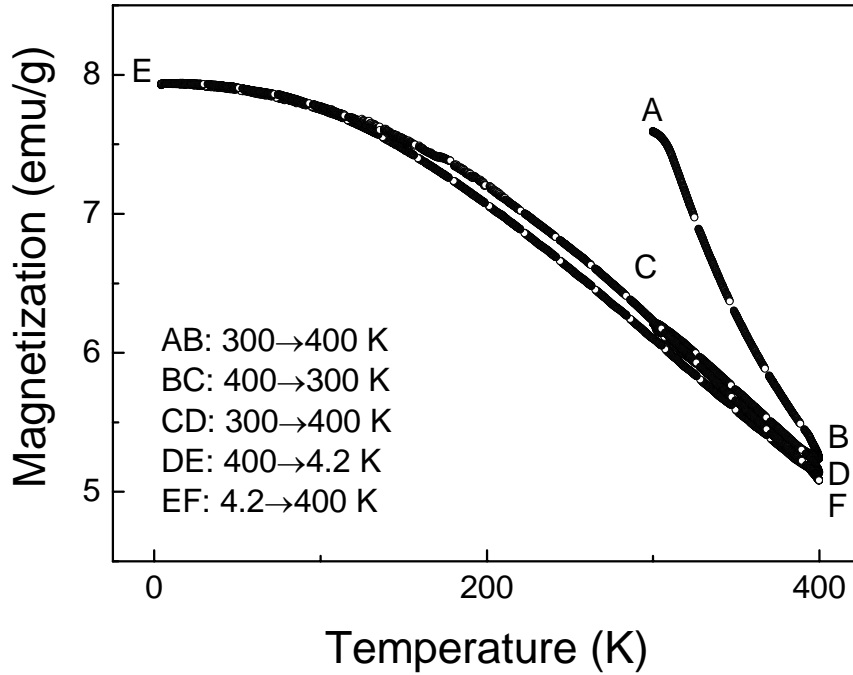


Fig.6. Temperature-dependent magnetization of the cobalt ferrite constituent in  $\text{CoFe}_2\text{O}_4\text{-BaTiO}_3$  core-shell structure composite under a magnetic field of 100 Oe.

The temperature-dependent magnetization of the studied composite measured in a constant magnetic field of 100 Oe showed a huge change in the magnetization of the  $\text{CoFe}_2\text{O}_4$  constituent when the alignment of the electric dipoles in  $\text{BaTiO}_3$  constituent is destroyed with increasing temperature to its ferroelectric Curie point (393 K), see Fig.6. With increasing temperature from 300 to 400 K, the part A-B, the magnetization of the  $\text{CoFe}_2\text{O}_4$  constituent in the electrically poled sample, i.e the electric dipoles of the  $\text{BaTiO}_3$  constituent are aligned, decreases from 7.6 to 5.25 emu/g. After that, decreasing the temperature from 400 to 300 K, the magnetization increases to only 6.2 emu/g which is about 18.4 % smaller than its initial value. This difference in the magnetization may result from the difference in the alignment of electric dipoles of the  $\text{BaTiO}_3$  constituent. In the first case, all electric dipoles were almost parallel at 300 K due to electrical poling of the sample. These parallel electric dipoles will interact with the magnetic moments of the  $\text{CoFe}_2\text{O}_4$  constituent as an “additional E-field”. When the temperature reached 400 K which is slightly higher than the Curie temperature of  $\text{BaTiO}_3$ , the alignment of the electric dipoles vanishes. Cooling back to 300 K, the part B-C, the electric dipoles increase again, however, in a random distribution, causing a total electric polarization of the  $\text{BaTiO}_3$  constituent which is almost zero. Therefore, the “additional E-

field” causing an interaction between electric dipoles and magnetic moments is now almost zero, resulting in a smaller “total field” compared to that in the first case, leading to a smaller magnetization as shown in Fig. 6. Increasing again the temperature from 300 to 400 K, the part C-D, as well as decreasing it from 400 to 4.2 K, the part D-E, and increasing up to 400 K, the part E-F, causes almost no change in the magnetization since the electric dipoles in these cases were already randomly distributed, giving no “additional E-field”.

The nature of the interaction between magnetic and electric moments, i.e the direct magneto-electric coupling, in this composite is not completely clear. However, according to the theory of electromagnetic field, a dynamic magnetic field induces an electric field and vice versa, i.e electric and magnetic fields are just two different aspects of the electromagnetic field. In matter, the electromagnetic field will act on both magnetic and electric moments, leading to the direct coupling between this moments, especially when the distance between them are very small as the case of single phase ME materials or the ME nanocomposite studied here.

#### **4. Conclusion**

Magnetoelectric studies in  $\text{CoFe}_2\text{O}_4\text{-BaTiO}_3$  core-shell structure nanocomposites showed that beside the mechanical coupling through magnetostriction of the  $\text{CoFe}_2\text{O}_4$  constituent, there may exist a direct coupling between dipoles of electric and magnetic domains which is evidenced by studying the AC susceptibility in bias field, angular dependent ME coefficient and temperature dependent magnetization of the composite.

#### **Acknowledgement**

This work is supported by the FWF Proj. Nr. P16500-N02, Proj. Nr. P15737 and the Austrian Exchange Service (ÖAD).

#### **Reference**

- [1]. P. Curie, J. Physique 3e series, 3, 393 (1894).
- [2]. L.D. Landau and E. Lifshitz, *Electrodynamics of Continuous Media* (Addison-Wesley: Translation of a Russian edition of 1958), (1960).
- [3]. I.E. Dzyaloshinskii, *Sov. Phys.–JETP*, 37, 628 (1960).

- [4]. D.N. Astrov, Sov. Phys.–JETP, 11, 708 (1960).
- [5]. G.T. Rado and V.J. Folen, Phys. Rev. Lett., 7, 310 (1961).
- [6]. N.A. Hill, J. Phys. Chem. B 104, 6694-6709 (2000).
- [7]. Jungho Ryu, Shashank Priya, Kenji Uchino & Hyoun-Ee Kim, J. Electroceramics., 8, 107–119, 2002.
- [8]. H. Zheng et al, Science 303 (2004) 661.
- [9]. Giap V. Duong, R. Groessinger, R. sato Turtelli, Magnetoelectric properties of  $\text{CoFe}_2\text{O}_4$ - $\text{BaTiO}_3$  core-shell structure composites, submitted to IEEE International Magnetic Conference, Intermag2006, San Diego, California, May 8-12, 2006.
- [10]. Giap V. Duong, R. Groessinger, M. Schoenhardt, D. Bueno-Basques, Lock-in technique for studying magnetoelectric effect, submitted for publication.
- [11]. R.P Manhajan, K.K Patankar, M.B. Kothale, S.C. Chaudhari, V.L. Mathe and S.A. Patil, PRAMANA-Journal of physics, Vol. 58, Nos 5 & 6 May & June 2002, pp. 1115–1124
- [12]. Manfred Fiebig, J. Phys. D: Appl. Phys. 38 (2005) R123–R152

# Magnetoelectric properties of $\text{CoFe}_2\text{O}_4 - \text{BaTiO}_3$ core-shell structure composite studied by a magnetic pulse method

Giap V. Duong<sup>1,2</sup>, R. Groessinger<sup>1</sup>

<sup>1</sup>*Institute for Solid State Physics, Vienna University of Technology  
Wiedner Hauptstrasse 8-10, A-1040, Vienna, Austria*

<sup>2</sup>*Faculty of Chemical Engineering, Hanoi University of Technology  
1 Dai Co Viet, Hai Ba Trung, Hanoi, Vietnam*

To be submitted for publication.

---

## Abstract:

A new method using a pulsed field in order to measure the ME effect of  $\text{CoFe}_2\text{O}_4$ - $\text{BaTiO}_3$  core-shell structure composite has been developed. The maximum ME coefficient of this composite is 5.5 and 4.2 mV/cmOe for longitudinal and transverse measurement, respectively. These values are bigger than those measured by the lock-in technique. Both pulse duration and field sweep rate  $dH/dt$  are found to affect the ME response of the composite.

*PACS:* 75.80.+q; 77.65.-j; 77.84.Lf

*Keywords:* Magnetoelectric effect, magnetoelectric interaction, magnetoelectric composite, magnetostriction, piezoelectricity, cobalt ferrite, barium titanate.

---

## 1. Introduction:

Magnetoelectric (ME) effect—the induction of electric polarization by means of a magnetic field and the induction of magnetization by means of an electric field—was predicted as early as 1894, when Curie pointed out that it would be possible for an asymmetric molecular body to polarize directionally under the influence of a magnetic field [1]. The ability of mutual control between magnetic and electric properties makes the ME materials become very attractive in both fundamental understanding of material physics and practical

applications, such as: multiple state memory elements, sensors, transducers, actuators, etc [2]. In single phase materials, the ME effect describes the interaction between magnetic and electric field in matters and requires the coexistence of ordered magnetic moments and electric dipoles. In composites, the ME effect is a “product property” of the constituents [3, 4]. In brief description, when exposing a ME composite to a magnetic field, a strain is produced in the magnetostrictive phase which is then passed into the piezoelectric phase through mechanical coupling, causing a stress, and as a result of it, producing an electric polarization in the piezoelectric constituent.

Despite the attractiveness of the ME materials and the revival of the ME effect [2], the measuring technique to characterize the ME properties is not established, i.e. a measuring system is not commercially available. For composites, most of the ME characterization involves the use of a small AC field superimposed onto a DC bias field. The ME response signal is registered at the frequency of the AC field. This method has advantage of exploring ME properties at different working points set by the DC bias field. However, it does not measure directly the ME response, and the discharging process due to the finite impedance of the sample and the lock-in amplifier under a periodic measurement condition influences significantly the measured values [5]. This paper will deal with the use of a pulse field technique—a new method to study the ME properties of a  $\text{CoFe}_2\text{O}_4\text{-BaTiO}_3$  ME composites. This method allows to measure directly the ME voltage across the sample under an applied magnetic field. Different aspects, including the set-up of measuring system, the magnetic and ME properties of the composite as well as the affect of the field sweep rate  $dH/dt$  to the ME behaviour will be discussed.

## **2. Experimental:**

The samples were synthesized using wet chemical method as described elsewhere [6]. Crystalline structures of single phase materials as well as composites were investigated by X-ray diffractometer (XRD). Magnetic properties were studied using a pulse field magnetometer (Hirst, PFM 11). Magnetostriction was measured using strain gauge method with a 50 kHz bridge (HBM Type KWS 85.A1). Magnetic properties were studied using pulse field method in a pulse field magnetometer with a pulse duration of about 50 ms (Hirst, PFM 11) or 4 ms (lab made pulse magnetometer) where the ME voltage across the sample was measured directly using a measuring card with input impedance of 10 M $\Omega$ . To avoid the induction voltage, the amplifier was operated in differential mode. Fig. 1 below showed the schema of

the measuring system. All measurements were carried out at room temperature and ambient pressure.

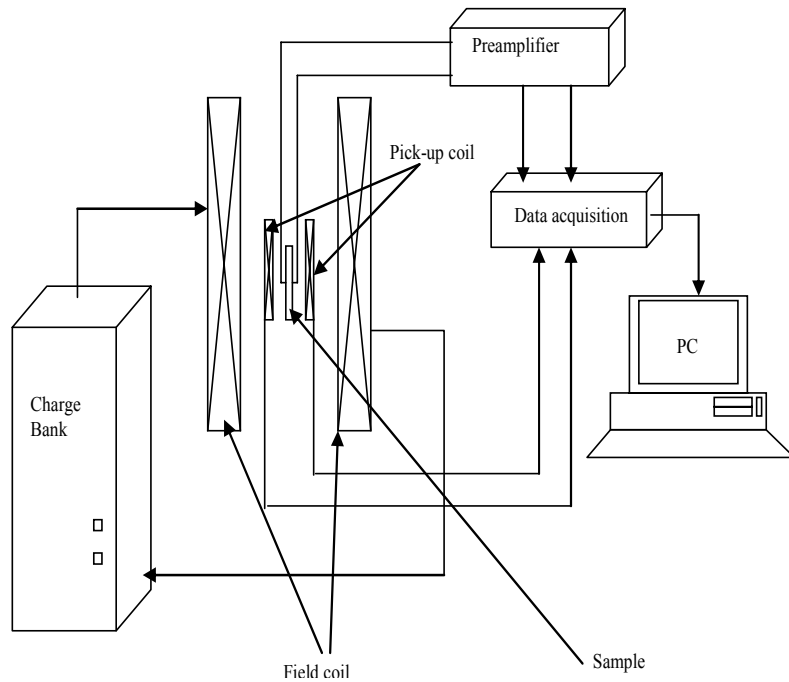


Fig.1. Schema of the pulse field method measuring system to study ME effect.

### 3. Results and Discussions:

The XRD pattern shown in Fig.2 suggested that the composite consists two single phases:  $\text{CoFe}_2\text{O}_4$  and  $\text{BaTiO}_3$ . Line broadening analysis showed that the grain size of the  $\text{CoFe}_2\text{O}_4$  core before sintering is about 10 nm. Magnetic measurements proved that the magnetic properties of the magnetostrictive component in the composite are similar to that one of the bulk sample. The saturation magnetization of the  $\text{CoFe}_2\text{O}_4$  constituent is about 80 emu/g as shown in Fig.3. The magnetostriction of the pure  $\text{CoFe}_2\text{O}_4$  is -130 and -70 ppm for parallel and perpendicular measurements, respectively. However, the magnetostriction of the 50% $\text{CoFe}_2\text{O}_4$ -50% $\text{BaTiO}_3$  (in mass) is less than half of the magnetostriction of the  $\text{CoFe}_2\text{O}_4$  constituent, only about 30 ppm, giving hint that part of the strain produced by the  $\text{CoFe}_2\text{O}_4$  component may be adsorbed due to the different elastic constants of the constituents as well as by the actual microstructure [6].



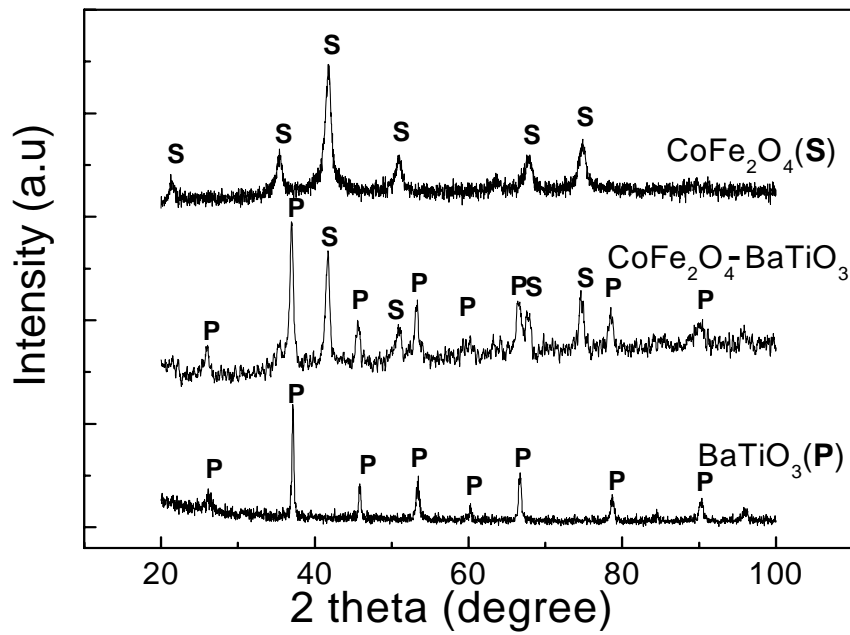


Fig. 2. XRD patterns of  $\text{CoFe}_2\text{O}_4$  (S),  $\text{BaTiO}_3$  (P) and  $\text{CoFe}_2\text{O}_4$ - $\text{BaTiO}_3$  composite.

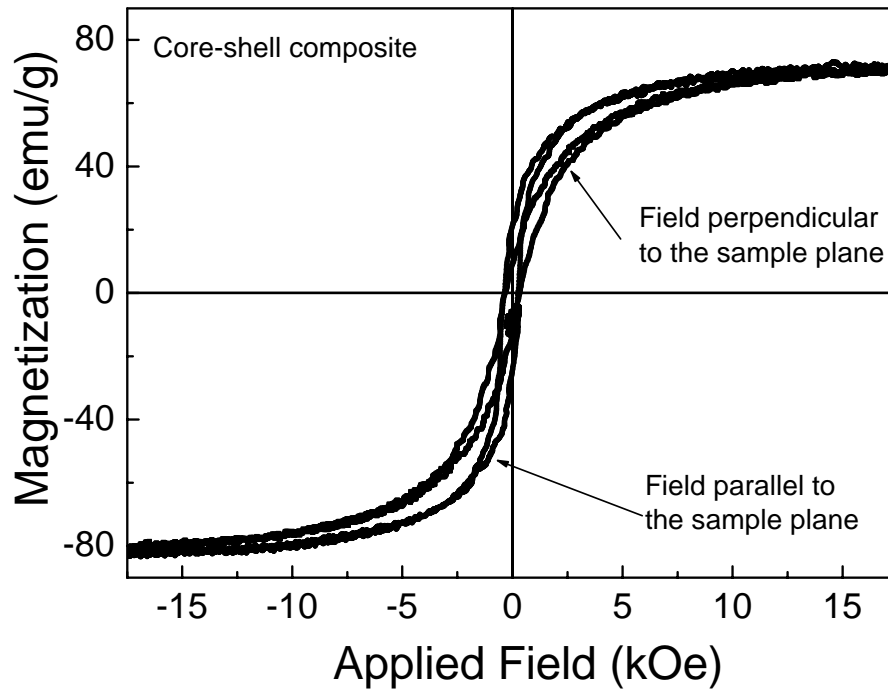


Fig.3. Hysteresis loops of  $\text{CoFe}_2\text{O}_4$  constituent measured in longitudinal and transverse position.

ME coefficient,  $\alpha_E$ , was determined using the equation  $\alpha_E = V/(d.H)$  where  $V$  is the voltage across the sample,  $d$  is the effective thickness of the sample and  $H$  is the applied magnetic field. The coefficient is called longitudinal if the surface of the sample is perpendicular to the applied magnetic field, and transverse if they are parallel. The ME coefficient – magnetic field curves,  $\alpha_E-H$ , is very similar to those measured by the lock-in technique in which a small AC magnetic field is superimposed onto a DC bias field [5, 6], see Fig.4. The maximum ME coefficient is 5.5 and 4.2 mV/cmOe for longitudinal and transverse measurements, respectively. These values are about 1.6 times bigger than those measured by the lock-in technique which can be explained by considering the fact that with a lock- in one measures the effective value of a periodic voltage, whereas with the pulsed field method one measures the amplitude which is a factor 1.4 larger.

The applied field where the maximum ME coefficient occurs,  $H_{max}$ , is ranging from 1000-2000 Oe, depending whether the measurement is longitudinal or transverse. The value of  $H_{max}$  for the case of longitudinal is bigger than that of transverse. The reason is the demagnetizing field which is in the former case bigger than in the later, which can be seen clearly in Fig.3. At higher fields, the ME coefficient decreases due to the decrease of magnetostriction of the magnetostrictive constituent which is in charge for the ME effect in the composite [2, 4, 7].

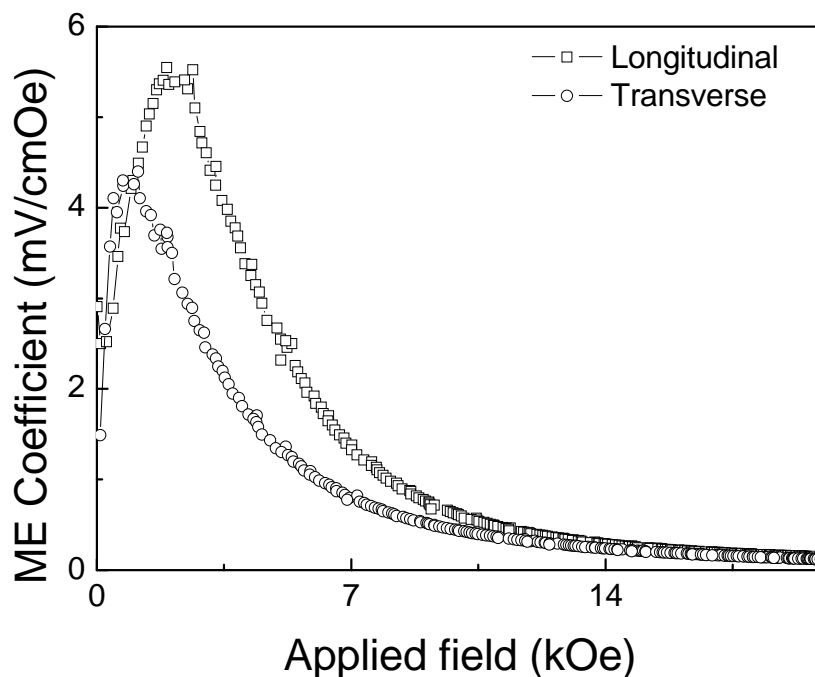


Fig.4. ME coefficient as function of applied magnetic field.

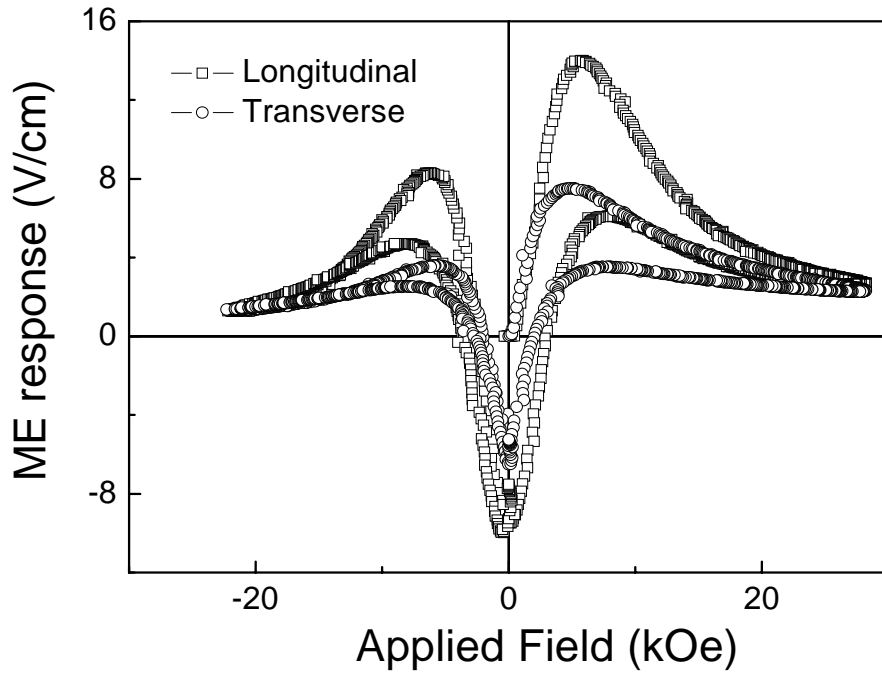


Fig.5. The ME voltage as function of a bipolar applied magnetic field.

With increasing magnetic field, a linear ME effect is observed up to 5000 Oe, see Fig.5. At higher field, the ME voltage decreases due to the decrease of the magnetostriction of the magnetic constituent as discussed above. When decreasing magnetic field, the magnetoelectric response voltage versus magnetic field curve does not follow exactly the increasing curve, resulting in a hysteretic behavior, and becoming even negative at low field region. The hysteresis may be attributed to the hysteretic nature of constituents, but also the discharging process during the measurement which is superimposed by the charge generation. The reason of the negative ME voltage may be the compensation of bound charges on the grains of piezoelectric constituent by free charges created by an electric current passing through the sample which has an opposite polarization [8]. With decreasing applied field to a certain value, the charge produced by the ME composite is smaller than the compensation charges, leading to the ME voltage of negative sign. Following this, the amplitude of this negative voltage is found to decrease exponentially as  $V=V_0\exp(e^{-t/\tau})$  with  $\tau = \sim 13$  ms because of the discharging process. To confirm this, the maximum ME response was measured as function of the field sweep rate  $dH/dt$ . The experiments showed that the faster the field increases, the bigger becomes the ME voltage. The reason is that the effect of the discharging process becomes smaller when the field increases faster, leading to a bigger ME voltage, see

Fig. 6. This means during such a pulsed field measurement, the charging and discharging process occurs simultaneously.

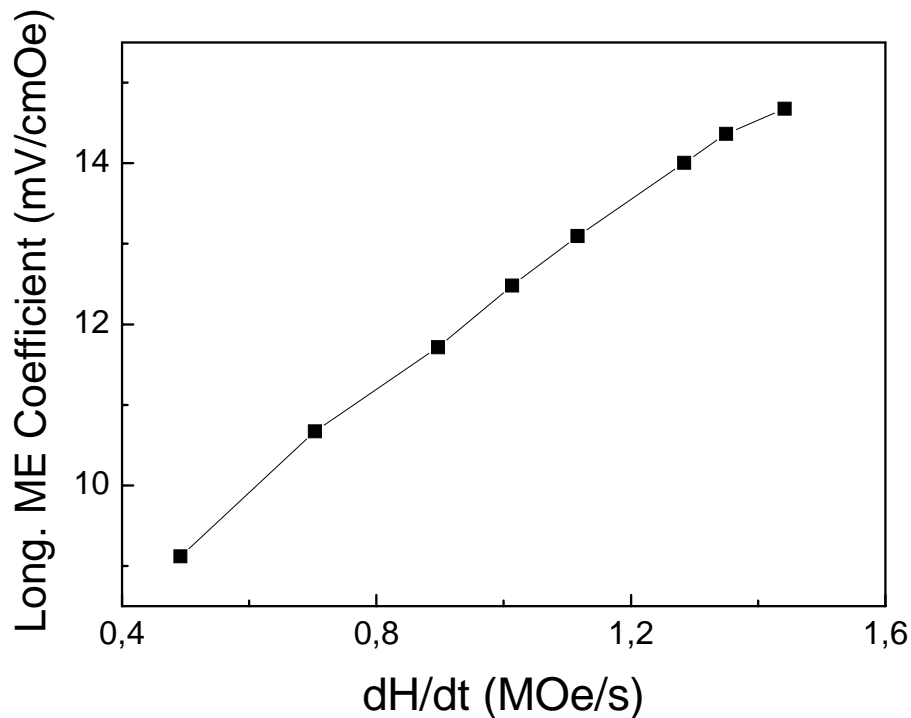


Fig.6. Maximum ME response as function of  $dH/dt$ .

Measuring ME response with different pulse durations between 50 and 4.2 ms, reveals that the ME voltage cannot follow the field if the pulse duration is smaller than 4.5 ms, see Fig.7 & 8. The reason may be attributed to the discharging process through the capacitance formed by the surface of the sample at higher frequencies similar as was found with the ac-method [5], i.e. short time duration. The frequency where the discharging through the capacitance part start to be dominant is about 200 Hz [5] which is in agreement with the pulse duration of 4.5 ms. Another reason of the mismatching between ME response and applied field by be due to the large ME viscosity, i.e. the time dependence of ME coupling. However, more experiments must be carried out to confirm this phenomenon.

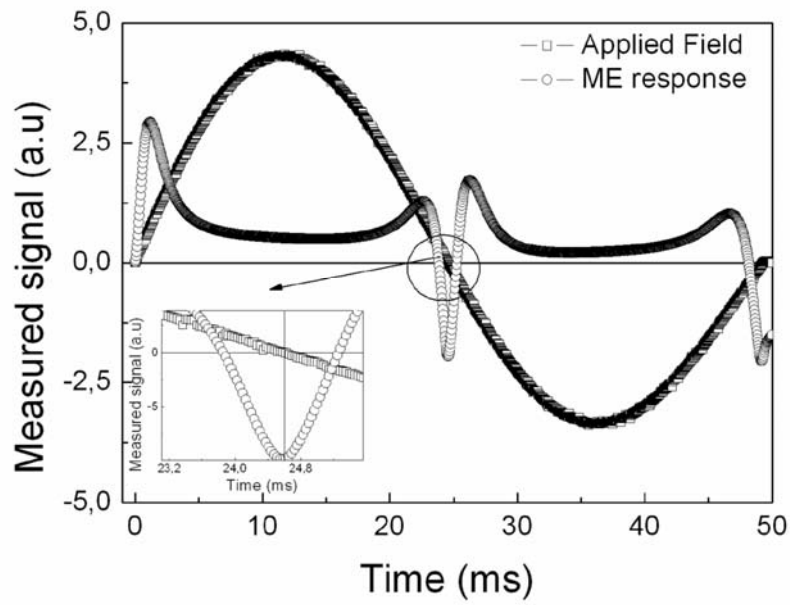


Fig.7. ME and field signal in a 50 ms pulse duration.

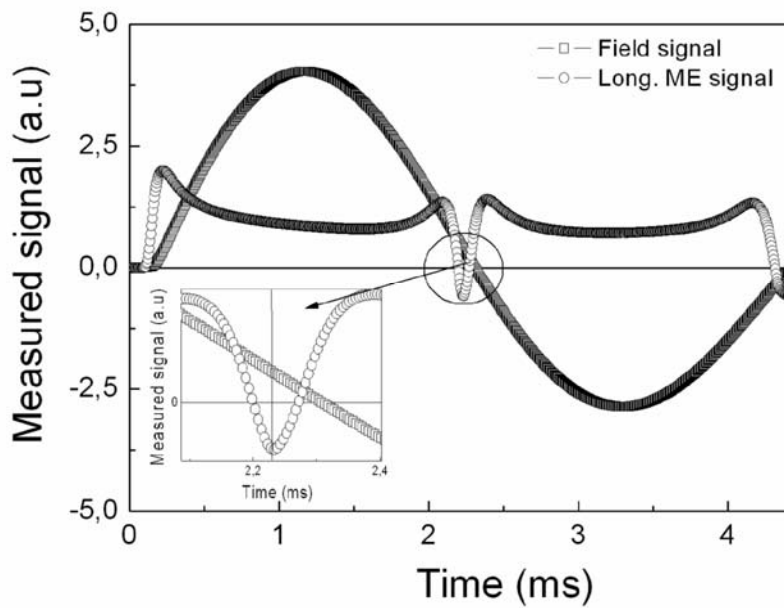


Fig.8. ME and field signal in a 4.2 ms pulse duration.

#### 4. Conclusion

Pulse field method is found to be convenient for a direct measurement of the ME response of ME composite under an applied pulsed magnetic field. The ME coefficient measured by this method is bigger than that measured by the lock-in technique. During this measurement also the effect of a competing charging and discharging process due to the

internal impedance of the sample is observed. Both pulse duration and the field sweep rate affect the response of the composite.

### **Acknowledgement**

This work is supported by the FWF Proj. Nr. P16500-N02, Proj. Nr. P15737 and the Austrian Exchange Service (ÖAD).

### **Reference**

- [19]. P. Curie, *J. Physique 3e series*, 3 (1894) 393.
- [2]. Manfred Fiebig, *J. Phys. D: Appl. Phys.* 38 (2005) R123–R152
- [3]. J. Van Suchetelene, *Philips Res. Rep.*, **27** (1972) 28.
- [4]. Jungho Ryu, Shashank Priya, Kenji Uchino & Hyoun-Ee Kim, *J. Electroceramics.*, 8 (2002) 107–119.
- [5]. Giap V. Duong, R. Groessinger, M. Schoenhart, D. Bueno-Basques, Lock-in technique for studying magnetoelectric effect, submitted for publication.
- [6]. Giap V. Duong, R. Groessinger, R. sato Turtelli, Magnetoelectric properties of  $\text{CoFe}_2\text{O}_4$ - $\text{BaTiO}_3$  core-shell structure composites, submitted to IEEE International Magnetic Conference, Intermag2006, San Diego, California, May 8-12, 2006.
- [7]. Giap V. Duong, R. Groessinger, R. Sato Turtelli, Driving mechanism for ME effect in  $\text{CoFe}_2\text{O}_4$ - $\text{BaTiO}_3$  multiferroic composite, *J. Magn. Mater.*, accepted for publication.
- [8]. Y.K. Fetisov, K.E. Kamentsev, A.Y. Ostashchenko and G. Srinivasan, *Solid State Comm.*, 132 (2004) 13-17.

# Magnetoelectric properties of $\text{Co}_{0.7}\text{Zn}_{0.3}\text{Fe}_2\text{O}_4 - \text{BaTiO}_3$ core-shell structure composite

Giap V. Duong<sup>1,2</sup>, R. Groessinger<sup>1</sup>

<sup>1</sup>*Institute for Solid State Physics, Vienna University of Technology*

*Wiedner Hauptstrasse 8-10, A-1040, Vienna, Austria*

<sup>2</sup>*Faculty of Chemical Engineering, Hanoi University of Technology*

*1 Dai Co Viet, Hai Ba Trung, Hanoi, Vietnam*

To be submitted for publication.

---

## Abstract:

A  $\text{Co}_{0.7}\text{Zn}_{0.3}\text{Fe}_2\text{O}_4$ - $\text{BaTiO}_3$  core-shell structure composite has been prepared by wet chemical method and studied with respect to its magnetoelectrical properties. It was found that the substitution of Co by Zn decreases the ME coefficient due to the decrease of the magnetostriction of the ferrite. The bias field where the maximum ME coefficient occurs decrease also compared to the pure  $\text{CoFe}_2\text{O}_4$  ferrite due to the increase of magnetic softness. The field dependence of the magnetoelectric coefficient is determined by the field dependence of  $k=\lambda \cdot \partial \lambda / \partial H$  as well as by the magnetization process of the magnetic constituent. Therefore, a magneto-mechanical coupling between the constituents and an additional direct coupling between magnetic and electric domains, both influencing the value and field dependence of the ME effect in the composite, is believed to exist.

*PACS:* 75.80.+q; 77.65.-j; 77.84.Lf

*Keywords:* Magnetoelectric effect, magnetoelectric interaction, magnetoelectric composite, magnetostriction, piezoelectricity, cobalt ferrite, barium titanate.

---

## 1. Introduction:

The magnetoelectric (ME) effect—the induction of electric polarization by means of a magnetic field and the induction of a magnetization by means of an electric field—was predicted as early as 1894, when Curie pointed out that it would be possible for an asymmetric molecular body to polarize directionally under the influence of a magnetic field [1]. The ability of mutual control between magnetic and electric properties makes the ME materials become very attractive in both fundamental understanding of material physics and practical applications, such as: multiple state memory elements, sensors, transducers, actuators, etc [2].

Recently we prepared a  $\text{CoFe}_2\text{O}_4\text{-BaTiO}_3$  ME composite in a core-shell structure which has a ME coefficient which was approximately 18 time higher than that of the mixed structure with the same composition [3]. The reason is the coupling between the constituents in the former is much better than that of the later. We also proved that the main driving mechanism is the magneto-mechanical coupling through magnetostriction of the magnetostrictive phase. The ME coefficient is found to be proportional to an efficiency factor  $k_0$  and a coupling coefficient  $k$ , defined as  $k = \lambda \cdot \partial\lambda / \partial H$  where  $\lambda$  is the linear magnetostriction [4]. We also found evidence of a “direct” coupling between magnetic and electric domains [5]. When substituting Co by Zn, the saturation magnetization increases but the magnetostriction decreases. If the mechanical coupling is the only driving mechanism for the ME effect in such composites, the expected ME coefficient should decrease linearly with the value of the magnetostriction. If an additional direct coupling between magnetic and electric domains exist, the ME coefficient will be bigger than the expected value determined by magneto-mechanical coupling since the zinc substituted ferrite has a larger saturation magnetization, which can consequently enhance the direct coupling between the constituents.

The aim of this work is to study the ME effect of  $\text{Co}_{0.7}\text{Zn}_{0.3}\text{Fe}_2\text{O}_4\text{-BaTiO}_3$  in a core-shell structure in order to investigate the effect of the zinc substitution, and hence, to study the possible contributions of the mechanical and the “direct” coupling between constituents, since zinc substitution affect both magnetostriction and magnetization of the the domains of the magnetic component.



## 2. Experimental:

The samples were synthesized using wet chemical methods. The  $\text{Co}_{0.7}\text{Zn}_{0.3}\text{Fe}_2\text{O}_4$  constituent was prepared by citrate gel method. The precursor salts,  $\text{Fe}(\text{NO}_3)_3 \cdot 9\text{H}_2\text{O}$ ,  $\text{Co}(\text{NO}_3)_2 \cdot 6\text{H}_2\text{O}$ ,  $\text{Zn}(\text{NO}_3)_2 \cdot 6\text{H}_2\text{O}$  and citric acid, all with analytical purity, were added to 150 ml of deionized water in stoichiometric ratio. The total metal concentration was 1 mol/l. The molar ratio between total metal ions and citric acid was fixed to 1. The starting mixture containing the salts, deionized water and citric acid was stirred to get homogeneous solution and heated to 80 °C with a heating rate of 5 °C/min using a hot plate magnetic stirrer. The pH of the solution was adjusted to 6 by dropping ammonia ( $\text{NH}_3$  25%). The sol was formed during stirring. Increasing the temperature of the hot plate up to 200 °C and keep stirring constantly, the water in the solution was evaporated and a viscous gel was formed. Keeping heating, the gel is dried and burnt as being ignited to form loose powder. It was pre-sintered at 450 °C for 3 hours to remove the organic substances before sintering at 1000 °C for 5 hours. The grain size of the obtained ferrite, estimated from the line broadening of the XRD pattern, as about 53 nm. To compare the magnetic properties of the ferrite constituents, a  $\text{CoFe}_2\text{O}_4$  sample was prepared under the same condition. The grain size of this ferrite, also estimated from XRD pattern, is about 40 nm.

To prepare the core-shell structure composite, the ferrite powder, calculated to get a composite containing 50% in mass of each constituent, was introduced into a solution of acetic acid, barium hydroxide and titanium (IV) n-Butoxide, which is then gelled on the surface of the  $\text{Co}_{0.7}\text{Zn}_{0.3}\text{Fe}_2\text{O}_4$  grains or particles during heating and stirring. The obtained material is dried, pre-sintered at 700°C for 2 hours, ground into fine powder, then pressed under a pressure of 6 tones/cm<sup>2</sup> to obtain a sample in shape of a disc of 10 mm in diameter and 1.5 mm thick. This sample is sintered at 1250°C for 4 hours to get a core-shell structure composite. After heat treatment, due to shrinkage, the diameter and thickness of the sample are 8.5 and 1.3mm, respectively. The sample was painted by silver paste for electric contacts, then poled electrically under an electric field of 7500V/cm (field direction is perpendicular to the surface of the sample) in silicon oil from 150°C down to room temperature. For comparison, a similar  $\text{CoFe}_2\text{O}_4$ - $\text{BaTiO}_3$  sample was produced under the same conditions, following the same heat treatment and poling procedure.

Crystalline structures of single phase materials as well as composites were investigated by X-ray diffractometer (XRD) using  $\text{CoK}_\alpha$  radiation. Magnetic properties of the ferrite constituent were studied using a pulse field magnetometer (Hirst, PFM 11).

Magnetostriction was measured using strain gauge method with a 50 kHz bridge (HBM Type KWS 85.A1). Magnetoelectric properties were studied using a lock-in technique [6], in which a small AC field with frequency of 1-4000 Hz and amplitude of 0.1-20 Oe was superimposed onto a DC bias field up to 6.5 kOe. The input resistance and capacitance of the lock-in (EG&G model 5210) is 100 M $\Omega$  and 25 pF, respectively. The measurements of the ME voltage were performed for two different field orientations with respect to the sample plane to obtain the transverse and longitudinal ME coefficients. The ME coefficient,  $\alpha_E$ , was determined using the equation  $\alpha_E = (\partial E / \partial H)_T = V / (d \cdot H_{AC})$ , where  $V$  is the voltage measured with the lock-in amplifier,  $d$  is the effective thickness of the piezoelectric phase. All measurements were carried out at room temperature and ambient pressure.

### 3. Results and Discussions

The XRD pattern of the composite and its constituents was shown in Fig.1. It is evident that the composite consists of only two single phases:  $\text{Co}_{0.7}\text{Zn}_{0.3}\text{Fe}_2\text{O}_4$  with spinel structure and  $\text{BaTiO}_3$  with perovskite structure. No foreign phase was detected by means of XRD characterization. The grain size of the ferrite powder, estimated by the line broadening of the strongest reflection at low angle [7], before introducing to the composite is 53 nm. However, it increases up to 64 nm in the composite after heat treatment.

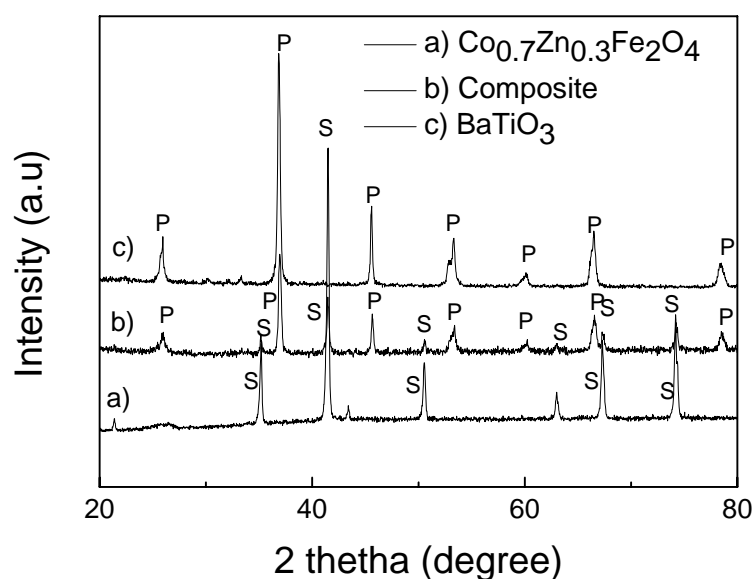


Fig. 1. XRD patterns of  $\text{Co}_{0.7}\text{Zn}_{0.3}\text{Fe}_2\text{O}_4$  (S),  $\text{BaTiO}_3$  (P) and  $\text{Co}_{0.7}\text{Zn}_{0.3}\text{Fe}_2\text{O}_4$ - $\text{BaTiO}_3$  composite.

Hysteresis loops of the ferrite constituents, i.e.  $\text{Co}_{0.7}\text{Zn}_{0.3}\text{Fe}_2\text{O}_4$  with an average grain size of 53 nm and  $\text{CoFe}_2\text{O}_4$  with average grain size of 40 nm, at room temperature are shown in Fig.2. In the zinc substituted sample, at room temperature, the saturation magnetization, under a magnetic field of 10 kOe, increases from 77.5 to 89.5 emu/g, and the coercivity decreases from 818 to 193 Oe. The reason for the increase of  $M_s$  when substituting Co by Zn is: the  $\text{Zn}^{2+}$  ions with a zero magnetic moment replace Co-ions on the tetrahedral A-sites, causing a decrease of the magnetic moment in this sublattice,  $M_A$ , resulting in an increase of the total magnetic moment,  $M$ , since  $M = M_B - M_A$  where  $M_B$  is the magnetic moment of the sublattice formed by the octahedral B-sites [8]. It is also found that the zinc substitution decreases the magnetic anisotropy of the cobalt ferrite [9]. This leads to a decrease of the coercivity in  $\text{Co}_{0.7}\text{Zn}_{0.3}\text{Fe}_2\text{O}_4$  sample as shown in Fig.2.

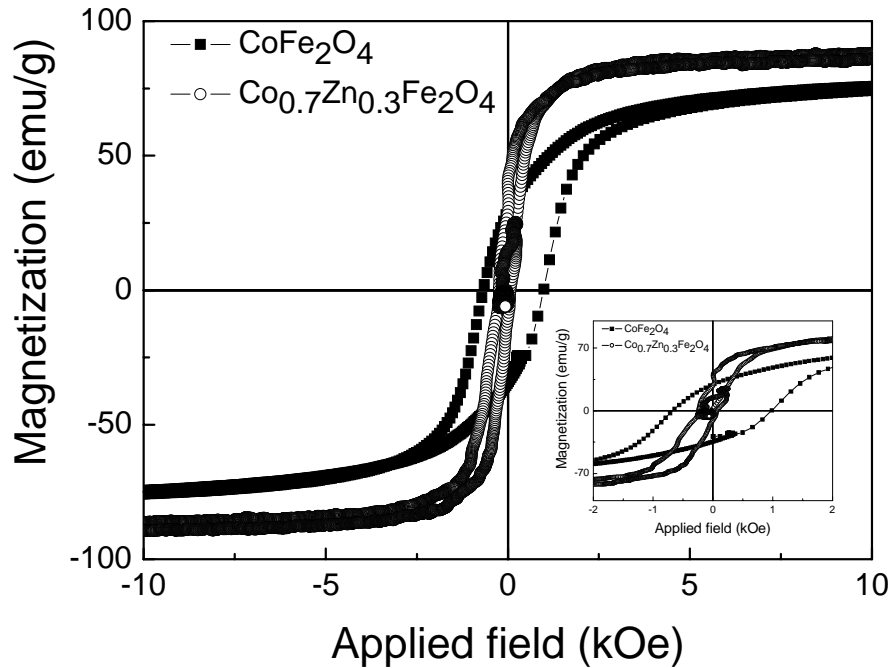


Fig.2. Hysteresis loops of  $\text{CoFe}_2\text{O}_4$  ( $D=40$  nm) and  $\text{Co}_{0.7}\text{Zn}_{0.3}\text{Fe}_2\text{O}_4$  ( $D=53$  nm). Inset is the loops close to the coercivity field range.

The magnetostrictions of the  $\text{Co}_{0.7}\text{Zn}_{0.3}\text{Fe}_2\text{O}_4$  and  $\text{CoFe}_2\text{O}_4$  ferrite are shown in Fig.3. The magnetostriction of pure  $\text{CoFe}_2\text{O}_4$  is about -130 and 70 ppm for  $\lambda$ -parallel and  $\lambda$ -perpendicular, respectively. However, in the zinc substituted sample, they decrease accordingly to -34 and 17 ppm. The reason is the substitution of  $\text{Co}^{2+}$  which has a large orbital moment by  $\text{Zn}^{2+}$  that has no magnetic moment which cause not only a reduction of the

anisotropy field but also of the magnetostriction since the contribution of  $\text{Co}^{2+}$  now is smaller. However, the decreases of the magnetostriction as well as the coercivity is not simply proportional to the degree of substitution. This deviation can be explained in terms of triangular arrangement of spins [10] or superparamagnetic spin clusters due to the breaking of exchange paths by non-magnetic  $\text{Zn}^{2+}$  ions [11]. The increase of saturation magnetization and the decrease of magnetostriction and coercivity suggest that mostly  $\text{Zn}^{+2}$  ions go into the  $\text{Co}^{2+}$  sites.

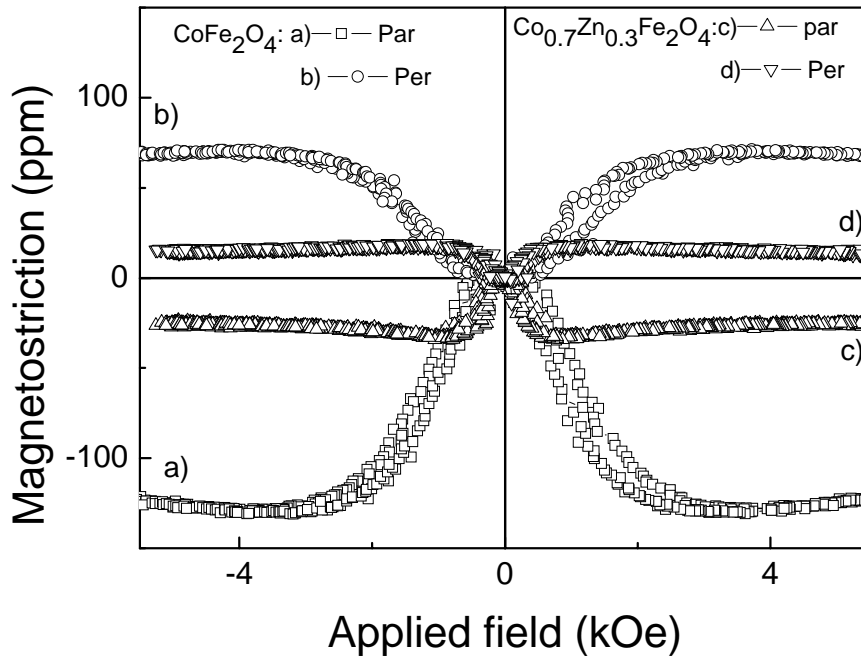


Fig. 3. Magnetostriction of  $\text{CoFe}_2\text{O}_4$  ( $D=40$  nm) and  $\text{Co}_{0.7}\text{Zn}_{0.3}\text{Fe}_2\text{O}_4$  ( $D=53$  nm).

The field dependence of the longitudinal ME coefficients of the  $\text{Co}_{0.7}\text{Zn}_{0.3}\text{Fe}_2\text{O}_4$ - $\text{BaTiO}_3$  and  $\text{CoFe}_2\text{O}_4$ - $\text{BaTiO}_3$  core-shell structure composites using the ferrite as a core are shown in Fig. 4. In the  $\text{CoFe}_2\text{O}_4$ - $\text{BaTiO}_3$  sample, the maximum longitudinal ME coefficient is about  $1.34$  mV/cmOe. However, it decreases to  $0.57$  mV/cmOe in the zinc substituted sample. The main reason may be due to the decrease of the magnetostriction in the  $\text{Co}_{0.7}\text{Zn}_{0.3}\text{Fe}_2\text{O}_4$  constituent, see Fig. 3. This leads to a decrease of the coupling coefficient  $k$ , defined as  $k=\lambda \cdot \partial \lambda / \partial H$  where  $\lambda$  is the linear magnetostriction, which is proved to be in charge for the ME effect in similar composites [4]. However, the decrease of the ME coefficient in  $\text{Co}_{0.7}\text{Zn}_{0.3}\text{Fe}_2\text{O}_4$ - $\text{BaTiO}_3$  is not proportional to the decrease of the linear magnetostriction value in the  $\text{Co}_{0.7}\text{Zn}_{0.3}\text{Fe}_2\text{O}_4$  constituent. In the zinc substituted sample, the parallel

magnetostriction, which is in charge for the longitudinal ME coefficient, of the ferrite constituent decrease 73.8%, from -130 to -34 ppm while the longitudinal ME coefficient decreases only 57.4%, from 1.34 to 0.57 mV/cmOe. The reason may be that the zinc substituted ferrite is magnetically softer than the cobalt ferrite, see Fig. 2, which leads to an increase of  $\partial\lambda/\partial H$ , and as a result of it, the mechanical coupling coefficient  $k=\lambda.\partial\lambda/\partial H$  increases too. Another reason may be due an additional direct coupling between magnetic and electric domains, which was already suggested in pure  $\text{CoFe}_2\text{O}_4\text{-BaTiO}_3$  composite [5]. In the zinc substituted sample this effect can be bigger since its magnetic moment is larger as discussed above. This may lead to a larger domain coupling contribution to the ME coefficient compared to that of the  $\text{CoFe}_2\text{O}_4\text{-BaTiO}_3$  sample.

The bias field where the maximum ME coefficient occurs is in case of the  $\text{Co}_{0.7}\text{Zn}_{0.3}\text{Fe}_2\text{O}_4\text{-BaTiO}_3$  sample smaller than that of the  $\text{CoFe}_2\text{O}_4\text{-BaTiO}_3$  one. The reason is that  $\text{Co}_{0.7}\text{Zn}_{0.3}\text{Fe}_2\text{O}_4$  is magnetically softer than  $\text{CoFe}_2\text{O}_4$  as shown in Fig.2. The decrease of the ME coefficient at higher bias field is attributed to the decrease of  $d\lambda/dH$ , that leads to a decrease of the mechanical coupling between constituents.

Another interesting feature in Fig.4 is the hysteretic behavior found in the  $\text{Co}_{0.7}\text{Zn}_{0.3}\text{Fe}_2\text{O}_4\text{-BaTiO}_3$  sample is much smaller than that of the  $\text{CoFe}_2\text{O}_4\text{-BaTiO}_3$  one. This indicates also the fact that the  $\text{Co}_{0.7}\text{Zn}_{0.3}\text{Fe}_2\text{O}_4$  is magnetically softer than the  $\text{CoFe}_2\text{O}_4$  as shown in Fig. 2. This suggests that the field dependence of the ME coefficient of such composites is affected by the  $\lambda.\partial\lambda/\partial H$  behaviour as well as by the magnetization process of its magnetic constituent, which can also be explained assuming a direct coupling between magnetic and electric domains on a nanoscale.

The longitudinal and transverse ME coefficients, measured when the magnetic field is perpendicular and parallel to the surface of the sample, are shown in Fig.5. The longitudinal ME coefficient is bigger than the transverse one since the parallel magnetostriction, which is in charge for the longitudinal ME coefficient, is bigger than the perpendicular magnetostriction, which is in charge for the transverse ME coefficient. The bias field where the maximum ME coefficient occurs in case of longitudinal measurement is smaller than that of the transverse one. The reason is the demagnetizing field which is in the former case smaller than that in the later one.

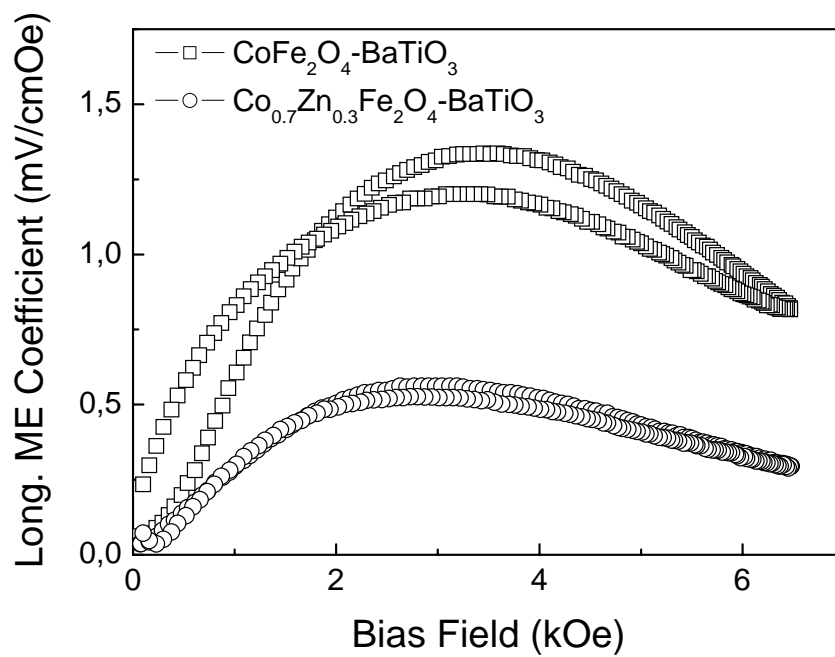


Fig.4. Longitudinal ME coefficient of CoFe<sub>2</sub>O<sub>4</sub>-BaTiO<sub>3</sub> and Co<sub>0.7</sub>Zn<sub>0.3</sub>Fe<sub>2</sub>O<sub>4</sub>-BaTiO<sub>3</sub> core-shell structure composites as function of bias field.

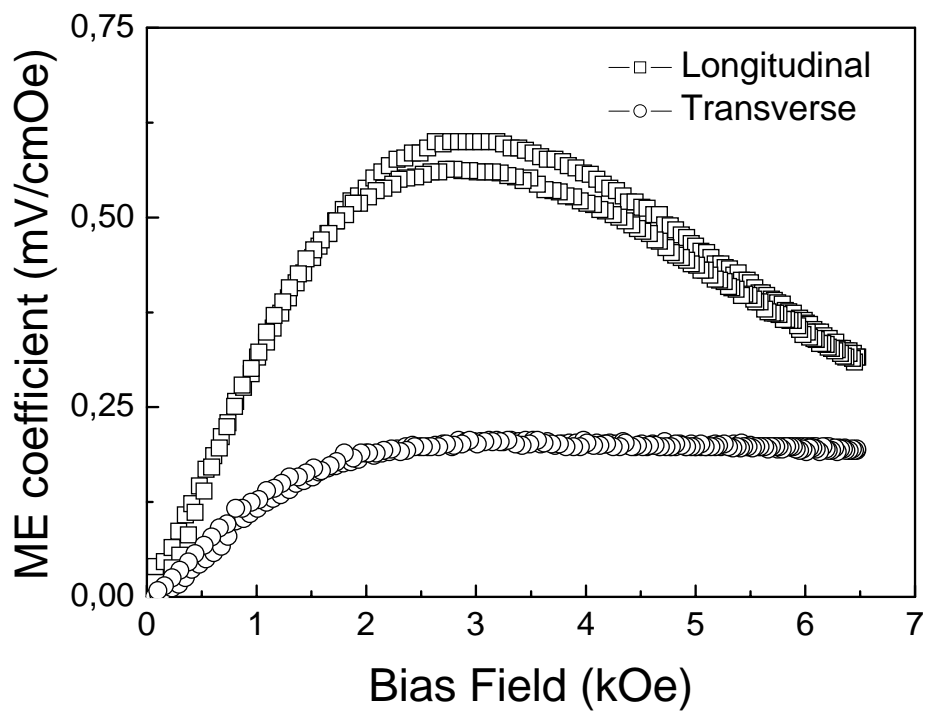


Fig.5. ME coefficients as function of bias field of Co<sub>0.7</sub>Zn<sub>0.3</sub>Fe<sub>2</sub>O<sub>4</sub>-BaTiO<sub>3</sub> composites.

The ME signal as function of the amplitude of the AC field is shown in Fig.6. The ME effect here is found to be linear up to 20 Oe with respect to the AC field. This value is almost two times higher than those assumed for other composites [12].

The longitudinal ME coefficient as function of AC field frequency is shown in Fig.7. It is clear that also here exists an optimum frequency where the ME coefficient is maximum. In the case of  $\text{Co}_{0.7}\text{Zn}_{0.3}\text{Fe}_2\text{O}_4\text{-BaTiO}_3$  composite, this optimum frequency is about 35 Hz, which is smaller compared to that of the  $\text{CoFe}_2\text{O}_4\text{-BaTiO}_3$  composite since the electrical resistance of the former is about 50% smaller than that of the later [6]. Below this frequency, the discharging process occurs through the resistance of the sample. At higher frequencies, it occurs through the capacitance formed by the two surface of the sample [6].

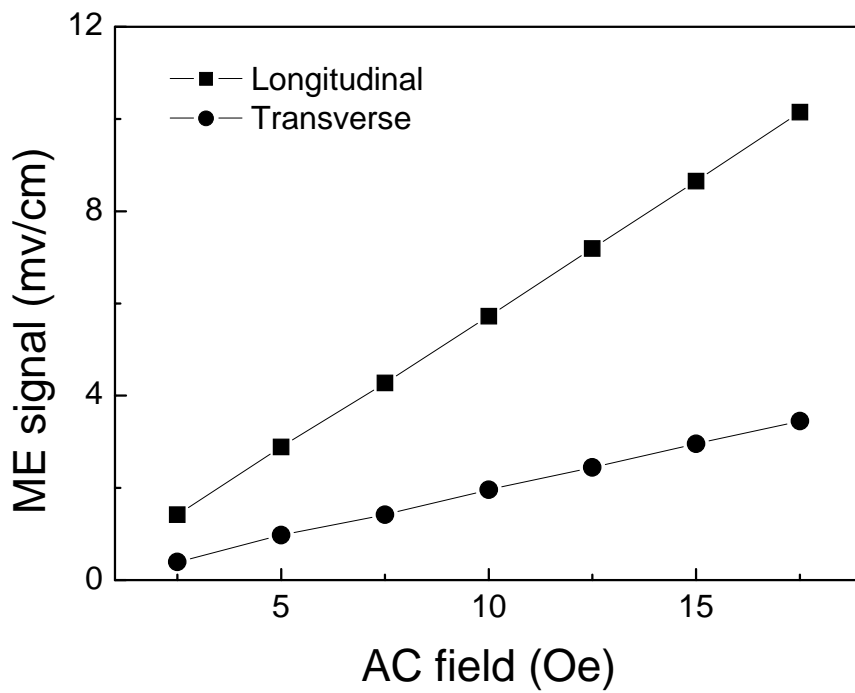


Fig.6. ME signal as function of the amplitude AC field with frequency of 270 Hz.

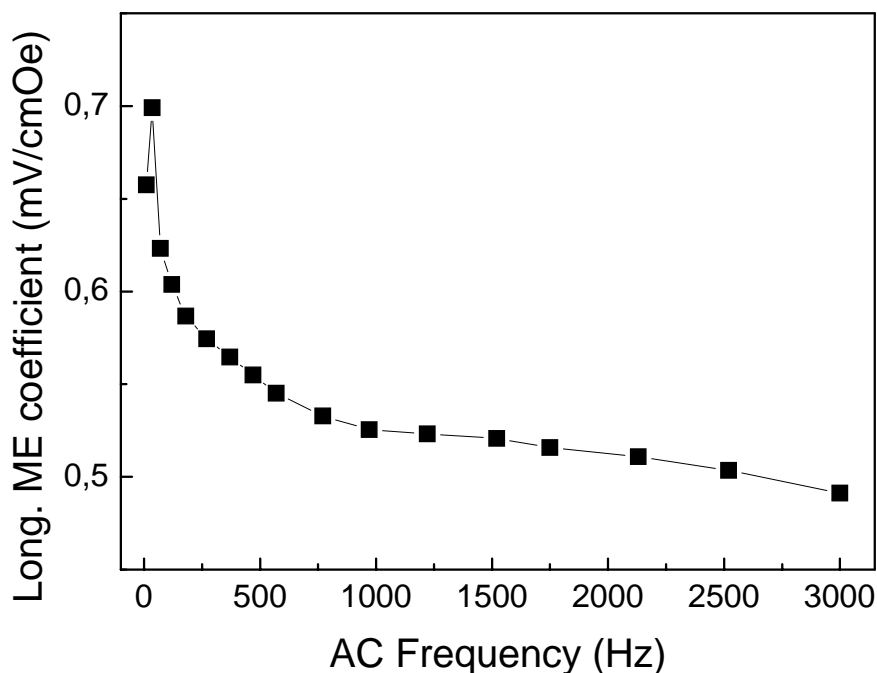


Fig.7. Longitudinal ME coefficient as function of the frequency of the AC field.

#### 4. Conclusion

A  $\text{Co}_{0.7}\text{Zn}_{0.3}\text{Fe}_2\text{O}_4\text{-BaTiO}_3$  core-shell structure composite has been prepared by wet chemical method. The substitution of Co by Zn decreases the magnetostriction and the coercivity of the magnetic constituent, leading to a decrease of the ME coefficient and the optimum bias field where the maximum ME coefficient occurs. The non-linear decrease of the ME coefficient with respect to the decrease of magnetostriction in the  $\text{Co}_{0.7}\text{Zn}_{0.3}\text{Fe}_2\text{O}_4\text{-BaTiO}_3$  composite is attributed to an increase of the mechanical coupling between the constituents due to the magnetic softness of the zinc substituted ferrite and the enhancement of direct coupling between magnetic and electric domains due to the increase of saturation magnetization. A direct connection between magnetic response of the composite and magnetization process of the magnetic constituent is shown. It is therefore concluded that a superposition of magneto-mechanical driven coupling between the constituents and a “direct” coupling between magnetic and electric domains, determines the value and the field dependence of the ME effect in such composites.



## Acknowledgement

This work is supported by the FWF Proj. Nr. P16500-N02 and the Austrian Exchange Service (ÖAD).

## Reference

- [19]. P. Curie, *J. Physique 3e series*, 3 (1894) 393.
- [2]. Manfred Fiebig, *J. Phys. D: Appl. Phys.* 38 (2005) R123–R152
- [3]. Giap V. Duong, R. Groessinger, R. sato Turtelli, Magnetolectric properties of  $\text{CoFe}_2\text{O}_4$ - $\text{BaTiO}_3$  core-shell structure composites, *IEEE Transaction on Magnetics*, accepted for publication.
- [4]. Giap V. Duong, R. Groessinger, R. Sato Turtelli, Driving mechanism for ME effect in  $\text{CoFe}_2\text{O}_4$ - $\text{BaTiO}_3$  multiferroic composite, *J. Magn. Magn. Mater.*, accepted for publication.
- [5] Giap V. Duong, R. Groessinger, Evidence of direct magneto-electric moment interaction in  $\text{CoFe}_2\text{O}_4$  –  $\text{BaTiO}_3$  core-shell structure composite, to be submitted for publication.
- [6] Giap V. Duong, R. Groessinger, M. Schoenhardt, D. Bueno-Basques, Lock-in technique for studying magnetolectric effect, *J. Magn. Magn. Mater.*, accepted for publication.
- [7] H.G. Jiang, M. Rühle and E.J. Lavernia, *J. Mater. Res.* 14, iss.2, 544-549, 1999.
- [8] Soshin Chikazumi, *Physics of Ferromagnetism*, 2<sup>nd</sup> edition, Oxford Science Publications (1997) 202-203.
- [9] Giap V. Duong *et al*, Magnetic properties of nanocrystalline  $\text{Co}_{1-x}\text{Zn}_x\text{Fe}_2\text{O}_4$  prepared by forced hydrolysis method, *J. Magn. Magn. Mater.*, in press.
- [10] Y. Yafet, C. Kittel, *Phys. Rev.*, 87 (1952) 290.
- [11] Y. Ishikawa, *J. Phy. Soc. Japan*, 17 (1962) 1877.
- [12] Manfred Fiebig, *J. Phys. D: Appl. Phys.*, 38 (2005) R123–R152.

*...your theory is crazy, but probably not crazy enough to be true...*

Niels Bohr

## **Conclusion**

*Concluding remarks and open questions will be shown here.*

## Conclusions

Regarding the self-proposed tasks as mentioned in the preface parts, and from the results achieved, some concluding remarks can be deduced as follow:

1. Various kind of nanocrystalline cobalt ferrites and Zn substitute Co-ferrites with different grain size ranging from 3 to 40 nm have been successfully synthesized by different wet chemical methods such as co-precipitation, forced hydrolysis, modified citrate gel. Structure and magnetic properties of these ferrites have been studied systematically. These nanocrystalline ferrites, proved to have very good magnetic properties, which are close to that of bulk materials. Such nanosized superparamagnetic particles can be used not only as initial materials for preparing ME composite as in this work but also for many other practical applications such ferrofluids, magnetic drug carriers, hyperthermias, etc.
2.  $\text{CoFe}_2\text{O}_4\text{-BaTiO}_3$  composites where prepared realising different microstructures. Most important is here the core-shell structure ME composites which have been successfully prepared by chemical methods, e.g. co-precipitation and sol-gel technique, and characterized structurally, magnetically and magnetoelectrically. This core-shell structure is new and proved to have a better coupling between magnetostrictive and piezoelectric constituents compared to the traditional mixed structure, giving a ME coefficient in former studies of almost 18 times higher compared to that in the later.
3. The effect of the microstructure, including the core-shell structure with  $\text{CoFe}_2\text{O}_4$  or  $\text{BaTiO}_3$  in the core, the mixed structure and the layer structure, and the effect of synthesis conditions such as synthesis temperature, pressure and annealing duration to the ME properties of the composites have been studied. The core-shell structure with  $\text{CoFe}_2\text{O}_4$  in core and  $\text{BaTiO}_3$  as shell, prepared by pressing the composite powder under a pressure of 6 tone/cm<sup>2</sup> and annealing at 1250 °C for 12 hours is found to give the highest ME coefficient. The microstructure is found to affect seriously the ME properties of the composites.

4. The main mechanism which is in charge for the ME effect in  $\text{CoFe}_2\text{O}_4\text{-BaTiO}_3$  composite is the mechanical coupling between the constituents through the magnetostriction of the magnetic phase. The ME coefficient is found to be proportional to an efficiency factor  $k_0$  and a coupling coefficient  $k$ , defined as  $k = \lambda \cdot \partial\lambda / \partial H$  where  $\lambda$  is the linear magnetostriction. This is different from the previous knowledge that the ME coefficient of composite is proportional to the piezomagnetic coupling  $q = d\lambda / dH$ .
5. The angular dependence of the ME coefficient may be used to investigate either the validity of the coupling model which predicts a proportionality to  $k = \lambda \cdot \partial\lambda / \partial H$  for different angles or to see here also the effect of coupling between different orientated domains.
6. Besides the magneto-mechanical coupling between the constituents through magnetostriction, a direct coupling between magnetic and electric domains has been evidenced when studying the AC susceptibility and the low field temperature dependent magnetization of the composite. This “direct” coupling becomes more evident when the grain size of the constituent reduces to nanoscale. This opens a new route of synthesizing an “subnanoscale” artificial quasi-single phase ME materials that exhibit room temperature ME properties which are very promising for some important applications such as high density information storage device since the information can be written with magnetic field and read out by electric field or vice versa, and as a result of it, overcoming the superparamagnetic limit which gives an upper boundary for the achievable bit density. However, more experiments have to be carried out to characterize the nature of this new direct coupling phenomenon.
7. Due to the complexity of ME composite systems, more experimental work such as controlling and optimizing the microstructure of the composites, improving the properties of the constituents etc., as well as improving a reliable measuring technique, and theoretical investigations (microstructurally as well as on an atomic scale). Here very basic questions should be studied such as: is ME coefficient a intrinsic property of the material, what is the nature of the coupling between constituents; between the magnetic and electric domains, what is the equivalent electric circuit to describe the ME effect in composite, etc. Also a comparison between the single phase multiferroic and nanoscale ME composites may show that they are

not so far from each others. Meanwhile, practical applications should be proceed to promote the scientific research of the field.

8. Two different measuring methods, called Lock-in Technique and Pulse Field Method, have been developed and were used to determine the ME properties of the  $\text{CoFe}_2\text{O}_4$ - $\text{BaTiO}_3$  composites at room temperature. By developing and comparing the results of these systems, deep knowledge and understanding of the time scale determining the measured value of the ME effect has been achieved. A pulse field method was used for the first time to measure the field dependence of the voltage which is proportional to the ME coefficient.
9. Analysing the results of the different measuring methods one can see that the charging and discharging processes occurs simultaneously. The ME coefficients measured by the Pulse Field Method is generally larger than those measured by the Lock-in Technique since the effect of the discharging process is smaller (for short pulse durations). The ME coefficient depends not only on the field amplitude and relative direction between the applied magnetic field and the internal alignment of magnetic and electric moments, but also on the measuring conditions such as input impedance of the measuring electronics and applied frequency. For the Pulse Field Method, the magnitude ME voltage depends also on the pulse duration and the field sweep rate,  $dH/dt$ . For a pulse duration smaller than 4.5 ms, a phase shift between the field and the ME signal occurs. For the Lock-in Technique, an optimum frequency which delivers the highest ME coefficient was found. The frequency dependence can be explained as following: at lower frequency, the discharging process occurs through the resistance of the sample; at higher frequency, it occurs through the capacitance formed by the sample surfaces. This means that the frequency dependence of the ME coefficient is determined by the resistance and the capacitance of the sample.

# Open Questions

## *8.1 What is the proper measuring technique?*

Until now, several techniques have been used to study the ME effect by different groups, such as the dynamic method with and without charge amplifier, the resonance technique, the magnetic pulse method, etc. Unfortunately, the results reported even on the same system but measured by different methods are very different. For example, the reported ME coefficient measured by different techniques of the  $\text{CoFe}_2\text{O}_4\text{-BaTiO}_3$  particulate composite scatters in a wide range, from 0.19 to 130 mV/cmOe. Reminding that no commercial system to measure the ME effect is up to now available. Additionally there exists no “well known sample” which can be used as a calibration standard. Every group who wants to study the ME effect have to create the measuring system by themselves and their system cannot compare to others due to the differences in instrumental parameters. This leads to the situation that the question of what is the proper and standard technique to measure the ME coefficient in composites is not yet clear.

## *8.2 What is the true value of ME coefficient?*

The ME coefficient is found to be dependent on the measuring conditions such as the frequency of the AC magnetic field and the input impedance of the measuring electronics. For example, we found that that the ME coefficient in  $\text{CoFe}_2\text{O}_4\text{-BaTiO}_3$  core-shell structure composite first increases with increasing the frequency of the AC field up about 200 Hz, then decreases for higher frequencies. Our explanation is: at low frequency, the ME coefficient is small due to the discharging process occurring through the resistance of the sample, but if high frequency is employed, the discharge will occur through the capacitance formed by two surfaces of the sample. Therefore, at a certain frequency the measured ME coefficient is not the “true” one. This leads to some questions: i) what is the true value of ME coefficient if it is independent of measuring conditions?, and ii) how to get this true ME coefficient? Here a modeling using an equivalent electric circuit of the sample including also the input circuit of the measuring system may help to solve the problem.

### *8.3 Is the ME coefficient an intrinsic property of the material?*

This question is consequence of the previous ones. Since we do not know the true value of the ME coefficient for a particular material, or even we still do not know how to get it– the truth – from the measured values, we therefore cannot say if the ME coefficient is an intrinsic property of the studied materials. This again makes the theoretical background of the ME effect in composite unclear as already discussed above.

The ME coefficient is only an intrinsic parameter for a single phase material. In the case of a composite the value of the ME coefficient depends strongly on the microstructure. The determination of the “true” ME coefficient is due to the experimental problems still open.

### *8.4 How to compare reported results?*

If we do not know the true value of ME coefficient for a particular material, and worse, we still do not know if it is possible to measure it, and if yes, what is the proper measurement technique, we are then very difficult to make an useful comparison between the results reported in literature.

### *8.5 Is mechanical coupling the only mechanism in charge for the ME effect in composites?*

It is common accepted that the mechanical coupling between the magnetostrictive and piezoelectric phases mediated by magneto/electrostriction is responsible for the ME effect in composite. However, from the expansion of free energy, one can derive the ME effect without the necessarily of magneto/electrostriction. Also here we observed: i) the huge difference in temperature dependent magnetization when the piezoelectric phase is in ordered and disordered state, ii) the large difference in AC susceptibility of the composite compared to that of the pure magnetostrictive component, and iii) the giant angular dependence of the ME coefficient with respect to applied magnetic field. These suggest the existence of the direct coupling between the dipoles of magnetostrictive and piezoelectric phases. However, the nature of this coupling is not completely understood. Therefore, more experiments need to be carried out to clarify this new coupling phenomenon between constituents in the ME composites.

### *8.6 What is the equivalent electric circuit?*

Since the ME materials convert the magnetic energy into electric one and vice versa, it is naturally to formulate them by an equivalent electric circuit. However, the complexity of the studied system and the lack of both theoretical and experimental understanding of the ME effect in composite make the question of what is the equivalent electric circuit not answered yet. Consequently, relevant questions such as how the discharging process which occurs due to finite impedance of the sample and measuring electronics affect the measured ME coefficient, and how to explain convincingly the negative sign of the ME signal when measured by magnetic pulse method, still need to be answered.



# Appendix

## Unit and Conversions of Magnetic Properties

Quantity	Symbol	Gaussian & CGS emu	Conversion factor	SI & Rationalized mks
Magnetic flux density	$B$	gauss (G)	$10^{-4}$	tesla (T)
Magnetic induction				Wb/m <sup>2</sup>
Magnetic flux	$\Phi$	maxwell (Mx), G.cm <sup>2</sup>	$10^{-8}$	weber (Wb) volt second (V.s)
Magnetic potential difference, magnetic force	$U, F$	gillbert (Gb)	$10/4\pi$	ampere (A)
Magnetic field strength	$H$	Oersted (Oe), Gb/cm	$10^3/4\pi$	A/m
Volume magnetization	$M$	emu/cm <sup>3</sup>	$10^3$	A/m
Volume magnetization	$4\pi M$	G	$10^3/4\pi$	A/m
Magnetic polarization	$J, I$	emu/cm <sup>3</sup>	$4\pi \cdot 10^{-4}$	T
Intensity of polarization				Wb/m <sup>2</sup>
Mass magnetization	$\sigma, M$	emu/g	1 $4\pi \cdot 10^{-7}$	A.m <sup>2</sup> /kg Wb.m/kg
Magnetic moment	$m$	emu, erg/G	$10^{-3}$	A.m <sup>2</sup> , joule per tesla (J/T)
Magnetic dipole moment	$j$	emu, erg/G	$4\pi \cdot 10^{-10}$	Wb.m
Volume susceptibility	$\chi, \kappa$	dimensionless emu/cm <sup>3</sup>	$4\pi$ $(4\pi)^2 \cdot 10^{-7}$	dimensionless henry per meter (H/m), Wb/(A.m)
Mass susceptibility	$\chi_\rho, \kappa_\rho$	cm <sup>3</sup> /g, emu/g	$4\pi \cdot 10^{-3}$ $4\pi \cdot 10^{-10}$	m <sup>3</sup> /kg H.m <sup>2</sup> /kg
Molar susceptibility	$\chi_{mol}$ $\kappa_{mol}$	cm <sup>3</sup> /mol emu/mol	$4\pi \cdot 10^{-6}$ $(4\pi)^2 \cdot 10^{-10}$	m <sup>3</sup> /mol H.m <sup>2</sup> /mol
Permeability	$\mu$	dimensionless	$4\pi \cdot 10^{-7}$	H/m, Wb/(A.m)
Relative permeability	$\mu_r$	not defined		dimensionless
Volume energy density	$W$	erg/cm <sup>3</sup>	$10^{-1}$	J/m <sup>3</sup>
Demagnetizing factor	$D, N$	dimensionless	$1/4\pi$	dimensionless

# Manual of the Lock-in System to Measure ME Coefficient

1. Turn on the Hall probe for at least 15 minutes before measuring.
2. Check all cables and connections if they are rightly connected.
3. Turn on the DC power supply, set it to programmable mode.
4. Turn on Computer, AC current generator, Lock-in amplifier, Keithley voltmeter.
5. Check if the Lock-in is in differential mode. If not, connect the cable in this mode and press A-B button.
6. Set the Lock-in sensitivity and time constant to the desired value, set FILTERS to BP and TRACK position.
7. Set the AC current amplitude and frequency, check the frequency in the DISPLAY 1 of the Lock-in.
8. Set DISPLAY 1 to DISP, DISPLAY 2 to R $\theta$  or XYV.
9. Put the sample into the sample holder and place it in the proper position to measure.
10. Press the button AUTO & PHASE to adjust the Lock-in automatically.
11. Open the LABVIEW interfere program.
12. Chose the Power Generator, set the current, amount of time to get maximum, dwell, sample rate to the desired values.
13. Run the program, press stop button to cancel the measurement. In this case, set the current to 0 and run the program again to reduce the DC current and voltage to zero.
14. Save the data when the measurement is finished and the dialog box appears.
15. Exit the program when finishing all measurements.
16. Turn of the DC power supply, the Hall probe, the Lock-in, the AC current generator and the Keithley voltmeter.
17. Take out the sample.

# Manual of the Pulse Field System to Measure ME Effect

1. Turn on the computer
2. Turn on the Pulse Field System (Hirst PFM 11).
3. Check all cables and connections if they are rightly connected.
4. Put the sample into the sample holder and place it in proper position.
5. Set the preamplifier to differential mode (A-B), set the amplifying factor to 1.
6. Open the LABVIEW interfere program.
7. Click the run button to activate the program.
8. Chose the pulse type: long or short.
9. Set the voltage.
10. Click “Start” button to measure.
11. Save the data when the measurement is finished.
12. Exit the LABVIEW program when finishing all measurements.
13. Turn of the Pulse Field System and the preamplifier.
14. Take out the sample.

## Acknowledgement

I express here my most sincere thanks to Prof. Dr. Roland Grössinger, my academic supervisor, and Dr. Reiko Sato Turtelli, for their kindness, their help and encouragement as well as many fruitful discussions during the course of this work. I deeply thank Prof. Nguyen Hanh for introducing me to Prof. Roland Grössinger and for his long-term encouragement and many scientific discussion and collaboration. I thank Prof. Dr. Hoang Ba Chu for the nice recommendation letter when I came here. And I thank the open-minded hard and soft magnetic materials working group where I learned not only magnetism but also many other things concerning most parts of the scientific job.

I am grateful the Austrian Exchange Service (ÖAD) for granting scholarship so that I can pursue my study in Austria.

I thank all my colleagues and all staff member at the Institute of Solid State Physics who are always nice and kind to help me as well as to provide me materials and facilities that without them I cannot finish my research and study. Particularly I thank Markus Schönhart, Micheala Küpferling, J. H. Espina-Hernandez, Martin Müller, Robert Lackner, Sabine Hoefinger, Saleh Mohammad, Peter Hundegger, Vladimira Piwetz, Andreas Lahner, Aurelia Witek, Dr. Cristina Bormio-Nunes, Dr. Herbert Sassik, Dr. Herbert Müller, for their help during experiment or administration, Prof. Dr. Walter Steiner, Prof. Dr. Michael Reissner, Prof. Dr. Ernst Bauer, Prof. Dr. Herwig Michor, Prof. Dr. Josef Fidler, Prof. Dr. Günter Wiesinger for their kindness and collaboration.

I thank all my colleagues at the Department of Inorganic & General Chemistry and at the Faculty of Chemical Engineering, Hanoi University of Technology, for their encouragement and for doing my teaching task during my stay in Austria now and Korea before. Particularly I thank the member of the sol-gel group who has a closed connection and collaboration during my stay abroad.

I thank all collaborators outside the Institute of Solid State Physics who are interested in my topic, helping me during some experiment and discussing the scientific problems. To mention, I should say: Prof. Nguyen Hanh at Faculty of Chemical Engineering, Hanoi University of Technology (Vietnam), Prof. Dr. Wolfgang Linert and Dr. Peter Wienberger at Institute of Applied Synthetic Chemistry, Vienna University of Technology (Austria), Prof. Dr. Michael Zehetbauer and Dr. Erhard Schafner at the Department of Materials Physics, Faculty of Physics, University of Vienna (Austria), Prof. Dr. Marcelo Knobel at Instituto de

Física, Universidade Estadual de Campinas (Brasil), Dr. Dario Bueno-Basques and Msc. Veronica Cores at Centro de Investigación en Materiales Avanzados (CIMA, Mexico), Dr. Sakura Pascarelli at European Synchrotron Radiation Facility, (ESRF, France).

Many thanks to my friends in Vietnam, Austria, Korea, Japan, America and other countries who encouraged and helped me during my staying abroad. Particular thanks to Lan Nguyen for her help when we arrived Vienna, Dung Vo & Hieu Nguyen for their help during my stay in San Diego, Trinh Xuan Anh and friends during my stay in Kyoto and Daniel Santos during my stay in Spain when I participated some scientific conferences.

Special thanks to all members of the Vietnamese Youth and Student Association in Austria (SVA) and the “family group” who helped us and shared a lot of joys with us during our stay in Vienna. I will not list their names here since there are many and we are so closed that it is not necessary to be mentioned formally.

Last but not most, I deeply thank our families for their long-term support and encouragement. Thank you, my beloved wife – Nam Anh, my lovely kid – Nam Duong, for your sharing of joys and sadness, your endless encouragement and your understanding of countless evenings and weekends that I was at work.

# Curriculum Vitae

Name: GIAP Van-Duong

Address: Hardtmuthgasse 88/3/9, A-1100, Vienna, Austria.

Telephone: +43 1 58801 13152

Mobile: +43 699 1277 1013

E-mail: [giap@ifp.tuwien.ac.at](mailto:giap@ifp.tuwien.ac.at)

Fax: +43 1 58801 13899

Date of birth: Feb. 23<sup>rd</sup> 1976      Place of birth: Bac Giang, Vietnam

Nationality: Vietnamese      Sex: male      Family Status: Married.

## Academic preparation

**Ph.D. in Technical Physics:** Academic years: 24/11/2003-11/10/2006.

Dissertation: Physics of Magnetolectric Composites

Advisor: Prof. Dr. Roland Groessinger,

Institute of Solid State Physics,

Vienna University of Technology,

Wiedner Hauptstrasse 8-10, 1040, Vienna, Austria.

### Concentrations:

1. Synthesizing nanocrystalline magnetic oxides and magnetolectric composites.
2. Charactering structures, electric, magnetic and magnetolectric properties of the synthesized materials.
3. Developing equipments to study magnetolectric effect.

**Master of Engineering:** Chemical Engineering, academic years: 9/2000-9/2002.

School of Chemical Engineering and Technology,

Chonbuk National University, Chonju, 561-756, South Korea.

Thesis: Photocatalytic Decomposition of Trimethylamine over TiO<sub>2</sub> photocatalysts

**Diploma Study:** Organic Synthesis and Petrochemicals, academic years: 1994-1999.

Faculty of Chemical Engineering, Hanoi University of Technology, No.1 Hai Ba Trung, Hanoi, Vietnam.

Thesis: Synthesis and characterization of catalytic copper oxides by citrate gel method

**High school:** 9/1991-6/1994.

Yen Dung No.2 high school, Yen Dung, Bac Giang, Vietnam.

**Primary & Secondary school:** 9/1982-6/1991.

Thai Dao Primary & Secondary school, Thai Dao, Lang Giang, Bac Giang, Vietnam.

## **Research skills**

### **Materials chemistry**

- Synthesis of various kinds of inorganic materials, including magnetic oxides and magnetoelectric composites such as ferrites, manganites, cobaltates, composites of ferrites and barium titanate, etc by different chemical methods.
- Synthesis of nanocrystalline materials down to 3 nm using wet chemical methods.

### **Chemical engineering**

- Organic synthesis and petrochemicals.
- Heterogeneous catalysis, environmental catalysis and photocatalysis.

### **Experimental physics:**

- X-ray diffraction for structure characterizations of materials.
- Electric and magnetic characterizations of materials.
- Developing equipments to measure magnetoelectric coefficients.
- High magnetic pulse field.

### **Solid state physics**

- Magnetic nanoparticles, hard and soft magnetic materials.
- Magnetoelectric effect, magnetoelectric composites.
- Transport phenomenon in solids.

## **Academic activities**

### **Participation of scientific conferences**

- 1) 21<sup>th</sup> Workshop on Novel Materials and Superconductors, 11-8. February, 2006, Planneralp, Austria.



- 2) IEEE International Magnetism Conference (INTERMAG 2006), May 8-12<sup>th</sup>, 2006, San Diego, California.
- 3) Sixth International Conference on Clinic and Scientific Applications of Magnetic Carriers, May 17-20<sup>th</sup>, 2006, Krems, Austria.
- 4) Eighth International Workshop on Non-Crystalline Solids, June 20-23, 2006, Gijón, Spain.
- 5) III Joint European Magnetic Symposia (JEMS 06), 26-30 June, 2006, San Sebastian, Spain.
- 6) 17th International Conference on Magnetism (ICM 2006), August 20-25, 2006, Kyoto, Japan.

### **Academic referee**

Reviewer of the “III Joint European Magnetic Symposia (JEMS 06), 26-30 June, 2006, San Sebastian, Spain”.

### **Professional experiences**

- + ) 9/1999-8/2000: Lecturer,  
Faculty of Chemical Engineering, Hanoi University of Technology,  
No.1, Hai Ba Trung, Hanoi, Vietnam.
- + ) 9/2002-10/2003: Lecturer,  
Faculty of Chemical Engineering, Hanoi University of Technology,  
No.1, Hai Ba Trung, Hanoi, Vietnam.

### **Honor and Awards**

1. Award for scientific research from the Hanoi University of Technology, Vietnam, 1999.
2. Award for scientific research from the Ministry of Education and Training, Vietnam, 1999.
3. Brain Korea scholarship award, South Korea, 9/2000-8/2002.
4. Technology Grant Southeast Asia scholarship award, Austrian Exchange Service, Republic of Austria, 11/2003-10/2006.

## Academic references

1. Prof. Dr. Roland Grössinger,  
Institute of Solid State Physics, Wiedner Hauptstrasse 8-10, A-1040, Vienna, Austria.  
Tel: +43 1 58801 13150, fax: +43 1 58801 13899.
2. Dr. Reiko Sato Turtelli,  
Institute of Solid State Physics, Wiedner Hauptstrasse 8-10, A-1040, Vienna, Austria.  
Tel: +43 1 58801 13150, fax: +43 1 58801 13899.

## Languages

- Fluent in English,
- Can speak some Korean, German, French, Russian, Italian and Spanish.

## Hobby and interest

Reading scientific and philosophy books, Art (painting and literature), Fishing, Travelling.

## Publications

1. Giap V. Duong, R.S. Turtelli, N. Hanh, D.V. Linh, M. Reissner, H. Michor, J. Fidler, G. Wiesinger, R. Grössinger, *Magnetic properties of nanocrystalline  $Co_{1-x}Zn_xFe_2O_4$  prepared by forced hydrolysis method*, Journal of Magnetism and Magnetic Materials, in press.
2. Giap V. Duong, R. Groessinger, R. Sato Turtelli, *Magnetoelectric Properties of  $CoFe_2O_4$ - $BaTiO_3$  Core-Shell Structure Composites*, IEEE Transactions on Magnetics, in press.
3. Giap V. Duong, R. Groessinger, *Evidence of Magneto-Electric Moment Interactions in  $CoFe_2O_4$ - $BaTiO_3$  Composites*, orally presented at the IEEE International Magnetics Conference (Intermag2006), San Diego, California, May 8-12, 2006.

4. Giap V. Duong, R. Groessinger, M. Schoenhardt, D. Bueno-Basques, *The Lock-in Technique for studying magnetoelectric effect*, accepted for publication (Journal of Magnetism and Magnetic Materials).
5. Giap V. Duong, R. Groessinger, *Effect of preparation conditions on the magnetoelectric properties of  $\text{CoFe}_2\text{O}_4\text{-BaTiO}_3$  multiferroic composites*, accepted for publication (Journal of Magnetism and Magnetic Materials).
6. Giap V. Duong, R. Groessinger, R. Sato Turtelli, *Effect of structure on the magnetoelectric properties of  $\text{CoFe}_2\text{O}_4\text{-BaTiO}_3$  multiferroic composites*, accepted for publication (Journal of Magnetism and Magnetic Materials).
7. Giap V. Duong, R. Groessinger, R. Sato Turtelli, *Driving mechanism for magnetoelectric effect in  $\text{CoFe}_2\text{O}_4\text{-BaTiO}_3$  multiferroic composites*, accepted for publication (Journal of Magnetism and Magnetic Materials).
8. Giap V. Duong, R. Sato Turtelli, W. Nunes, E. Schafler, N. Hanh, R. Grössinger, M. Knobel, *Ultrafine  $\text{Co}_{1-x}\text{Zn}_x\text{Fe}_2\text{O}_4$  synthesized by hydrolysis: Effect of thermal treatment and its relationship with magnetic properties*, orally presented at the 8<sup>th</sup> International Workshop on Non-Crystalline Solids, June 20<sup>th</sup>-23<sup>rd</sup> 2006, Gijon, Spain, submitted for publication.
9. Giap V. Duong, R. Sato Turtelli, B.D. Thuan, N. Hanh, R. Grössinger, *Magnetic properties of nanocrystalline  $\text{BaFe}_{12}\text{O}_{19}$  prepared by hydrothermal method*, accepted for publication (Journal of Non-Crystalline Solids).
10. Giap V. Duong, N. Hanh, R. Grössinger, P. Weinberger, *Monodispersed nanocrystalline  $\text{Co}_{1-x}\text{Zn}_x\text{Fe}_2\text{O}_4$  by forced hydrolysis: Synthesis and characterization*, accepted for publication (Journal of Magnetism and Magnetic Materials).
11. Giap V. Duong, B.D. Thuan, N. Hanh, R. Grössinger, *Size controlled nanocrystalline  $\text{BaFe}_{12}\text{O}_{19}$  by hydrothermal method: Synthesis and Characterization*, presented at the 6<sup>th</sup> International Conference on Scientific and Clinical Applications of Magnetic Carriers, May 17<sup>th</sup>-20<sup>th</sup> 2006, Krems, Austria.
12. R.Grössinger, Giap Van Duong, D. Bueno-Baqués, *Magnetoelectric materials-New materials for Applications*, Invited talk at International Symposium on Interdisciplinary Electromagnetic, Mechani & Biomedical Problems (ISEM 2005), September 12-14, 2005, Bad Gastein (Salzburg), Austria (proceedings in press).
13. Giap V. Duong, R. Grössinger, R. Sato Turtelli, M. Knobel, *Magnetic properties of nanocrystalline  $\text{CoFe}_2\text{O}_4$  synthesized by modified citrate-gel method*, to be submitted for publication.

14. Giap V. Duong, R. Grössinger, R. Sato Turtelli, M. Reissner, Magnetic properties of nanocrystalline cobalt ferrite in  $\text{CoFe}_2\text{O}_4$ - $\text{BaTiO}_3$  core-shell structure composite, to be submitted for publication.
15. Giap V. Duong, R. Groessinger, Evidence of direct magneto-electric moment interaction in  $\text{CoFe}_2\text{O}_4$  –  $\text{BaTiO}_3$  core-shell structure composite, to be submitted for publication.
16. Giap V. Duong, R. Groessinger, Magnetoelectric properties of  $\text{CoFe}_2\text{O}_4$  –  $\text{BaTiO}_3$  core-shell structure composite studied by magnetic pulse method, to be submitted for publication.
17. Dario Bueno Baques, Roland Grossinger, Markus Schonhart, Giap V. Duong, Reiko Sato, Veronica Corral Flores, Jose Matutes Aquino, *J. Appl. Phys.* 99, 08D908, 2006.
18. Van-Duong Giap, R. Grössinger: *Magnetoelectric materials* (talk), 21<sup>th</sup>. Workshop on Novel materials and superconductivity, Planneralm, Österreich; 02-11-2006 - 02-18-2006.

*...to live is to find the hidden truth...*

GVD